Liposome-Micelle Hybrid Systems for Oral Delivery of Poorly Water-Soluble Cardiovascular Drug Lovastatin and Anticancer Drugs Paclitaxel and 5-fluorouracil

Bilquis Romana

B. Pharm (Honors) and M. Pharm (Pharmaceutical Technology)

A thesis submitted for the degree of

DOCTOR OF PHILOSOPHY

(Pharmacy)

School of Pharmacy and Medical Sciences

University of South Australia



7th April' 2018

Dedicate to my

Parents

Mrs. Tahmina Khatun & Shaikh Auboyedullah

Children

Ruhama & Bilhaan

উৎসর্গ

মাতা-পিতা

(তাহমিনা খাতুন এবং শেখ ওবায়দুল্লাহ)

সন্তান

(রুহামা এবং বিলহান)

Table of Content

Table of Content i

List of Figures vi

List of Tables xv

Abbreviations xvii

Abstract xxii

Thesis Outline xxv

Publication xxvi

Conference Presentation xxvi

Acknowledgments xxvii

Author's Statement of Originality xxx

1. Introduction 1

1.1. Project scope and significance 1

1.2. Aims of the research project 5

2.1. Literature Review 11

2.1.1. Poorly water-soluble drugs for oral drug delivery, challenges, and current strategy 11

2.1.2. Biopharmaceutical Classification System (BCS) and the Model Drugs 12

2.1.3. Strategies for oral delivery of poorly soluble drugs 16

2.2. Overview of liposome-based drug delivery system and commercial liposomes 18

2.2.1. Background 18

2.2.2. What are Liposomes? 18

2.2.3. The rational for Liposome Delivery Systems 20

2.2.4. Classification of liposomes 21

2.2.5. Liposome preparation methods and drug incorporation in liposomes 24

2.2.6. Formation process of liposomes 27

2.2.7. Factors influencing drug loading in liposome 27

2.2.8. Factors affecting drug release from liposome 31

2.2.9. Drug release mechanism and kinetics 34

2.3. Micelle based drug delivery systems 35

2.3.1. What are micelles? 35
2.3.2. Drug delivery using micelles 36
2.3.3. Drug incorporation in micelles 36
2.3.4. Micelle preparation methods 37
2.3.5. Factors affecting drug loading in micelles 42
2.3.6. In vitro drug release from micelles 42
2.3.7. Factors affecting drug release from micelles 44
2.3.8. Drug release mechanism from micelles 46
2.4. Cellular activity of liposome and micelles and drug absorption 48
2.4.1. Mucosal Surface as Potential Site for Liposome Uptake 49
2.4.2. Improved cellular activity of drugs encapsulated in liposomes or micelles 52
2.4.2.1. Liposomes 52
2.4.2.2. Micelles 53
2.5. Liposomes and micelles as a temperature-sensitive carrier for chemotherapy 54
2.6. Current challenges of liposome and micelles as drug delivery 57
2.7. Liposome-micelles-hybrid system (LMH) as a project goal 58
3. Liposome-Micelle-Hybrid System for Oral Delivery of Poorly Water-Soluble Drugs 59
3.1. Introduction 60
3.2. Materials 63
3.3. Experimental methodology 63
3.3.1. Preparation of LMH system 63
3.3.1.1. Formulation of LOV loaded micelles 63
3.3.1.2. Formulation of liposomes 64
3.3.1.3. Formulation of liposome-micelle-hybrid 65
3.3.2. LOV assay method 66
3.3.3. Encapsulation efficiency and drug loading 66
3.3.4. Physicochemical characterisation of the LMH system 67
3.3.4.1. Particle size and zeta potential 67
3.3.4.2. Morphology and surface characteristics 67
3.3.4.3. LMH physical and chemical stability 68
3.3.4.4. Short-time physical and chemical stability 68
3.3.4.5. LOV *in vitro* release study 69
3.4. Results and discussion 70

3.4.1. Physicochemical characterisation of LMH 70
3.4.1.1. The size, zeta potential and size distribution of micelles 70
3.4.1.2. The size, zeta potential and size distribution of PC and DSPG Liposomes ... 79
3.4.1.3. Preparation and physical characterisation of LMH. 82
3.4.2. Microscopic characterisation of LMH 86
3.4.3. LOV release study from LMH system 87
3.4.4. *In vitro* drug release kinetics 92
3.4.5. Short–term stability test of liposomes and micelles 95
3.4.5.1. Physical stability of micelles and liposomes indifferent preparation (different pH) conditions 95
3.4.5.2. LOV content stability at different pH values 99
3.4.5.1. LMH Physical stability with storage 100
3.5. Conclusion 101
4. Evaluation of a Liposome-Micelle Hybrid System to Improve the Intestinal Transport of Lovastatin using Caco-2 Cell Monolayers 103
4.1. Introduction 104
4.2. Materials and equipment 108
4.3. Experimental methodology 109
4.3.1. Assessment of cell viability by Alamar blue method 109
4.3.2. Permeability assessment of LOV-LMH 109
4.3.3. Evaluation of the Caco-2 cell monolayer integrity using lucifer yellow 111
4.3.4. LOV assay method 113
4.3.5. Transportation and cellular uptake of LOV 113
4.3.6. Intracellular uptake and accumulation 113
4.3.7. Statistics analysis method 113
4.4. Results and discussion 114
4.4.1. Cell viability assessment of LOV-LMH 114
4.4.2. Caco-2 cell monolayer permeability assessment of LOV-LMH 115
4.4.3. Evaluation of the Caco-2 cell monolayer integrity using Lucifer yellow 122
4.4.4. Transport of LOV with different nanocarriers (micelles, liposomes, and LMH) across a Caco-2 cell monolayer 124
4.4.5. Intracellular uptake and accumulation 126
4.5. Conclusion 129

5. Development of a Temperature-Sensitive Liposome-Micelle-Hybrid (TS-LMH) System for Anticancer Drugs Paclitaxel and 5-fluorouracil 130
5.1. Introduction 133
5.2. Materials 137
5.3. Experimental Methodology for preparation and characterisation 139
5.3.1. Preparation of PTX encapsulated thermosensitive micelles 139
5.3.2. Formulation of PTX encapsulated thermosensitive liposome 139
5.3.3. Formulation of PTX encapsulated thermosensitive LMH 140
5.3.4. Preparation of 5-FU-PTX dual-encapsulated LMH 140
5.3.4.1. Preparation of 5-FU loaded micelles 140
5.3.4.2. Preparation of PTX loaded liposome 140
5.3.4.3. Preparation of PTX-5-FU loaded LMH 140
5.4. Encapsulation efficiency and drug loading 140
5.4.1. PTX assay method 141
5.4.2. 5-Fluorouracil assay method 141
5.5. Physical characterisation of PTX-loaded LMH 142
5.5.1. Particle diameter and size distribution 142
5.5.2. Morphological characterisation of PTX loaded LMH 142
5.5.2. Temperature-triggered release of PTX and 5-FU from TS-LMH 143
5.5.4. Dry sample preparation (Sample drying) for cell studies 143
5.5.5. Permeability assessment of PTX-LMH 144
5.5.6. Transport and cellular uptake of PTX study of PTX with different nanocarriers (micelles, liposome, and LMH) to the apical-to-basolateral (A→B) direction 147
5.5.7. Statistics analysis method 148
5.6. Results and discussion 148
5.6.1. Physical characterisation of PTX-LMH 148
5.6.3. Drug loading efficiency 151
5.6.4. Morphological characterisation 154
5.6.5. Temperature-triggered release of PTX from micelles, liposomes, and LMH 156
5.6.6. Temperature-triggered release of PTX and 5-FU from PTX-5-FU-LMH and 5-FU from micelles 163
5.6.7. Release kinetics of PTX and 5-FU from LMH 166
5.6.8. Assessment of cytotoxicity 169

5.6.9. Measurements of permeation co-efficient or apparent permeability..... 171
5.6.10. Evaluation of the Caco-2 cell monolayer integrity using Lucifer yellow 175
5.6.11. Transport studies of PTX with different nanocarriers (micelles, liposome, and LMH) in the apical-to-basolateral (A→B) direction..... 177
5.7. Conclusion..... 178
6. Conclusions and Future Direction 180
6.1. Summary of research findings 180
6.1.1. Liposome-micelles-hybrid system for oral delivery of poorly water-soluble drugs 181
6.1.2. Cell permeability, transportation and cell viability studies of lovastatin loaded liposome-micelle-hybrid system..... 182
6.1.3. Development of a temperature sensitive liposome-micelle-hybrid system for anticancer drugs 183
6.2. Future direction..... 184
7.Reference..... 186

List of Figures

Figure No.	Description of Figure	Page No.
Figure 1-1	Schematic representation of a liposome (>100 nm), micelles (< 50 nm) and a liposome-micelle hybrid (LMH) as drug delivery systems for a poorly water-soluble drug.	3
Figure 1-2	Schematic presentation of the research presented in this thesis.	6
Figure 2-1	Representation of the BCS indicating that improved formulation design can highly improve the solubility of class II drugs, which results in higher absorption, while drugs of classes III and IV require chemical modification. Biopharmaceutical classification system (BCS) of therapeutic defined by FDA. Image reproduced from Wu *et al*.	11
Figure 2-2	Schematic representation of different nanotechnology-based drug delivery systems. Image adapted from Romana *et al*.	16
Figure 2-3	Schematic showing spherical liposomes plus the bilayer where hydrophobic and hydrophilic substances can be incorporated. Image adapted from Lasic *et al.* and Bergstrand *et al.*	19
Figure 2-4	Schematic illustration of liposomes of different size and number of lamellae resulting from different formulation/manufacturing techniques. Image adapted and edited from Storm *et al*.	21
Figure 2-5	Four types of liposomes utilised to date; A) conventional, B) sterically-stabilized liposomes (pegylated or stealth liposome), C) ligand-targeted and D) a combination of the as theranostic. Image adapted from Sercombe *et al*.	22
Figure 2-6	The relationship between liposomal (PC: cholesterol, 89:11 mol %) bilayer encapsulation of the drug and (A) lipophilicity or (B) molecular weight of the drug. Image adapted from Mohammed *et al*.	28
Figure 2-7	The influence of long-chain symmetric and asymmetric lipids on midazolam or propofol encapsulation. Liposomes were prepared from a combination of (A) PC, DMPC, DPPC, DSPC, DGPC, POPC or MSPC (89 mol %) and (B) DSPC or DPPC (44.5 mol %) with POPC or MSPC (44.5 mol %). Keeping constant cholesterol (11 mol %) and drug loading in a total lipid concentration of 18 µmol for the formulations. Image adapted from Mohammed *et al*.	29
Figure 2-8	Comparison of midazolam encapsulation by MSPC: cholesterol or DMPC: cholesterol (89:11 mol %) liposomes prepared using increasing amounts of cholesterol. Results are expressed as the means of three experiments ± S.D. Image adapted from Mohammed *et al*.	30

Figure 2-9	(A) Effect of alkyl chain length of positively charged TAP series on bilayer release of propofol. (B) Effect of vesicle surface charge on the rate of propofol release. Image reproduced from Mohammed *et al*.	31
Figure 2-10	The effect of incorporation of 9 mol% stearylamine (positively charged) or dicetylphosphate (negatively charged) lipids induced significantly more release of ibuprofen compared to neutral liposomes. Image reproduced from Mohammed *et al*.	32
Figure 2-11	The effect of lipid alkyl chain length on the release profile of ibuprofen from liposomes in order of PC > DMPC > DSPC > PC24. Multilamellar vesicles incorporating ibuprofen composed of 16 mol PC, 4 mol cholesterol (CHO); 16 mol DMPC, 4 mol CHO; 16 mol DSPC, 4mol CHO; 16 mol C_{24}PC, 4 mol CHO were incubated 0.01M PBS at 37 $^{\circ}$C for up to 24 h. Results represent mean ± S.D., n = 3.Image Mohammed *et al.*	33
Figure 2-12	The general scheme of micelle formation from amphiphilic molecules. Image modified from Gutman *et al*.	34
Figure 2-13	Physical methods of drug encapsulation into polymeric micelles: (A) direct dissolution; (B) dialysis; (C) oil-in-water emulsion; (D) solvent evaporation; (E) co-solvent evaporation; (F) freeze-drying. Image adapted from Aliabadi *et al.*	38
Figure 2-14	Drug release profiles of free 5-FU and 5-FU micelles in PBS solution at pH 7.4 Image reproduced from Yan *et al*.	42
Figure 2-15	*In vitro* drug release kinetics of the docetaxel-loaded d-α-tocopheryl polyethylene glycol 1000 succinate micelles prepared by a solvent casting method in phosphate-buffered saline (pH 7.4). Bars represent (Mean ± SD, n = 3). DTXSC-50: Docetaxel-loaded micelles prepared with 2.5 mg docetaxel and 50 mg D -α-tocopheryl polyethylene glycol 1000 succinate (TPGS); DTXSC-100: Docetaxel-loaded micelles prepared with 2.5 mg docetaxel and 100 mg TPGS; DTXSC-150: Docetaxel-loaded micelles prepared with 2.5 mg docetaxel and 150 mg TPGS. Image reproduced from Muthu *et al.*	43
Figure 2-16	Mechanism of drug release from polymeric micelles. (A) drug release from block copolymer-drug conjugates, (B) drug release from drug encapsulated micellar carriers and (C) drug release from poly ion complex micelles. Image adapted from Aliabadi *et al*.	46
Figure 2-17	Schematic drawing of mucus (MU) covered absorptive enterocytes (EC) and M cells (MC) in the small intestine. Lymphocytes (LC) and macrophages (MP) from underlying lymphoid tissue can pass the basal lamina (BL) and reach the epithelial cell layer which is sealed by tight junctions (TJ). Possible translocation routes for liposomes (LP) are (I) paracellular uptake, (II) endocytotic uptake by enterocytes and (III) M	48

cells. Image adapted from Jung *et al*.

Figure 2-18 Different interactions of liposomes to the cell. Image adapted from Lasic *et al*. 49

Figure 2-19 The viability of Caco-2 cells after the cells were treated with different concentrations of the SMV/G5-NH2 (A) or the SMV-liposomes (B) compared with the control group. n = 3. Image reproduced from Qi *et al*. 51

Figure 2-20 Cell viability of MCF-7 cells after 48 h of treatment with PTX, blank single micelles (Soluplus®), blank mixed micelles (Soluplus®: TPGS), PTX-loaded Soluplus®micelles and PTX-loaded Soluplus®: TPGS mixed micelles. Image reproduced from Bernabeu *et al*. 52

Figure 2-21 Schematic representation of temperature-triggered release from temperature sensitive liposome. 54

Figure 2-22 Transmission electron microscope photos of (A) PTX-TSL and (B) NTSL. (C) In vitro, drug release from PTXTSL and NTSL in vitro, determined at 37°C and 42°C, respectively in PBS (pH 7.4) containing 0.5 M sodium salicylate. Image reproduced from Wang *et al*. 55

Figure 2-23 Release profile in PBS of encapsulated 5-FU-Cu-PEI from 5-FU-Cu-PEI-loaded liposomes upon heating for 10min in (a) water bath at 37, 39, 42, 45 and 49°C after dilution by 10 mM PBS (1776 mM dextrose). Image reproduced from Al Sabbagh *et al*. 55

Figure 3-1 Schematically presentation of LOV liposomes-micelles hybrid system (LOV-LMH). 58

Figure 3-2 Formation of poloxamer micelles from amphiphilic block copolymer (407 /188). 69

Figure 3-3 Hypothetical model showing A) helical deoxycholate-LOV micelles (seen from top), (1,2) different primary micelles, (3) disclike micelle B) the molecular structure of DC composed of a rigid steroid backbone with I) hydrophobic group: α-oriented hydroxyl and the carboxyl group of the side chain on the concave side of the steroid skeleton and ii) hydrophobic group: β-oriented methyl groups positioned on the opposite convex side conjugated to an anionic chain, C) the structure of LOV molecule with hydrophobic ring and D) the structure of DC molecule with hydrophobic rings; a nucleus composed of four fused rings: three cyclohexane rings, labeled A, B and C, and a cyclopentane ring, labeled D. Image adapted from Kumar *et al*. and Nicola *et al*., Madenci *et al*. and modified. 72

Figure 3-4 Hypothetical model showing A) self-assembly of Deoxycholate-Poloxamer mixed micelles and B) the molecular structure of lovastatin, DC and Poloxamer with structural similarity and dissimilarity (already 73

discussed above) Image adapted from Kumar *et al*. Nicola *et al*. Maarten *et al*. and modified.

Figure 3-5 The amphiphilic structure of TPGS shows A) a hydrophilic head (polyethylene glycol chain) and B) a hydrophobic tail (tocopheryl group) and C) formation of TPGS micelles. Adapted and modified from Jhaveri *et al*. 75

Figure 3-6 A) The relationship between added LOV to the polymers/surfactants and drug loading amount in different polymeric/surfactants micelles, B) The LOV loading levels (% w/w) in different polymeric/ surfactant micelles and C) The relationship between added LOV to the polymers/surfactants and encapsulation efficiency (%) in different polymeric/surfactant micelles (mean ± SD, n=3). 76

Figure 3-7 The space within the liposomes; lipid bilayer and aqueous inner core for drug loading. Image modified from Narvekar *et al*. 78

Figure 3-8 Showing comparative % of drug loading for LMH system; the same mass of carrier material (polymers and lipids) in different preparation methods (mean ± SD, n = 3). 81

Figure 3-9 The size distribution after ultracentrifuge: pellets (B) and supernatant (A). 82

Figure 3-10 The size distribution of the nanocarriers; A) LMH, B) DSPG/PC liposomes and C) TPGS micelles respectively. 82

Figure 3-11 Cryo-TEM images of A) LMH and B) DSPG/PC liposomes (mean ± SD, n = 3). 83

Figure 3-12 Investigation of the LOV solubility in different percentages of PEG-400 (0.2, 0.5 and 10- 40 % w/v) in PBS solution to find the maximum solubility of LOV in PEG-400 (mean ± SD, n = 3). 84

Figure 3-13 LOV releases from A) micelles and LMH (blank lipid bilayer + loaded aqueous inner core), B) liposomes and LMH (loaded lipid bilayer + blank aqueous inner core) at 37 °C for 24 hours (inset graphs) and and up to 10 days with (PBS + PEG-400 (0.5%) dialysis bag (mean ± SD, n = 3). 85

Figure 3-14 Schematic presentation of different nanocarriers A) Micelles, B) LMH (blank lipid bilayer + loaded micelles in inner aqueous core), C) Liposome, D) LMH (loaded lipid bilayer + blank micelles in inner aqueous core). 87

Figure 3-15 LOV release from micelles, liposomes and LMH (lipid bilayer and aqueous inner core) in release media (PBS with 0.2% of tween 80) and 20 % ethanol (mean ± SD, n = 3). 88

Figure 3-16	Calculated diffusion coefficients (*D*) from eqution 3-2 for micelles, liposomes and LMH A) PEG-400 (0.5%) and B) Tween 80 + ethanol.	90
Figure 3-17	Effect of different hydration pH on LOV micelles.	92
Figure 3-18	Effect of different hydration pH on (A) particle size of liposomes and micelles and (B) zeta potential for DSPG/PC liposomes (mean ± SD, n =3).	93
Figure 3-19	Effect of different hydration pH on LOV liposomes.	95
Figure 3-20	The percentage of LOV content in A) liposomes and B) micelles with i) 1 mM NaCl (ionic strength) and ii) 1 mM NaCl + different hydration pH over 3 months (mean ± SD, n = 3).	96
Figure 3-21	(A) The size distribution and (B) zeta potential of LMH after 3 months kept in the freezer (4°C) (mean ± SD, n = 3).	97
Figure 4-1	Schematic representation of Caco-2 cell monolayer (CCM) cultured on permeable supports to trace the permeability of the LMH in two directions, from the apical to the basolateral (A-B) side or basolateral to apical (B-A).	100
Figure 4-2	Schematic representation of routes and mechanisms of drug transport across the intestinal epithelium: (1) passive transcellular route, (2) passive paracellular route, (3) carrier-mediated transport, (4) carrier-mediated efflux, and (5) vesicular transport. Modified from Shah *et al*.	103
Figure 4-3	Caco-2 cell viability as a function of various levels of LOV-LMH inclusion. Viability determined after 48 hours of treatment by Alamar blue assay. Data presented as the mean ± SD (n = 4) from two individual experiments in quadruplicate. **control without the drug.	111
Figure 4-4	The resistance of Caco-2 Cell monolayers (CCM) measured on the 14th day and 21st day (2 days) of monolayer formation in DMEM control media. The data are presented as mean ± SD (n = 4).	112
Figure 4-5	Effect of 100 µM LOV encapsulated in micelles, liposomes, LMH and free LOV on the TEER in Caco-2 cell monolayers (21 days old) in HBSS over 2 hours of the treatment period. Control without treatment (Cells with buffer and buffer only). The data are presented as mean ± SD (n = 4).	113
Figure 4-6	A) The A→B and B→A fluxes of LOV and LOV loaded nanocarriers (100 µM) were determined at pH 7.4 as a function of time (2 hours at 37°C) and B) Transepithelial efflux of LOV across CCM. Each point represents the mean (4 S.E.M.) of 4 determinations (CCM).	114
Figure 4-7	Model for the proposed LOV transport, Left) blocking the apical transporter reduces LOV, A→B transport, reduced LOV transport,	115

Right) LOV is taken up by a basolateral transporter from the basolateral membrane and excreted by apical efflux transporters at the apical membrane; Image modified from Li *et al.*

Figure 4-8 Percent permeability of LY (100 µM) from A→B; added to the apical chamber of CCM treated with 100 µM LOV and 100 µM LOV incorporated into each nanocarrier; micelles, liposomes, and LMH; were incubated for 1-hour with 100 µM LY. After 1-hour samples were collected from the basal chamber. Here the control was only the cells. LY was measured by fluorescence intensity at excitation and emission wavelengths of 485 and 520 nm, respectively. Results are means ± SD (n = 4). 118

Figure 4-9 LOV transported across Caco-2 monolayers after 8 hours of incubation in the A→B direction at 37 °C in the presence of micelles, liposomes and LMH containing 100 µM of LOV and LOV 100 µM, expressed as a percentage of the initial concentration of 100 µM LOV, added to the apical compartment, as a function of time, mean ± SD (n=4). 120

Figure 4-10 Scheme of different possible transport ways of LOV and nanocarriers: micelles, liposome and LMH (1) degradation of nanocarriers and release of LOV(2) Inhibition of LOV absorption by the effect of the multidrug efflux transporter P-gp in the apical membrane of intestinal epithelium cells (3) The hypothetical paracellular way of transport of LOV (4) Other P-gp independent transport way of nanocarriers micelles, liposome and LMH. Modified image from Mo *et al*. 121

Figure 4-11 Caco-2 cell uptake of LOV and LOV loaded nanocarriers (all containing 100 µM LOV. The average particle diameter of the nanocarriers, micelles, liposome, and LMH are 12.96 94.27 and 149.65 nm. respectively shown above the standard deviation bars (reported in Chapter 3) 122

Figure 4-12 Model for the proposed LOV, A→B transport across Caco-2 cell monolayers. A) LOV is taken up by an apical transporter from the apical membrane and excreted by basolateral efflux transporters at the basolateral membrane; B) blocking the apical transporter reduces LOV, A→B transport, reduced LOV transport C) blocking the basolateral efflux transporter reduces LOV, A→B transport but increases its intracellular accumulation. Image modified from Li *et al.* 123

Figure 5-1 Schematic presentation of PTX encapsulated thermoresponsive liposome-micelles-LMH system (PTX-TS-LMH) 127

Figure 5-2 Schematic presentation of the thermoresponsive PTX-5FU encapsulated liposome- micelles-hybrid system (PTX-5FU-TS-LMH). 127

Figure 5-3 Schematically representation of Caco-2 cell monolayer (CCM) cultured on a permeable supports to monitor the permeability of the LMH in two directions, from the apical to the basolateral (A-B) side or 128

basolateral to apical (B-A).

Figure 5-4 Particle size distributions of nanocarriers (mean ± SD, n=3). 146

Figure 5-5 A) The relationship between added drug to the polymers/lipids and drug loading amount in different carriers and B) Average drug loading in different nanocarriers (mean ± SD, n=3). 147

Figure 5-6 The average drug loading in LMH with different drugs, (mean ± SD, n=3). 148

Figure 5-7 Representative transmission electron microscope image of TPGS micelles: A) low resolution view showing uniform distribution and B) a single micelle (10-15 nm in diameter). 149

Figure 5-8 Representative transmission electron microscope image of liposomes: A) low resolution view showing uniform distribution and B) a single liposome (< 200 nm). 150

Figure 5-9 Representative transmission electron microscope image of LMH: A) low resolution view showing uniform distribution and B) a single LMH < 200 nm (mean ± SD, n=3). 150

Figure 5-10 The release of PTX from TPGS micelles. Each data point represents the mean ± SD (n=3). 151

Figure 5-11 Schematic representation of drug-release mechanisms from polymer micelles. The drugs get released from the micellar core by two major pathways i.e. dissociation of the micelle followed by the separation of the drug from monomers and drug-polymer bond breakage within the micelle followed by diffusional escape from the delivery system. The image is adapted from Ahmad *et al*. 152

Figure 5-12 Schematic illustration of thermoresponsive polymeric micelle drug carrier system and drug release mechanism upon temperature increase. Image adapted from Nakayama *et al*. 153

Figure 5-13 PTX release from PTX liposomes determined at 37°C and 42°C, respectively for 48 hours in sink conditions (PBS + 0.5% PEG 400). Each data represents the mean ± SD (n=3). 154

Figure 5-14 Schematic presentation of the phase transition behavior of TSL. When the lipid membrane passes through the transition temperature, the bilayer permeability increases, while below that temperature, lipid membranes exist in solid phase only and therefore no drug release is expected. At the *Tm*, the existence of both the solid and the liquid phases leads to the formation of grain boundary defects in the bilayer through which drug release occurs. Image modified from Needham *et al*. 155

Figure 5-15	PTX release from LMH (PTX in micelles core) determined at 37 °C and 42 °C, respectively for 48 hours in sink condition (PBS + 0.5% PEG 400). Each data represents the mean ± SD (n=3).	156
Figure 5-16	Schematic diagrams of drug release barriers from different carriers; A) PTX from micelles' core, B) PTX from liposome bilayer and C) PTX from LMH (micelles' core only) drug not loaded in the bilayer.	157
Figure 5-17	The % release of A) PTX from liposome bilayer of PTX-5-FU-LMH for 24 hours (inset graph) and 192 hours, B) 5-FU from PTX-5-FU-LMH micelles for 24 hours (inset graph) and 192 hours at 37°C and 42°C in release media PBS + PEG-400 (0.5%) pH: 7.4). Each data represents the (mean ± SD, n = 3).	158
Figure 5-18	The release of 5-FU from micelles for 24 hours (inset graph) and 120 hours at 37°C and 42°C in release media (PBS + PEG-400 0.5% with pH 7.4). Each data represents the (mean ± SD, n = 3).	160
Figure 5-19	Calculated diffusion coefficient values (*D*) from **equation (5-10)** for PTX from A) micelles, liposomes, LMH inner micelles' core, and both LMH bilayer and inner micelles' core at 37ºC and B) inner micelles' core of LMH and both lipid bilayer and inner micelles' core of LMH at temperatures 37ºC and 42ºC.	162
Figure 5-20	Hela cells treatment of 96-well plate, A) initial image after Alamar blue treatment, B) image after 2 hours, and C) 4 hours.	163
Figure 5-21	The effect of (A) free PTX and PTX- micelles B) free PTX and PTX-liposome and C) free PTX and PTX-LMH on cells viability using HeLa cell lines after 4 hours of treatment (mean ± SD, n = 4), three different 96 well plates are cultured for different nanocarriers formulations separately with the control free paclitaxel. Statistical significance (P < 0.05) differences between free PTX and nanocarriers was 0.05 and between the nanocarriers was 0.04.	164
Figure 5-22	The resistance of Caco-2 Cell monolayers (CCM) measured on the 14th day and 21st day (2 days) of monolayer formation in DMEM control media. The data are presented as mean ± SD (*n* = 4).	165
Figure 5-23	Effect of 100 µM PTX encapsulated LMH, liposome, micelles and free PTX on the TEER in Caco-2 cell monolayers (21 days old) in HBSS over 2 hours of the treatment period. Control without treatment (Cells with buffer only). The data are presented as mean ± SD (*n* = 4).	166
Figure 5-24	The B→A fluxes of PTX and PTX loaded nanocarriers (100 µM) were determined at pH 7.4 as a function of time (2 hours at 37°C). Each point represents the mean (4 S.E.M.) of 4 determinations (CCM). The P*app* values, expressed in centimeters per second. The statistical analysis of data showed that the p-value (P < 0.05) among the free	168

PTX and nanocarriers was 4.1 X 10^{-12} which is statistical significance.

Figure 5-25 Percent permeability of LY (100 µM) from A→B; added to the apical chamber of CCM treated with 100 µM PTX and 100 µM PTX incorporated into each nanocarrier; micelles, liposomes, and LMH; were incubated for 1-hour with 100 µM LY. After 1-hour samples were collected from the basal chamber. Here the control was only the cells. LY was measured by fluorescence intensity at excitation and emission wavelengths of 485 and 520 nm, respectively. Results are means ± SD (n = 4). 170

Figure 5-26 PTX transported across Caco-2 monolayers after 24 hours of incubation in the A→B direction at 37°C in the presence of micelles, liposome, and LMH containing 100 µM of PTX and PTX 100 µM, expressed as a percentage of the initial concentration of 100 µM PTX, added to the apical compartment, as a function of time, mean ± SD (n=4). 171

List of Tables

Table No.	Description of Table	Page No.
Table 2-1	Physico-chemical properties of model drugs.	15
Table 3-1	Different poloxamer polymers with a different number of the block.	69
Table 3-2	Average particle diameter, PDI, zeta potential, the drug loading and encapsulation efficiency of LOV into different polymeric micelles, mean ± SD, (n = 3)	70
Table 3-3	Physical characterization of different liposomes (mean ± SD, n = 3)	77
Table 3-4	Physicochemical characterization of drug loaded LMH by different preparation methods (mean ± SD, n=3).	79
Table 3-5	The exponent value (n) used to characterise the drug release mechanism and the diffusion coefficient (*D*) for LOV, for their release from micelles-liposome and LMH (release media PEG-400, 0.5% and 0.2 % Tween 80 + ethanol). The exponent value (n) and the diffusion coefficient (*D*) was obtained by non-linear fitting (MATLAB) of the fractional drug (M_t/M_∞) release data to Equation 3-2 as a function of time over 48 h.	90
Table 3-6	The relationship between the diffusion exponent (*n*) and the solute (drug) release mechanism as proposed by Korsmeyer Peppas.	91
Table 3-7	Effect of different hydrations pH on size and PDI of TPGS micelles and DSPG/PC/CHO liposomes (mean ± SD, n = 3) 24 hours after preparation.	91
Table 3-8	data presented here of the size and zeta potential up to 3 months (mean ± SD, n = 3)	97
Table 4-1	The parameters determined from permeability assay of LOV through CCM using different carriers.	117
Table 4-2	The average diameter and zeta of LOV loaded nanocarriers.	123
Table 5-1	Average particle size, particle size distribution (PDI) and zeta potential of PTX loaded micelles, liposome, and LMH (mean ± SD, n = 3).	144

Table 5-2	Drug loading of PTX and 5-FU in individual carriers and LMH system (mean ± SD, n=3)	148
Table 5-3	Physiochemical properties of 5-FU and PTX.	149
Table 5-4	The exponent value (*n*) used to characterise the drug release mechanism and the diffusion coefficient (*D*) for PTX, for its release from micelles-liposome and LMH at temperatures 37ºC and 42ºC. The exponent value (*n*) and the diffusion coefficient (*D*) was obtained by non-linear fitting (MATLAB) of the fractional drug (M_t/M_∞) release data (**Figure 5-10, Figure 5-13, and Figure 5-15**) to **equation 5-9** as a function of time over 48 hours.	161
Table 5-5	The relationship between the diffusion exponent (*n*) and the solute (drug) release mechanism.	161
Table 5-6	The parameters determined from permeability assay of PTX through CCM using different carriers	169

Abbreviations

A	Area	MWCO	Molecular Weight Cut-Off
A-B	Apical to the Basolateral	M∞	The total amount of molecules that are kept in the matrix
ACN	Acetonitrile	MC	M Cells
ADME	Absorption, Distribution, Metabolism, and Excretion	MCF-7	Human Caucasian Breast Adenocarcinoma Cell Line
Al-Alg	Aluminium -Alginate	MDR	Multi Drug Resistance
ANOVA	Analysis of Variance	MPS	Mononuclear Phagocytic System
API	Active Pharmaceutical Ingredients	MRP	Multidrug Resistance-Associated Protein
ATV	Atorvastatin	MRP1	Multidrug Resistance-Associated Protein 1
AUC	Area Under The Curve	µg	Microgram
B-A	Basolateral to Apical	mL	Millilitre
Ba-Alg	Barium-Alginate	MLV	Multi Lamellar Vesicle
BCS	Biopharmaceutical Classification System	mV	Milli Volt
BL	Basal Lamina	NaCl	Sodium Chloride
BS	Bile Salt	NaOH	Sodium Hydroxide
CCM	Caco-2 Cell Monolayer	N-DMF	N, N-Di-Methyl-Formamide
$Ca^{2}+$	Calcium	N_{agg}	Aggregation Number
Ca-Alg	Calcium-Alginate	nm	Nanometer
Caco-2	Human Epithelial Colorectal Adenocarcinoma Cells	NSCL	Non-Small Cell Lung Cancer
CHO	Cholesterol	NP	Nanoparticle
C_o	Mass of compound initially in the donor compartment	NTSL	Non-Thermosensitive Liposome
CMC	Critical Micelle Concentration	n	Exponent Coefficient
Cryo-	Cryo-Transmission Electron	OEP	Octaethylporphine

TEM	Microscopy		
CPT	Camptothecin	*P*	Statistically Significant Difference
CYP3A4	Cytochrome P450 3A4	PALS	Phase Analysis Light Scattering
D	The Diffusion Coefficient	PCEC	Poly-(E-Caprolactone)-Poly(Ethylene-Glycol)-Poly(E-Caprolactone
DC	Deoxycholate	PDI	Polydispersity Index
DDS	Drug Delivery System	P*app*	Apparent Permeability
DEX-C_{16}	Dextran-Grafted-Polyoxyethylene Cetyl Ether	PBS	Phosphate Buffer Solution
DL	Drug Loading	PBLA	Poly-Beta-Benzyl L-Aspartate
DLS	Dynamic Light Scattering	PC	Phosphatidylcholine
dMr/dt	The rate of drug permeation across the cells	PDI	Polydispersity Index
DMEM	Dulbecco's Modified Eagle`S Medium	PCL	Polycaprolactone
DMSO	Dimethyl Sulfoxide	PE	Phosphatidylethanolamines
DMPC	1,2-Dimyristoyl-Sn-Glycero-3-Phosphorylcholine	PECL	Poly(Ethylene Glycol)-Poly(Ɛ-Caprolactone)
DNA	Deoxyribonucleic Acid	PEG	Polyethylene Glycol
DOX	Doxorubicin	PEG-PE	Polyethylene Glycol-Poly-Ethanolamine
DOPS	1,2-Dioleoyl-Sn-Glycero-3-Phospho-L-Serine (Sodium Salt).	PEI	Polyethylenimine
DTX	Docetaxel	PEO	Polyethylene Oxide
DTXSC	Docetaxel Succinate	P-gp	P-Glycoprotein
DPPC	Dipalmitoylphosphatidylcholine	pk_a	Acid Dissociation Constant
DSPE	1,2-Distearoyl-Sn-Glycero-3-Phosphoethanolamine	PLGA	Poly Lactic-Co-Glycolic Acid
DPPG	Dipalmitoyl-*Sn*-Glycero-3-Phosphorylglycerol	PLA/PEG-PPG-	Poly(DL-Lactic Acid) / Poly (Ethylene Glycol)-Block-Poly (Propylene Glycol)-Block-Poly

		PEG	(Ethylene Glycol) Copolymer
DSPC	1,2-Distearoyl-Sn-Glycero-3-Phosphocholine	P-407	Poloxamer 407
DSPG-Na	1,2-Distearoyl-Sn-Glycero-3-Phospho-1'-Rac-Glycerol Sodium-Salt	P-188	Poloxamer 188
DSTAP	1, 2-Distearoyl-3-Trimethylammonium-Propane	P-123	Pluronic P-123
EC	Enterocytes	F-68	Pluronic F- 68
EDTA	Ethylene Diamine Tetraacetic Acid	POPC	1-Palmitoyl-2-Oleoyl-Sn-Glycero-3-Phosphocholine
EE	Encapsulation Efficiency	PPO	Polypropylene Oxide
EPR	Enhanced Permeability and Retention Effect	PS	Phosphatidylserines
ER	Efflux Ratio	PTX	Paclitaxel
FAE	Follicle-Associated Epithelia	PTX-LMH	Paclitaxel Liposome-Micelles-Hybrid
FBS	Fetal Bovine Serum	PTX-PTX LMH	Paclitaxel -Paclitaxel-Liposome-Micelles-Hybrid
FT	Freezing Thawing	PTX-5FU LMH	Paclitaxel -5fluorouracil-Liposome-Micelles-Hybrid
5-FU	5-Fluorouracil	PWSD	Poorly Water-Soluble Drugs
GIT	Gastrointestinal Tract	PTX-TS-LMH	Paclitaxel Thermosensitive Liposome-Micelles-Hybrid
λ	Thickness of nanocarriers	PTX-5FU TS-LMH	Paclitaxel-5fluorouracil Thermosensitive Liposome-Micelles-Hybrid
GM1	Mono Sialoganglioside	R	Resistance
h	Hours	Rb	Blank Resistance
HBSS	Transport Buffer Hank's Balanced Salt Solution	RES	Reticuloendothelial System
HCT-116	Human Colon Carcinoma Cell Line	RI	Refractive Index

HeLa	Human Cervical Adenocarcinoma	RPE	Reverse Phase Evaporation
HMG-CoA	Hydroxymethyl Glutaryl Coenzyme A Reductase	SA	Stearyl Amine
HEPES	4-(2-Hydroxyethyl)-1-Piperazineethanesulfonic Acid	SC	Stearyl Chitosan
HLB	Hydrophilic-Lipophilic Balance	SD	Standard Deviation
HPC-C16	Hydroxy Propyl Cellulose-Grafted-Polyoxyethylene Cetyl Ether	SDC	Sodium Deoxycholate (3α,12α-Dihydroxy-5β-Cholanic Acid Sodium Salt)
HPLC	High-Performance Liquid Chromatography	SMV	Simvastatin
IR	Immediate Release	SPC	Soy Phosphatidylcholine
K	Kinetic/Constant	S-SC	Sulfated Stearyl Chitosan
Kpcs	Kiloparsecs	SUV	Small Unilamellar Vesicles
LC	Lymphocytes	Tc	Gel-Liquid Crystalline Transition Temperature
LE	Loading Efficiency	TEER	Transepithelial Electric Resistance
LY	Lucifer Yellow	TEM	Transmission Electron Microscope
LMH	Liposome-Micelle-Hybrid	TFH	Thin Film Evaporation
LOV	Lovastatin	TFF	Tangential Flow Filtration
Log P	Partition Co-Efficient	TJs	Tight Junctions
LOQ	Limit Of Quantification	Tm	Transition Temperature
LP	Possible Translocation Routes For Liposomes	TSLs	Thermosensitive Liposomes
LUVs	Large Unilamellar Vesicles	TPGS	d-α -Tocopherol Polyethylene Glycol 1000 Succinate
MATLAB	Matrix Laboratory	TS-LMH	Thermosensitive Liposome-Micelles-Hybrid
MDR	Multidrug-Resistant	TSH-PTX	Temperature-Sensitive Hybrid Loading Paclitaxel

MP	Macrophages	UV	Ultraviolet
MSPC	1-Myristoyl-2-Stearoyl-*Sn*-Glycero-3-Phosphocholine	USP-NF	United States Pharmacopoeia And National Formulary
MRT	Multidrug-Resistant Tumors	US FDA	U.S. Food And Drug Administration
Mt	The total amount of molecules released during the measurement	*We*	The amount of the entrapped drug in the nanocarriers
mTPP	Meso-Tetraphenyl Porphine	*Wi*	The initial drug concentration.
MU	Mucus	WHO	World Health Organization
mV	Milli Volt	*Wnp*	The total weight of nanocarriers.
MW	Molecular Weight	Z-average	Average Particle Diameter

Abstract

Poor aqueous solubility has been identified as a key obstacle to the formulation development of pharmaceutical dosage forms and for selecting the route of administration for many drugs. The aim of this thesis is to describe the fabrication and characterisation of novel hybrid nanoparticle systems based on micelles and liposomes for establishing better loading and release properties of water-insoluble drug molecules and to mitigate the challenges associated with low solubility. The study also includes the manipulation of these hybrid nanoparticle systems to confer efficient stimuli (temperature)-sensitive drug release of chemotherapy drugs, for potential application in targeted cancer therapy. The cellular activity of these hybrid nanoparticles is also explored to better assimilate their potential for therapeutic application.

Firstly, a novel liposome-micelle-hybrid (LMH) system was developed based on liposomes (phosphatidylcholine (PC), cholesterol and distearoyl phosphatidyl glycerol-Na (DSPG)) and micelles (Vitamin E, d-α-tocopherol polyethylene glycol 1000 succinate (TPGS). Physical characterisation of all drug-free and drug-loaded TPGS micelles, liposomes (DSPG-PC-CHOL) and LMH (TPGS-DSPG-PC-CHOL) were performed using the poorly soluble cardiovascular drug lovastatin (LOV). The nano/microscopic structure of LMH was elucidated using cryo-transmission electron microscopy (Cryo-TEM) and showed unilamellar spherical vesicles with an average diameter < 200 nm, with worm-like spherical-shaped branched micelles scattered within the interior aqueous core. The zeta potential (ζ) of the LMH was a high negative value (- 46.3 ± 1.93 mV) and offered better colloidal stability with monodisperse particle size distribution (PDI < 0.3). When LOV was encapsulated in the LMH system, its equilibrium solubility in water was 665 µg/ml, i.e. 166-fold higher than for pure LOV (4µg/ml). Furthermore, its solubility was 50 or 125-fold higher than when encapsulated in micelles or liposomes alone, indicating that synergistic loading was achieved in LMH. Under simulated intestinal conditions, LOV showed extended /controlled release behaviour from LMH nanoparticles, i.e. 70% drug release over 12 days compared to 90% release from individual micelles and liposomes over 10 and 3 days, respectively. Moreover, physical stability of micelles and liposomes were monitored upon storage at 4 °C for up to 3 months at different pH and drug levels and showed no significant changes in size and zeta potential. The size and zeta potential of the LMH also showed no significant changes for that

period. Therefore, the LMH system provides enhanced water solubility of LOV, extended release kinetics, and improved storage stability.

Secondly, the cellular activity of LOV encapsulated in LMH was investigated in a Caco-2 cell monolayer (CCM) *in vitro* model of the intestine. The LMH system was biocompatible with the Caco-2 cell line model and enhanced cellular permeability was evident. The apparent permeability *(Papp)* of LOV increased by 2.95-fold, 2.90-fold, and 1.84-fold for LMH, liposomes, and micelles, respectively. This confirms that LMH and liposomes are more rapidly and effectively absorbed by intestinal epithelial cells than micelles. The permeability enhancement by LMH is considered paracellular. It is suggested that specific P-Glycoprotein (P-gp) transporters on the apical side help nanocarrier transport from the apical to the basolateral membrane. The observed transport kinetics was biphasic with respect to the incubation time: slow for first 2 hours followed by an enhanced increase in transport around 8 hours for the LOV-nanocarriers and including free LOV. This may be due to the saturation of the P-gp by the nanocarriers and LOV initially (first 2 hours) and then the LOV transport starts to increase gradually with rest of the time. The LMH exhibits significant enhancement of LOV transport, i.e. approximately 2-fold compared to free LOV. Therefore, the LMH system provides further promise as an oral delivery approach for enhancing the oral bioavailability of the poorly water-soluble drug LOV.

Finally, a temperature sensitive liposome-micelle-hybrid (TS-LMH) system was developed for the poorly soluble chemotherapy drugs paclitaxel (PTX) and 5-Fluorouracil (5-FU). This was achieved by adding dipalmitoyl-sn-glycero-3-phosphorylglycerol (DPPG, which has a phase transition at 41.5°C) and polyethylene glycol (PEG) 1500 in DSPG-PC-CHOL liposomes to facilitate thermoresponsive drug release characteristics at the targeted site (hyperthermia). The average particle diameter (< 200 nm), PDI and zeta potential for PTX free and loaded carriers were equivalent. The microscopic structure (determined using TEM) of the TS-LMH was observed to be roughly spherical in shape with hair-like projections on the surface (PEG coating around the LMH). The drug loading of PTX and 5-FU in LMH were 47.33 and 2.91- fold (drugs loaded only in micelles core of the LMH) higher than in their general state. It was also notable that the solubility of PTX was increased 73.40 and 157.33 fold for micelles and liposomes. This is also applicable for 5-FU in micelles (3.2 fold). Most importantly, the LMH and other nanocarriers exhibit thermoresponsive release characteristics at an elevated temperature (i.e. 5-20% greater than body temperature). The

integration of liposomes and micelles augmented the loading and influenced the control release profile by tuning their thermoresponsive behaviour.

The chemotherapeutic effects of PTX-encapsulated LMH, liposomes and micelles were evaluated in human cervical adenocarcinoma (HeLa) cells and the LMH formulation exhibited greater toxicity compared to liposomes and micelles. The Caco-2 monolayer permeability of PTX was enhanced 2.6-fold, 2.4-fold and 2.13-fold for LMH, liposomes, and micelles respectively. Correspondingly, a more significant reduction of the TEER values was evident for the LMH than liposomes and micelles. The LMH, liposomes, and micelles were considered able to open the tight junction of the Caco-2 cells. Additionally, the reduced TEER value for TS-LMH compared to the LMH is likely due to the presence of the PEG/DPPG. The transport of LMH was 1.12 times higher than free PTX. It was also observed that transport of PEGylated TS-LMH occurred in a controlled manner in comparison to biphasic trend of the previous LMH system.

The work present in this thesis has addressed some of the current challenges of poorly soluble drug delivery by improving the loading, controlling release and further exploring the cellular activity. A significant outcome is achieved in this research by designing the LMH which shows promising potential as an advanced drug delivery system, which should now advance to *in vivo* studies prior to potential translation into the clinic.

Thesis Outline

Chapter No.	Chapter Title	Keywords
1	Introduction	Project scope and significance, aims of the research project, model drugs used in the research
2	Literature Review	Oral drug delivery: background and challenge, poorly water soluble drugs, liposome-micelles based drug delivery system, temperature-sensitive carrier, chemotherapy, liposome-micelles-hybrid system (LMH)
3	Liposome-Micelles-Hybrid Nanoparticles for Oral Delivery of Poorly Water-Soluble Drugs	Formulation, different methods, drug loading, characterization, drug release, stability.
4	Evaluation of a Liposome-Micelle Hybrid System to Improve the Intestinal Transport of Lovastatin using Caco-2 Cell Monolayers	Cell viability, permeability, TEER, apparent permeability, efflux ratio, transportation, cellular accumulation.
5	Development of a Temperature-Sensitive Liposome-Micelle-Hybrid (TS-LMH) System for Enhanced Anticancer Activity	Formulation, different methods, drug loading, characterization, drug release, stability, cell viability, permeability, TEER, apparent permeability, efflux ratio, transportation, cellular accumulation.
6	Conclusion and Future Direction	Thesis conclusion and future directions
7	Reference	References

Publication

Romana, B. Batger, M. Prestidge, C. A. Colombo, G. Sonvico, F. *Expanding the Therapeutic Potential of Statins by Means of Nanotechnology Enabled Drug Delivery Systems*, Current Topics in Medicinal Chemistry 2014, 14(9): p1182-1193

Conference Presentation

Australian Centre of Nanomedicine (ACN) and ARC Centre of Excellence in Convergent Bio-Nano Science and Technology

1. *Sydney International Nanomedicine Conference 30th June-2nd July 2014*, Sydney Australia.
2. "Hybrid nanovectors for oral delivery of poorly water-soluble drugs", Bilquis Romana, Alexander F. Mason, Pall Thordarson, Fabio Sonvico, Clive A Prestidge, *Sydney International Nanomedicine Conference.6-8th July 2015*, Sydney Australia.
3. *Sydney International Nanomedicine Conference, 27-29th July 2016*, Sydney Australia.

Controlled release society (CRS)

1. *Drug Delivery Australia*-Australian Chapter of the Controlled Release Society, 2012, Melbourne, Australia.
2. *Drug Delivery Australia*-Australian Chapter of the Controlled Release Society, 2013, Sydney, Australia.
3. "Hybrid nanovector for oral delivery of Poorly Water-Soluble Statin Drugs'' International Conference on Nanoscience and Nanotechnology 2014, Adelaide, Australia.
4. "Development of Hybrid Nanovector for Insoluble Drugs Delivery'' Bilquis Romana, Clive A Prestidge, Fabio Sonvico, Pall Thordarson. *Drug Delivery Australia*-Australian Chapter of the Controlled Release Society, University of New South Wales, Sydney, Australia, and 27-28th October 2016. (Poster presentation)**.**

Acknowledgments

This thesis is the great achievement of my career and brings the pride of my family and relatives, friends and whose inspiration, help and continuous support over the past four years have been made it possible.

First of all, I would like to sincerely thank my principle Ph.D. supervisor, Professor Clive Prestidge who from beginning to the end, enormously helpful, kind support and guide me to start, run and accomplish the project. His passion, insight and keen attention to details has helped to sustain me throughout this life-changing experience and I know I could not have asked for a better supervisor. I am grateful for all the help and support provided throughout my research program: time, knowledge, encouragement, motivation, advice and believing in me. I have no words to describe my appreciation for Clive's fantastic supervision from the first day of my Ph.D. project. I am greatly indebted to Clive for his contribution to the success of my Ph.D.

My gratitude goes to Senior Lecturer Kristen Bremmell, for her tremendous feedback during my thesis writing. I should appreciate her patient for consistently giving me suggestions to write my thesis in an organised way. I am thankful for her continuous response to improve my writing, to give the thesis a good shape and make it submittable.

I am also grateful to Senior Lecturer Timothy Barnes, for his incredible support for writing my thesis in systematically. His guidance and supervision helped me to describe a logical explanation of my results and improve my attention details. I am also thankful for his direct communication at the starting the thesis writing.

I wish to thank Dr. Angel Tan and Dr. Shasha Rao helping in the laboratory work and understanding the project at the beginning of my research work and My gratitude goes to all of my lab mates; Achal Bharatkumar, Vaskor Bala, Jin Jau, Rokhsana Yasmin, Tahnee Jade, and Paul Matthew.

My special thanks to Dr. Fabio Sonvico, from University of Technology Sydney (UTS), a graduate school of health (Pharmacy), who helped me to continue my Ph.D. in his lab. He did guide me to keep tracking of my project. I am also grateful to Dr. Samira Ali, Dr. Michele Pozzoli, and Dr. Gabriela Garrastazu for their support and help in the lab.

My appreciation and gratitude to Professor Pall Thordarson, from University of New South Wales, School of Chemistry, for a greater contribution to this work, especially additional work, Cryo-TEM, TEM, Cell biology experiments. Without his involvement, a big proportion of this work would not be possible. Thanks to Dr. Celine Heu from the Children's Cancer Institute Australia and BMIF for providing the cell lines, expertise and the inspiration for the cell studies of my project. My special thanks to Professor. Fazlul Huq, from the University of Sydney, for kindly donating Caco-2 cell line in the most critical time that helped me to accomplish the cell work project for my Ph.D. I also add my thank to Pall Thordarson group; Jonathan Wojciechowski, Andrew B Robinson, Genevieve Duche, Alex Mason, Alistair Laos and Chin Ken Wong for helping me in the lab experience. Thanks to Dr. Adam Martin, who helped me to write my thesis initially. Special thanks to Md. Musfizur Hassan of this group who helped me in some after hour works. I am fortunate to have the chance to work with this fantastic group. Thank you to Svetislav Videnovic for helping in HPLC and LCMS and gave me his full support when required. Thanks to the academic and staff members of the school of Chemistry who have helped in various ways; Dr. Toby Jackson, Ken McGuffin, and Jodee Anning for administrative matters; and Ian Aldred from the Chemistry Store.

I am very proud and grateful for the opportunity to start my Ph.D. at the Future Industry Institute (former Ian Wark Research Institute) University of South Australia. I am indebted to IWRI for financial support by means of a Top-up Scholarship and conference support during the last three and half years. I would also like to show my appreciation to all the staff at the Ian Wark Institute and School of Pharmacy and Medical Sciences for providing me with the necessary training and administrative support. Special thanks go to Louise Jennings, Andrew Robinson, Dr. Scott Abbott, Philip Moore and Vicky Foreman for their constant support provided to the students of the aforementioned institutes. A big thanks to Monica Behrend and Judy Ford, for the fantastic job in conducting the Writer's Circle workshops, which helped me to write the research proposal.

I am grateful to Australian Government for APA for my scholarship and financial support of this work. I would also like to thank my supervisors who helped me to present my work at the DDA and Nanomedicine conference in Melbourne, Adelaide and Sydney.

My deepest thanks go to my beloved parents; Shaikh Auboyedullah (father) and Mrs. Tahmina Khatun (mother), and siblings; Shamima Arju, Asma Dilruba, Talat Shahnaj, Arif

Ahsanullah and Ishrat Nimmi for their unconditional love and support from my childhood and until now. Thanks to my elder sisters, Asma Dilruba and Talat Shahnaj for teaching me the importance of education at an early age and taking care of it. I love them so much. Specially, I would like to thanks, Ishrat Nimni (my twin sister) and Md Mahabubul Haque (brother in law).

Last but not least, I would like to thank my beloved husband, Dr. Md. Musfizur Hassan, lovely daughter Ruhama Musfiz and cute son Bilhann Musfiz. The fundamental inspiration arises in my life in contact with my husband. He gives me a beautiful family life that I never forget. He is my all-time inspiration guardians in my life for inspiration and suggests me in the different stage of my life and Ph.D. I'm really owed to them as they accepted a huge pain and negligence throughout my Ph.D. time. I'm really sorry to them that I didn't able to pay much attention and time to them as they disserved. Special thanks to Dr. Md. Musfizur Hassan as through the Ph.D. period, he cared for the whole family, sometimes take responsibilities for new baby Bilhann while I needed. Despite all, the love and support you have given me helped to shape the person I am today.

Author's Statement of Originality

This thesis presents work carried out by myself and does not incorporate without acknowledgment any material previously submitted for a degree or diploma in any university; to the best of my knowledge it does not contain any materials previously published or written by another person except where due reference is made in the text; and all substantive contributions by others to the work presented, including jointly authored publications, are clearly acknowledged. The work described in this Thesis was performed in The University of South Australia (UniSA), The University of Technology, Sydney, (UTS), School of Chemistry at the University of New South Wales (UNSW) and University of Sydney (USYD). All results discussed herein are my own work except where specific reference to the work of others is made in the text.

Bilquis Romana 06/04/2018

[Signature] [date]

Chapter One

1. Introduction

1.1. Project scope and significance

Poor aqueous solubility has been identified as a key obstacle to the development and clinical application of many drugs, including anticancer compounds. The low solubility profile of a drug molecule is one of the most common challenges for the development of pharmaceutical dosage forms to deliver their site of action in the body.[1-3] More than 40% of compounds identified through combinatorial screening programs are discarded due to solubility problems in phase III pre-clinical studies; this is a significant cost to the pharmaceutical industry.[4-6] Most of the side effects of existing anticancer drug formulations are due to low solubility related issues, e.g. the use of high concentrations of co-solvents and/or surfactants required for drug solubilisation is responsible for adverse side effects.[7] In addition, oral delivery of poorly water-soluble drugs is not suitable because they have a tendency to distribute and accumulate in the peripheral tissues.

Oral administration of drugs is considered highly desirable in terms of both obtaining therapeutic effects as well as maximising patient compliance. However, for drug absorption to occur upon oral administration, the drug molecules must be dissolved in the gastrointestinal (GI) fluids. In the case of poorly soluble drugs, the dissolution rate is significantly slower than the absorption rate, thus making dissolution the rate-limiting step in the absorption process. Other barriers to the oral delivery of poorly soluble drugs include; issues with drug stability during transit through the low-pH environment of the stomach, as well as pre-absorption or pre-hepatic metabolism of drug molecules in the enterocytes, and impact of digestive enzymes. Some additional factors that are encountered by oral dosage forms include GI motility, mucus barriers, high metabolic activity and low relative permeability of the epithelium.[8-9]

A variety of formulation approaches are available to facilitate the oral delivery of poorly soluble drugs, which can be broadly defined as either chemical or physical methods. Chemical methods include the use of salts (although this requires the compound to be acidic/basic) and the preparation of pro-drugs. Similarly, a variety of physical methods are

available, including reducing particle size (e.g. nano suspensions),[10] modification of the crystal structure (e.g. polymorphs, co-crystals),[11] solid solutions (e.g. nano dispersions,[12-13] nanoparticles,[14] nanospheres,[15] nanocapsules,[10]) as well as the preparation of more complex nanostructured systems to encapsulate the drug. Nanostructured drug carriers have been prepared from a variety of materials, such as inorganics (e.g. mesoporous silica,[16-17] graphene[18-19]), polymers[20-22] (e.g. Poly Lactic-co-Glycolic Acid (PLGA),[23] d-α -tocopherol polyethylene glycol 1000 succinate (TPGS),[24]) as well as lipid-based systems (e.g. liposomes,[25-26] solid lipid nanoparticles,[27-28] emulsions and nano-emulsions[29]). There is ongoing interest in the use of nanostructured systems for oral drug delivery, as they both protect the encapsulated drug from degradation within the GI tract, as well as offering the potential for targeting of the therapeutic by attaching specific ligands to the carrier surface.[30-34]

Liposomes and micelles offer numerous advantages in the area of pharmaceutical drug delivery, e.g. for improving bioavailability by accumulating at the site of action as well as through improving solubility of the poorly water-soluble drugs over the range from 1.5- 29 fold higher compared to the parent drug.[20-21, 25] These liposomes and micelles also offer "stimuli-sensitive" drug delivery of chemotherapeutic drugs.[35-38] Such a stimulus-sensitive nanocarrier are expected to release their contents in targeted tissues or cell compartments and greatly increase the drug's efficacy to the targeted site when exposed to a certain internal stimulus such as elevated temperature arise in mild hyperthermia (defined as 39–43 °C).[39-40,38,41-42] They deliver drugs to minimise the toxicity as well as the dose-limiting side effects by increasing the control of drug delivery to the diseased tissues while reducing harmful interactions with healthy tissues by increasing the solubility of the drug through physical encapsulation in these nanocarriers.[43-49]

The incorporation of PEG or "PEGylation" is a commonly used approach for improving the efficiency of drug release control to target cells and tissues[13,14] by increasing the circulation time of an entrapped drug at a hyperthermic site *in vivo* along with thermosensitive liposome.[50] Most of the early examples of TSL systems were composed mainly of Dipalmitoylphosphatidylcholine (DPPC) or Dipalmitoyl-*sn*-glycero-3-phosphorylglycerol (DPPG) lipids mixed with other types of lipids like DSPC and HSPC lipids to tune the phase transition temperature (T_m) and the rate of drug release.[43, 51-54] There is a significant amount of research being performed in the field of liposomes and micelles include thermally sensitive

polymers into delivery systems, which have been reviewed thoroughly, however, challenges still exist there.[36, 55-57]

It is hypothesized that the combination of liposomes and micelles will increase drug loading, improve release profiles, result in greater bioavailability and offer an oral dosage form for many insoluble drug molecules. The liposome-micelle-hybrid (LMH) **(Figure 1-1)** may provide additional advantages over the liposomes and micelles alone; e.g. improve the solubility and control the drug release profile compared to the individual micelles or liposomes. A similar type of research is introduced recently naming of hybrid drug-in-micelles-in-liposome system.[58 59]

Different types of hybrids of liposomes and nanoparticles are available as drug delivery systems, some examples of the hybrid are: liposomal hybrid nanoparticle containing antibody and quantum dot functionalities (QD-immuno liposomes),[60] hybrid elastin-like polypeptide (ELP)/ liposome nanoparticles,[61] and exosome–Liposome Hybrid Nanoparticles.[62] There are several benefits of using micelles-liposomes hybrid over the unique strengths of polymeric NPs and liposomes in improving oral bioavailability. The hybrid NPs can be a robust drug delivery platform with high drug encapsulation yield, tunable and sustained drug release profile, excellent serum stability and potential for differential targeting of cells or tissues, GI stability, improved absorption and bioavailability as reported in literature.[58 59]

The hybrid will be composed of two distinct compartments: (i) an aqueous hydrophilic core, where drug-loaded polymeric micelles can be encapsulated, and (ii) a lipid bilayer at the interface of the core that acts as a molecular fence to promote drug retention inside the polymeric core, thereby potentially enhancing drug encapsulation efficiency. These two compartments together will increase the drug loading and also control the drug release. The core-shell structure will facilitate double benefits; one is encapsulating the drug-loaded micelles in the core, while the outer shell or the lipid bilayer of the hybrid will protect the encapsulated drug from inactivation in biological media, such as the gastrointestinal fluid.

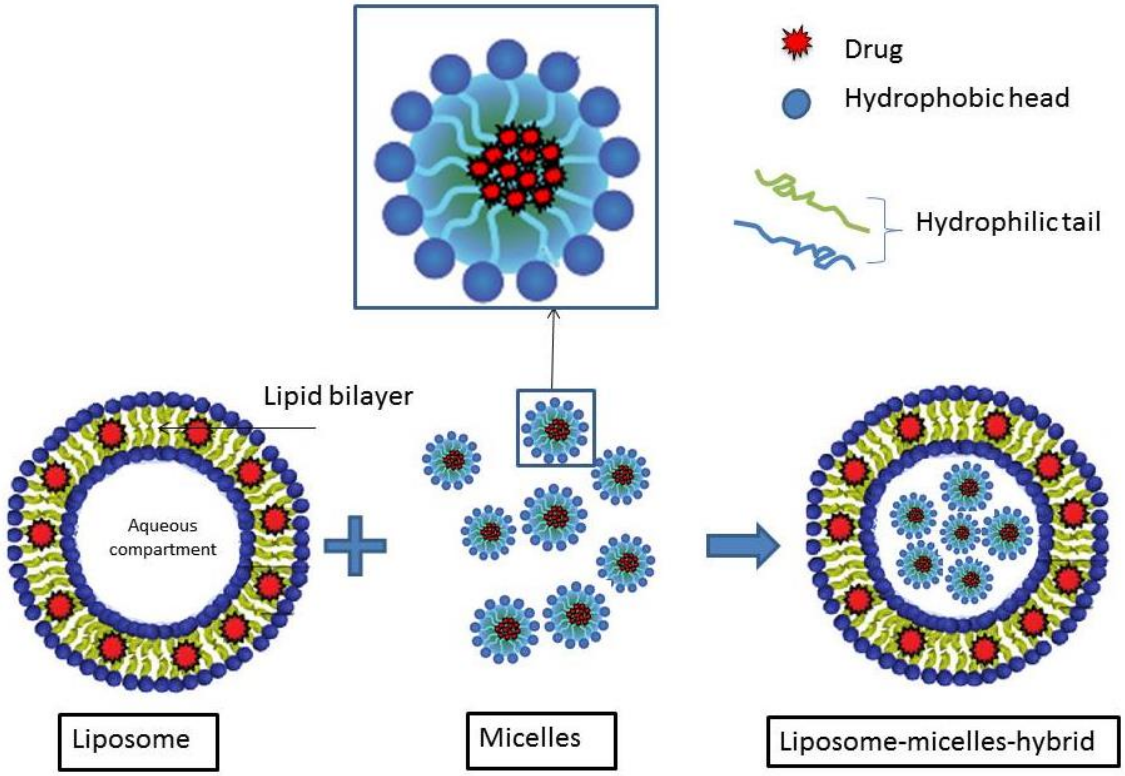


Figure 1-1: Schematic representation of a liposome (>100 nm), micelles (< 50 nm) and a liposome-micelle hybrid (LMH) as drug delivery systems for a poorly water-soluble drug.

Moreover, incorporation of drug-containing micelles into LMH may improve the colloidal stability of the encapsulated drug.[63-65] In addition, the LMH may enhance the cellular activity, as well as increase cellular permeability and transport compared to the drug alone or drug-containing micelles, due to encapsulation into the lipid bilayer structure of the liposome-based drug delivery system.[66-70] Additionally PEGylation into liposome may improve the efficiency of drug release to target cells and tissues in hyperthermia.[41-42, 50] Furthermore, a thermosensitive liposome-micelles-hybrid (TS-LMH) may be developed to tune the rate of drug release exploring phase transition temperature (T_m) of lipids (commonly used for liposome preparation).[43, 51-54]

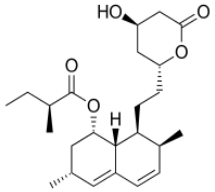
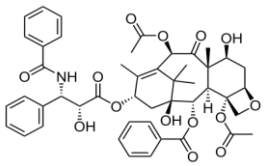
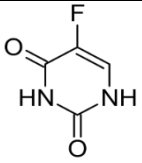
A series of model poorly water-soluble drugs have been selected for use in this research project, that is lovastatin (LOV), paclitaxel (PTX) and 5-fluorouracil (5-FU). These drugs represent three different drug classes which possess different physicochemical properties while presenting distinct challenges with respect to their oral delivery. As in this research, we focused on oral delivery of the selected drugs. Yet, for PTX, the parenteral infusion is the

only administration route used in the clinic. However several studies have demonstrated enhanced bioavailability as well as enhances the drug therapeutic efficacy of PTX facilitated by liposome formulations.[71] The development of an oral dosage form is impeded by their toxicity to rapid-proliferating intestinal epithelium. A great deal of effort is still needed to minimize the drug-associated GI toxicity as well as carrier-associated toxicity before oral PTX administration becomes practicable.

In this study, we assess the influence of various physicochemical properties (e.g. lipophilicity, molecular weight, diameter and geometry) of these model drugs **(Table 1-1)** to undertake an extensive evaluation of drug delivery vectors of the proposed liposome-micelle-hybrid system using a range of *in vitro* biophysical assessment tools, including drug analysis (HPLC), diameter and zeta potential (Zetasizer), transmission electron microscopy (TEM), cryo-transmission electron microscopy (Cryo-TEM). This research offers new potential formulation strategies for many poorly water-soluble drugs with problematic oral absorption challenges like solubility and cell permeability.

The physicochemical properties of the model drugs are shown in **Table 1-1**

Table 1-1: Physico-chemical properties of model drugs used in this study.[72-74]

Properties	**Lovastatin**	**Paclitaxel**	**5-Fluorouracil**
Chemical structure			
Molecular weight (g/mole)	404.54	853.91	130.08
Chemical Formula	$C_{24}H_{36}O_5$	$C_{47}H_{51}NO_{14}$	$C_4H_3FN_{2O2}$
Drug class	Cardiovascular	Anti-cancer	Anti-cancer
Aqueous solubility (pH 7.0)	0.4 mg/L	Insoluble	< 12 mg/mL at 66° F
Log P	4.26	3.96	-0.89
pKa	14.9	10.9	8.02
Melting point	174.5 °C	213 °C	282°C (decompose)

1.2. Aims of the research project

The overall aim of this research is to develop a LMH system for drug LOV and a thermoresponsive LMH (TS-LMH) system for drugs PTX and 5-FU to improve their solubility. The study also includes the cellular activities of both types LMH. Thus the research will focus to address problems associated with (i) low drug loading efficiency of liposomes, (ii) colloidal stability, (iii) release kinetics (iv) delivery efficiency by stimuli-response vi) lack of control release rate (vii) low permeability into cellular environment and (viii) low cellular uptake that rely on oral administration.

Chapter 3 is focused on the design and application of a LMH system for the poorly water-soluble and widely used cardiovascular drug lovastatin (LOV) through the combination of liposomes and micelles as an innovative oral dosage form (**Figure 1-2)**. Different types of polymeric micelles and lipids are explored for the optimisation of the LMH carrier system. Their preparation, drug loading, physiochemical characterization, morphology and *in vitro* drug release is investigated and compared (**Figure 1-2**).

Chapter 4 is focused on the investigation of the cellular activity of LOV encapsulated LMH systems in a Caco-2 cell monolayer (CCM) *in vitro* model of the intestinal epithelium to monitor permeability (as a predictor of oral absorption). The study includes cellular permeability, measurements of transepithelial electric resistance (TEER), apparent permeability (*Papp*), efflux ratio (ER), drug transportation, cellular uptake and accumulation of LMH within cell monolayers. The apparent permeability was used to trace the perviousness of LMH in comparison to free drug from the apical to the basolateral (A-B) or basolateral to apical (B-A) side and by either passive or active transport processes. This chapter also focused on the cell viability assessment on the LMH system by using an Alamar blue assay.

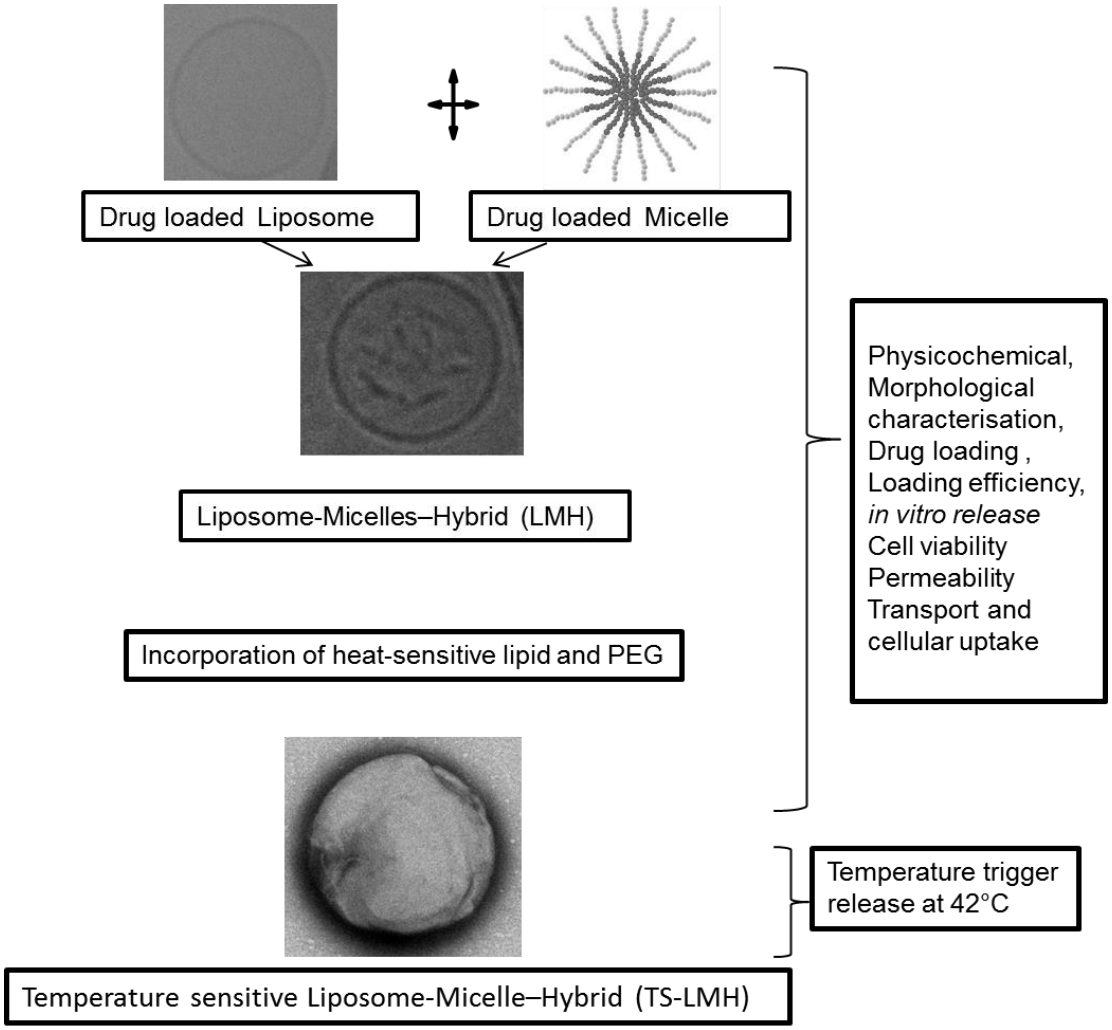


Figure 1-2: Schematic presentation of the research presented in this thesis.

Chapter 5 is focused on the development of a temperature sensitive liposome-micelle-hybrid (TS-LMH) system to control the drug release of encapsulated anticancer drugs at elevated temperature 42 °C (mild clinical hyperthermia). Initially, only a single drug (PTX) will be encapsulated into the micelles core and these will be encapsulated within a liposomal bilayer to prepare a PTX encapsulated liposome-micelles-hybrid system. Then, a combination of PTX and 5-FU will be loaded into the hybrid system, i.e. PTX will be encapsulated into the liposomal bilayer and 5-FU will be loaded in the TPGS micelles of the hybrid aqueous core to distinguish their loading and release profiles. The procedure used to prepare TS-LMH is thin film evaporation method and Vitamin E (d-α-tocopherol polyethylene glycol 1000 succinate-TPGS) is for micelles and 1, 2-Dipalmitoyl-sn-glycero-3-phosphorylglycerol (DPPG) and PEG-1500 for liposomes contribute thermosensitivity along with distearoyl

phosphatidyl glycerol-Na (DSPG), phosphatidylcholine (PC) and cholesterol. The therapeutic effect of the PTX-LMH will be performed by Alamar blue assay against HeLa cells. The cellular permeability and transport of PTX-LMH will also investigate using Caco-2 monolayers as a model system to trace the potential for oral absorption of the PTX.
The following hypotheses, with associated specific aims, are explored:

1. A LMH system, based on polymeric micelles and different lipid-containing liposomes will provide improved drug loading levels and release behaviour for oral delivery of the poorly water-soluble drug LOV (Chapter 3).

   Specific Aims:

   i. Develop a LMH system with different polymeric micelles and varying lipids.
   ii. Investigate and compare the physicochemical characteristics of different LOV loaded micelles, liposomes and hybrid nanocarriers, including encapsulation efficiency, average particle diameter, polydispersity and zeta potential.
   iii. Investigate the morphology and surface characteristics of the LOV loaded LMH systems to confirm its successful formation.
   iv. Investigate and compare LOV release behaviour from liposomes, micelles and the LMH system, and also analyse the release kinetics.
   v. Investigate the long-term physicochemical stability of LMH.

2. The LMH system can control drug permeability of LOV across a model epithelium as investigated with a human colon carcinoma cell line (Caco-2) monolayer (Chapter 4).

Specific aims:

   i. Investigate the influence of liposomes, micelles, and LMH system on Caco-2 cell viability.

   ii. Investigate the permeability of micelles, liposomes, and LMH across Caco-2 cell monolayers. Investigate the transportation and cellular uptake of pure LOV and LOV loaded micelles, liposomes, and LMH across the

cell monolayer from the apical to basolateral and basolateral to apical side of the Caco-2 cell monolayer.

iii. Evaluate the impact of micelles, liposomes, and LMH on the integrity of a Caco-2 monolayer.

3. A thermoresponsive LMH system can provide temperature controlled delivery of poorly water-soluble anticancer drugs paclitaxel (PTX) and 5-fluorouracil (5-FU) for improving bioavailability (Chapter 5).

Specific aims:

i. Investigate the impact of thermosensitive lipids on drug release behaviour from TS-LMH at physiological and elevated body temperatures.

ii. Investigate the dual or combination drug release behaviour from inner aqueous core and lipid bilayer of the LMH system at physiological and elevated body temperature.

iii. Investigate and compare the physicochemical and morphological characteristics of different paclitaxel loaded nanocarriers: encapsulation efficiency, diameter, zeta, and PDI.

iv. Investigate the killing ability of the LMH compared to individual nanocarriers and free drug PTX on the HeLa cancer cell line.

v. Investigate the cellular permeability of PTX-LMH carriers using Caco-2 *in vitro* cell model to confirm enhancement of loaded formulation across the cell membrane in comparison to the pure PTX. Also, study the transportation and cellular uptake of pure and loaded paclitaxel formulations across the cell monolayer from the apical-to-basolateral side of Caco-2 cell monolayers.

This thesis describes an investigation of a liposome-micelle-hybrid particle for oral delivery of LOV, prepared using polymeric micelles and phospholipid liposomes, which act

synergistically to stabilise the payloads and solubilise the drugs. Utilising different chambers facilitates better loading and combination of lipids and polymer offer greater colloidal stability. Improvement of release profile is also observed with double core matrix system that better protection as well as enhances bioavailability. Secondly, the study is extended to temperature sensitive hybrid particles with addition thermosensitive lipid and polymer to encapsulate anticancer drugs paclitaxel and 5-fluorouracil to get a better therapeutic effect. The cancer cells can easily develop resistance to specific drugs, or type of drugs. Combining of different types of chemotherapy agents, treatments can overcome this type of resistance. On the basis of this, Paclitaxel and 5-Fluorouracil could be encapsulated in the hybrid system in two separate chambers for a better chemotherapeutic response.

Besides these, a LMH system could be developed for improved permeability and transport in Caco-2 cells. It is also investigated that hybrid system shows better cellular activity that also enhances the extent of dissolution and membrane transport and serves as an ideal carrier for oral delivery of drugs with low water solubility. It provided protection to the particulate system from drug retention as well as water permeation, initiations of biliary and pancreatic secretions, increased GIT residence time, stimulation of lymphatic transport, variation in mesenteric and liver blood flow, enhanced intestinal wall permeability and reduced metabolism, efflux activity which enhances bioavailability.

Overall, the main focus in this research is to develop a LMH system for cardiovascular drug LOV, a TS-LMH system for anticancer drugs; PTX and 5-FU and finally, the cellular activities are monitored to address the current drug delivery challenges for oral drug delivery.

Chapter Two

2.1. Literature Review

2.1.1. Poorly water-soluble drugs for oral drug delivery, challenges, and current strategy

Oral delivery of therapeutic drugs is preferred as it presents the easiest route of drug delivery while minimising the risk of disease transmission when compared to parenteral therapeutic delivery.[75] It increases patient compliance, allows flexible and controlled dosing schedules, especially for chronic therapy.[76-78]

Despite the potential advantages for oral delivery, oral formulations face several common problems, particularly for poorly water-soluble drugs (PWSDs). For absorption to occur, a drug must be present in its dissolved form within the human GI tract, making bioavailability highly dependent on both solubility and dissolution rate. Indeed, drugs with poor water solubility such as lovastatin,[79] paclitaxel,[80] and 5-fluorouracil have been shown to exhibit limited bioavailability.[1, 79-80]

Several technologies exist for increasing the solubility and oral bioavailability of poorly water-soluble drugs, including; particle size reduction, use of surfactants, controlled crystal habit formation, salt formation, prodrugs, as well as the use of nanoparticle or nanotechnology-based drug delivery system.[2, 81]

Poorly water-soluble drugs (PWSDs) are defined by Wu *et al.*[82] as having an aqueous solubility in the range of 0.1 to 1 mg/mL, whereas if the compound solubility is < 0.1 mg/mL, it is considered to be practically insoluble according to the United States Pharmacopoeia and National Formulary (USP-NF).[82] Although low water solubility of drug candidates presents varied and significant challenges throughout drug discovery and development, the greatest concern is generally the risk of reduced and variable absorption after oral administration. The value at which limited solubility begins to impact absorption is difficult to state definitively since it is dependent on a number of other system variables, including drug permeation, dose, and the environment present within the gastrointestinal (GI) tract.[83]

2.1.2. Biopharmaceutical Classification System (BCS) and the Model Drugs

An application of the solubility-permeability relationship to oral drug absorption is the Biopharmaceutics Classification System (BCS) (**Figure 2-1**), a scientific framework used by the U.S. Food and Drug Administration (US FDA) for differentiating drugs based on their solubility and intestinal permeability.[84] The BCS was originally developed by Amidon *et al.* [85] with subsequent variations by others (Wu and Benet;[82, 86] Butler and Dressman; [87] Chen *et al.*[88]). Principles of the BCS are well described elsewhere (Amidon *et al.*[85] Yu *et al.*[89] Dahan *et al.*[90]).

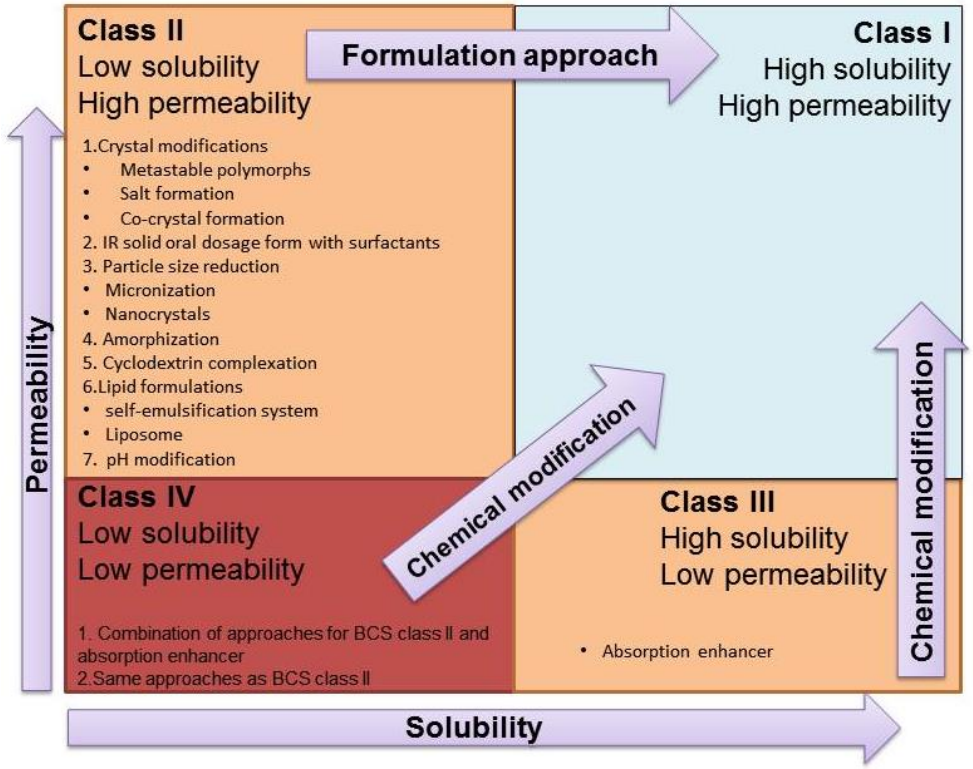


Figure 2-1: Representation of the BCS indicating that improved formulation design can highly improve the solubility of class II drugs, which results in higher absorption, while drugs of classes III and IV require chemical modification. Biopharmaceutical classification system (BCS) of therapeutic defined by FDA. Image modified from Wu *et al.*[82]

According to the BCS, class I molecules are those having both high solubility and high permeability (and therefore likely to have problems with oral absorption); class II compounds are those that have low solubility and high permeability (where solubility is the primary

limitation to absorption); class III compounds have high solubility but low permeability (where absorption is limited by membrane permeation and not solubility); and class IV compounds are those in which both poor solubility and poor permeability limit drug absorption. The focus of the current review is BCS class II compounds, which often exhibit solubility-limited absorption. Class IV compounds are also relevant, although they have additional problems associated with low permeability. Since both BCS class I and class II compounds show high permeability, the rate and extent at which the drug becomes available in the systemic circulation are primarily dependent on the availability of dissolved drug at the intestinal absorption site, at least if there is no significant transporter effect. Once these solubility limitations are overcome by optimized drug formulation, differences in the rate of absorption should become the primary drivers for changes in oral drug absorption.

According to the World Health Organization (WHO), Class II and Class IV drugs contribute about 27% of the list of Essential Medicines, facing challenges such as poor oral bioavailability, high fed-fasted variability, lack of dose-response proportionality and precipitation in the GI tract.[91] BCS Class IV drugs often require optimisation and chemical modification e.g. designing prodrugs to improve the oral absorption.[92] In contrast, several delivery options are available for BCS Class II drugs to improve their dissolution rate limited low oral bioavailability, which will be discussed in Section 2.1.3.

Three different drugs will be investigated in this research. Lovastatin is a Class II drug (high permeability and low solubility)[93] and paclitaxel is a Class IV drug (low permeability and low solubility).[94] They exhibit many characteristics that are problematic for effective oral delivery. Some of the problems associated include low aqueous solubility, poor permeability, erratic and poor absorption, inter and intra subject variability and significant positive food effect which leads to low and variable bioavailability. Also, most of the class IV drugs are a substrate for P-glycoprotein (low permeability) and for Cytochrome P450 3A4 (CYP3A4) (extensive pre-systemic metabolism) which further potentiates the problem of the poor therapeutic potential of these drugs. A decade back, extreme examples of class IV compounds were an exception rather than the rule, however today many drug candidates under development pipeline fall into this category. Formulation and development of an efficacious delivery system for BCS class IV drugs are staggering tasks for any formulator.

As an example of BCS Class III, 5-fluorouracil (5-FU)[95] has a high solubility but low permeability, where absorption is limited by membrane permeation and not solubility.[96] Many approaches, including prodrugs,[97] chemical enhancers,[98] physical methods,[99] formulation approaches (nano-emulsion and micro-emulsion)[100-101] liposomes[102-105] polymers (PLA/PEG-PPG-PEG)[106-107] etc., have been evaluated to enhance the permeability of 5-FU with different degrees of success.

The physicochemical properties (e.g. lipophilicity, molecular weight, particle size, geometry) of lovastatin, paclitaxel, and 5-FU are described below:

Lovastatin

Lovastatin (LOV) is widely used and the first of a new class of cholesterol-lowering drugs that reversibly and competitively inhibit hydroxymethyl glutaryl coenzyme A reductase (HMG-CoA), an enzyme involved in the biosynthesis of cholesterol.[108] It is also classified in the anti-lipemic agent pharmacological group. According to the Biopharmaceutical Classification System (BCS), it belongs to Class II (high permeability and low solubility).[93]

Due to high lipophilicity and poor water solubility (0.4 mg/L),[79] LOV undergoes extensive first-pass extraction in the liver, resulting in low and variable bioavailability and pre-systemic metabolism; it shows < 5% bioavailability and only 30% of the oral dose is absorbed. [109]Moreover, LOV (a lactone) is hydrolysed *in vivo* to its corresponding β-hydroxy acid, which is a strong inhibitor of HMG-CoA reductase. LOV and its β-hydroxy acid metabolite are both are highly bound (> 95%) to human plasma proteins and can cross the blood-brain and placental barriers. The plasma half-life is 1.1-1.7 hour.[109]

LOV is a white, non-hygroscopic crystalline powder. It is sparingly soluble in ethanol, methanol, and acetonitrile.[109-110] The structural formula of LOV is $C_{24}H_{36}O_5$ and its molecular weight is 404.55 g/mol. It has a high *log P* value (4.3) and is soluble in lipids. The low oral dose (10–40 mg), suitable *log P*, low oral bioavailability and being a BCS class II drug strongly provide a rationale to develop a more efficient and controllable oral delivery system for LOV to improve its oral bioavailability; e.g. using nanocarriers liposome and micelles.[93, 111]

Paclitaxel

Paclitaxel (PTX) is one of the most widely used and effective antineoplastic agents isolated from natural sources, the bark of *Taxus brevifolia*.[112] It is a pseudo alkaloid that has a taxane ring as its nucleus ($C_{47}H_{51}NO_{14}$, MW 853.93).[113] It is a microtubule inhibitor and approved for chemotherapy of various types of solid tumors, e.g. ovarian, breast, pulmonary prostate, melanoma, oesophageal cancer, and Kaposi's sarcoma. However, its clinical use is limited due to its low aqueous solubility (< 0.03 mg/mL).[80] It has been a great challenge to formulation scientists due to its water-insolubility and efflux by p-glycoprotein (p-gp) expressed in the intestinal epithelial cells which are considered as a major reason for poor absorption of orally administered paclitaxel.[114-115]

Moreover, PTX can bind to plasma proteins and decreases the ability to penetrate the tumor interstitium at an effective concentration and increases the toxicity to healthy tissues.[112, 116] Also, the excipients used in commercial formulations cause adverse effects.[117-121] Hence, to increase the solubility, reduce toxicity and selectively target to tumor tissue, PTX has been encapsulated in liposomes[71, 122-123] and micelles[76, 124] which show greater accumulation at the tumor site and enhanced permeability and retention (EPR).[121, 125-126]

Paclitaxel is a colourless to slightly yellow or (in pure form) an off-white crystalline powder. It is a highly lipophilic compound with a *log P* value of 3.96.[127]Among non-aqueous solvents, the solubility is found to be ~46 mM in ethanol, ~20 mM in methylene chloride or acetonitrile, and ~14 mM in isopropanol. It is also soluble in methanol, tertiary-butanol, and dimethyl sulfoxide.

5-Fluorouracil

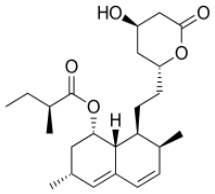
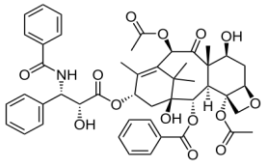
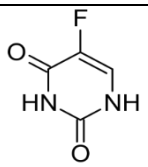
5-Fluorouracil (5-FU) is an effective and widely used chemotherapeutic agent for more than 50 years in the treatment of colorectal,[128] breasts,[129] and skin cancer.[130] However, 5-FU suffers from several drawbacks; e.g. a short plasma half-life after intravenous bolus administration and drug resistance by tumor cells.[131] Therefore, requiring high doses that lead to severe side effects, including gastrointestinal, haematological, neuronal, dermatological effects, pancytopenia, and cardio-toxicity.[132]

To overcome these limitations, 5-FU has been encapsulated into liposomes to prolong its circulation time, reduce the associated side effects, improve its therapeutic index and efficacy, and favour drug accumulation in tumors.[102-103]

5-FU is a white to nearly white crystalline powder; practically odourless with a *log P* value of -0.89 and *pKa* 8.02. It is soluble in methanol.[74]

The physicochemical properties of the model drugs are shown in **Table 2-1**

Table 2-1: Physico-chemical properties of model drugs used in this study.[72-74]

Properties	**Lovastatin**	**Paclitaxel**	**5-Fluorouracil**
Chemical structure			
Molecular weight (g/mole)	404.54	853.91	130.08
Chemical Formula	$C_{24}H_{36}O_5$	$C_{47}H_{51}NO_{14}$	$C_4H_3FN_{2O2}$
Drug class	Cardiovascular	Anti-cancer	Anti-cancer
Aqueous solubility (pH 7.0)	0.4 mg/L	Insoluble	< 12 mg/mL at 66° F
Log P	4.26	3.96	-0.89
pKa	14.9	10.9	8.02
Melting point	174.5 °C	213 °C	282°C (decompose)

2.1.3. Strategies for oral delivery of poorly soluble drugs

It was proposed that some BCS II drugs could be formulated using just micronisation for particle size reduction or with added surfactants in a simple solid dosage form. However, for more challenging BCS II compounds in terms of dose volume, more sophisticated formulations would be required. There is a significant opportunity for enabling technologies to facilitate the development of BCS Class II drugs into a viable therapy. A number of technologies have been developed to address reduced solubility of BCS Class II drugs, including amorphous formulations (e.g. solid solutions),[91, 133-134] particle size reduction[81] (e.g. nanocrystals), formulation strategies (e.g. cyclodextrin),[135-136] porous silica-based systems,[137] and lipid-based formulations [3, 30, 138-139]) as summarized in **Figure 2-2.**

Detailed descriptions of all these systems are beyond the scope of the present study. Among these, liposomes and micelles are of interest that encapsulate, protect and shield drugs against enzymatic degradation, pre-absorption or pre-hepatic metabolism in the enterocytes and release them in a controlled manner. Owing to their nano-sized, they offer numerous benefits for oral administration. Their surface can be modified to enhance or reduce bioadhesion, or to target specific cells.[140-142] This modification helps the drug to diffuse inside the intestinal mucus, improving the capability for the nanocarrier-associated drug to be absorbed.[143] Liposomes and micelles are widely investigated for poorly water-soluble drugs such as statins[111] and anticancer drugs[144-145] to challenge the issue of its poor solubility and low stability.

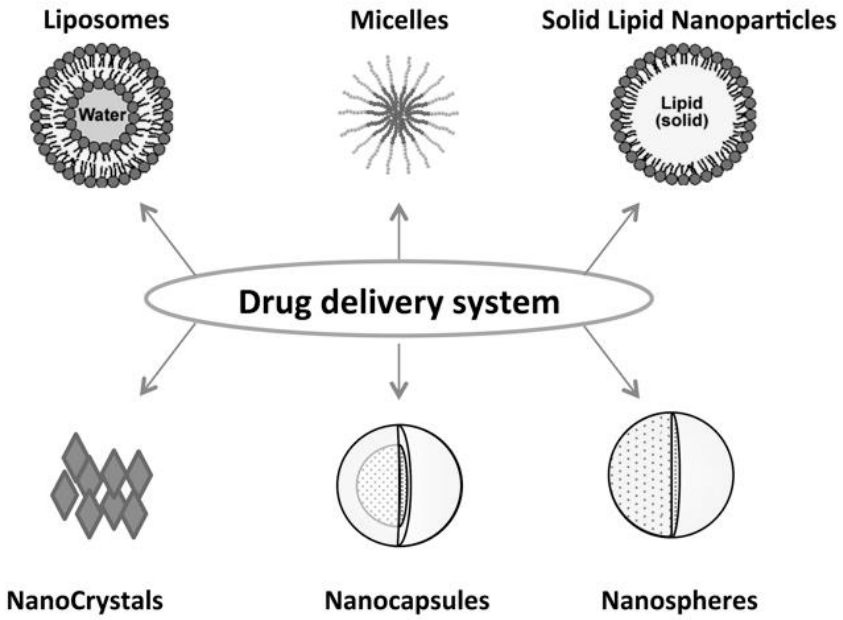


Figure 2-2: Schematic representation of different nanotechnology-based drug delivery systems. Image adapted from Romana *et al*.[111]

Due to the high relevancy in the current research, specific examples of liposome and micelle-based drug delivery approaches have been reviewed in the following sections.

2.2. Overview of liposome-based drug delivery system and commercial liposomes

2.2.1. Background

Liposomes were first developed by Alexander Bangham in 1960[146] as an analytical tool to study bio-membrane dynamics, e.g. phase transition, fluidity, and diffusion characteristics.[146] Liposomes offer significant potential as a drug delivery system,[147] owing to their similarity in composition to biological membranes, their ability to encapsulate both hydrophilic[148] and hydrophobic therapeutics while offering control over release kinetics, as well as being easily surface modified to enhance circulation or provide specific targeting.[149]

Liposomes have long been considered for use in therapeutic delivery, with the first *in vivo* experiments undertaken in the early 1970's, by Sapra *et at.* (2003).[145] It was not until the 1980's that research different diseases, particularly cancer.[145] Doxil®, the first FDA-approved nano-drug (1995) is based on three unrelated principles of the liposomal formulation: (i) prolonged drug circulation time and avoidance of the RES due to the use of PEGylated nano-liposomes; (ii) high and stable remote loading of doxorubicin driven by a transmembrane ammonium sulfate gradient, which also allows for drug release at the tumor; and (iii) having the liposome lipid bilayer in a "liquid ordered" phase composed of the high-T_m (53 °C) phosphatidylcholine, and cholesterol. Due to the EPR effect, Doxil is "passively targeted" to tumors and its doxorubicin is released.[150]

These carriers have advantages particularly in oral drug delivery and they allow delivery of poorly water-soluble drugs, targeting of drugs to specific parts of the gastrointestinal tract, transcytosis of drugs across the tight intestinal barrier, intracellular and transcellular delivery of large macromolecules, the increase in efficacy, specificity, tolerability and therapeutic index of corresponding drugs.[151-155]

2.2.2. What are Liposomes?

Liposomes are microscopic spherical vesicular structures of hydrated phospholipid-bilayers, consisting of one or more lipid bilayers, generally including cholesterol and lecithin, and form spontaneously when phospholipids are dispersed in water,[156] and are amphiphilic i.e.,

they have defined polar and non-polar regions **(Figure 2-3)**.[157-158] The lipid components which are used to form liposomes either occur naturally or are synthetically manufactured.[157] They encapsulate a fraction of the solvent in which they are suspended into their interior.[159] Studies during the 1970s and 1980s typically used imprecise large multilamellar vesicles in the micrometre size range, while more recent investigations mostly use homogeneous unilamellar vesicles in the size range 50–150 nm. This size range is a compromise between loading efficiency of liposomes (increases with increasing size), liposome stability (decreases with increasing size above an optimal 80–200 nm range) and ability to extravasate (decreases with increasing size). The thickness of the membrane is around 4 nm, and it can contain a polymer coating and/or ligands with defined functions, such as specific binding or fusogenic activity.[159]

Liposome properties differ considerably with lipid composition, surface charge, size, and the method of preparation. Furthermore, the choice of bilayer components determines the 'rigidity' or 'fluidity' and the charge of the bilayer. For instance, unsaturated phosphatidylcholine species from natural sources (egg or soybean phosphatidylcholine) give much more permeable and less stable bilayers, whereas the saturated phospholipids with long acyl chains (for example, dipalmitoyl phosphatidylcholine) form a rigid, rather impermeable bilayer structure.[160-162]

Phospholipids are the main component of naturally occurring bilayers, including; Phosphatidylcholines (PC), phosphatidylethanolamines (PE) and phosphatidylserines (PS).[163] This aqueous core is used as the medium for delivery of water-soluble substances such as proteins and peptides and hydrophilic drugs,[157-158] whilst the amphiphilic and lipophilic substances, i.e. oil soluble, can be incorporated into the lipid bilayer.

When the phospholipids dissolve in water they spontaneously self-assemble to minimize unfavourable hydrophobic interactions with water. They arrange themselves tail to tail (including hydrophilic interactions between polar heads and van der Waals interactions between hydrocarbon tails), forming a spherical bi-layer, thus encapsulating the aqueous environment **(Figure 2-3)**.

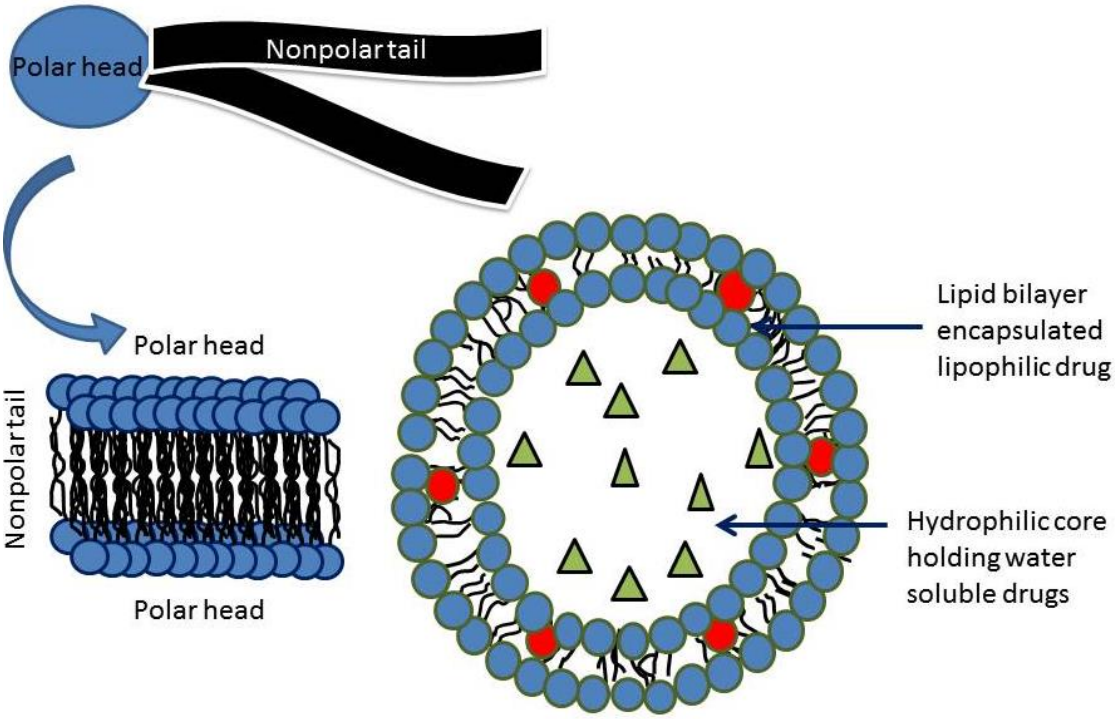


Figure 2-3: Schematic showing spherical liposomes plus the bilayer where hydrophobic and hydrophilic substances can be incorporated. Image adapted from Lasic *et al.* and Bergstrand *et al.*[89,91]

2.2.3. The rational for Liposome Delivery Systems

Due to their size and hydrophobic and hydrophilic character (amphiphilicity), liposomes are promising systems for drug delivery. The rationale for using liposomes as drug delivery systems to cells was originally based on the possibility of fusion between the liposome and the target cell membranes.[164] Therefore, liposomes had to be prepared from lipids that are present in cell plasma membranes or from synthetic lipids with structural and physicochemical properties that resemble those of natural lipids. Liposomes are relatively non-toxic, biodegradable, non-immunogenic, delay drug elimination and their nanometer size and large specific surface area favour their absorption compared to larger traditional therapeutic delivery systems such as microspheres and emulsions.[165] Early research in liposomal drug preparations was beset with problems–there was insufficient understanding of liposome absorption and clearance *in vivo*, inaccurate extrapolation of *in vitro* liposome-cell interactions, and insufficient stability and circulation time of liposome-based drugs *in vivo.*[166-167] Advances in the late 1980's and early 1990's, including a detailed understanding

of physiological mechanisms of *in vivo* liposome absorption, and lipid-drug interaction overcame many of the early disappointments. The result was liposome designs with improved biodistribution, enhanced stability both *in vitro* and *in vivo*, and optimized residence times of liposomes in systemic circulation.[26]

2.2.4. Classification of liposomes

Liposomes can be classified by either their structural properties, size or by the basis of their preparation methods. The liposome size can vary from very small (0.025 μm) to large (2.5 μm) vesicles. Moreover, liposomes may have one or more bilayer membranes. The vesicle size is a crucial parameter in determining the circulation half-life of liposomes, and both size and number of bilayers affect the amount of drug encapsulated in the liposomes.

On the basis of their size and number of bilayers, liposomes can be classified into one of two categories: multilamellar vesicles (MLV) and unilamellar vesicles. Unilamellar vesicles can also be classified into two categories: large unilamellar vesicles (LUV) and small unilamellar vesicles (SUV) **Figure 2-4**.[153 168]

SUVs have a diameter of 20 to approximately 100 nm. LUVs, MLVs, and SUVs range in size from a few hundred nanometers to several microns.[168-169] The thickness of the membrane (phospholipid bilayer) measures approximately 5 to 6 nm. Large liposomes form spontaneously when phospholipids are dispersed in water above their phase transition temperature. The preparations of SUVs start usually with MLVs, which are then transformed into small vesicles using an appropriate manufacturing technique.

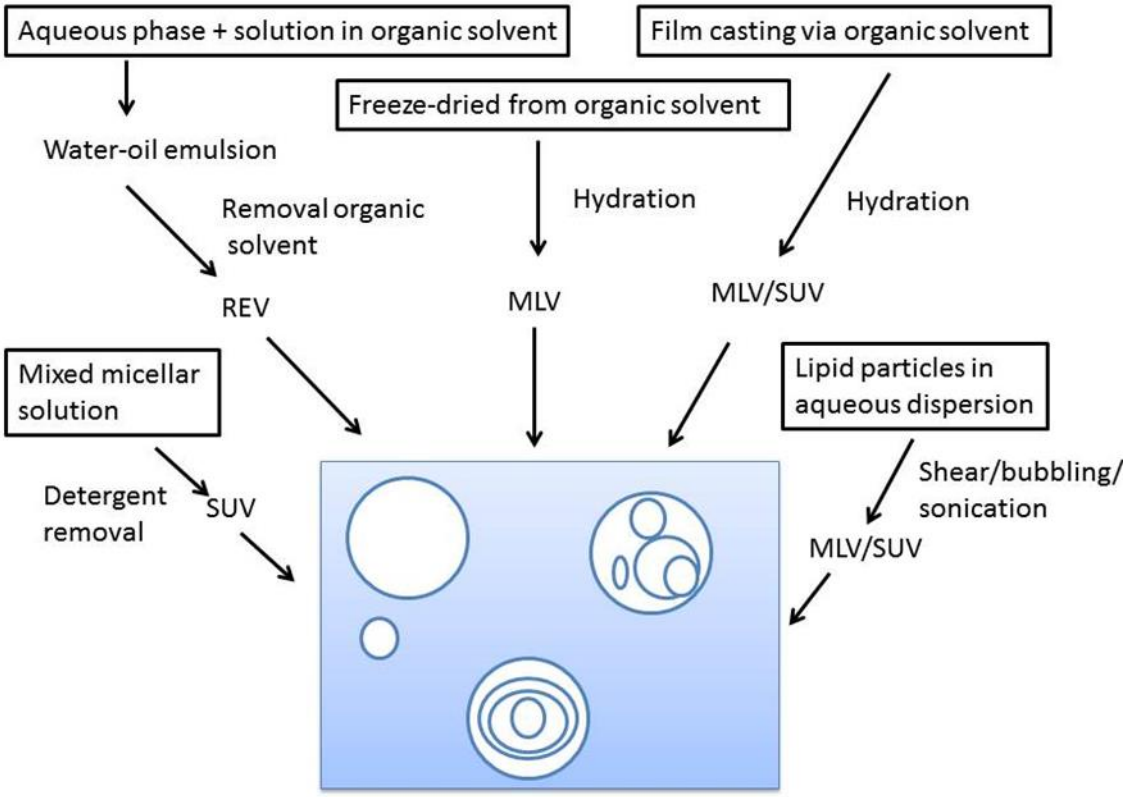


Figure 2-4: Schematic illustration of liposomes of different size and number of lamellae resulting from different formulation/manufacturing techniques. Image modified from Storm *et at*.[168]

The four major liposome types utilized to date are conventional liposomes, sterically-stabilized liposomes (pegylated or stealth liposome), ligand-targeted liposome and a combination of the above into theranostic liposomes (**Figure 2-5)**.[170]

Conventional liposomes are either neutral or negatively charged when formed by natural phospholipids plus cholesterol, and have shown promise in effectively delivering some drugs. However, they have very short circulation times and are generally recognized by the body's immune system as foreign bodies and are often destroyed before significant amounts of the drug can reach the intended disease site.[171-172]

To increase the likelihood of the success in drug targeting by liposomes, it is necessary to minimize the opsonisation and to prolong the circulation of liposomes *in vivo*. Different approaches have been reported to achieve a long circulation of a liposome *in vivo,* including modification with certain lipids such as monosialoganglioside (GM1), palmityl-D-glucoronic

acid and polyethylene glycol-poly-ethanolamine (PEG-PE).[171, 173] These liposomes have reported significantly longer circulation in blood than conventional liposomes. Attachment of

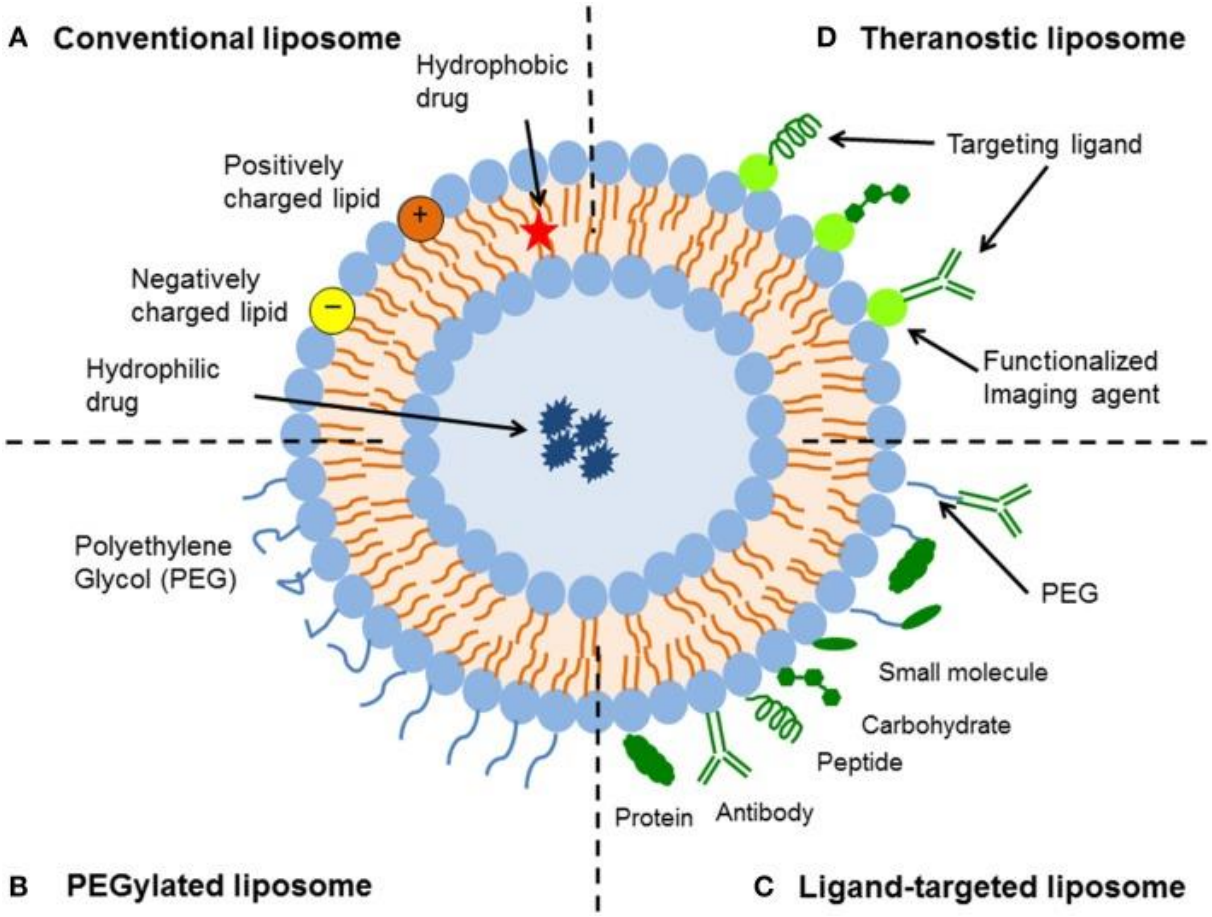


Figure 2-5: Four types of liposomes utilised to date; A) conventional, B) sterically-stabilized liposomes (pegylated or stealth liposome), C) ligand-targeted and D) a combination of the as theranostic. Image adapted from Sercombe *et al*.[170]

various ligands such as polyethylene glycol (PEG) to a liposomal surface is the patented delivery form termed Stealth® liposomes.[171] Sterically stabilised (stealth) liposomes carry polymer coatings to obtain prolonged circulation times and drug residence time in blood and are developed for state-of-the-art drug delivery.[157]

The mechanism whereby steric stabilization increases circulation longevity is that PEG possesses a flexible chain that occupies the space adjacent to the liposome surface. Given this occupancy, access and binding of plasma proteins to liposome surfaces are hindered, resulting in inhibition of such a liposome's interactions with MPS macrophages.[174] It has been reported that the terminal half-life of PEG-liposomes in humans is 90 h.[175] Other

polymers that have been investigated are gelatine with multivalent ions such as calcium (Ca^{2+}), alginate with Ca^{2+} (Ca-Alg), aluminium Al^{3+} (Al-Alg) and Ba^{2+} (Ba-Alg)[176] and mucoadhesive polymers such as carbopol and chitosan,[177] which are also reported to have exhibited prolonged circulation, sustained release profiles and increased protection of encapsulated drugs, thereby creating more favourable drug pharmacokinetic profiles.

This stealth principle has been used to develop the successful doxorubicin-loaded liposome product that is presently marketed as Doxil (Janssen Biotech, Inc., Horsham, USA) or Caelyx (Schering-Plough Corporation, Kenilworth, USA) for the treatment of solid tumors. Recently, impressive therapeutic improvements were described with the use of corticosteroid-loaded liposomes in experimental arthritic models.[178-179] The application of stealth liposomes has been on their potential to increase the blood circulation time. However, long-circulating liposomes may also act as a reservoir for prolonged release of a therapeutic agent. Pharmacological action of vasopressin is formulated in long-circulating liposome.[178-179]

Ligand-targeting liposomes usually involve coating with functionalized ligands (i.e. monoclonal antibodies, peptides, growth factors, glycoproteins, and receptor ligands) that can bind specifically with cell surfaces and cell receptors, and hence induce the internalization of liposomes or encapsulated drugs; these may be either conventional or stealth.[145, 168, 180]

2.2.5. Liposome preparation methods and drug incorporation in liposomes

Three different strategies used to prepare liposomes are: (a) Mechanical methods such as thin film and ultrasonic methods; (b) Methods based on organic solvent replacement such as reverse phase evaporation and ether vaporization; and finally (c) Methods based on size transformation or fusion of preformed vesicle such as freeze thaw extrusion and dehydration-rehydration.[154] Preparative methods also can be divided into two groups depending on the liposome size; (1) those which produce large vesicles; e.g. multilamellar (MLV) or large unilamellar (LUV) and (2) methods which produce small unilamellar vesicles (SUV). The major advantages of the large vesicles are that they have a much higher encapsulation capacity and efficiency than SUV and that they allow the encapsulation of macromolecules of high molecular weight; their major drawback is that they are usually heterogeneous with respect to particle size and in the case of MLV also with respect to the number of lamellae.

The main advantage of SUV is their fairly homogeneous particle size distribution and that their geometry is usually well characterised. Their principal disadvantages are limitations in terms of capacity and efficiency of encapsulation.[181-182]

Multilamellar liposomes (MLV) usually range from 500 to 10,000 nm. Unilamellar liposomes can be categorized as small (SUV), usually smaller than 50 nm, and as large (LUV), usually larger than 50 nm. The liposomes of very large size are called giant liposomes (10,000 - 10, 00,000 nm). They can be either unilamellar or multilamellar. The liposomes containing encapsulated vesicles are called multi-vesicular liposomes. Their size range from 2,000-40,000 nm.[182]

A) Multilamellar Liposomes (MLV)

Multilamellar liposomes are prepared by the lipid hydration method and solvent spherule method as described by Riaz *et al*.[182] The lipid hydration method is the most widely used method for preparation of multi lamellar vesicles (MLV).[153, 183] The method involves drying a solution of lipids to form a thin film at the bottom of a round bottom flask. The film is then hydrated with aqueous buffer and the dispersion vortexed. The hydration step is done at a temperature above the gel-liquid crystalline transition temperature (Tc) of the lipid or above the Tc of the highest melting component in the lipid mixture. The compounds to be encapsulated are added either to aqueous buffer or to the organic solvent containing lipids, depending upon their solubilities. MLVs are simple to prepare by this method and a variety of substances can be encapsulated in these liposomes. Drawbacks of the method are low internal volume, low encapsulation efficiency and the size distribution is heterogeneous due to the exposure of the materials (to be encapsulated) to organic solvent and sonication.[146, 184]

However, high drug loading can be achieved by hydrating the lipids in the presence of an immiscible organic solvent (petroleum ether, diethyl ether). The contents are emulsified by vigorous vortexing or sonication. The organic solvent is removed by passing a stream of nitrogen gas over the mixture. MLVs are formed immediately in the aqueous phase after the removal of the organic solvent.[185-186] Kan *et al.* (2010) prepared paclitaxel loaded liposome by this method and achieved high drug loading.[187]

The formation of multivesicular liposomes has been reported by Kim *et al.* (1983).[188] A water in oil emulsion (lipids solution in organic solvents) was converted to organic solvent

spherules by the addition of the lipid solution into water. The evaporation of organic solvent resulted in the formation of multivesicular vesicles. The materials which can be encapsulated include glucose, Ethylene-diamine-tetraacetic acid (EDTA), human deoxyribonucleic acid (DNA). These liposomes have very high encapsulation efficiency (up to 89%).[188]

The lipid hydration method appears to be a simpler method compared with the other techniques used for drug loading in the liposome.[146, 156, 182]

B. Large Unilamellar Liposomes (LUV)

LUVs have high internal volume/encapsulation efficiency and are now being used for the encapsulation of drugs and macromolecules. The following methods are widely used to prepared large unilamellar liposomes (LUV), e.g. solvent injection (ether infusion method, or ethanol injection method), detergent removal, reverse phase evaporation, calcium-induced fusion, micro-fluidization and freeze-thaw method.[182] The two most widely used methods are described below;

I. Reverse Phase Evaporation Method

First, a water in oil emulsion is formed by brief sonication of a two-phase system containing phospholipids in an organic solvent (diethyl ether or isopropyl ether or a mixture of isopropyl ether and chloroform) and aqueous buffer. The organic solvents are removed under reduced pressure, resulting in the formation of a viscous gel. The liposomes are formed when residual solvent is removed by continued rotary evaporation under reduced pressure. With this method, high encapsulation efficiency (up to 65%) can be obtained in a low ionic strength medium of 0.01 M NaCl. The method has been used to encapsulate small and large macromolecules.[185]

II. Freeze-Thaw Method

Small unilamellar vesicles (SUV)s are rapidly frozen, then followed by slow thawing.[153, 183] Brief sonication disperses aggregated materials to large unilamellar vesicles (LUV)s. The formation of unilamellar vesicles is due to the fusion of SUV during the processes of freezing and or thawing. This type of fusion is strongly inhibited by increasing the ionic strength of

the medium and by increasing the phospholipid concentration. Drug encapsulation efficiencies of 20 to 30% have been obtained.[189-190]

Ostro *et al*.[191] found that when MLV preparations were subjected to five cycles of a freeze on liquid nitrogen-thaw and followed by thawing in warm water, liposomes of high encapsulation efficiency (up to 88%) could be obtained.[192]

2.2.6. Formation process of liposomes

An important parameter to consider when addressing the formation process of liposomes is the rigidity of the bilayer. Hydrated-single component phospholipid bilayers can be in a liquid-crystalline (fluid) state or in a gel state. By increasing the temperature, the gel state bilayer melts and is converted into the liquid state. This occurs at a temperature known as the transition temperature (Tc). The Tc of a bilayer depends on the acyl chain length, degree of saturation and polar head group.[193] The transition temperature of egg yolk phosphatidylcholine due to a high degree of unsaturation is 15 ºC while that of fully saturated di-stearoyl-phosphatidylcholine is over 50 ºC.[193]

Hence the selection of lipid is important for the formation and intended use of liposomes. Phosphatidylcholine (PC), phosphatidyl ethanolamine (PE) and phosphatidyl serine (PS) are commonly used phospholipids for liposome preparation. Cholesterol can be added to the bilayer mixture to reduce the permeability of fluid crystalline state bilayers.[194]

2.2.7. Factors influencing drug loading in liposome

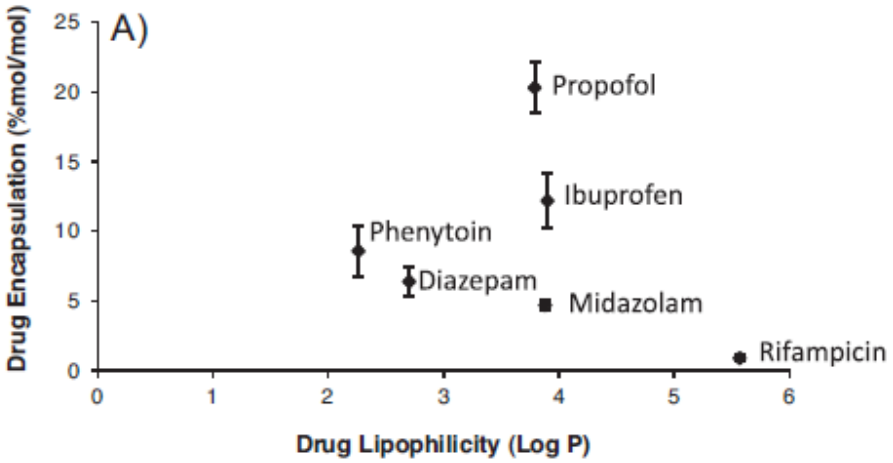
Currently, there are few liposome preparation methods which are capable of achieving high encapsulation efficiencies.[195] In addition, the success of entrapment depends on the size, charge, fluidity, the number of lamellae and the type of lipid, drug and hydration medium used in the preparation.[156] The extent of drug loading depends on the available trapping volume by a given amount of lipid, lipid composition, the geometry of the lipid and method of preparation. A concentration of drug and lipid and the specific affinity of the drug for lipids are also important for higher drug loading. In order to increase the entrapment efficiency of a drug, liposomes encapsulating water-soluble drugs should have a large encapsulated volume. On the other hand, the amount of water-insoluble drug encapsulation depends on the quantities of lipids used.[196] It is known that the higher lipid concentrations

and larger the liposome diameter the larger the entrapment efficiency due to increased internal volume.[197-198]

Drug loading efficiency of a liposome is affected by the molecular weight (MW) and lipophilicity (*Log P*) of the drug, composition of the phospholipids, surface charge, bilayer area and lipid geometry such as; length of the alkyl chain, cholesterol content, presence of charged group on the lipids, lipid quantity, presence of bile salts and the method of liposome preparation.[199-200] Factors influencing drug loading in liposomes are described below:

I. Molecular weight (MW) and the drug lipophilicity (*Log P*)

A molecular weight of the drug (MW) plays a major role in controlling levels of drug encapsulation compared to the drug lipophilicity (*Log P*). Recently, a series of poorly soluble drugs including diazepam, ibuprofen, midazolam, phenytoin, propofol and rifampicin with MW ranging from ~178- 823 g/mol, and *LogP* between 2.3- 3.84 were investigated in terms of their bilayer drug loading in a liposome formulation (PC: cholesterol, 89:11 mol %). No trend was detected for lipophilicity **(Figure 2-6A)**, but for MW **(Figure 2-6B),** the trend was, the larger the MW, the lower the incorporation efficiency.[201]



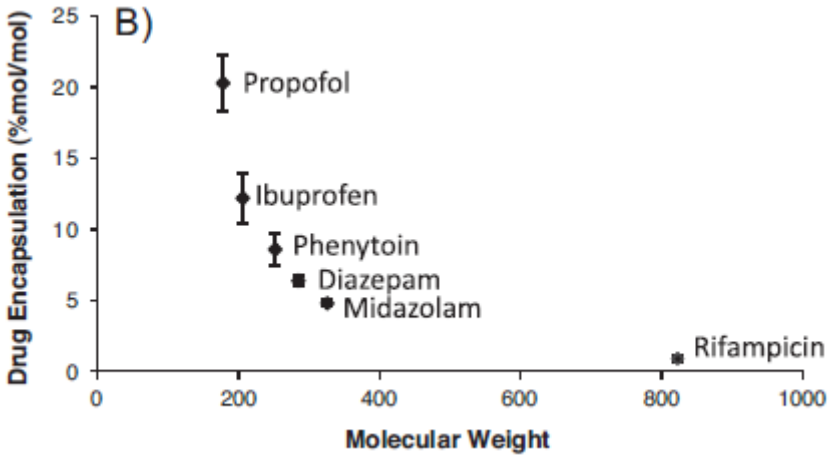


Figure 2-6: The relationship between liposomal (PC: cholesterol, 89:11 mol %) bilayer encapsulation of the drug and (A) lipophilicity or (B) molecular weight of the drug. Image adapted from Mohammed *et al*.[200]

II. Surface charge

A surface charge also has an influence on drug loading. For example, the addition of 2 μmol cationic lipids (stearyl amine-SA) enhanced the incorporation efficiency of ibuprofen by approximately 8% to 47%. A further increase in the concentration of SA decreased the encapsulation efficiency and drug loading.[199]

III. Bilayer area and lipid geometry

Mohammed *et al*. 2004 demonstrated that the drug loading of propofol and midazolam in a lipid bilayer increased with increased lipid chain length in the order of DGPC > DSPC > DMPC ≈ DPPC > PC **(Figure 2-7A)**[200] and revealed a tendency of increasing encapsulation levels of water-insoluble ibuprofen with increasing lipid chain length in the order of DGPC > DSPC > DMPC > PC, with drug loading being improved by approximately 50% when DGPC was substituted for PC.[200, 202]

When considering the asymmetrical PC derivatives, MSPC and POPC provided significantly lower incorporation rates for propofol when compared to their symmetrical counterparts, DSPC and DMPC **(Figure 2-7B)**. Similarly, incorporation studies using midazolam suggest that symmetrical PC derivatives provide significantly higher encapsulation of midazolam when compared their asymmetrical counterparts **(Figure 2-7B).** This generally reduced drug loading by liposomes formulated from asymmetrical lipids may be attributed to bilayer

formation via a mismatch interaction between alkyl side-chains of asymmetric lipids, therefore reducing the overall hydrophobic area available for hydrophobic drug interaction, when compared to that of symmetric lipid bilayers (**Figure 2-7A**).[200]

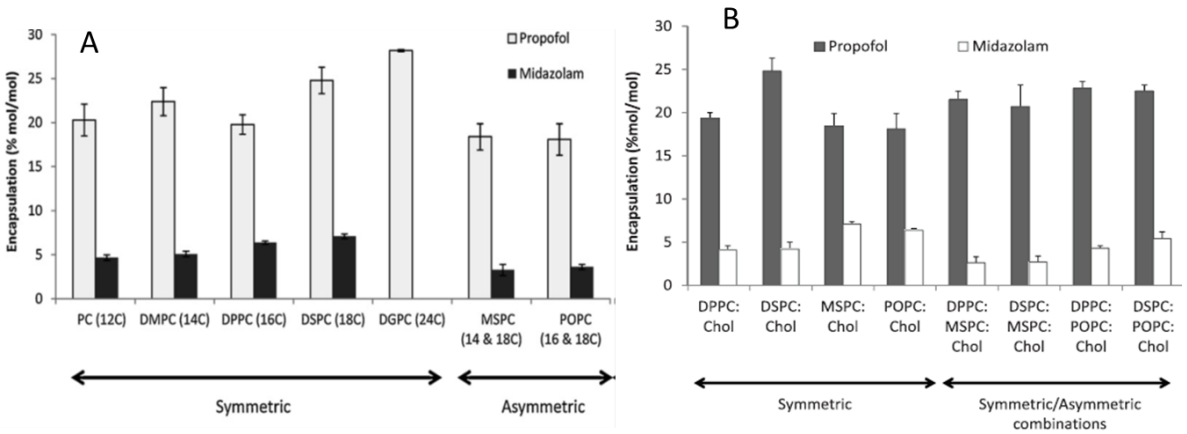


Figure 2-7: The influence of long-chain symmetric and asymmetric lipids on midazolam or propofol encapsulation. Liposomes were prepared from a combination of (A) PC, 1,2-Dimyristoyl-sn-glycero-3-phosphorylcholine (DMPC), Dipalmitoylphosphatidylcholine (DPPC), 1,2-distearoyl-sn-glycero-3-phosphocholine (DSPC), DGPC, 1-palmitoyl-2-oleoyl-sn-glycero-3-phosphocholine (POPC) or 1-myristoyl-2-stearoyl-sn-glycero-3-phosphocholine (MSPC) (89 mol %) and (B) DSPC or DPPC (44.5 mol %) with POPC or MSPC (44.5 mol %). Keeping constant cholesterol (11 mol %) and drug loading in a total lipid concentration of 18 µmol for the formulations. Image adapted from Mohammed *et al*.[200]

Addition of cholesterol to liposomes has been shown to improve drug loading, however, the extent to which this occurs is dependent on the bilayer volume (length of the phospholipid) (**Figure 2-8**). Therefore, for lipids with a reduced hydrophobic region, the competitive space-filling action of cholesterol is more notable in the decreased bilayer volume of the MSPC liposomes. Therefore the reduced hydrophobic region of the MSPC combined with the competing action of cholesterol for packaging within the bilayer reduces bilayer drug loading.[202] Cholesterol improves drug loading at 10%, but decreases at higher concentrations; actually, at higher concentrations, it is worse than the lipids alone.

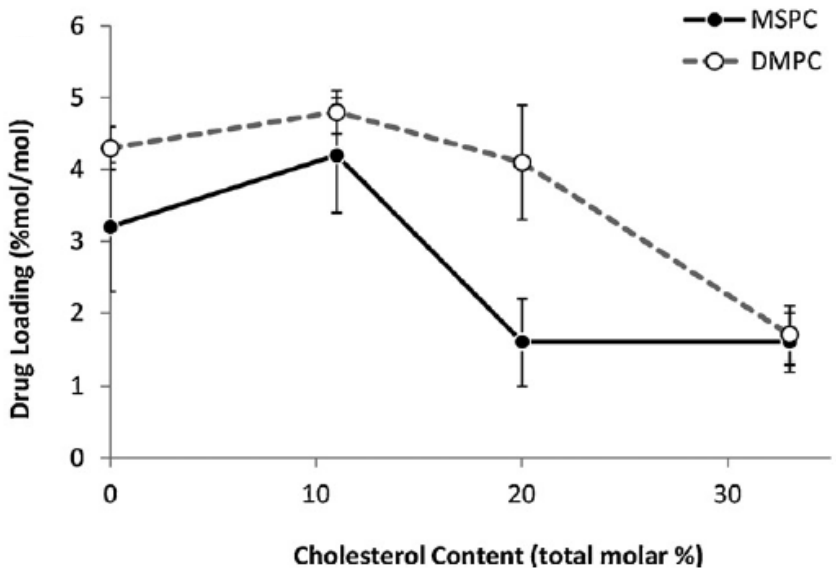


Figure 2-8: Comparison of midazolam encapsulation by MSPC: cholesterol or DMPC: cholesterol (89:11 mol %) liposomes prepared using increasing amounts of cholesterol. Results are expressed as the means of three experiments ± S.D. Image adapted from Mohammed *et al*.[200]

2.2.8. Factors affecting drug release from liposome

The *in vitro* release profile of a poorly soluble drug is improved when loaded into liposomes due to the decreased particle size, increased surface area and the altered physical state of the drug. For example; LOV loaded liposomal formulation reported by Arora *et al*.[203] The release study demonstrated sustained release of LOV from liposomal formulations compared to free LOV. Nounou *et al.*[204] also reported sustained drug release of LOV from liposomal formulations.[204] The release of anticancer drugs are also widely investigated to challenge the issue of its poor solubility.[144,205-206] D-α-tocopherol polyethylene glycol 1000 succinate (TPGS)-based liposomes have been used to deliver anticancer agents like doxorubicin[207] and docetaxel.[208-211] The liposomal formulations of vancomycin,[212] vinpocetine,[213] fenofibrate,[214] ibuprofen,[199] and cyclosporin A[69] have also been reported to show sustained release.

Factors affecting drug release from liposomes are highly dependent on the physical properties of the drug, drug loading level, the molecular weight of the solutes, drug solubility in the lipid and drug diffusibility through the lipid are important parameters. Solubility is the fundamental parameters for drug release, which is the process by which a drug leaves a drug product and is subjected to absorption, distribution, metabolism, and excretion (ADME), available for pharmacological action.

Surface charge

A surface charge has an influence on drug release. Studies have shown that positively charged liposomes prepared with lipid 1, 2-distearoyl-3-trimethylammonium-propane (DSTAP) demonstrated fast release of propofol compared with neutral 1,2-distearoyl-sn-glycero-3-phosphocholine (DSPC) and negatively charged 1,2-distearoyl-3-phosphatidyl glycerol (DSPG) liposome preparations (**Figure 2-9**).[199, 204]

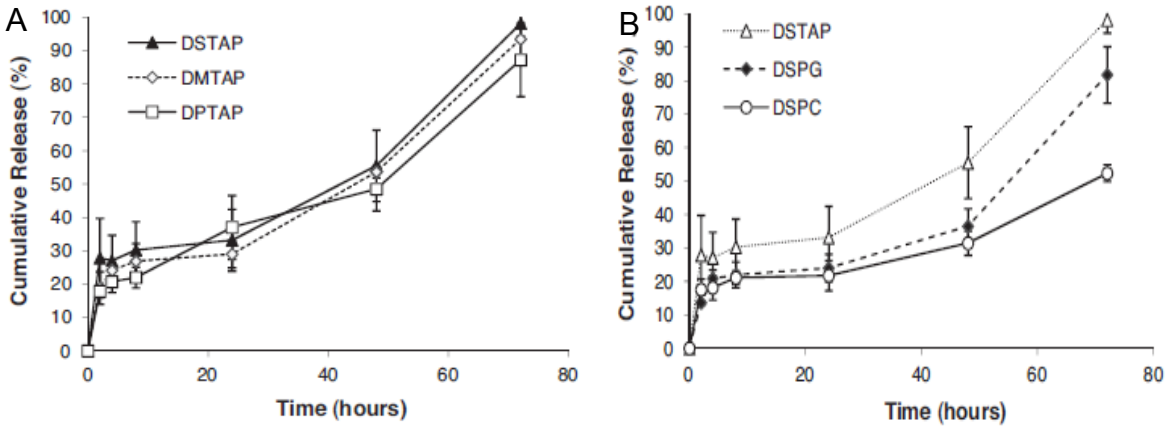


Figure 2-9: (A) Effect of alkyl chain length of positively charged TAP series on bilayer release of propofol. (B) Effect of vesicle surface charge on the rate of propofol release. Image reproduced from Mohammed *et al.*[200]

Drug release from cationic DSTAP formulation was the highest and the slowest release rate was noted for the neutral DSPC preparation, suggesting that both charge and alkyl chain length is contributing to the release rates. The effect of charge on drug permeability has been previously documented; results collated by Nounou *et al.*[204] revealed that positively charged liposomes exhibited the fastest release compared with neutral and negatively charged preparations. Furthermore, Mohammed *et al.*[200] demonstrated that the inclusion of 9 mol% stearylamine (positively charged) or dicetylphosphate (negatively charged) induced significantly more release of ibuprofen compared to neutral liposomes.

Mohammed *et al.*[200] demonstrated that the incorporation of charged lipids in PC: cholesterol liposomes also resulted in increased drug release compared with unmodified PC: cholesterol vesicles.[199] The positively charged liposomes exhibited the fastest release compared with neutral and negatively charged preparations. The inclusion of 9 mol% stearylamine

(positively charged) or dicetylphosphate (negatively charged) induced significantly more release of ibuprofen compared to neutral liposomes **Figure 2-10.**

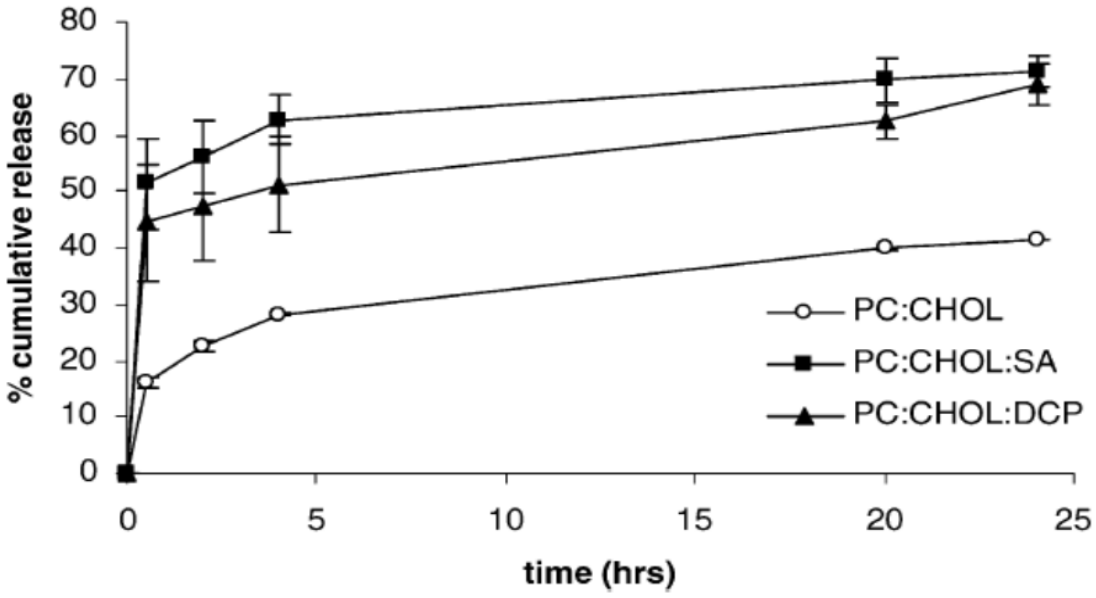


Figure 2-10: The effect of incorporation of 9 mol% stearylamine (positively charged) or dicetylphosphate (negatively charged) lipids induced significantly more release of ibuprofen compared to neutral liposomes. Image reproduced from Mohammed *et al*.[200]

Lipid Composition

Mohammed *et al*.[200] establish that the lipid composition also affects the drug release. The addition of a long alkyl chain lipid with PC-cholesterol resulted in an enhanced release rate of the drug, as shown in **Figure 2-11**. The influence of lipid alkyl chain length on ibuprofen encapsulation was investigated using liposomes prepared from Egg PC, DMPC (C14 alkyl chain length), DSPC (C18 alkyl chain length) or C24PC (C24 alkyl chain length). The substitution of PC by longer alkyl chain lipids influenced both ibuprofen incorporation and release rates. A trend of increasing ibuprofen loading and encapsulation efficiency with increasing lipid chain length was apparent.[200]

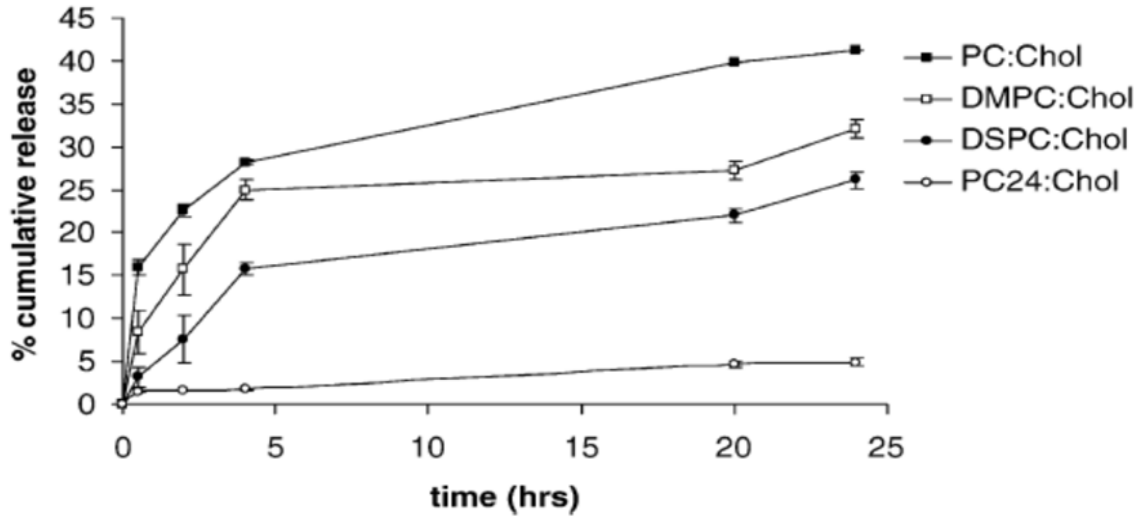


Figure 2-11: The effect of lipid alkyl chain length on the release profile of ibuprofen from liposomes in order of PC > DMPC > DSPC > PC24. Multilamellar vesicles incorporating ibuprofen composed of 16 mol PC, 4 mol cholesterol (Chol); 16 mol DMPC, 4 mol Chol; 16 mol DSPC, 4mol Chol; 16 mol C_{24}PC, 4 mol Chol were incubated 0.01M PBS at 37 ˚C for up to 24 h. Results represent mean ± S.D., n = 3. Image Mohammed *et al.*[200]

2.2.9. Drug release mechanism and kinetics

The mechanism of drug release from liposome was first proposed by Gregoriadis in 1973,[215] where he suggested that drug release was a result of accelerated diffusion through the liposomal membrane. The liposomal content release is based on the fact that liposomes lose all or some of their stability in different media and as a result expel some or all of their contents to the external environment over time. Two main parameters are involved in drug release from liposomes; the lipophilicity of the drug (or its ability to diffuse through lipid membranes), its aqueous solubility which will be the driving force moving drug molecules out of liposomes (for partitioning in the aqueous dispersion media).[216]

There are several behaviours used to describe drug release. Immediate release drug products are designed to dissolve drugs with no intent of delaying dissolution or absorption of the drug. Modified release dosage forms include both delayed and extended release drug products. Delayed release is defined as the release of a drug at a time other than immediately following administration. Extended-release drugs are formulated to make the drug available over an extended period after administration. And lastly, controlled release, which includes

the extended and pulsatile release of the drug. A pulsatile release is defined as the release of predictable amounts of drug at distinct time intervals that are loaded into the dosage form.[217]

2.3. Micelle based drug delivery systems

2.3.1. What are micelles?

Micelles are self-assembling colloidal dispersions of 5 to 100 nm in diameter with a hydrophobic core and hydrophilic shell that form spontaneously from amphiphilic or surface-active agents (surfactants), molecules of which consist of two clearly distinct regions with opposite affinities towards a given solvent.[218] At low concentrations in a liquid medium, these amphiphilic molecules exist separately; however, as their concentration is increased, aggregation takes place within a rather narrow concentration interval (see the principal scheme of micelle formation from an amphiphilic molecule in an aqueous medium in **Figure 2-12**). The aggregates include several dozens of amphiphilic molecules; usually, have a shape close to spherical, and are known as micelles. The concentration of a monomeric amphiphile at which micelles appear is called the critical micelle concentration (CMC).

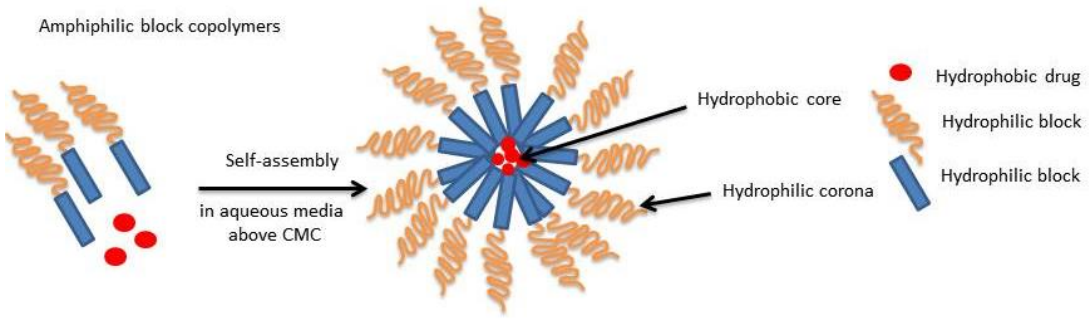


Figure 2-12: The general scheme of micelle formation from amphiphilic molecules. Image modified from Gutman *et al*.[218]

Polymeric micelles represent a specific class of micelles and are formed from copolymers consisting of both hydrophilic and hydrophobic monomer units. There exist several possible classifications of polymers and copolymers. Co-polymers include two types of monomeric

units differing in their solubility. The two types of monomeric groups can be polymerized into a polymeric chain in different fashions providing random, block and graft copolymers.[219]

2.3.2. Drug delivery using micelles

Micelle based drug delivery is specially focused on the hydrophobic character of the core which enables the inclusion of hydrophobic drugs, by physical means or chemical conjugation, and their dispersion at the molecular level, resulting in enhanced water-solubility.[65, 220-221]

The hydrophobic core of micelles is capable of carrying PWSDs with high loading capacity (i.e. 5–25% weight). Their core-shell structures facilitate the solubility and encapsulation of PWSDs and thus improve bioavailability and protect the drugs from degradation in biological systems. Micelles demonstrate a series of attractive properties as drug carriers; e.g. colloidal size, specific cell targeting capacity, minimised toxicity, their stability in the GI tract, good biocompatibility, and solubilizing property, high stability both *in vitro* and *in vivo* and can solubilize a broad variety of poorly soluble drugs.[65, 222-223]

Polymeric micelles are used in pharmaceutical formulations as a non-ionic, biodegradable and biocompatible polymer with effective micellization in aqueous solution.[224] They provide lower aggregation concentration values and are more thermodynamically stable than conventional or low molecular weight surfactants.[65, 76, 223] The dynamic structure, size (20–50 nm), hydrophilic corona, hydrophobic core and drug solubilizing capacity make polymeric micelles efficient and promising drug delivery carrier for PWSDs.[225-227] The most frequently used polymers are Pluronics and TPGS are reported as an effective drug delivery carrier for the poorly soluble anticancer drugs paclitaxel,[228-229 230] and tamoxifen,[230] 5 fluorouracil,[231-232] doxorubicin,[233-234] octaethylporphine (OEP), meso-tetraphenyl porphine (mTPP) and camptothecin (CPT),[222] and another drug Genistein.[235]

2.3.3. Drug incorporation in micelles

The solubilization and stable encapsulation of drug into polymeric micelles can primarily be achieved by chemical and physical methods. Chemical methods involve covalent core cross-linking of the drug with the polymers consisting of side-chain or end-group-functionalized block copolymers. An important factor to be considered using chemical methods is that the

reactive groups of the polymers should be sufficiently hydrophobic or low in number so that they do not interfere with the formation of monodisperse micelles. The most commonly employed methods for preparing core cross-linked polymeric micelles are: (i) radical polymerization, used for micelles containing polymerizable groups in their core; (ii) addition of bi-functional cross-linkers, used for micelles containing reactive groups in their core; and (iii) disulphide bridges, used for micelles containing thiol groups. The last method allows for stimuli-responsive disintegration and drug release. Although chemical crosslinking allows significant improvements in circulation kinetics, biodistribution and target site accumulation of micelles, the series of chemical reactions involved may sometimes be challenging and complicated. On the other hand, physical methods including (i) direct dissolution, (ii) dialysis, (iii) oil-in-water emulsion, (iv) solvent evaporation, (v) co-solvent evaporation and (vi) freeze-drying methods (**Figure 2-12**) are much simpler and practical.

Several modifications of polymeric micelles have been explored by scientists to improve drug loading (DL) including the size of both cores and corona-forming blocks. In the first case, the larger the hydrophobic block the bigger core size and its ability to entrap hydrophobic drugs. In the second case, the increase in the length of the hydrophilic block results in the increase of the critical micellar concentration (CMC) value, i.e. at a given concentration where micelles begin to form.[65] Drug loading efficiency was also found to be dependent on the aggregation number of the copolymer. Micelles showing a higher aggregation number allow a greater amount of drug to be solubilized in their inner core.[236] Additional mixed micelle-forming compounds may be added to polymeric micelles to improve drug loading. For example, egg phosphatidylcholine (PC) was added to the Polyethylene glycol-poly-ethanolamine (PEG-PE) based micelle composition to increase the encapsulation efficiency of paclitaxel.[223] Adding TPGS in the formulation also increased PTX loading[237] and cytotoxicity against multidrug-resistant (MDR) tumor significantly.[238]

2.3.4. Micelle preparation methods

There are several methods for preparation of drug-loaded micelles; i.e. the direct dissolution method, the dialysis method, oil/water emulsion method, solvent evaporation methods, co-solvent evaporation method and freeze-drying method (**Figure 2-13)**. In each particular case, the choice of the method is usually determined by the extent of the solubility of a micelle-forming block co-polymer in an aqueous medium.[218, 239223, 236, 240-241]

1. Direct dissolution method

The direct dissolution method (**Figure 2-13A)** is the simplest technique for the preparation of drug-loaded polymeric micelles.[242] This method is frequently applied for polymers possessing a certain degree of solubility in water. In direct dissolution, the co-polymer is simply directly dissolve in an aqueous medium (distilled water or buffer) at a normal or elevated temperature and at a concentration well above its CMC value. However, this technique is associated with low drug-loading which can be enhanced by increasing the temperature of the system before the addition of the copolymer. Preparation of a thin film of a drug before the addition of the polymer into the system can also result in higher drug loading.[242] The drug is then loaded into the micelles by stirring, heating and/or sonicating the mixture. This method is frequently applied for micelle preparation from pluronics and similar block co-polymers possessing a certain degree of solubility in water. Micelle-forming co-polymers with very low water solubility are converted into micelles by direct dissolution in a water-miscible organic solvent, such as dimethylsulfoxide dimethyl formamide, acetonitrile, tetrahydrofuran, etc., and subsequent dialysis against water.[218] Several water-insoluble drugs such as doxorubicin (DOX), nystatin, etoposide, and haloperidol have been successfully loaded into Pluronic® micelles using this method.[243-244]

However, the simple equilibration of the drug and micelles in water may not result in high levels of an incorporated drug. So, insoluble drugs can be incorporated in micelles by chemical conjugation or by physical entrapment through dialysis or emulsification techniques. Physical entrapment of drugs is generally done by the dialysis or oil-in-water emulsion procedure.

2. Dialysis method

The dialysis method (**Figure 2-13B**) is most frequently employed for preparation of micelles from copolymers that have fairly low aqueous solubility.[245-251] The drug along with the block copolymer is dissolved in a water-miscible organic solvent (such as N, N-di-methyl-formamide (N-DMF), dimethylsulfoxide (DMSO), dimethyl formamide (DMF), acetonitrile (ACN), tetrahydrofuran.) and the resultant solution is dialysed against water [252-255].

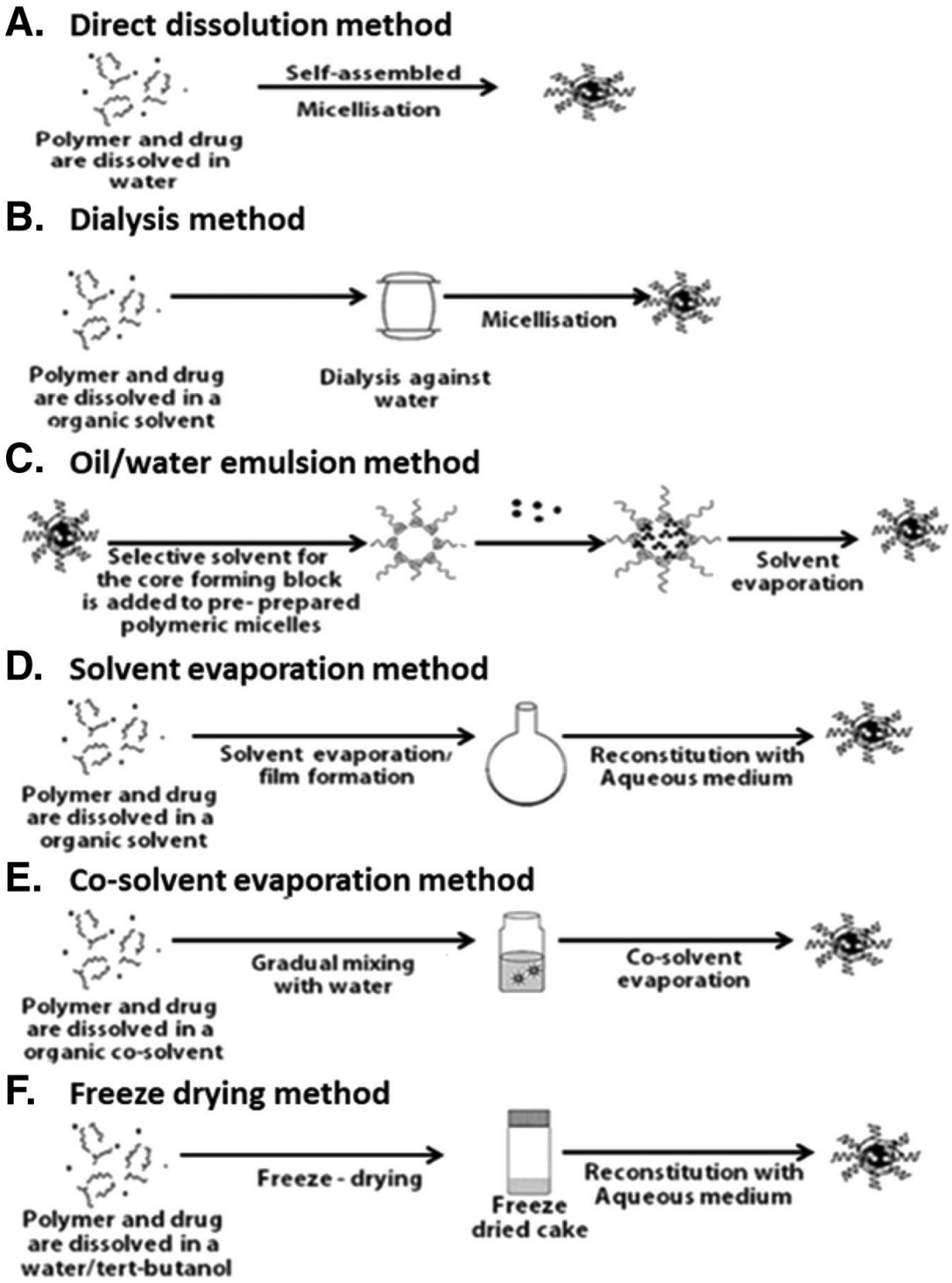


Figure 2-13: Physical methods of drug encapsulation into polymeric micelles: (A) direct dissolution; (B) dialysis; (C) oil-in-water emulsion; (D) solvent evaporation; (E) co-solvent evaporation; (F) freeze-drying (Image adapted from Aliabadi *et al*).[256]

During the dialysis process, the organic solvent is replaced by water which induces self-association of block copolymers and the entrapment of drug. The semipermeable membrane

of the dialysis bag keeps the drug encapsulated polymeric micelles inside. At the same time unloaded or free drug remains outside the dialysis bag. However, this method is only suitable for lab scale production, while incomplete removal of the free drug from the polymeric assemblies is another drawback. Alternatively, tangential flow filtration (TFF) is a fast and simple method that can be used for scalable manufacturing processes of polymeric micelles.[245-251, 257] This is one of the most widely used methods for preparation of drug-loaded micelles and has been employed to load various agents including ellipticine, DOX, FK506 and di-hydro-testosterone into a wide range of systems.[247, 249, 258]

For this method, it has been shown that the choice of solvent employed has a significant influence on the physical and drug loading properties of the micelles. Extending the dialysis over several days is required to ensure the complete removal of organic solvent. The dialysis method is the most commonly and widely used method for preparation of drug-loaded micelles.

3. Oil-in-water emulsion method

The drug is dissolved in a water-immiscible organic solvent (such as chloroform or methylene chloride), followed by addition of this organic to the aqueous phase under vigorous stirring. The polymer may be dissolved in either the organic or the aqueous phase and the organic solvent is then removed by evaporation (**Figure 2-13C**). The micelle-drug conjugate is formed as the solvent evaporates.[259-260] The main advantage of the dialysis procedure compared to the oil-in-water emulsion method is that the use of potentially toxic solvents such as chlorinated solvents can be avoided. Both dialysis and oil-in-water emulsion methods were compared for the incorporation of DOX in polyethylene oxide (PEO) ± (Poly-beta-benzyl L-aspartate) PBLA micelles. The emulsification method was more efficient since the DOX content of the micelles was estimated to be 12% (w/w) compared to 8% (w/w) for the dialysis technique.[236]

4. Solvent evaporation method

Another frequently used method for preparation of drug-loaded micelles is the solvent evaporation method (**Figure 2-13D**). In this method, polymer and drug are first dissolved in a common solvent or mixture of two miscible volatile organic solvents. A thin film of drug/polymer is formed at the bottom of the flask after the evaporation of the organic solvent.

This film is then reconstituted in an aqueous phase (water or buffer) by vigorous shaking.[247, 261-263] This method can be applied to micelle-forming block copolymers having high hydrophilic-lipophilic balance (HLB) values so that the polymer film can be easily reconstituted in an aqueous medium.[262, 264-266] In some cases, in order to obtain a mono-modal size distribution, the reconstituted samples are sonicated.[247, 267] For drug loading via this method, the extent of drug incorporation has been demonstrated to be largely dependent on the common solvent employed for initial dissolution of the copolymer and drug. Zhang *et al*. investigated a wide range of solvents in search for the most suitable co-solvent for both the drug and the copolymer concluded that only acetonitrile resulted in a clear solution following reconstitution of the dried copolymer-drug film.[262]

5. Co-solvent evaporation method

Drug and polymer are dissolved in a volatile water-miscible organic solvent (co-solvent) followed by addition of the aqueous phase (non-solvent for the core-forming block) which triggers the formation of micelles and drug entrapment. The organic co-solvent is evaporated at the end resulting in drug-loaded polymeric micelles (**Figure 2-13**E).[266, 268-270]

6. Freeze-drying method

This method is applicable for freeze-dryable organic solvents such as tert-butanol which can dissolve the polymer and the drug. The drug/polymer solution is then mixed with water, freeze-dried and reconstituted with isotonic aqueous media. This method is suitable for large-scale production. However, it is applicable only to block copolymers and drugs that can be solubilized in tert-butanol (**Figure 2-13F**).[271]

7. Poly ion complex method

Electrostatic interactions between oppositely charged polymer/drug combinations result in poly ion complex micelles. This method is suitable for different therapeutic moieties that carry charge including peptides and DNA. Upon neutralization of the charge, the core-forming segment of the block copolymer can induce self-assembly of the poly ion complex and further stabilization of the micelle.[272-275]

2.3.5. Factors affecting drug loading in micelles

Factors affecting drug loading in micelles are:

i. The degree of hydrophobicity of the micelles-forming polymers and the size of the micelle are the two main factors that affect drug loading levels in micelles. Studies have also shown that for a particular block copolymer micelle system, an increase in the length of the core-forming block can result in a higher level of drug loading.[239] In a study by Jette *et al.* micelles were formed with diameters of 22 nm and 41 nm and the loading levels of fenofibrate achieved were 35 mg/mL and 95 mg/mL, respectively.[276] Similar results were observed by Shuai *et al.* where the diameters of DOX-loaded copolymer micelles were 30 nm, 41 nm, 57 nm, and 86 nm, respectively, and the level of DOX-loaded in the micelles increased from 3.1% to 4.3% (w/w).[277]

ii. The miscibility and/or presence of specific interactions between the drug and the core-forming block have also been shown to have a large influence on the loading capacity and loading efficiency of micelles as reported in the literature.[247, 278]

iii. The preparation method of drug-loaded micelles influences the physicochemical properties of the micelle as well as the drug loading efficiency.[279-280]

iv. A balance exists between the drug loading level and the stability of the micelles. If the concentration of drugs increased to a point where it exceeds the solubilization capacity of the micelles notable precipitation will occur.[277]

2.3.6. In vitro drug release from micelles

Drug release studies from polymeric micelles have commonly been conducted using the dialysis method, e.g. a synthetic membrane separates the drug-loaded micelles from the free drug molecules.[225] Yan *et al.* [107] Investigated 5-FU release from micelles. A long-term sustained released of 5-FU was observed from micelles compared to free drug and provided a satisfactory delivery system **(Figure 2-14)**.

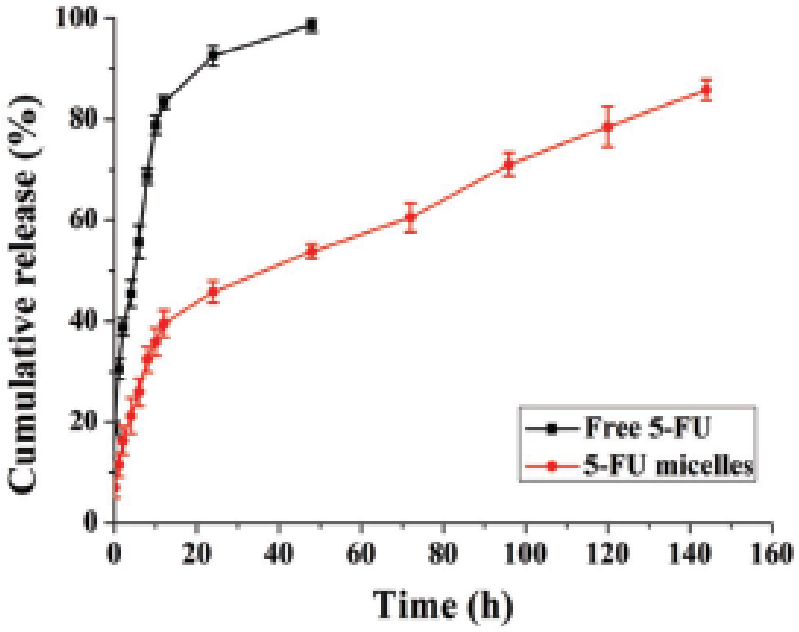


Figure 2-14: Drug release profiles of free 5-FU and 5-FU micelles in PBS solution at pH 7.4
Image reproduced from Yan *et al*.[107]

PTX loaded poly-(ε-caprolactone)-poly(ethylene-glycol)-poly(ε-caprolactone) PCEC copolymer mixed micelles with TPGS was developed by Bernabeu *et al*.[228] The mixed micelle system provided a sustained release of PTX compared to the pure micelles. Francis *et al*. investigated Cyclosporin A, a PWSD, release from polymeric micelles by the dialysis method and observed that < 12% drug was released from the micelles within 4 h.[70] TPGS micelles containing docetaxel was prepared by Muthu *et al.*[281] The percentage release of docetaxel (DTX) in PBS (pH 7.4) containing 0.1% w/v Tween 80 showed initial burst release (approximately 20–40% of DTX) followed by first-order release for more than 3 days **(Figure 2-15)**.

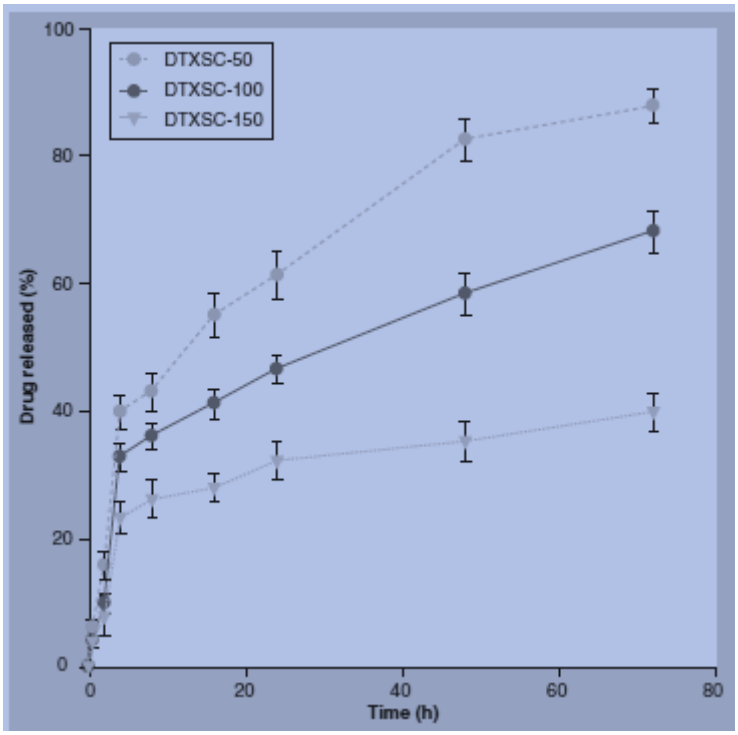


Figure 2-15: *In vitro* drug release kinetics of the docetaxel-loaded d-α-tocopheryl polyethylene glycol 1000 succinate micelles prepared by a solvent casting method in phosphate-buffered saline (pH 7.4). Bars represent (Mean ± SD, n = 3). DTXSC-50: Docetaxel-loaded micelles prepared with 2.5 mg docetaxel and 50 mg D -α-tocopheryl polyethylene glycol 1000 succinate (TPGS); DTXSC-100: Docetaxel-loaded micelles prepared with 2.5 mg docetaxel and 100 mg TPGS; DTXSC-150: Docetaxel-loaded micelles prepared with 2.5 mg docetaxel and 150 mg TPGS. Image reproduced from Muthu *et al.*[281]

2.3.7. Factors affecting drug release from micelles

Factors such as molecular weight and degree of hydrophobicity of the core-forming block have a significant influence on the rate of drug release from micelles along with the rigidity or flexibility of the micelles.[239]

Additional factors that affect drug release are-

i. **Crystallinity of the Drug**

When the drug is molecularly dissolved in the micelle core, the rate of release will be determined by the rate of diffusion of the drug from the micelles in the condition when there is no significant interaction present between the drug and the core-forming block. In this case, it has been found that the rate of drug release from the system is relatively fast. By contrast, if

the drug is dispersed in a crystalline state and/or phase separated from the polymer, the rate of release will depend on both the rates of dissolution and diffusion of the drug.

ii. Level of Drug Loaded

It has been reported that the rate of drug released from micelles decreases as the drug load is increased. For example, Lim *et al*. [245] studied the release profile for benzo[a]pyrene from polyethylene glycol -b-polycaprolactone (PEG-b-PCL) micelles as a function of the amount of agent loaded (i.e. 14 mM or 89 mM). Their study revealed that the probe was released more slowly when the drug was loaded at a higher level. Approximately 65% of the encapsulated drug was found to be released within 60 hours when loaded at 89 mM and 100% was released within the same period of time when the probe was present at 14 mM.[245] Liu *et al*. also found that for ellipticine loaded in PEG-b-PLA micelles, the drug release rate was significantly decreased when the drug loading level was increased from 4% to 10% (drug to polymer ratio wt/wt).[247]

However, the reverse trend also has been observed. Huh *et al*. reported an increase in the drug release rate with an increase in the amount of drug loaded for PTX from PEG-b-poly(2-(4-vinylbenzyloxy)-N, N-diethylnicotinamide) micelles.[282]

iii. Influence of Polymer-Drug Compatibility on Drug Release

The degree of miscibility between the drug and the core-forming block is known to influence the rate of release of drug from the micelles. If there is a high degree of miscibility between the drug and the core-forming block it is likely that the drug will be molecularly dissolved within the core. In this way, the drug will not be present in a crystalline form and thus dissolution will not be required prior to diffusion mediated release of the drug from the micelles. Therefore, it may be anticipated that molecularly dissolved drug that is homogeneously distributed throughout the core would be released more quickly from the micelles.

iv. Molecular Weight and Molecular Volume of the Drug

The diffusion of small molecules or drugs in a polymer matrix is sensitive to the molecular weight and molecular volume of the diffusate. This is due to the fact that with an increase in the molecular weight of the diffusate, more segments of the polymer must reorient in order to

allow the molecule to move from one site to another. Studies have shown a critical dependence of the diffusion coefficient on the molecular weight and volume of the diffusate.[283-284] Berens *et al*. [283] reported an exponential relationship between the molecular size and the diffusion coefficient of various diffusates in polymer matrices.[283]

2.3.8. Drug release mechanism from micelles

Drug release from polymeric micelles mainly depends upon the number of factors including the design and method used for their preparation, the structure of the micelle-forming block copolymer and the drug, their physicochemical properties; and the localization of the drug in the polymeric micelles. This was shown in **Figure 2-16** the various modes of drug release from polymeric micelles. Drug release from polymer-drug conjugates generally follows two mechanisms, firstly, dissociation of micelles followed by drug cleavage from the polymeric unimers or drug cleavage inside the micellar structure followed by diffusion out of the carrier (**Figure 2-16A**). Drug release from drug-loaded micellar carriers is usually preceded by diffusion (Figure 2-17B), whereas drug release from poly ion complex micelles is triggered via ion exchange in physiological media (**Figure 2-16C**).[256]

Apart from these basic drug release mechanisms, instant, sustained, pulsed or delayed drug release can be achieved by modifying the chemical structure of the micelle-forming block copolymers which will ultimately modify the physicochemical properties of the core/shell forming blocks,[285] For example the rigidity of the micellar core which limits the movement of water and free ions to the micellar core in micelle-forming drug conjugates and poly ion complex micelles.[286-287]

The lower rate of micellar dissociation, the diffusion of drug and the overall drug release from micellar carriers can also be achieved via crosslinking of the micellar core structure and the induction of strong hydrophobic interactions or hydrogen bonds between the core-forming blocks and the drug.[288-289] The incorporation of hydrophilic or stimuli-responsive groups to the core structure may be another avenue to provide an instant or pulsed mode of drug delivery.[289-291]

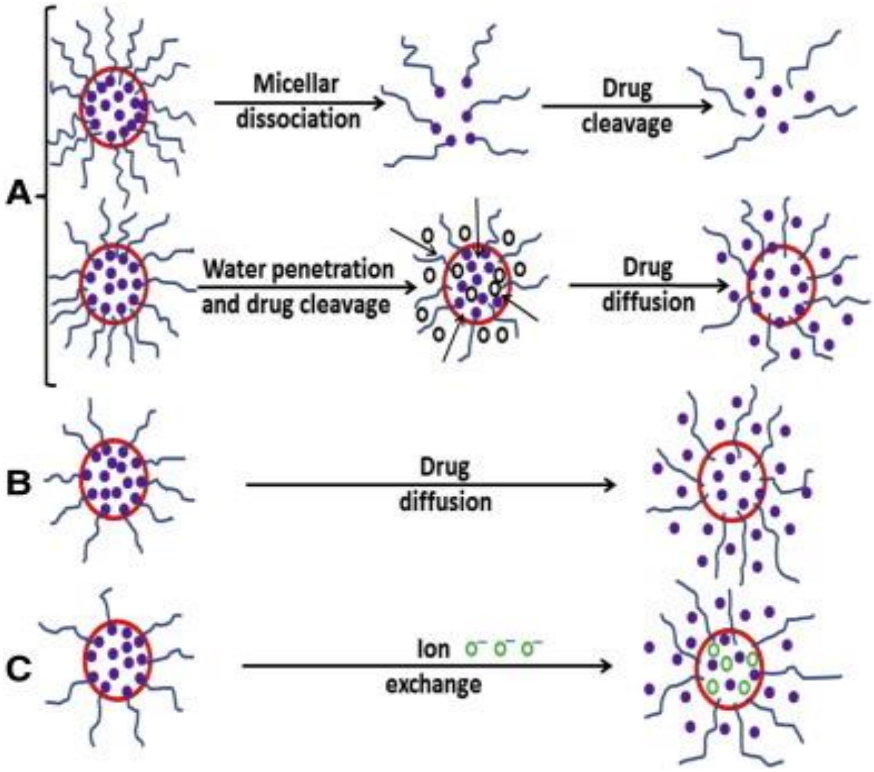


Figure 2-16: Mechanism of drug release from polymeric micelles. (A) drug release from block copolymer-drug conjugates, (B) drug release from drug encapsulated micellar carriers and (C) drug release from poly ion complex micelles. Image adapted from Aliabadi *et al.*[256]

Some mathematical models used to describe drug release phenomena are the Higuchi, zero-order, first order and Korsmeyer-Peppas models.[292] Korsmeyer *et al.*[292] derived a simple relationship widely used to describe drug release from a polymeric system (**Equation 2-1**). To determine the mechanism of drug release, drug release data were fitted to the Korsmeyer–Pappas model:

$$\frac{Mt}{M\infty} = Kt^n \quad \text{..... Equation 2-1}$$

Where Mt/M_∞ is the fraction of the drug released at time t, k is the rate constant and n is the release exponent. The n value is used to characterise different release mechanisms; *e.g.* Fickian diffusion, anomalous (non-Fickian).

In order to access more details of the release mechanism, the diffusion coefficient (D) of the drug molecules in the nanocarrier matrix may be derived using the non-steady-state diffusion model equation as described elsewhere,[293] (Equation 2-2)

$$M_t/M_\infty = 4(Dt/\pi\lambda^2)^{1/2} \qquad \textit{Equation (2-2)}$$

Where M_t is the total amount of molecules released during the measurement, M_∞ is the total amount of molecules that are kept in the matrix, λ is the thickness, (t) is the time of the measurement, and D is the diffusion coefficient of the molecule.

To date, the overall mechanism for the release of physically entrapped drug from micelles has not been fully clarified. However, it is hypothesised that, as for most polymer-based nano-sized delivery systems, diffusion and polymer degradation are the major mechanisms for drug release.[294-295] Multiple mechanisms are involved in the release of drug from a polymer, where diffusion was predominant.

Diffusion of the drug may be considered as the dominant mechanism for a drug release. The diffusion of a drug in a polymer matrix may be described by Fick's first law.[296] The amount of a diffusate crossing a given area is proportional to the spatial gradient of concentration and the diffusion coefficient of the diffusate (**Eqn 2-3**).

$$\frac{dMt}{dt} = ADCsm/x \ldots\ldots\ldots\ldots\ldots\ldots\ldots \textbf{Eqn 2-3}$$

Where M_t is the amount of drug released at time t, A is the total surface area of the micelles, D is the diffusion coefficient of the drug and C_{sm} is the solubility of the drug in the polymer core.

In Kim's study, a Fickian model was employed to evaluate the release behaviour of indomethacin from a PEG-b-PLLA micelle system.[294] A Higuchi model was used by Lim *et al*. to evaluate the release kinetics of two hydrophobic drugs in PEG-b-PCL micelle systems.[245] Saxena *et al*. demonstrated that the release of Gambolic acid from Poloxamer 407/TPGS mixed micelles might be followed by diffusion, polymer erosion or swelling mechanisms.[297]

2.4. Cellular activity of liposome and micelles and drug absorption

Drug absorption across biological membranes is a complex multi-pathway process which is directly related to its permeability.[298] The cell permeability of biological membranes is one of the most important determinants of the absorption processes of a drug in early stages of drug

development for orally administered drugs. Human colon carcinoma (Caco-2) cells are well-established, simple, reproducible, commonly and most widely used as an *in vitro* model[299] that mimic the desired intestinal epithelial tight junctions to determine the permeability, cellular uptake,[300] oral drug absorption mechanism and rate[301] and bioavailability of drugs[302-306] encapsulated in liposomes[66] and micelles.[67-68] Both liposomes and micelles have demonstrated improved cellular permeability and transport of their formulation on the Caco-2 cell line compared to free drug.[69-70]

2.4.1. Mucosal Surface as Potential Site for Liposome Uptake

Human mucosa extends to a surface area of at least 200 times that of the skin, amounting to more than 400 m^2 in adults. Mucus-covered enterocytes (**Figure 2-17**), representing the largest population of cells in the mucosa of the small intestine (around 90%), are arranged as a single cell monolayer at the gastrointestinal surface.[307] Although the penetration of potentially toxic materials and harmful pathogens is restricted, the mucosal surface is not a completely impenetrable barrier.

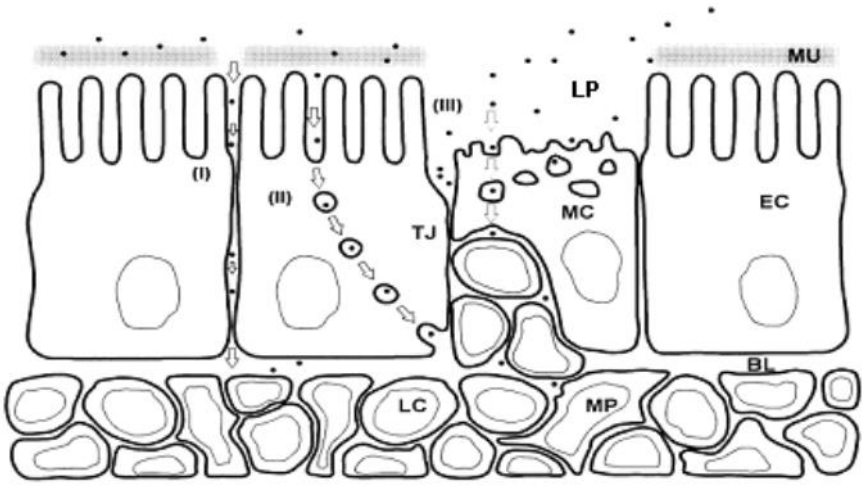


Figure 2-17: Schematic drawing of mucus (MU) covered absorptive enterocytes (EC) and M cells (MC) in the small intestine. Lymphocytes (LC) and macrophages (MP) from underlying lymphoid tissue can pass the basal lamina (BL) and reach the epithelial cell layer which is sealed by tight junctions (TJ). Possible translocation routes for liposomes (LP) are (I) paracellular uptake, (II) endocytotic uptake by enterocytes and (III) M cells. Image adapted from Jung *et al*.[307]

In intestinal tissues, highly specialized enterocytes, the membranous micro-fold (M) cells, collect antigens and macromolecules from the gastrointestinal surface. Absorptive enterocytes and M cells constitute the follicle-associated epithelia (FAE). The FAE shuttle

colloidal antigens, small bacteria, and viruses, via a transcytotic mechanism to lymphoid micro compartments which are in close contact with their covering epithelia.[308] This physiological transport mechanism is thought to be of particular relevance for colloidal carriers, such as liposomes which are capable of enhancing the interaction mechanisms of the drug delivery systems and the epithelial cells in the GIT i.e. hydrophobic particles are transported through the gut-associated lymphoid tissue, whereas hydrophilic particles are transported across the enterocytes.[309] The surface of enterocytes and M cells display cell-specific carbohydrates, which may serve as binding sites to liposomes containing appropriate ligands.[310] Certain glycoproteins and lectins bind selectively to this type of surface structure by a specific receptor-mediated mechanism.

In general, the gastrointestinal absorption of liposomes involves either the paracellular route or by interaction with cells (enterocytes and M cells) and occurs through a variety of postulated mechanisms such as endocytosis, fusion, adsorption and lipid exchange,[311] which are shown schematically in **Figure 2-18.**

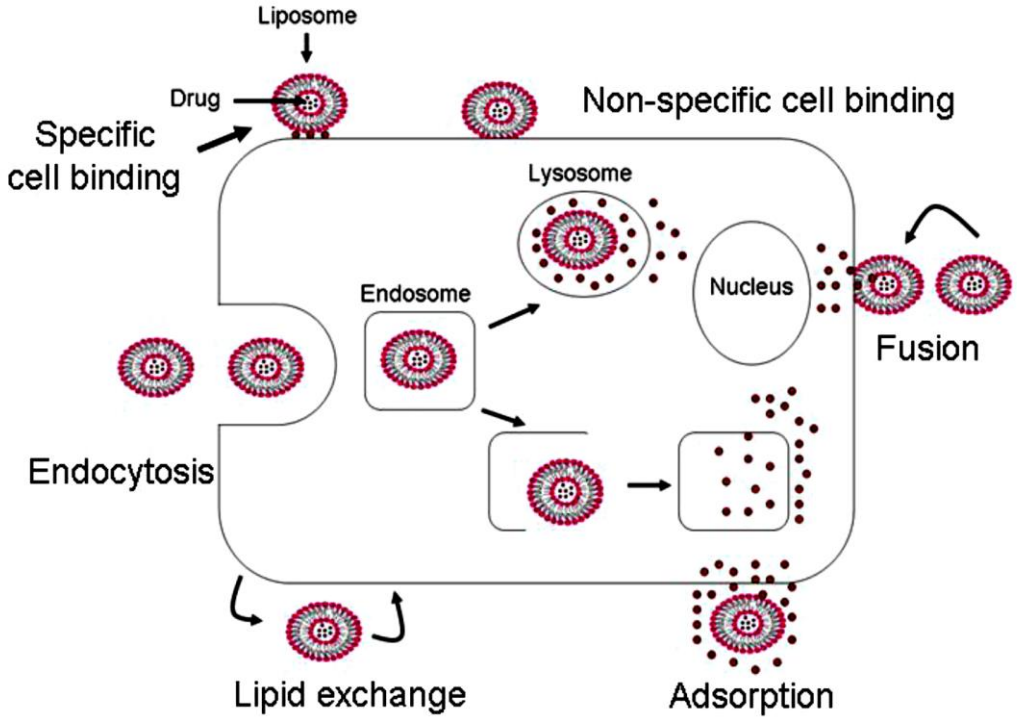


Figure 2-18: Different interactions of liposomes to the cell. Image adapted from Lasic *et al*.[311]

The paracellular route of absorption of liposomes utilizes less than 1% of a mucosal surface area.[307] Using polymers such as chitosan, starch or poly (acrylate) the paracellular permeability of liposomes can be enhanced. The endocytotic pathway for absorption of liposomes is either by receptor-mediated endocytosis or absorptive endocytosis which does not need any ligands.[312] In the case of endocytosis, a liposome can be delivered by the endosome into the lysosome; the liposome can provoke endosome destabilization resulting in drug liberation into the cell cytoplasm. Adsorptive endocytosis depends primarily on the size and surface properties of the liposomes. If liposomes are positive or uncharged, it will provide an affinity to adsorptive enterocytes through hydrophobic interaction, whereas negatively charged and hydrophilic liposomes show a greater affinity to adsorptive enterocytes and M-cells. This shows that a combination of size, surface charge, and hydrophilicity play a major role in affinity. Making use of the fact that the gastrointestinal mucosal surfaces are negatively charged and the mucus is composed of glycoproteins bearing different sugar moieties, such as N-acetylgalactosamine, N-acetyl glucosamine, galactose and L-fucose, drug delivery systems can be made adhesive to the mucus layer via non-specific binding, or by specific ligand-receptor interactions with the mucosal cells.[313]

Liposomes can also fuse with the cell membrane and release their drug contents into the cell cytoplasm, or when absorbed on the cell surface can be destabilized by the cell membrane components resulting in the released drug to enter the cell via micro pinocytosis.[314] Adsorption is, in the case of smaller liposomes, largely independent of the fluidity of the membrane. If adsorbed liposomes may leak part of their encapsulated drug, which can then enter the cell by diffusion. In addition, liposomes can even undergo the direct or transfer-protein mediated exchange of lipid components with the cell membrane. Lipid exchange occurs due to the fact that lipids themselves have small aqueous solubility and therefore the liposomes and cell membranes can exchange lipid molecules. Such exchange is higher for liposomes in a liquid crystalline phase and for lipids with shorter hydrocarbon chains.[315] However, all of these interaction mechanisms are initiated by an adsorption step; this may or may not be followed by an endocytic sequence of events or by fusion with the plasma membrane.[316]

2.4.2. Improved cellular activity of drugs encapsulated in liposomes or micelles

Some examples are provided below as evidence of improved cellular activity of liposome and micelle encapsulated drugs compared to un-encapsulated drugs.

2.4.2.1. Liposomes

Qi *et al.*[317] developed a simvastatin (SMV) loaded liposome to compare the cytotoxicity of free drug and liposomal formulation. A decreased cell viability with increasing SMV concentration in the liposomes was observed. SMV loaded liposomes significantly improved the transport through Caco-2 cell monolayers compared to free SMV. The small particle size and negative zeta potential 141.7 nm and -4.54 (mV) respectively improved the transport through Caco-2 cell monolayers **(Figure 2-19).** Guan *et al.*[69] also showed with different bile salt (BS) liposomes containing stable Cyclosporin A cell monolayer permeability was size and concentration dependent. Muthu and co-workers developed a PTX-liposome which showed a significantly higher cytotoxic effect compared with the commercial docetaxel (Taxotere) preparation in Human Caucasian breast adenocarcinoma (MCF-7) cells (IC_{50}=0.23 for liposomes versus 9.54 for Taxotere).[208]

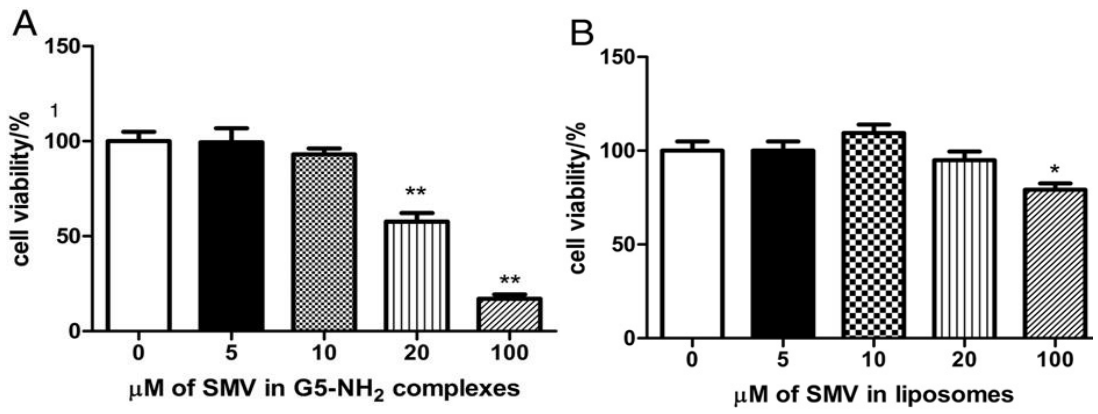


Figure 2-19: Viability of Caco-2 cells after the cells were treated with different concentrations of the SMV/G5-NH2 (A) or the SMV-liposomes (B) compared with the control group. n = 3. Image reproduced from Qi *et al.*[317]

2.4.2.2. Micelles

Similarly to liposomes, micelles have been reported to improve cellular permeability of loaded drug molecules compared to free drug. The apical to basal permeability of Cyclosporin A across Caco-2 cells, increased 1.5- and 3-fold (compared to free cyclosporin A) of two polymeric micelles, hydroxy propyl cellulose-grafted-polyoxyethylene cetyl ether (HPC-C_{16}) and dextran-grafted-polyoxyethylene cetyl ether (DEX-C_{16}).[70] Similar results were found with PTX and parthenolide when co-administered through mixed DSPE-PEG/TPGS micelles against Taxol-sensitive and resistant non-small cell lung cancer (NSCL) cell lines[318] and for atorvastatin (ATV) loaded stearyl chitosan (SC) and sulfated stearyl chitosan (S-SC) micelles in two cell lines; human breast adenocarcinoma cell line (MCF-7) and human colon carcinoma cell line (HCT-116) compared to free drug.[319] It was also reported that docetaxel-loaded TPGS micelles[281] exhibit higher cytotoxicity compared to Taxotere®. It was reported by Bernabeu *et al.* that increased intracellular uptake of micelles occurred as a result of the accumulation of the slightly negatively charged micelles at the few cationic sites present on the cancer cell surface (**Figure 2-20**).[228]

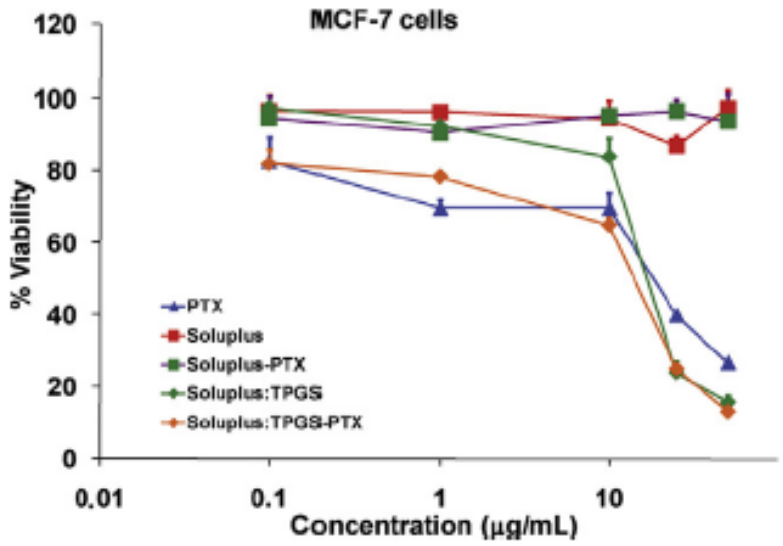


Figure 2-20: Cell viability of MCF-7 cells after 48 h of treatment with PTX, blank single micelles (Soluplus®), blank mixed micelles (Soluplus®: TPGS), PTX-loaded Soluplus®micelles and PTX-loaded Soluplus®: TPGS mixed micelles. Image reproduced from Bernabeu *et al.*[228]

Although many PWSDs are successfully encapsulated into liposomes and micelles, limitations still exist. There is a gap between current research of liposomes and micelles to a successful formulation for oral delivery.

2.5. Liposomes and micelles as a temperature-sensitive carrier for chemotherapy

Liposomes respond to a variety of basic signals generated by the tumor microenvironment like low pH, elevated redox potential, over-expressed enzymes and hyperthermia as well as to externally applied stimuli such as a magnetic field, ultrasound or light have been developed to trigger site-specific drug release.[37]

Hyperthermia is a pathophysiological condition. Inflammation and cancer promote cell environmental conditions with lowered pH and elevated temperature; in the range of 40–45°C with higher blood flow that also causes vasculature permeability as compared to that in normal tissues (37°C).[320-321] In the clinic, hyperthermia has been administered as an adjuvant therapy to improve the therapeutic effect combined with radiation or chemotherapy. It is now considered the fourth modality of cancer treatment. Mild hyperthermia has not been found to be associated with any toxicity in contrast to radiotherapy and chemotherapy. Instead, when tumors are exposed to hyperthermia, the tumor blood flow and oxygenation increased, which would improve the delivery of liposomal drugs to tumors.[322-325]

On the basis of hyperthermia, thermosensitive liposomes (TSLs) were first suggested by Yatvin *et al.* in the late 1970s.[43] Thermo Dox® (Celsion Corporation), a temperature-sensitive PEGylated liposomal doxorubicin (DOX) delivered via intravenous injection [326], is already in phase III study for unresectable hepatocellular carcinoma, and in earlier phases of clinical trials for other tumor types.[207, 327-328] Liposome thermosensitivity arises by mild hyperthermia (up to 42°C) on thermosensitive carriers, from the property of some lipids to possess a phase transition temperature (T_m) higher than physiological temperature **(Figure 2-21)**. Above the phase transition temperature, lipids exhibit a conformational change leading to liposome rupture and release of the encapsulated drug.

Commonly used lipids in TSL systems were composed mainly of DPPC or DPPG lipids mixed with other types of lipids like DSPC and HSPC lipids to tune the T_m, rate

of drug release, and their crystalline transition temperature (T_g). The rate of drug release upon heating was more than 3- 4 times that of normal/conventional liposomes.[51-52, 207]

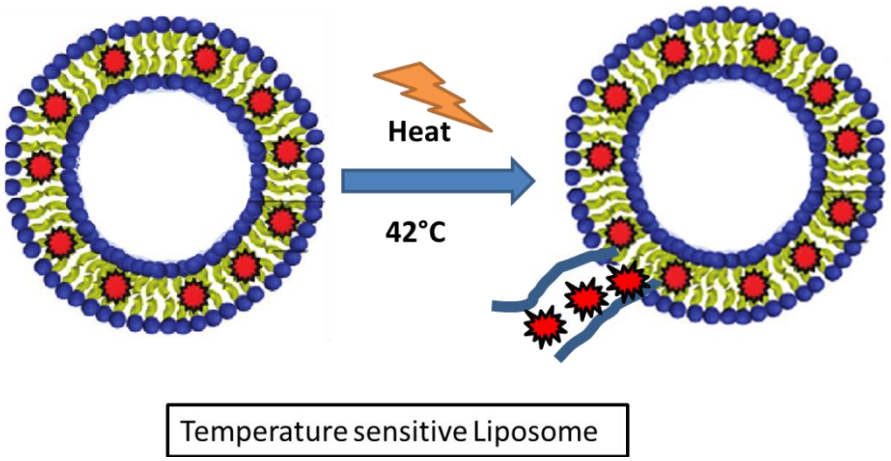


Figure 2-21: Schematic representation of temperature-triggered release from temperature sensitive liposome.

For example, physically and chemically stable paclitaxel loaded thermoresponsive liposomes were formulated by Wang *et al.*[329] using the thermosensitive lipid, dipalmitoyl phosphatidylcholine (DPPC-a T_m of 41.5±0.5°C) with PTX to increase the anti-tumor activity of PTX liposomes. The mean particle diameter was about 100 nm, and the entrapment efficiency was larger than 95%. The resulting drug release rate was higher at 42°C compared to 37°C from PTX-TSL **(Figure 2-22)**.

Another anticancer drug 5-fluorouracil (5-FU) was also encapsulated into a thermosensitive liposome with dipalmitoyl-sn-glycero-3-phosphocholine, cholesterol and 1,2-distearoyl-sn-glycero-3-phosphoethanolamine-N-PEG2000 (thermosensitive lipid dipalmitoylphosphatidylcholine DPPC with T_m of 41.5±0.5°C),[330] with an encapsulation efficiency of 37%. At 42°C, heat-triggered 5-FU release from TSLs was 63% within 10 min, whereas it remained below 20% for the non-thermosensitive formulation. The cytotoxicity assay revealed that formulation toxicity arose from 5-FU and not from the excipients. In addition, 5-FU complex encapsulation into TSLs induced a reduction of the IC_{50} from 115 down to 49 µM **(Figure 2-23)**.

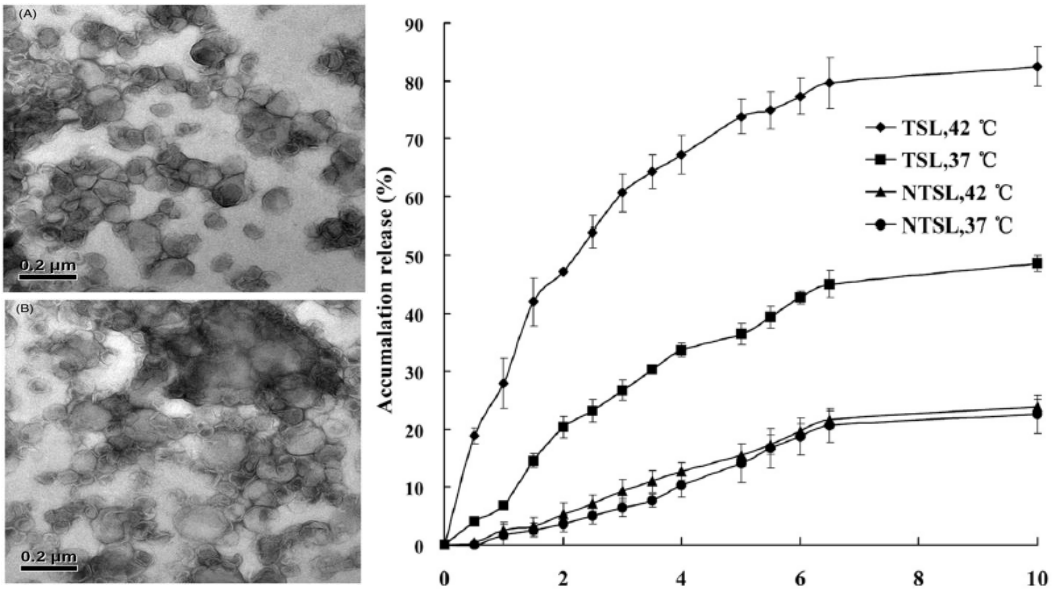


Figure 2-22: Transmission electron microscope photos of (A) PTX-TSL and (B) NTSL. (C) In vitro, drug release from PTX-TSL and NTSL in vitro, determined at 37°C and 42°C, respectively in PBS (pH 7.4) containing 0.5 M sodium salicylate. Image reproduced from Wang *et al*.[329]

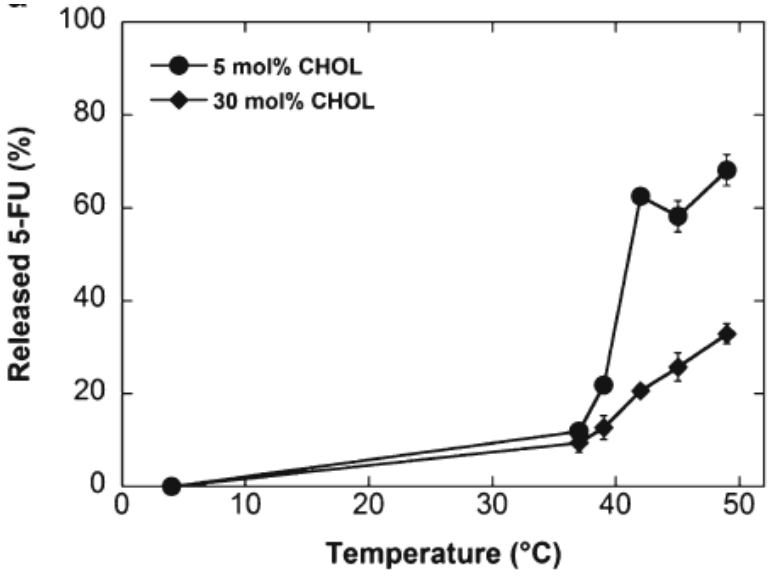


Figure 2-23: Release profile in PBS of encapsulated 5-FU-Cu-PEI from 5-FU-Cu-PEI-loaded liposomes upon heating for 10min in (a) water bath at 37, 39, 42, 45 and 49°C after dilution by 10 mM PBS (1776 mM dextrose). Image reproduced from Al Sabbagh *et al*.[330]

Moreover, additional studies also reported that thermosensitive mixed liposomes with lipids and copolymer of N-isopropyl-acrylamide and N-acryloyl-pyrrolidine increased the release rate of the content from the liposomes under mild hyperthermic conditions (41-42°C).[331-333]

Thus, several new studies have introduced the idea of modifications to the bilayer composition or surface of liposomes with temperature-sensitive polymers that retain temperature-triggered release from the liposome. Such modifications may prove useful but require further investigation.

2.6. Current challenges of liposome and micelles as drug delivery

Formulation scientists are continuously trying to develop robust drug delivery vectors by using polymers lipid or combination of them. Among them, liposomes are often cited as the dominant nanocarrier today[25] though there are series of problems including low encapsulation efficiency, physical instability and poor cellular activities that limit their use.[71, 80, 121, 125-126,170] Polymeric micellar oral formulations from bench to the clinic have been challenging. The main hurdles are low loading efficiency and poor GI stability, complexity in transport through GI membrane, efflux by some transporters and lack of stability in blood.[65, 68, 334-335] Moreover, polymeric micelles with sustained release characteristics are desired to further improve patient compliance and decrease related side effect.[335]

In recent years, there have been many developments and improvements in thermosensitive liposomal drug delivery system; however, there are many barriers to the thermosensitive liposomal formulations demonstrated improved therapeutic activity.[325, 336-337] A promising approach is required very precise heating of the tumor and fast release from the nanocarriers in combination with drugs that are rapidly taken up by tumor vasculature and/or tumor cells. Up to now, only a limited number of studies focused on the targeted thermosensitive drug delivery approach of the formulation are that the unloading of the drug at the target site is very poor. This opens up a new challenge to trigger drug release at the target site, while still retaining most of the drug inside the carrier while it resides in the bloodstream.[170]

In addition, multidrug resistance (MDR) is a major challenge to the effective treatment of cancer and refers to a state of resilience against functionally and structurally unrelated chemotherapeutic agents.[338] However, over the past several years the concept of using combination drug delivery overcomes MDR by addressing tumor heterogeneity as well as to improve the clinical efficacy of acceptable clinical toxicity profile.[339-340] by reducing the dosage of the drugs to reduce cytotoxicity while maintaining treatment efficacy by inducing

synergistic killing cancer cells,[341-344] yet, the proper combination with optimum therapeutic effect is not achieved.

Extensive studies in this field, especially pharmacokinetics and anti-tumor efficacy, are required. Still, the bioavailability of some polymeric micelles is quite low after oral administration, some novel strategies need to be taken to further increase their absorption across the intestinal membrane with high safety for the promise of clinical application.[335]

2.7. Liposome-micelles-hybrid system (LMH) as a project goal

Both liposome and micelle-based drug delivery systems have advantages and limitations for the oral delivery of poorly water-soluble drugs. In this research, it is proposed that a combination of liposomes and micelles, as a dual drug loading system, may provide benefits as a new robust drug delivery platform. A few lipid-polymer hybrid nanoparticle studies have been reported in the literature,[345-346] indicating there is enormous potential to improve the oral absorption of poorly soluble drugs by combining the operation of liposomes and micelles in hybrid formulations (LMH), which will also be beneficial in terms of resolving the limitations of the individual delivery systems.

Specifically, an LMH carrier based on different types of polymeric micelles and lipids will be engineered to address the major challenges associated with conventional liposome-based drug delivery systems: (i) drug loading efficiency, (ii) colloidal stability, (iii) release profile, and (iv) poor absorption of water-insoluble drugs. A thermoresponsive liposomal-micellar hybrid (LMH) system could also be developed for improved drug loading efficiency and colloidal stability with a controlled oral delivery of PWSDs, paclitaxel, and 5-FU to tune their water solubility, entrapment efficiency, particle size, greater controlled release and tumor cell uptake.

Chapter Three

3. Liposome-Micelle-Hybrid System for Oral Delivery of Poorly Water-Soluble Drugs

Chapter outline

In this chapter, the development of a novel liposome-micelle-hybrid (LMH) system is described, along with the drug delivery performance of the LMH system compared with the individual liposomes and micelles systems. Specifically, the micelles were developed based on commonly used polymers and surfactants that are widely used for drug delivery, including poloxamer 407 (P-407), deoxycholate (DC) a bile salt, vitamin E, d-α-tocopherol polyethylene glycol 1000 succinate (TPGS), to rationalise their physical characteristics and influence of their chemical structure on drug loading and release capabilities. Similarly, liposomes were also developed using different lipids: including phosphatidylcholine (PC), cholesterol (CHO) and distearoyl phosphatidyl glycerol-Na (DSPG), as well as combinations of these lipids to optimise their physical characteristics and drug loading. Finally, a combination of micelles and liposomes, a LMH was developed. Different methods of lovastatin (LOV) loading were investigated to determine how to incorporate the micelles into the liposomes. A key part of this study was to optimize the drug loading and the drug encapsulation efficiency of LOV into LMH.

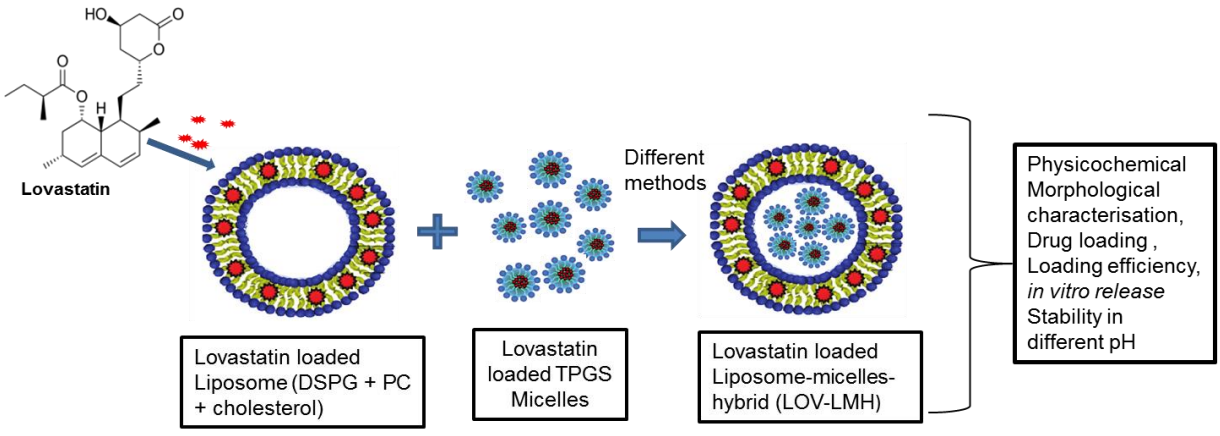


Figure 3-1: Schematically presentation of LOV-LMH.

Initially, micelles were prepared using a P-407 and then poloxamer 188 thin film hydration method. After that mixed micelles were prepared with P-407, DC and TPGS using the same method for optimising the physical properties as well as to improve physical characteristics and drug loading. Micelles prepared with TPGS were found to be more stable and with greater drug loading capability compared to the other polymers used.

Next, liposomes were prepared with PC/CHO, that were neutral or slightly negatively charged and found to be unstable in 1 mM NaCl solution (pH 5.5) after 1 week in 4 °C. DSPG was then included in PC/CHO to optimise the physicochemical properties and drug loading of the liposomes. Negatively charged DSPG lipids were included in the liposomes, as charged liposomes (DSPG/PC) were more stable (more than 3 months) than the neutral liposomes prepared from PC/CHO alone. LMHs were prepared using a combination of the DSPG/PC/CHO liposomes and TPGS micelles described above. Several critical parameters for successful preparation of a stable hybrid system were identified, including: optimised physical properties of the micelles, charge of the lipids used for liposomes preparation, temperature during preparation, pH of the hydration media, solvent composition for complete solubility of the lipids and drugs, and finally different preparation methods to improve drug loading. LMH's underwent physicochemical characterisation with and without encapsulated drug LOV.

Encapsulation efficiency and loading were determined. The structure of the hybrid was assessed using cryo-transmission electron microscopy (Cryo-TEM) to image the LMH structure, as well as visualising any morphological changes taking place upon encapsulation of micelles within the liposomes. Under simulated intestinal conditions, *in vitro* drug release was performed. Physical stability studies were monitored at different pH and drug quantity was assayed upon storage condition at 4 °C for up to 3 months.

3.1. Introduction

Poorly water-soluble drug candidates often emerge from contemporary drug discovery programs, and present formulators with considerable technical challenges and difficulties; for formulation design such as; low/poor encapsulation efficiency, poor drug release kinetics i.e. burst release, no sustained release effect, stability i.e. drug leakage, aggregation, drug expulsion, biological issues i.e. poor biodistribution, toxicity and other issues; i.e. scalability,

lack of good manufacturing practice, etc.[6, 138, 347] LOV is a BCS Class II drug *(*i.e. high permeability and low solubility) with limited aqueous solubility (0.4 mg/L), highly lipophilic (log P 4.26) and low oral bioavailability, typically < 5%.[79,93, 348] It is widely used and the first of a new class of cholesterol-lowering drugs that reversibly and competitively inhibit hydroxymethyl glutaryl coenzyme A reductase (HMG-CoA), an enzyme involved in the biosynthesis of cholesterol.[108, 349] Due to insolubility and high lipophilicity, LOV undergoes extensive first-pass extraction in the liver, resulting in low and variable bioavailability and pre-systemic metabolism.[111, 350]

To overcome this challenge and enhance its aqueous solubility and oral bioavailability, numerous drug delivery systems (DDS) are utilised,[351-356] such as; mesoporous nano matrix-supported delivery systems,[357-358] solid lipid nanoparticles,[359-361] emulsions (micro/nano),[362-363] microspheres,[364] nanostructured lipid carriers,[365-366] micelles[111] and liposomes.[203, 367-368] Among them, micelles have been considered excellent candidates for encapsulation of statin drugs due to their mainly hydrophobic characteristics. Micelles are a promising DDS for enhancing the bioavailability and reducing the toxic side effects of hydrophobic drugs as a result of significant benefits in terms of drug loading, release, delivery, and stability.[369-370] In recent years, there has been an increasing interest in the development of novel approaches using liposome-based drug delivery systems, e.g. elastic liposomes, conventional liposomes, proliposomes and niosomes etc.[371] These systems improve drug uptake by presenting the drug in a solubilised form rather than a crystalline material from which absorption may occur easily.[31-34]

Micelles are also widely investigated for the poorly water-soluble drugs delivery challenge because of their unique core-shell architecture in which the hydrophobic core serves as a reservoir for hydrophobic drugs.[111, 370] This hydrophobic core can protect drugs from decomposition and control their release, while the hydrophilic shell imparts steric stabilization in physiological fluids and enables active targeting. Because of the unique core-shell architecture and small size (diameter usually less than 100 nm), such micelles are not susceptible to recognition and uptake by the reticuloendothelial system (RES), hepatic excretion, or renal excretion.[241, 372] Therefore, they are normally used as sustained-release drug carriers to prolong the circulation time of the drug in the blood and improve bioavailability.[373] In earlier studies, a micellar formulation of another statin drug (SMV) loaded poly(ethylene glycol)-poly(Ɛ-caprolactone) (PECL) was reported by Liu *et al.* that

showed enhanced solubility and prolonged release behavior of SV.[370] Another statin drug Atorvastatin encapsulated in micelles exhibited a sustained release.[319] Despite these promising results, research based on micellar DDSs for statin drugs is still at an early stage and powerful delivery formulations are still required clinically for oral administration.

There has been increasing interest in liposome-based formulations to improve the oral bioavailability of LOV due to their potential to enhance the intestinal absorption of the drug avoiding hepatic metabolism.[203, 368,151, 367, 374] A recent study described the development of a proliposomal formulation of LOV to decrease the hepatic first-pass metabolism and there by improving the bioavailability of the highly metabolized LOV.[368] Another study also demonstrated that elastic liposomes could be used as a potential carrier in prolonging drug release and enhancing bioavailability of LOV[203] and clotrimazole to enhance the anti-fungal activity of the drug.[375] The vesicle membrane of elastic liposomes is ultra-flexible, making the vesicles highly deformable, and metastable. A subsequent study went on to refine the formulation of elastic liposomes of clotrimazole that will release the drug over a prolonged period of time i.e. sustained release, enhanced anti-fungal activity.[375]

However, there are few micelles and liposome-based LOV formulations and there is a clear demand for a controlled delivery system which could be achieved by micelle and liposome-based formulations. Therefore, to overcome the drawbacks of both micelles and liposomes; instead of their single use as a DDS, micelles can be assimilated into liposomes for comprehensive applications as a robust drug delivery platform, where the micelle controls the drug release and the liposome increases the loading efficiency. A lipid-polymer hybrid nanoparticle (NP) with high drug encapsulation yield and sustained drug release profile has been reported.[345,346] NPs have been reported by Yuk *et al.* to provide sustained release of Docetaxel compared to polymeric micelles alone.[376]

The aim of the current study was to fabricate a novel hybrid system composed of micelles encapsulated within liposomes, namely the LMH, (**Figure 3-1**) for improved oral delivery of the poorly water-soluble drug, LOV. The proposed combination of the liposomes and micellar carriers are hypothesized to increase drug loading, improve the release profile as well as providing greater bioavailability and offer an oral dosage form for many insoluble drug molecules. Our specific interest was to determine the drug loading and release properties

of the LMH hybrid system in comparison to the individual nanocarriers, liposomes, and micelles.

3.2. Materials

1,2-Distearoyl-sn-glycero-3-phospho-1'-rac-glycerol, sodium-salt (DSPG-Na) with C18:0, < 99%, (Molecular Weight: 801.058), was purchased from Avanti polar lipids, (INC. Lipoid). Cholesterol (CHO) with 99% purity with MW 386.65 was purchased from Sigma-Aldrich (USA). LOV (crystalline powder), with 98% purity was purchased from International Laboratory (USA). Poloxamer 407 (P407) and 3α,12α-Dihydroxy-5β-cholanic acid sodium salt (Sodium deoxycholate-SDC) were purchased from Sigma-Aldrich Pty. Ltd.(Australia). d-α -Tocopheryl polyethylene glycol 1000 succinate (TPGS) was purchased from Antares, Health Products, INC, (US/Canada). All reagents; NaCl, NaOH, H_3PO_4, Tween 20, PEG-400 and buffer (PBS tablets) solution components were an analytical grade, purchased from Ajax Chemicals, Australia). HPLC grade acetonitrile and analytical grade chloroform, methanol, and ethanol were used as supplied and purchased from Sigma-Aldrich, Australia.

3.3. Experimental methodology

3.3.1. Preparation of LMH system

3.3.1.1. Formulation of LOV loaded micelles

The method used for the preparation of micelles was modified from direct dissolution[222-223, 241, 377-378] and solvent evaporation methods.[377, 379-381] Different types of polymers (poloxamer 407, TPGS) and surfactants (DC) were used in the preparation of micelles. The polymer (100- 800 mg) was weighed into a round bottom flask and dissolved in chloroform (10 mL) by gentle hand shaking to form a clear solution. A 1 mg/mL LOV solution in chloroform (10 mL) was added to the polymer solution. The polymer-drug solution was subjected to vacuum evaporation in a rotary evaporator to evaporate chloroform by rotating the round bottle flask at 80 rpm at room temperature. After 2-3 hours, a thin polymer-drug film was formed. The thin film was hydrated with 10 mL of 1 mM freshly prepared and filtered (0.2 μm) NaCl solution by sonication for 30 minutes to form micelles. Clear drug-loaded micelles were formed. The free drug was separated by centrifugation at 10,000 rpm for 20 minutes. Only

simple centrifugation was reported in most of the literature and one wash was enough for free drug separation as reported previously.[200]

3.3.1.2. Formulation of liposomes

Liposomes were prepared by a thin-film hydration method previously described by Bangham *et al.*[146] Two different compositions were used to prepare the liposomes; PC and DSPG: PC with a molar ratio of 7:3.[382-384] 2 molar LOV was used for each of the formulations. The lipids (82 mg) and LOV (8 mg) were weighed, mixed, and dissolved in a mixture of methanol-chloroform-water (10 mL) with a ratio of 1:5:0.1[384] in a round bottom flask by gentle hand shaking and sonication (1-2 min) to form a clear solution. The round-bottom flask was connected to a rotary evaporator (BUCHI rotavapor R-124 and water bath B-480). The excipient-solvent mixture was allowed to evaporation under vacuum for 3 h, with gentle rotation (60 rpm) to prepare uniform thin drug-lipid films upon complete evaporation of the organic solvents at 60°C, which is above the phase transition temperature (Tc) of the lipids (55°C).[385] The homogeneously dry, thin lipid film was dried for an additional hour under N_2 gas before leaving the flask open in a fume hood overnight in order to ensure complete removal of the solvent.

The resultant dry drug-lipid film was hydrated with 1 mM NaCl for 2 h in a water bath with controlled temperature (60°C) with constant rotation at slow speed. The solution of 1 mM NaCl was just used to provide a simple background electrolyte concentration (to enable determination of physicochemical parameters such as zeta potential for film hydration as reported in literature.[383] The hydrated solution was subsequently sonicated in an ice bath for 10 minutes. The ice bath was used to improve the rigidity of the obtained liposomes. The drug-loaded liposomes (pellets) were separated from the unencapsulated free drug (supernatant) by ultracentrifugation (32,000 rpm at 4°C). Ultracentrifugation is a method mostly applied for liposome separation. Excessive sample dilution may cause a loss of drug from inside the liposome that's why excess dilution should be avoided. If the formulation was washed more than one time, the encapsulation efficacy may decrease as reported in previous articles. It seems that dilution causes the medicine to leak from the liposomal structure, thus dilution is not appropriate when evaluating liposomal formulations.[200] The collected pellets were suspended in 1 mM NaCl solution, extruded through polycarbonate filters of 400 - 800 nm pore diameter for about 8–10 times to obtain highly monodispersed (PDI < 0.25) and

unilamellar liposomes.[386,157] The final liposomes product appeared as a transparent light bluish suspension. The suspension was kept in the freezer (4°C) prior to use.

3.3.1.3. Formulation of liposome-micelle-hybrid

To fabricate the LMH system, the drug-loaded TPGS micelles were prepared and subsequently mixed with the composition used in DSPG: PC liposome formation. Different methods of mixing the pre-formed micelles with the liposome-forming lipids were used to get the highest amount of drug loading into the hybrid system, including thin film evaporation (TFH), reverse phase evaporation (RPE), and RPE combined with freezing and thawing (FT). The drug was loaded into LMH, both in the bilayer and micelles, and also separately. e.g, 1. LMH (blank lipid bilayer + loaded aqueous inner core (micelles) and 2. LMH (loaded lipid bilayer + blank aqueous inner core (micelles))

3.3.1.3.1. Thin film evaporation method

The LMH was prepared in a similar manner as the liposomes as described in **Section 3.3.1.1**, however, the thin drug-lipid film was hydrated in the pre-formed LOV micelles suspension instead of the NaCl solution. After rehydration, the suspension was sonicated and ultracentrifuged as described in **Section 3.3.1.1.** The drug present in the pellet and the supernatant was analysed separately. The drug present in the pellet was considered as encapsulated within the hybrid, and the drug present in the supernatant was considered as encapsulated within the free micelles.

3.3.1.3.*2*. Reverse phase evaporation method

All the lipids were solubilised together in the same solvent mixture of methanol-chloroform-water (10 mL) with a ratio of 1:5:0.1 as described in S**ection 3.3.1.1.** for liposomes preparation. Then 3 mL of the pre-formed LOV micelles suspension (LOV containing 1 mg/mL) was mixed with the lipid-solvent mixture in the ratio of 3:1 in a round bottom flask.[385] The solvent-micelles mixture (total volume 12 mL) was evaporated to form a drug-lipid film as described in **Section 3.3.1.2.** The resultant dry drug-lipid film was hydrated with 1 mM NaCl solution followed by sonication, ultracentrifugation and extrusion followed the methods as described in **Section 3.3.1.1**.

3.3.1.3.3. Reverse phase evaporation and freeze-thawing method

The hybrid suspension was prepared by following the same procedure of RPE. The hybrid suspension was then frozen for 20 minutes using dry ice (frozen carbon dioxide, a block of dry ice has a surface temperature of -78.5 °C). This frozen icy suspension was then thawed for another 20 minutes in a beaker containing hot water (60 °C) with continuous stirring at 200 rpm. The freeze-thaw cycle was repeated 3 times.[387]

3.3.2. LOV assay method

The concentration of LOV in LMH was analysed using an HPLC system (Shimadzu, Scientific Instruments) assembled with a UV-detector **(**PD-M2OA) set at 237 nm with a Phenomenex hyper clone 5 µm-ODS C18 column (125 x 4.0 mm, 120A). The mobile phase was a mixture of 65% (v/v) of acetonitrile and 35% (v/v) of an aqueous solution containing filtered 10 mM phosphoric acid. The pH of the solution was adjusted to 3 with 1 M NaOH solution. The mobile phase was degassed by ultra-sonication for 30 minutes before use and was not allowed to recirculate during the analysis. The samples were injected at a volume of 20 µL at ambient temperature. An isocratic method was used at a flow rate of 1.5 mL/min. A series of working solutions with concentrations ranging from 0.1 to 100 µg/mL was used to generate the linear calibration curve (n = 4) by plotting the chromatographic peak area versus LOV concentrations (R^2 > 0.9998). The limit of quantification (LOQ) value was 0.1 µg/mL. The precision and accuracy for both intra and inter-day analyses were within the acceptable analytical limits (i.e. < 10%). The specificity and reproducibility of the assay were within 102- 108%. Repeated analysis showed excellent precision (< 3%) in the peak area results. Therefore, the selected HPLC method was highly applicable for LOV quantification. All analytes were diluted suitably to meet the calibration concentration range prior to analysis.

3.3.3. Encapsulation efficiency and drug loading

The LOV content in the LMH and other nanocarriers formulation was determined by diluting 100 µL of each formulation with 900 µL of methanol and then vortexing and sonication to breakdown to disrupt the carriers. The samples were centrifuged before analysis to free the nanocarriers. The samples were centrifuged before analysis to free from any nanocarriers and the supernatant was taken for the HPLC analysis. LOV content was measured according to

the LOV assay methods as described in **Section 3.3.2**. The encapsulation efficiency (*EE*%) of LOV in the nanocarriers was calculated using the following **equation 3-1**:

$$EE\% = \frac{We}{Wi}\ X\ 100 \quad \text{.....Equation } \textit{3-1}$$

Where, *We*, is the amount of the entrapped drug in the nanocarriers and *Wi*, is the initial drug concentration.

The drug loading (DL%) of the LOV in the nanocarriers was calculated using the following **equation 3-2**

$$DL\% = \frac{We}{Wnp} \ldots\ldots\ldots\ldots\ldots\ldots\ldots\ldots\ldots\ldots\ldots \textbf{Equation } \mathbf{3-2}$$

Where, *We*, is the amount of entrapped drug in the nanocarriers and *Wnp*, is the total weight of nanocarriers.

3.3.4. Physicochemical characterisation of the LMH system

3.3.4.1. Particle size and zeta potential

Average particle diameter (Z-average), size distribution (polydispersity index-PDI) and zeta potential of the LMH were measured by dynamic light scattering and Phase Analysis Light Scattering (PALS) techniques using a Zetasizer Nano instrument (Malvern, UK) ZS, respectively. The sample was placed into a disposable sizing cuvette (for size) and clear disposable Zeta cell (for zeta potential measurement). The micelles were analysed without any treatment beforehand, and the liposomes or the LMH systems were diluted 100 times with Milli-Q water prior to size and zeta analysis. For each sample, the size was measured 3 times with 6 runs for 4 minutes (1 minute for equilibrium and 3 minutes for 3 measurements) at 25 ºC; the attenuation was set at 7 and 9 and the material RI was set at 1.59. The correlation function and count rate were observed (approximately 300- 500 kpcs) which represents the average scattering intensity during the measurement with the sample.

3.3.4.2. Morphology and surface characteristics

Morphological characterisation of the LMH was performed by Cryo-TEM at the Australian Centre for Microscopy & Microanalysis, the University of Sydney.

Blotting and plunging were done using a Vitrobot Mk III (FEI, The Netherlands). For thin specimens such as suspensions of liposomes, cryo-immobilisation was achieved by blotting to generate a thin film of liquid containing the sample liposome, and then rapidly freezing it by plunging into a cryogen. The most widely used cryogens liquid ethane was used after cooled by liquid nitrogen.[388] Being an aqueous biological sample it was stabilized before placed in the high vacuum of an electron microscope. As plunge freezing maintains the sample in the most native state among the various approaches that have been developed therefore it is selected. Plunge freezing for standard electron cryomicroscopy applications proceeds by spreading the sample into a thin film across an EM grid and then rapidly submerging it in a cryogen (usually liquid ethane),[389] A 3 μL aliquot of the liposomal suspension was pipetted onto a lacey formvar grid (GSCU 300FL-50, ProSciTech) and blotted for 2 seconds using a blot offset of -2 mm at 23 °C and 100 % relative humidity. The grid was plunged into liquid ethane at -183 °C and transferred to a grid box immersed in liquid nitrogen until required for imaging. Vitrified samples were transferred to a JEOL 2100 transmission electron microscope (JEOL, Japan) using a Gatan model 915 cryo-transfer holder (Gatan, The United States). Images were taken at an accelerating voltage of 200 kV.

3.3.4.3. LMH physical and chemical stability

The LMH nanocarriers average particle diameter (Z-average), size distribution, PDI and zeta potential were observed at different hydration pH's as a function of time over 3 months to assess particle stability. For this purpose, the micelles and liposome films were hydrated using hydration media at different pH's (1 mM NaCl solution adjusted to pH 2, 4, 5 or 6) and the impact in pH change on the drug content and physical properties of the nanocarriers was observed. The pH was adjusted by adding an appropriate amount of 1% acetic acid or 1 M NaOH in 1 mM NaCl solution and measured by a pH meter. These solutions of different pH were used to prepare micelles and liposomes and the particle diameter and charge were observed after 24 hours as fresh samples and at each month up to 3 months using DLS as described earlier in subsection-3.3.4.1.

3.3.4.4. Short-time physical and chemical stability

The physical stability study of different formulations was observed using DLS as described earlier in subsection-3.3.4.1.The physical parameters were reported were size of the

nanoparticles and their polydispersibility index. These properties were monitored over one, two and 3 months consequently. The stability test of LOV in the formulation was also done by storing it in a freezer at 4°C temperature for up to 3 months. Stability of the LOV formulation was quantified by analysing the drug quantity using HPLC.

3.3.4.5. LOV *in vitro* release study

In vitro LOV release from the hybrid LMH, liposome and micelle systems were estimated by a dynamic dialysis membrane diffusion technique using cellulose membrane dialysis tubing (MWCO 14,000; Sigma Aldrich Inc-USA).[214, 390] The dialysis bag was soaked for 2 hours before the sample was inserted. 10 mL of sample was filled into a dialysis bag and dipped in a beaker containing the release medium (90 mL) under magnetic stirring (100 rpm). The release medium was composed of PBS (pH 7) and the surfactant, PEG-400 (0.5%) and "sink'' conditions maintained at 37 °C. At predetermined time intervals, a 1 mL sample was withdrawn from the beaker and replaced with the same volume of fresh release medium. To investigate the LOV content in release samples, initially the samples containing micelles/liposomes/hybrid were treated with methanol to breakdown the nanocarriers by vortexing and sonication and then centrifuged to separate the supernatant (LOV) and the nanocarriers. Secondly, the LOV content in the supernatant for the nanocarrier formulations was determined by diluting 100 µL of each formulation with 900 µL of methanol and then vortexing and sonication to breakdown to disrupt any nanocarriers left. The samples were centrifuged at 10,000 rpm for 10 minutes at room temperature before analysis to ensure they were free from any nanocarriers and the supernatant was collected was taken for analysed in HPLC using the LOV assay method (described above in **Section 3.3.2**) to quantify the amount of LOV released. Therefore, there is minimal possibility for micelles/liposomes /LMHs to get through to the sample and even if it is in collected sample, it should be either separated with centrifugation or broken down by dilution. Details have been described in **section 3.3.3.**

The release study was carried out over 10 days to observe the complete drug release (100%) from the carriers. Here also the first 60% of the drug release data is fitted using the Korsemeyer-Peppas model to explain the mechanism of drug release.

3.4. Results and discussion

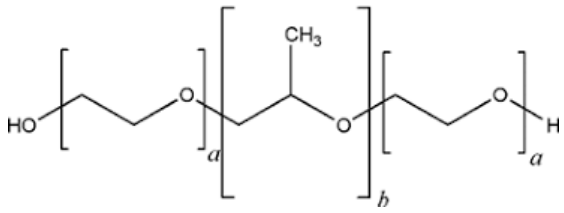
3.4.1. Physicochemical characterisation of LMH

3.4.1.1. The size, zeta potential and size distribution of micelles

Initially, a series of micellar systems were prepared using different polymers. Two types of non-ionic micelles systems, e.g. P-407 ($PEO_{98}PPO_{67}PEO_{98}$), poloxamer 188 ($PEO_{75}PPO_{30}PEO_{75}$), a charged micelles system, DC micelles and mixed micelles systems of P- 407 and DC and TPGS both with and without loaded LOV were developed.

The poloxamers possess different PEO block mass (11500 and 8350 $gmol^{-1}$ respectively) and PPO block size (**Table 3-1**). P-407 self-assembles into spherical micelles, with the polyethylene oxide (PEO) forming a hydrophilic outer shell and polypropylene oxide (PPO) the hydrophobic inner core where the LOV is incorporated (**Figure 3-2**). Similar micelle forming mechanisms have been described in the literature.[73, 391] Increasing the length of PEO blocks increases hydrophilicity and an increase in the length of the PPO block increases hydrophobicity.[392]

Table 3-1: Different poloxamer polymers with different number of block.[391]



General structure of poloxamer
Different number of blocks/segments

Poloxamer	Polyethylene oxide (PEO) [a]	Polypropylene oxide (PPO) [b]
188	75	30
407	98	67

The Poloxamer 188 micelles are larger than the P-407 analogs because the length of hydrophobic blocks of poloxamer 407 is higher than the hydrophobic blocks of poloxamer 188. Here, the size of the poloxamer 407 micelles is influenced by the balance of hydrophobic and hydrophilic blocks.[335, 393] Both micelle size and association number decrease with the increased length of the hydrophobic blocks.[335, 394]

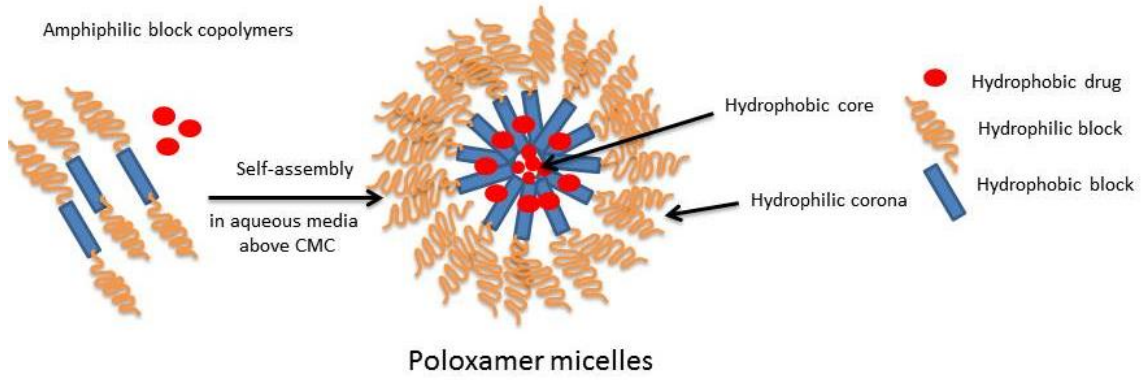


Figure 3-2: Formation of poloxamer micelles from amphiphilic block copolymer (407 /188).

For Poloxamer 407, the average diameter of the LOV loaded and blank micelles were 22.31 ± 0.63 nm and 22.96 ± 0.6 nm which was smaller than the Poloxamer 188 micelles which were 32.8 ± 7 nm and 32.8 ± 0.2 nm, for the blank and drug-loaded micelles, respectively **(Table 3-2)**. These values are in good agreement with literature for polymer-based micelles (10-150 nm).[21, 235, 241, 395] PDI for the P-407 and Poloxamer 188 micelles were 0.35 ± 0.1 and 0.20 ± 0.045, respectively (**Table 3-2**), indicating that the micelles are relatively monodisperse (typically PDI < 0.3 is considered to be monodispersed).

Table 3-2: Average particle diameter, PDI, zeta potential, the drug loading and EE of LOV into different polymeric micelles, mean ± SD, (n = 3)

Micelles Type		Average particle diameter size (d.nm)	Polydispersity index (PDI)	Zeta potential (mV)	Drug loading (%) w/w	Encapsulation efficiency (%)
Poloxamer 407	Loaded	22.31 ± 0.63	0.355 ± 0.1	0.30 ± 1.3	0.181 ± 0.0	14.61 ± 18.27
	Blank	22.96 ± 0.56	0.205 ± 0.04	-0.31 ± 0.1		
Poloxamer 188	Loaded	32.82 ± 0.18	0.357 ± 0.0	0.03 ± 0.2	*Nd	
	Blank	32.80 ± 7.69	0.355 ± 0.1	-1.22 ± 1.6		
DC	Loaded	40.13 ± 20	0.558 ± 0.3	-4.27 ± 0.9	2.89 ± 0.03	90.34 ± 12.94
	Blank	63.54 ± 80	0.6 ± 0.3	-0.46 ± 1.2		
DC-poloxamer	Loaded	33 ± 24	0.216 ± 0.08	-4.66 ± 1.6	0.926 ± 0.17	54.37 ± 33.89
	Blank	130.49 ± 80	0.291 ± 0.3	-0.35 ± 0.3		
TPGS	Loaded	11 ± 0.24	0.135 ± 0.02	-1.26 ± 1.5	2.05 ± 0.08	71.81 ± 19.10
	Blank	12.96 ± 1	0.258 ± 0.05	-1.41 ± 1.9		

*nd= not done as smaller size (below 20 nm) was our priority, so TPGS were used, based on size. Hence, drug load was not measured for all polymer micelles.

Loading poloxamer micelles with LOV did not visibly affect their average particle diameter and size distribution. Very slight and insignificant average size increase after LOV loading might nevertheless reflect a certain increase in the hydrophobic micelles core size because of solubilization of LOV there.

Zhao *et al*. reported that the average size of blank mixed micelles composed of P123/F68 was 23 nm with PDI 0.304.[396] An increase to the average size was observed after loading a drug, curcumin, from 23 nm to 68.2 nm, and the PDI from 0.304 to 0.197, respectively. The mean diameter of blank micelles was close to 20 nm, which was similar to the LOV loaded micelles. However, the loading of curcumin in micelles visibly affected their size and size distribution.[396] Wei *et al*. reported mixed micelles of poloxamer P123 / F127 with an average particle diameter of about 25 nm.[397] The P188/F407 mixed micelles were prepared with Paclitaxel (PTX)-loaded by Zhang *et al.* by thin-film hydration method and the optimized formulation showed a mean diameter of blank and drug-loaded mixed micelles was 20.1 and 23.5 nm with a PDI 0.14 and 0.23.[396, 398]

The PDI of the loaded and blank micelle for Poloxamer-407 was 0.355 ± 0.1, 0.205 ± 0.04, and for Poloxamer 188 micelles 0.357 ± 0.0 and 0.355 ± 0.1, respectively. The zeta potential of Poloxamer-407 and 188 micelles was weakly negative, they were -0.31 ± 0.1 mV and-1.2 ± 1.6 mV. The LOV loading was 0.181% (w/w) for Poloxamer-407. Though their sizes were within ranges previously observed for polymer-based micelles, however, the loading observed for both poloxamer-based micelles was low (0.181% w/w) **(Table 3-2)**. To improve LOV loading in the micelles, they were prepared with a different amphiphile, i.e. DC using the same micelles preparation method. It was hypothesized that as deoxycholate micelles have a larger hydrophobic micellar core, therefore, it may be possible to encapsulate higher quantity of LOV compared to poloxamer micelles (**Figure 3-3**).

After LOV loading, the average particle diameter of the DC micelles decreased significantly, from 63.54 ± 80.29 nm to 40.13 ± 20.32 nm. This is due to encapsulation of the hydrophobic drug molecules into the micelles' core enhancing the hydrophobic interaction within the hydrophobic micelle' core. This phenomenon has previously been described by Hu *et al*.[399] with the reduction of average diameter attributed to a decrease in aggregation number (N_{agg}) which is just beyond the Critical Micelle Concentration (CMC ~ 2-6 mM or ~0.083-0.249% (w/v)). The trend of N_{agg} for amphiphiles is $2 \leq Nagg \leq 15$ [400-405] and for DC, the N_{agg} is

10.[406] The aggregation of DC is shown in **Figure 3-3A** and these aggregates are also known as facial micelles.[407]

The SDs was quite large and this is because of the variation of size. The greater variation of size could be due to the rapid aggregation properties of the anionic surfactants, deoxycholate.[408] This is apparently possible for nano-size particles. A light-scattering study has been made of the effect of concentration and temperature on the micellar size in a series of homogeneous non-ionic detergents in aqueous solution. It has been found that above the critical micelle concentration, as determined by surface tension measurements, an increase in micellar size takes place until a critical concentration is reached.[409]

The PDI of the loaded and blank DC micelles was 0.558 ± 0.382 and 0.6 ± 0.3, respectively (Table 3-3), indicating that the micelles were relatively polydisperse (typically PDI > 0.3 is considered to be polydispersed). The micelles were weakly negative, with zeta potentials of - 4.27 ± 0.908 mV and - 0.461 ± 1.24 mV (~ 0 mV) loaded and blank, respectively. For the DC micelles, we obtained loading of 2.89% (w/w) which is 16-fold higher than the poloxamer micelles, 0.181% (w/w). It was clearly observed that LOV loading was improved in DC micelles compared to poloxamer micelles. This enhanced drug loading into DC micelles was due to the structural similarity of the hydrophobic part of the LOV molecule with the hydrophobic part of the DC molecule.[410-411]

Drug loading was lower into poloxamer micelles due to the structure dissimilarity with the hydrophobic part PPO of poloxamer (**see Figure 3-3 and Table 3-1**) as drug loading is often correlated with the solubility of the drug in the hydrophobic part of the amphiphile.[412] It has been previously reported by Moriarty *et al*. that drug loading is associated with the size, shape, chemical structure of the LOV.[411] LOV has a hydrophobic ring-structure[410] like the DC molecule[411] **(see Figure 3-3C and 3D).** Structural similarity enhanced the solubility of LOV molecules with the hydrophobic core of the DC molecules compared to the hydrophobic core of the poloxamer molecules.[349]

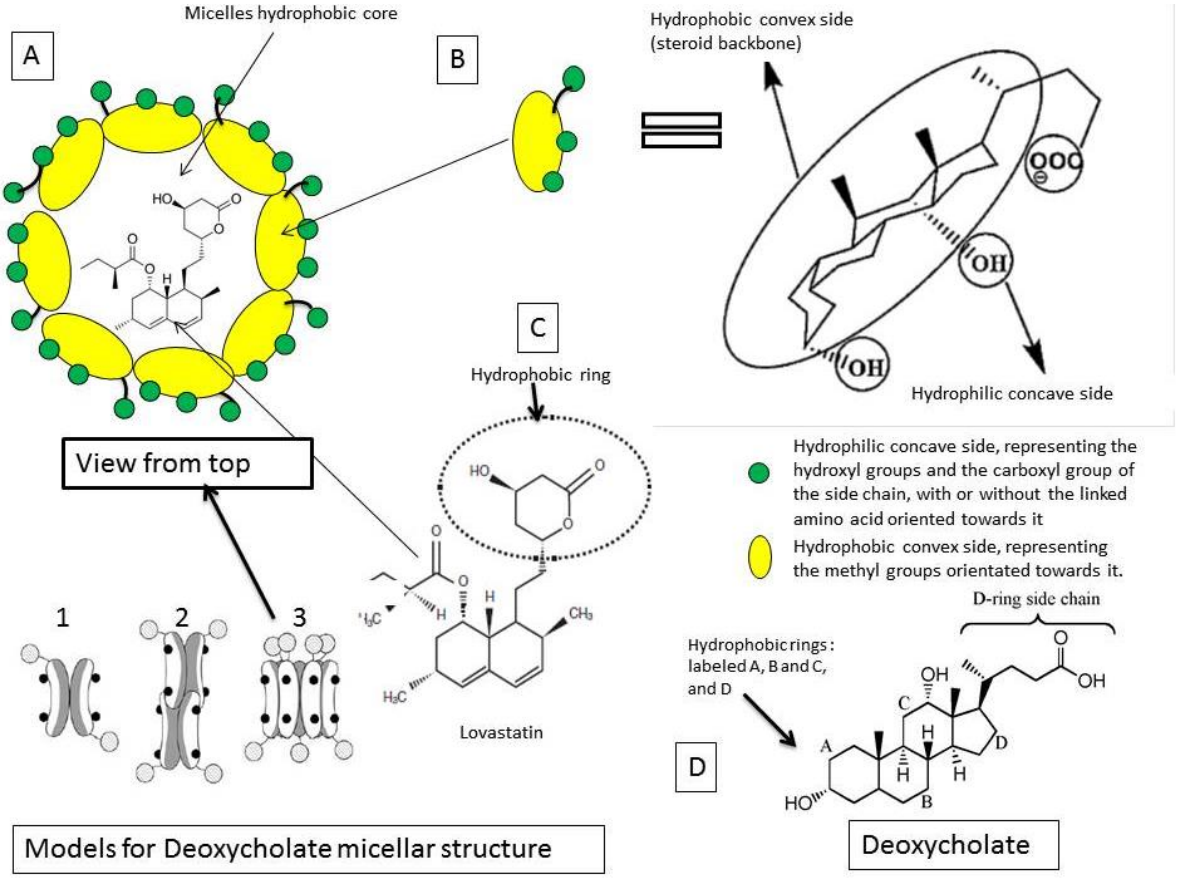


Figure 3-3: Hypothetical model showing A) helical deoxycholate-LOV micelles (seen from top), (1,2) different primary micelles, (3) disclike micelle[413] B) the molecular structure of DC composed of a rigid steroid backbone with I) hydrophobic group: α-oriented hydroxyl and the carboxyl group of the side chain on the concave side of the steroid skeleton and ii) hydrophobic group: β-oriented methyl groups positioned on the opposite convex side conjugated to an anionic chain, C) the structure of LOV molecule with hydrophobic ring[410] and D) the structure of DC molecule with hydrophobic rings; a nucleus composed of four fused rings: three cyclohexane rings, labeled A, B and C, and a cyclopentane ring, labeled D.[411] Image adapted and modified from Kumar *et al*.[414] and Nicola *et al*.[407] and Madenci *et al*.[413]

A generally accepted model for DC aggregates[413] is depicted in **Figure 3-3A**, which are different from conventional head-tail amphiphilic poloxamer and known as facial micelles **(Figure 3-3B)**.[407] Consequently, the aggregation behavior of DC is also different from that of conventional amphiphilic surfactants, and they form primary aggregates due to hydrophobic interactions and secondary aggregates at higher concentration due to hydrogen bonding between the hydroxyl groups (see **Figure 3-3E)**.[413]

Next, mixed micelles were prepared with P-407 and DC with (1:1) w/w ratio (only ratio) for characterisation of properties and to investigate the drug loading (**Figure 3-4**). Similar mixed micelle preparation were investigated in the literature for Camptothecin[415] and Cefotaxime.[416]

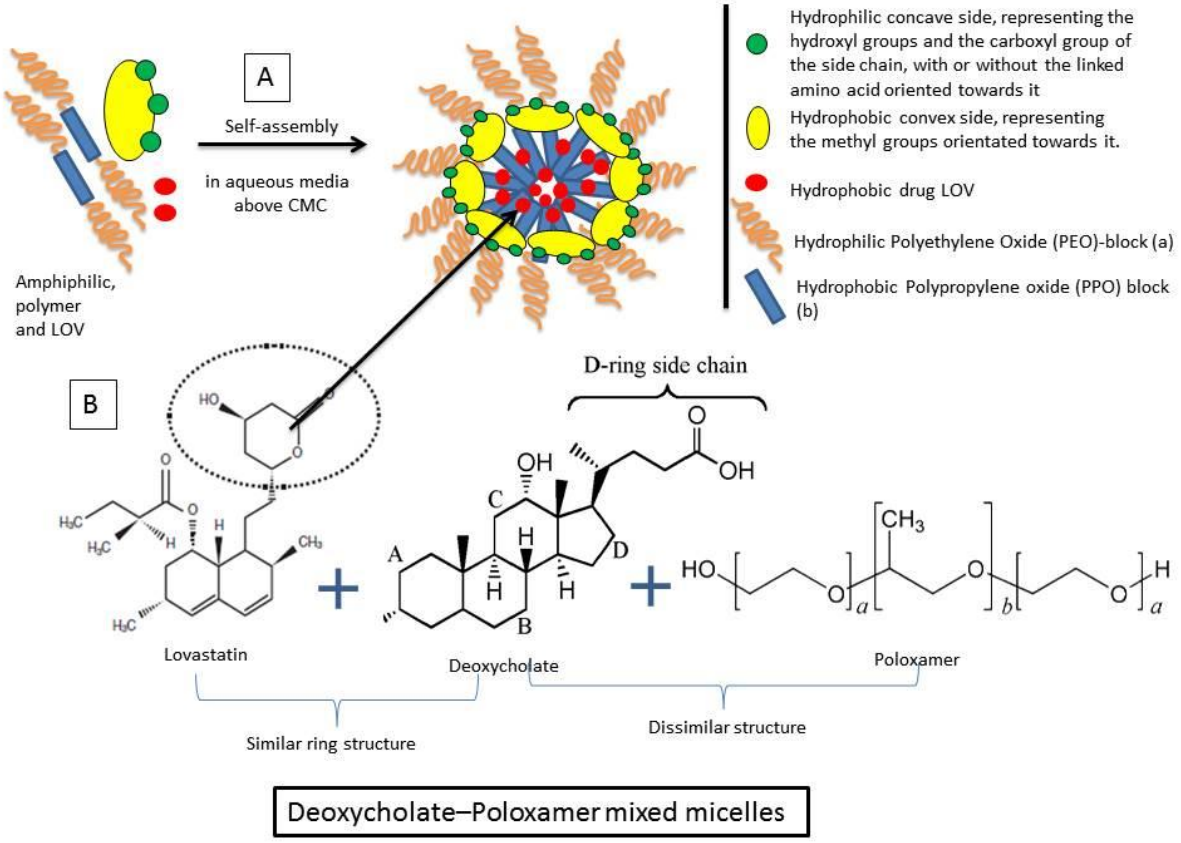


Figure 3-4: Hypothetical model showing A) self-assembly of deoxycholate-Poloxamer mixed micelles and B) the molecular structure of LOV, DC and Poloxamer with structural similarity and dissimilarity (already discussed above)[410-411] Image adapted from Kumar *et al.* [414] Nicola *et al.* [407] Maarten *et al.* [391]and modified.

For loaded and blank DC-poloxamer mixed micelles of diameter 33.07 ± 23.7 nm and 130.49 ± 79.91 nm and zeta potential of - 4.66 ± 1.61 and - 0.352 ± 0.35 were observed, respectively. After the loading, it was found that their diameter decreased significantly. A similar reduction of diameter after drug loading was reported in the literature.[399] The reason for the reduction of diameter after drug loading already has been described above for DC micelles.[399] The SDs was quite large value this because of greater variation of size. The greater variation of size could be for rapid aggregation property of the anionic surfactants, deoxycholate.[408]

The PDI of the loaded and blank Poloxamer-DC mixed micelles was 0.216 ± 0.086 and 0.291 ± 0.336, respectively (**Table 3-2**), indicating that the micelles are relatively monodisperse (typically PDI < 0.3 is considered to be monodispersed). The micelles were weakly negative, with zeta potentials of -4.66 ± 1.61 and -0.352 ± 0.35 (~ 0 mV) for loaded and blank micelles, respectively. It has been reported that for low molecular weight surfactant the zeta values in

the range of ± 5 indicates fast aggregation.[417-418] The drug loading and encapsulating efficiency of LOV in DC-poloxamer mixed micelles was 0.926 ± 0.17 % (w/w) and 54.37 ± 33.32 %, respectively which was 5-fold lower than the poloxamer micelles (0.181% w/w) and 3-fold lower than DC micelles (2.89 % w/w) (**Table 3-2**). Therefore, it was observed that using this mixed micelle formulation did not significantly improve LOV loading and even it was lower than DC micelles alone. For encapsulation efficiency, the large deviation is observed because the % EE value is the average EE% of 2, 5, 10, 15 mg and 20 mg samples. The deviation for either of them by itself was not so high

To further investigate drug loading and stability, TPGS micelles were investigated as the TPGS has a large hydrophobic tail which might enable encapsulation of more hydrophobic LOV.[24, 211, 281] TPGS has an amphiphilic skeleton that gives TPGS, a non-ionic surfactant property. The TPGS structure shows a hydrophilic head (polyethylene glycol chain) and a large hydrophobic tail (tocopheryl group), shown in **Figure 3-5A, 5B**.

The average diameter of the LOV loaded and blank micelles prepared from TPGS was 11.08 ± 0.247 and 12.96 ± 1.61 nm, respectively (Table 3-2), which were smaller than poloxamer and DC micelles mentioned above. LOV loading into TPGS micelles exhibited no significant changes in size. The PDI was 0.135 (< 0.2) for the TPGS micelles, which indicates that the systems can be considered to be monodispersed (**Table 3-2)**. Literature published for TPGS micelles reports a comparable micelle size to that reported here. Zhang *et al.* prepared a PTX loaded and blank TPGS micelles with diameter 13 nm.[419] Muthu *et al*. also reported docetaxel-loaded TPGS micelles diameter ranged between 12 and 14 nm using different preparation methods.[208, 281] Similar results were published by Mu *et al*. and Yan *et al*. for TPGS micelles with the diameter of 12 nm with or without the drug (camptothecin)[420] and mean size of 12.7 nm (blank) and 11 nm loaded with fullerene.[381]

The average size of the LOV loaded and blank micelles prepared from TPGS were smaller than other polymeric micelles mentioned above, with diameter 11.08 ± 0.247 and 12.96 ± 1.61 nm, respectively **Table 3-2**. LOV loading into TPGS micelles exhibited no significant changes in size. The PDI was 0.135 (< 0.2) for the TPGS micelles, which indicates that the systems can be considered to be mono dispersed (**Table 3-2)**. Literature published for TPGS micelles reports a comparable micelle size to that reported here.

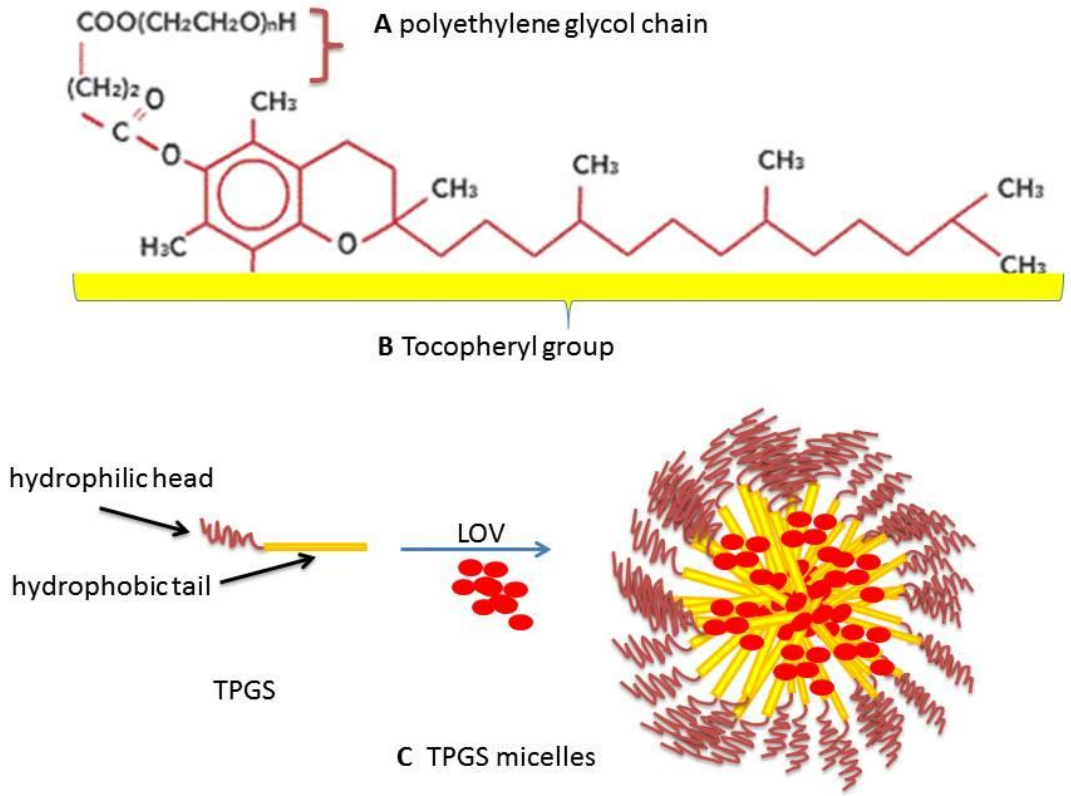


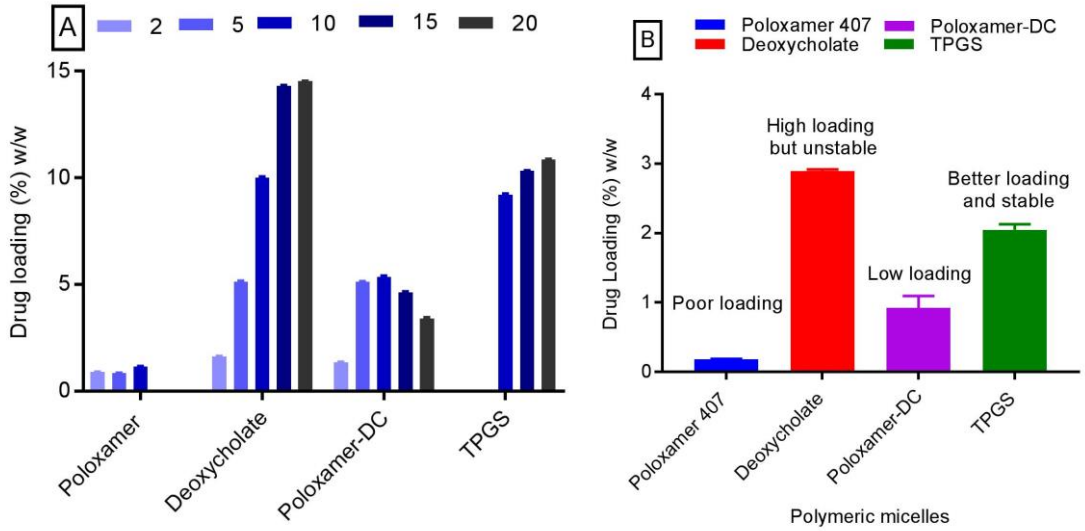
Figure 3-5: The amphiphilic structure of TPGS shows A) a hydrophilic head (polyethylene glycol chain) and B) a hydrophobic tail (tocopheryl group) and C) formation of TPGS micelles. Adapted and modified from Jhaveri *et al.*[421]

Zhang *et al.* prepared a PTX loaded and blank TPGS micelles with diameter 13 nm.[419] Muthu *et al*. also reported docetaxel-loaded TPGS micelles diameter ranged between 12 and 14 nm using different preparation methods.[208, 281] Similar results were published by Mu *et al*. and Yan *et al*. for TPGS micelles with the diameter of 12 nm with or without the drug (camptothecin)[420] and mean size of 12.7 nm (blank) and 11 nm loaded with fullerene.[381]

Smaller size (below 20 nm) was our priority, so TPGS was preceded with, based on size, and drug load was not measured for all polymer micelles. The loading of LOV within TGPS micelles was 2.05 (% w/w), **(Figure 3-6B)** which was an improvement from previous results (0.181 % w/w for poloxamer micelles and 0.926 % w/w for poloxamer and DC mixed micelles). The TPGS micelles demonstrated good stability and appearance over time by visual inspection and of size measurement for 3 months (as described in this chapter in section 3.4.5.1. in Table 3.8). Therefore, TPGS micelles were selected for encapsulation within liposomes due to their small particle size and high LOV loading capacity and stability compared to other micelles (**Figure 3-6B**). Although the drug loading levels of DC-based

micelles was greater, their long-term stability at room temperature was poor, rendering them unsuitable for future applications. The loading of LOV within micelles was then investigated as a function of LOV concentration, by loading and using a fixed amount of polymers and surfactants **(Figure 3-6A)**.

Keeping the polymer/surfactant quantity at a constant (500 mg), it was found that the drug loading was not increased in each micelle with increasing amount of added LOV up to 20 mg. For poloxamer micelles, the loading was similar for 5 and 10 mg of LOV. However, in DC micelles, the drug loading was increased with an increase in added amounts of LOV from 2, 5, 10 and 15 mg while unchanged for 20 mg. For mixed micelles (P- 407 and deoxycholate 250/250 mg), the drug loading increased gradually from 2, 5 and after 10 mg the loading is decreased with the increased of the LOV quantity. For, TPGS micelles the increase not significantly differs between 10, 15 and 20 mg of added LOV.



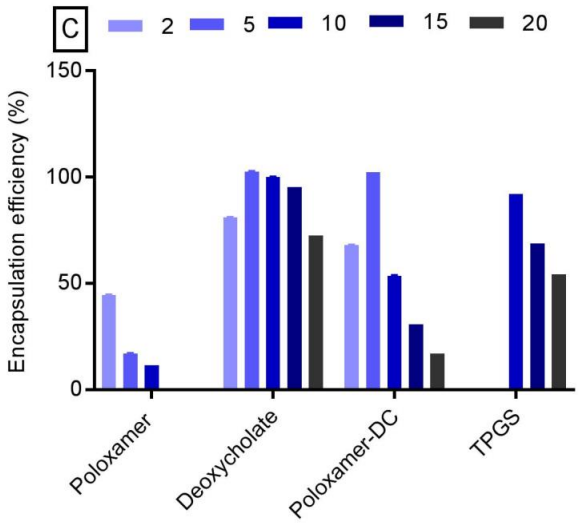


Figure 3-6: A) The relationship between added LOV to the polymers/surfactants and drug loading amount in different polymeric/surfactant micelles, B) The LOV loading levels (% w/w) in different polymeric/surfactant micelles and C) The relationship between added LOV to the polymers/surfactants and encapsulation efficiency (%) in different polymeric/surfactant micelles (mean ± SD, n=3).

However, the relationship between EE and the drug added is inversely proportional, i.e. the EE decreased with increased added drug. We investigated drug loading maxima with definite amount of polymer (500 mg). Increasing the added drug quantity from 2, 5, 10, 15 and 20 mg into fixed weight of polymeric micelles, the loading was varied based upon the polymers. The loading also varied for each polymer that is stated in **Figure 3-6A**. However, it was found that the encapsulation efficiency was decreased in each micelle with increasing amount of added LOV after certain amount (highest loading) as shown in **Figure 3-6C**.

3.4.1.2. The size, zeta potential and size distribution of PC and DSPG Liposomes

The average diameter of the blank and LOV loaded liposomes prepared with PC/CHO/LOV (molar ratio 7:3:2) was 271 ± 6 and 407 ± 5 nm, respectively **(Table 3-3)**. The size of loaded liposomes increased due to the incorporation of LOV molecules compared to blank liposomes, in agreement with previously published data,[422] where the increase in liposome size upon loading of LOV was attributed to its filling the free void space within the liposome bilayer. Previously, Xiang *et al* found that doxorubicin-loaded liposomes and chlorotoxin-loaded liposomes were slightly larger than the blank ones.[422] For LOV loaded and blank PC/CHO liposomes the PDI was 0.298 ± 0.02 and 0.266 ± 0.01, indicating the PDI < 0.3

were considered to be monodisperse. Xiang *et al.* reported the size of blank liposomes prepared with lipids; HSPC/CHO/DSPE-PEG was about 85 nm with a PDI below 0.182, while both the DOX- and DiR-loaded (carbocyanine DiOC18, a near IR lipophilic fluorescent) liposomes were larger than blank ones with an average particles size of below 130 nm and the low PDI (between 0.171 and 0.240) with weak negative surface charge of less than − 5 mV.[422]

Table 3-3: Physical characterization of different liposomes (mean ± SD, n = 3)

Liposome Type		Size (d.nm)	Polydispersity index (PDI)	Zeta potential (mV)	Drug loading (%) w/w	EE (%)
PC/CHO	Loaded	406 ± 5	0.298 ± 0.02	-0.94 ± 2.6	5.74 ± 0.32	92.78 ± 2
	Blank	271 ± 7	0.266 ± 0.01	-1.19 ± 2.5		
PC/CHO/ DSPC	Loaded	94 ± 2	0.264 ± 0.01	-42.3 ± 1.1	5.04 ± 0.29	91.48 ± 4
	Blank	107 ± 4	0.229 ± 0.01	-33 ± 8.9		

The drug loading and drug EE of PC/CHO/LOV liposomes were 5.74 ± 0.32 (% w/w) and 92.78 ± 2.01%, calculated according to **equation 3-1 and 3-2**, described at **Section 3.3.3**). Previously, Afergan *et al*. also reported a simvastatin loaded liposome with different composition of lipids (DSPC: DSPG: CHOL). The drug loading was reported of 0.70 ± 0.04 mg/mL and the lipids were 11.6 ± 1.8 mg/mL in the liposome. The liposomes obtained had a mean diameter of 164 ± 25 nm, with a PDI below 0.1, and a negative zeta potential of −14.3 ± 0.3 mV.[384] Achieving high drug loading for lipophilic drug LOV in liposomes was confined to the lipid bilayer (**Figure 3-7**). As reported in the literature that liposomes have a large hydrophilic inner aqueous core for water-insoluble drugs compared to a smaller volume lipid bilayer for lipophilic drugs.[7, 208] A variety of factors such as bilayer composition, physicochemical properties of the drug entity and method of preparation need to be well optimized to achieve higher drug loading.[7, 199]

The zeta potential of PC/CHO liposomes was close to zero and unchanged after LOV loading. Thus, these liposomes are electrostatically unstable due to the absence of an electrostatic potential.

The liposomes remain slightly negative, indicating that the incorporation of LOV within the lipid bilayer was not affecting the electrical double layer of the lipid bilayer-water interface. Zeta potential values > 25 mV (either positive or negative), were considered necessary to

provide colloidal stability due to electrostatic repulsion.[423] Lack of surface charge either positive or negative reduces the physical stability of small unilamellar liposomes (SUV) by increasing their aggregation, as reported by Sharma *et al*.[424]

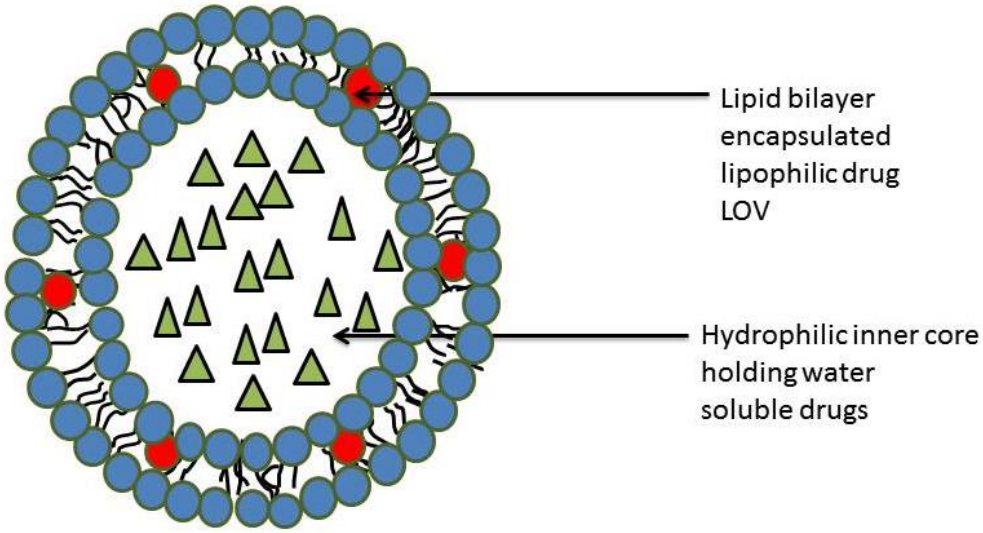


Figure 3-7: The space within the liposomes; lipid bilayer and aqueous inner core for drug loading. Image modified from Narvekar *et al*.[7]

Therefore, to improve the liposome colloidal stability, a negatively charged lipid, DSPG, was added to the PC/CHO liposome. The average size of loaded and blank DSPG/PC/CHO liposomes was 94 ± 1 and 107 ± 4 d.nm, with the PDI being 0.26 ± 0.01 and 0.23 ± 0.01. The drug loading of DSPG/PC/CHO liposomes was 5.04 ± 0.29 (% w/w). Here, the size of the LOV loaded liposomes was smaller compared to the blank liposomes. A similar reduction of size after drug loading has been reported in the literature.[200, 202] When the drug is dissolved together with the lipid mixture, it is located within the liposomal bilayer, where the acyl chains of phospholipids provide a favorable environment for the lipophilic LOV molecules. However, the intercalating incorporation of the drug into the bilayer alters the microstructure of the vesicular membrane, thus giving rise to a re-arrangement of the membrane structure and a decrease in ordering the system for drug entrapment. This hypothesis is supported by the reduction of the liposomal membrane organization order and reduces the average particle size of the liposome. A similar reduction of liposomal size after drug loading also has been reported for Benzocaine-loaded liposomes,[425] Prilocaine-loaded liposomes,[426] and for other lipophilic drugs.[427]

The diameter of the PC/CHO liposome were within the small unilamellar vesicle (SUV < 200 nm) size range as reported in the literature.[153, 183] For drug delivery applications, the suitable liposomes are usually unilamellar and range, 50-200 nm.[428] The DSPG/PC/CHO liposomes should retain greater stability due to the negative charge (-33.02 mV) of the DSPG lipids that was evident from their retaining clear solution rather than forming precipitation.

3.4.1.3. Preparation and physical characterisation of LMH.

Next liposome-micelle-hybrids were prepared using the DSPG/PC/CHO liposomes and TPGS micelles. Given the smaller particle size, acceptable PDI value and drug loading of TPGS micelles and greater stability of PC/CHO/DSPG liposomes, they were chosen for the LMH preparation (**Table 3-4**). Three different preparation methods were trialed, with the average particle diameter, PDI and zeta potential of the LMH particles determined.

Table 3-4: Physicochemical characterization of drug loaded LMH by different preparation methods (mean ± SD, n=3).

Different preparation methods	Diameter (nm)	Polydispersity index (PDI)	Zeta potential (mV)	Drug loading (%) w/w (Aqueous core)	Encapsulation efficiency (%)
Thin film hydration	149 ± 2	0.246 ± 0.01	- 46.3 ± 1.93	0.15 ± 0.03	4.44 ± 0.94
Freeze-thaw	197 ± 41	0.516 ± 0.05	-35.28 ± 2.5	1.04 ± 0.28	29.91 ± 8.62
Reverse phase evaporation	167 ± 2	0.505 ± 0.26	-22 ± 2.7	1.61 ± 0.37	47.80 ± 11

The average particle diameter and size distribution of LMH obtained from the thin film hydration (TFH) method were, 149 ± 2 nm and 0.246 ± 0.01, respectively. The PDI was 0.246 (< 0.2) for the LMH, which indicates that the systems can be considered to be monodispersed (**Table 3-4)**. The zeta potential of the LMH was - 46.3 ± 1.93 (mV) which was higher negative value for the colloidal stability of LMH. The drug loading and EE was 0.15 ± 0.03 (%) w/w and 4.44 ± 0.94 (%). When the TPGS micelles were loaded into its inner aqueous core, the LMH size increased from liposomes diameter (94.27 ± 0.27 nm.) to 149.65 ± 1.8 nm using the TFH method.

The average particle diameter and size distribution of LMH obtained from the Freeze-thaw (FT) method were, 197 ± 41 nm and 0.516 ± 0.05, respectively. The PDI was 0.516 (> 0.3)

for the LMH, which indicates that the systems can be considered to be polydispersed (**Table 3-4)**. The zeta potential of the LMH was – 35.28 ± 2.59 (mV) which was also considered as high negative value for the colloidal stability of LMH. The drug loading and EE was 1.04 ± 0.28 (%) w/w and 29.91 ± 8.62 (%).

When the TPGS micelles were loaded into its inner aqueous core, the LMH diameter increased from liposome diameter (94.27 ± 0.27 nm.) to 197 ± 41 nm using FT method. In this method, larger particles were found compared to the TFH methods. This larger particle diameter was found in this method because freezing changed the structure of the liposomes. Before FT, the liposomes were significantly smaller, however, the internal volumes of liposomes were increased after freeze-thawing cycle (typically 3). Subsequently increasing the number of freeze-thaw cycles resulted in a further increase of the entrapped volume and the average particle size increased. In addition, during freezing, the bilayer of the liposomes was destabilised through expansion of inner water phase by ice formation and dehydration of the hydrated head group of lipid. While thawing, the exposed hydrophobic cores fuse to form new vesicles, which may also increase the average size of the particle. A similar increase in size was also reported by Sriwongsitanont *et al* for an Egg-PC and DSPE-PEG2000 liposomes.[429] Similarly, MacDonald *et al*. [430] reported that large size liposomes are produced from SUV by repeated FT cycles. The FT cycles aggregate and ruptures the vesicles to enlarged liposomes and increase their internal concentration of polar compound thus improved the drug loading.

The average particle diameter and size distribution of LMH obtained from the RPE method were, 167 ± 2 nm and 0.505 ± 0.26, respectively. The diameter was smaller than the LMH obtained by FT methods and larger than TFH method. The PDI was 0.516 (> 0.3) for the LMH, which indicates that the systems can be considered to be polydispersed (**Table 3-4)**. The PDI results show polydispersed for both FT and RPE, however, monodispersed for the TFH method. The zeta potential of the LMH was - 22.09 ± 2.71 (mV) which was also considerable negative value (~ 25 mV as mention above) for sufficient stabilization of the LMH as reported in the literature. However, the zeta potential below 20 mV provides only short-term stability.[417-418] The zeta potential value in RPE was lower than other two different methods, TFH and FT described above. This lower zeta potential value in RPE method may be due to the migration of some TPGS from the micelles to the liposomes bilayer. The drug loading and EE was 1.61 ± 0.37 (%) w/w and 47.80 ± 11.04 (%). The loading of LOV in

LMH was higher in RPE method compared to the TFH and FT method. It was one magnitude higher from FT method and nearly six magnitudes higher than TFH method (**Figure 3-8**).

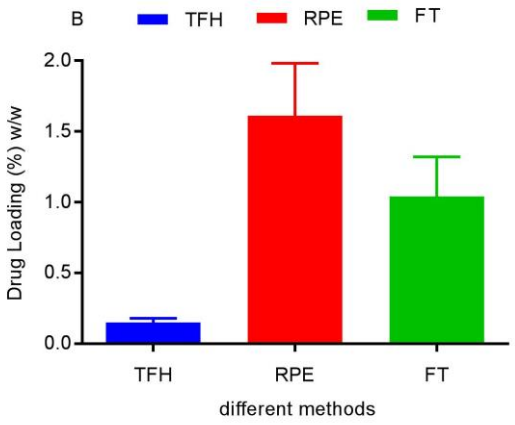
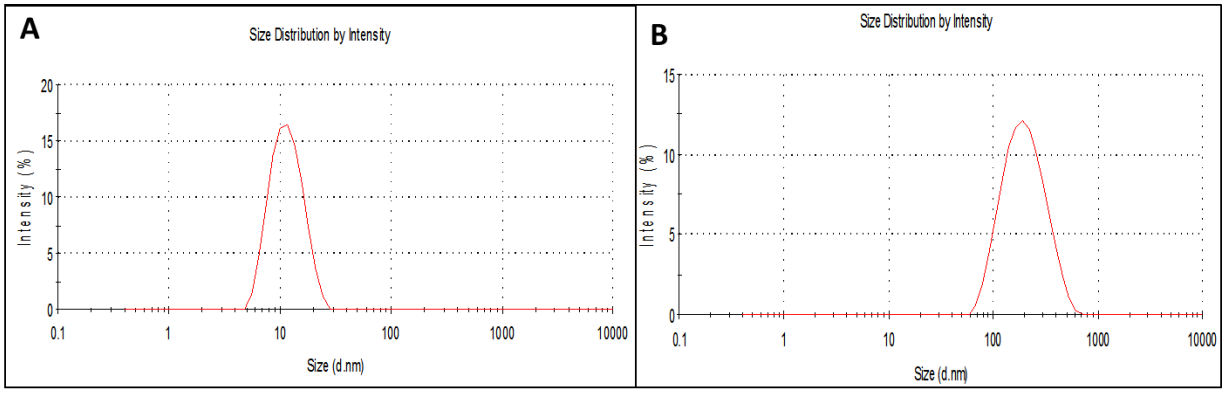


Figure 3-8: Showing comparative % of drug loading for LMH system; the same mass of carrier material (polymers and lipids) in different preparation methods (mean ± SD, n = 3).

The RPE method acquired the higher drug loading as in this method it allowed the preparation of liposomes with a high aqueous space-to-lipid ratio and enhanced the capability to entrap a large percentage of the aqueous materials presented. The slow elimination of the organic solvent allowed liposome formulations to have aqueous volume-to-lipid ratios that were up to four times higher than liposomes prepared by other methods. It has been demonstrated by Szoka *et al*. and that by using this method, more than 65% EE could be obtained.[185]

The presence of micelles in the supernatant (the unencapsulated LOV-Micelles) may correlate to the drug loading in the TFH method compared to the RPE method that results in greater loading in the RPE method. However, the TFH method was selected due to its simple, direct and efficient nature for large-scale production.

In order to quantify the number of micelles not encapsulated within the LMH, the size distribution of the supernatant and pellets was investigated separately (after ultracentrifuge of the LMH suspension). As illustrated in **Figure 3-9**, only a single peak in the size distribution was observed, i.e. monodisperse for the supernatant (containing micelles only **Figure 3-9 A**) and the pellets (containing LMH only **Figure 3-9 B**), respectively.



LMH supernatant containing micelles

LMH pellets containing LMH only

Figure 3-9: The size distribution after ultracentrifuge: (A) supernatant and (B) pellets.

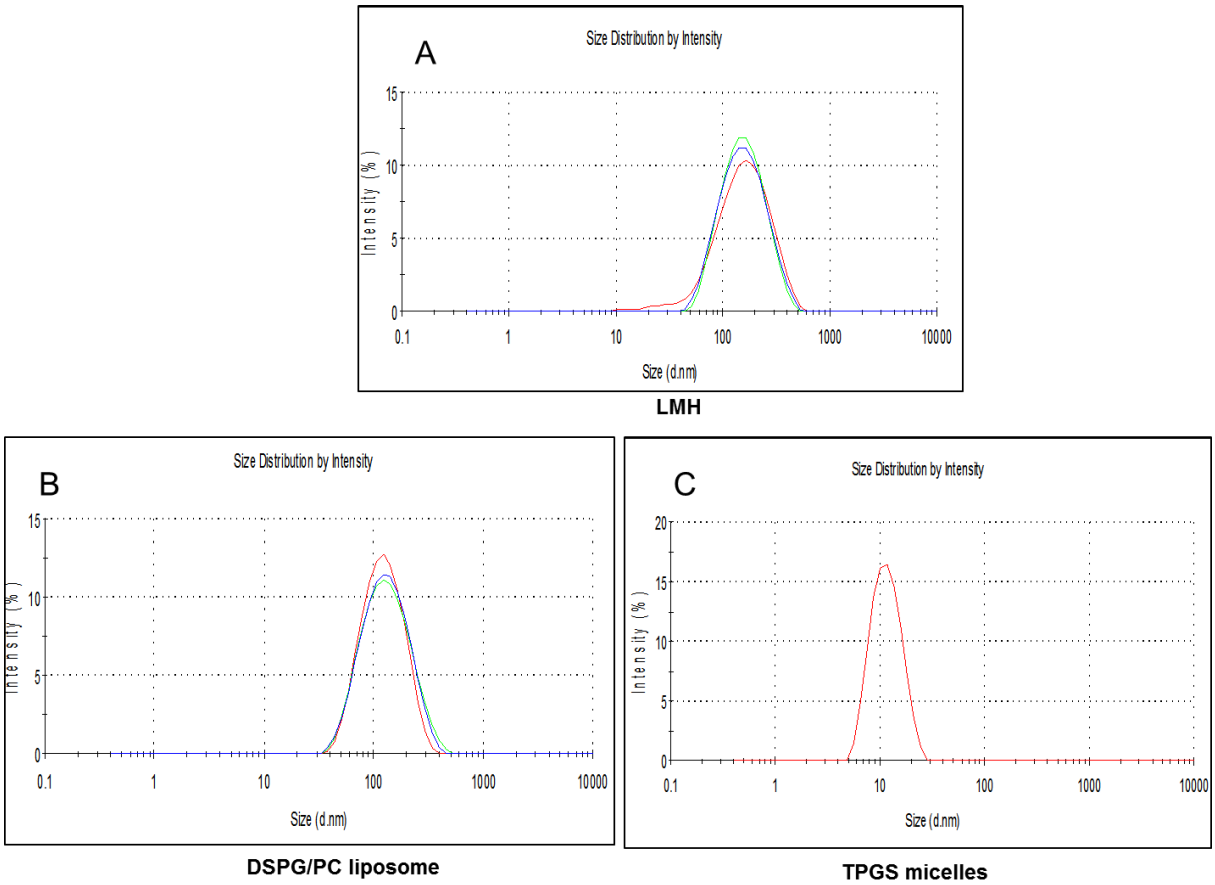


Figure 3-10: The size distribution of the nanocarriers; A) LMH, B) DSPG/PC liposomes and C) TPGS micelles respectively.

It was also revealed that there were no changes in size or breakdown of the LOV-LMH or no trace of bigger or smaller particles in the LMH formulation compared to the single micelles

or liposome particle size distribution. For all systems, only one peak was observed **(Figure 3-10)**, confirming that they remain unchanged even after ultrasonication and separation.

3.4.2. Microscopic characterisation of LMH

Cryo-transmission electron microscopy (Cryo-TEM) of LMH (PC: DSPG-TPGS) and liposomes reveal important information about the morphology, particle size and inner structure (**Figure 3-11**).

The images of liposomes and LMH displayed a spherical shape surrounded by a thin lipid bilayer (unilamellar) with an average diameter of > 100 nm (**Figure 3-11B and 11A**), correlating with the diameter determined using dynamic light scattering (**Figure 3-10**). These structures are similar to the liposomes observed by Ashley *et al.*[431] and in other literature.[428, 432-433] However, additionally, there were some worm-like micelles scattered inside the inner aqueous core of the LMH (**Figure 3-11A**). Notably, these structures were not observed inside the blank liposomes (without micelles).

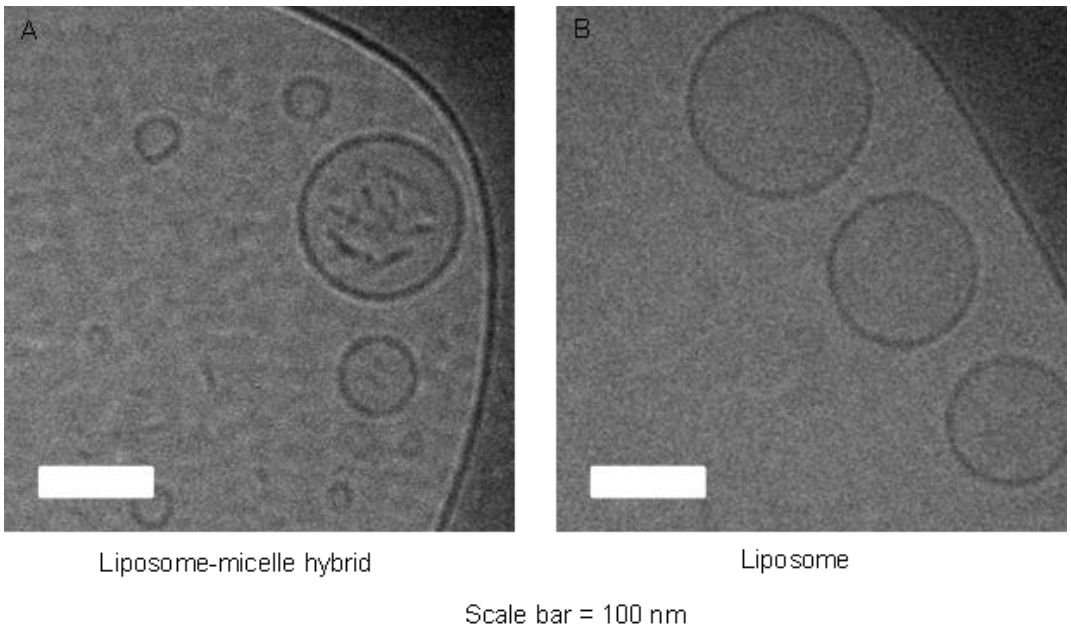


Figure 3-11: Cryo-TEM images of A) LMH and B) DSPG/PC liposomes (mean ± SD, n = 3).

Cautela *et al.*[434] also found worm-like micelles, formed by very long cylindrical and flexible aggregates of different amphiphiles, have been extensively investigated in the past several decades because of their remarkable visco-elastic properties that are exploited in numerous

technological fields.[434] It was also found that the LMH exists as unilamellar vesicles, where the micelles fill the void space and are surrounded by thin lipid single layer. Similar unilamellar, spherical shaped vesicles were previously observed for an elastic liposome containing ketorolac tromethamine.[423] Cai *et al.* also observed a worm-like poly(ethylene oxide)-b-poly(Ɛ-caprolactone) micelles and reported that these worm-like micelles have an improved solubilisation and stabilizing efficiency of hydrophobic drug paclitaxel.[435]

3.4.3. LOV release study from LMH system

The release study of poorly soluble drugs requires surfactants in the release media to achieve drug solubility and simulate intestinal conditions *in vitro*.[89] Initially, the solubility of LOV at different concentrations (% w/v) was investigated using PEG 400 in phosphate buffered solution (PBS).

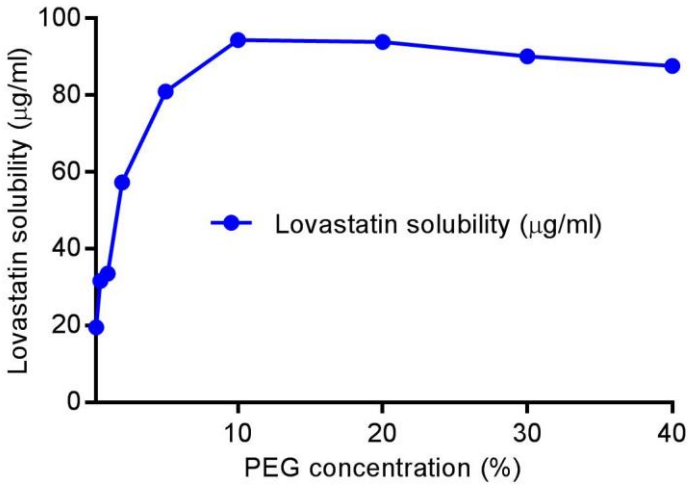


Figure 3-12: Investigation of the LOV solubility in different percentages of PEG-400 (0.2, 0.5 and 10- 40 % w/v) in PBS solution to find the maximum solubility of LOV in PEG-400 (mean ± SD, n = 3).

It was found that LOV solubility increased with increased PEG-400 concentration (**Figure 3-12**). The highest solubility (90%) was found at 10% (v/v) PEG-400, before plateauing up to 40%. To maintain the sink condition for LOV release from different formulations, the 0.5% PEG-400 (31.63 µg/mL drug dissolved) was used with PBS (which is simulated to physiological pH of 7.4). PEG impacted on drug release by increasing solubility in release

media. Here PEG was used to create sink conditions as surfactants are commonly added to create sink conditions.

The release of LOV from micelles, liposomes and LMH were determined *in vitro* at a temperature of 37 °C by dialysis method[39, 333](**Figure 3-13).** For micelles, controlled release characteristics were observed, with 40% of LOV released within 12 hours followed by a more gradual release of 90% over 240 hours. Here, the micelle might act as a barrier against the release of LOV and that the hydrophobic core of the micelle strongly restricts the release of the drug into the media. This might be due to the more hydrophobic domain of the polymer providing stronger hydrophobic interactions with the hydrophobic drug. Similar results have been reported in the literature for doxorubicin loaded chitosan micelles.[436] In addition, the PEG layer (from release media) may act as a molecular fence that helps to retain the drugs inside the micelles.[437]

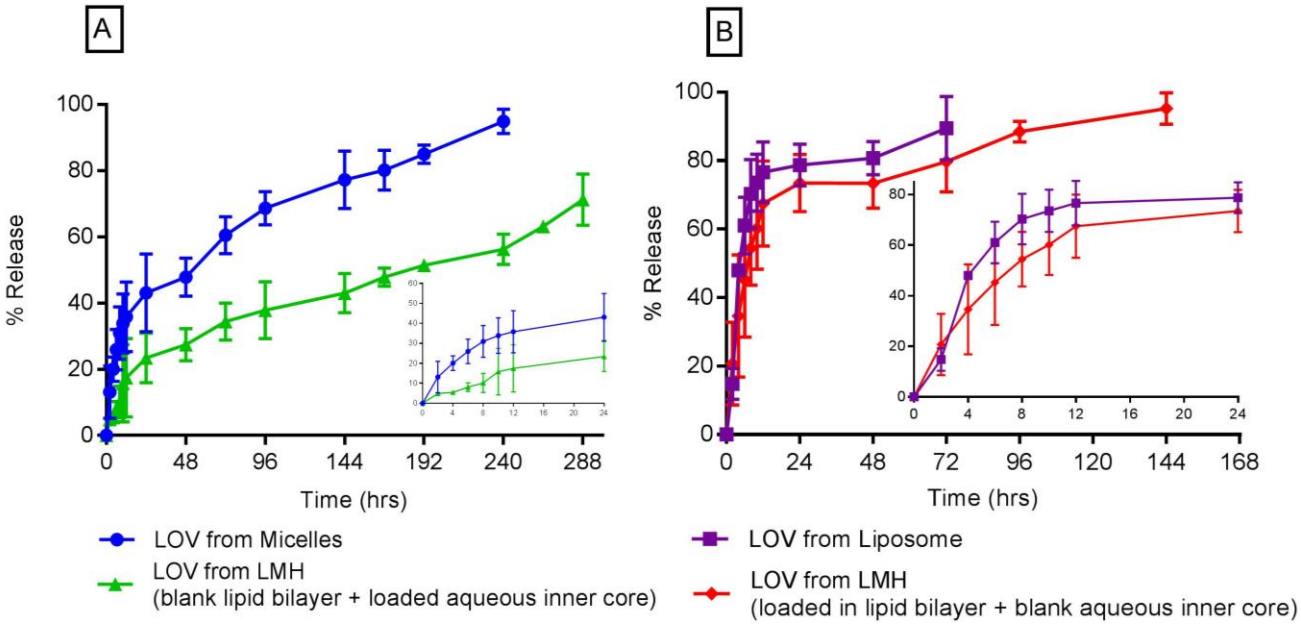


Figure 3-13: LOV release from A) micelles and LMH (blank lipid bilayer + loaded aqueous inner core), B) liposomes and LMH (loaded lipid bilayer + blank aqueous inner core) at 37 °C for 24 hours (inset graphs) and up to 10 days with (PBS + PEG-400 (0.5%) dialysis bag (mean ± SD, n = 3).

For LOV release from LMH (blank lipid bilayer and loaded micelle aqueous core**, Figure 3-13 A, B**), the LOV release rate was characteristic of controlled release and noticeably slower compared to the micelles. Controlled release was observed over extended periods of time for

10 days. Only 17 % (where micelles were 40%) of LOV was released within 12 hours, followed sustained behaviour and almost 56% at 240 hours (compared to 90% from micelles) and finally reached to 71 % of LOV released after 288 hours. For the LMH, the LOV from micelles has to pass through the hydrophobic micellar core and then the liposome bilayer, therefore, the release rate is slower than the micelles alone. Moreover, TPGS molecules may stabilize and modify the liposome bilayer structure, which may control the release of the drug (**Figure 3-14 A, B**).

However, in liposomes, LOV showed fast release over 12 hours, with 75% of LOV released at 24 hours before a plateau over 48 hours and finally 85% of drug release after 72 hours. The initial fast release was related to the detachment of drugs from the surface or near to the surface in the bilayer, while the later slow release is ascribed to the sustained release of the lipophilic drugs from the core (**Figure 3-14 B**). Similar results have been reported for doxorubicin loaded phosphatidyl ethanolamine (PE)-conjugated nanoliposomes.[438] It was also described the fast release of LOV from liposome bilayer is due to the presence of the PEG in the release media which have the ability to induce lipid bilayer fusion that enhanced release rate. PEG has been widely used to induce lipid bilayer fusion as reported by Malinin *et al*. PEG is a hydrophilic polymer that causes fusion of lipid vesicles.[439-440]

From the LMH (loaded lipid bilayer and blank micelle aqueous core), the LOV release rate was characteristic of controlled release over 24 hours and release rate is relatively slow compared to liposomes. Only 67 % of LOV was released within 12 hours and 73% drug released at 24 hours before starting to plateau at 48 hours. After that, it is gradually increased and almost 95 % of LOV released after 240 hours. For the LMH, LOV release from lipid bilayer is slower than the release from liposomes alone. This is because LOV has to pass through the liposomes bilayer similar to liposome however due to TPGS micelles loaded inside, the liposome bilayer structure can be stabilized and modified, providing better control of drug release compared to liposomes alone (**Figure 3-14 C, D**). Similarly, a nanohybrid system of non-ionic surfactant (i.e. Solutol) inserting into liposomes bilayer loaded with paclitaxel used as a stabilizers has been reported by Ji *et al*.[441] Liangfang *et al*. also stabilized a liposome using nanoparticles (NPs), poly D, L-lactic-co-glycolic acid (PLGA) polymer to form the polymeric core of the NPs and 1,2-distearoyl-sn-glycero-3-phosphoethanolamine (DSPE), to form the "stealth" shell of the NPs; to control the paclitaxel release from lipid-polymer hybrid NPs.[442]

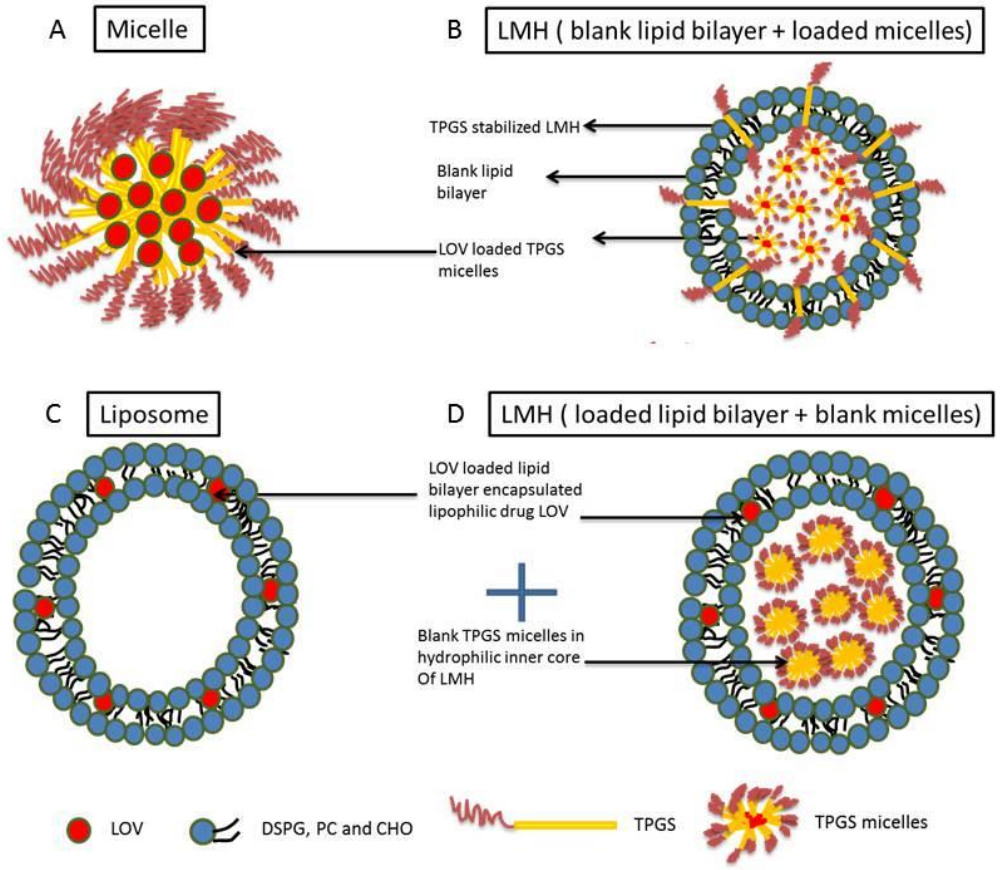


Figure 3-14: Schematic presentation of different nanocarriers A) Micelles, B) LMH (blank lipid bilayer + loaded micelles in inner aqueous core), C) Liposome, D) LMH (loaded lipid bilayer + blank micelles in inner aqueous core).

Arora *et al*. [203] reported the sustained release of LOV by formulating of an elastic liposomal formulation using different proportions of surfactants, i.e. sodium cholate, sodium DC.[203] In another study, Yanamandra *et al*. [374] reported that a proliposomal formulation shows the very fast LOV released (about 99% within 2 hours).[374]

Literature also reported that the release of insoluble drugs is increased with the addition of ethanol in release media.[443] Therefore, further release studies were performed with the addition of 20% ethanol in water in addition to Tween-80 (0.2% w/v) to see how solubility enhancement in media with ethanol influenced the release profile.

For micelles, a fast release profile of about 95 % of LOV released within 48 hours **(Figure 3-15)** in comparison to 48% of PEG-400 in PBS **(Figure 3-13A).** However, for liposomes, the release was not varied significantly compared to micelles. Though a faster release profile

compared to micelles was observed initially and after that about 90 % of LOV released within 48 hours in comparison to 80% of PEG-400 in PBS **(Figure 3-13B)**. The release of LOV from liposomes was faster in this media compared to the release of LOV in previous media above due to the presence of ethanol that destabilising the liposomes by acting as a permeation enhancer, penetrating into the liposome lipid bilayer to reversibly decrease the barrier resistance. A similar mechanism of permeation enhancer ability of ethanol was also reported by Williams *et al*.[444] Literature also reported the use of ethanol for the release of water-insoluble drugs. For example; Kuo-Sheng *et al*.[443] used 30% ethanol with PBS for the release of Apomorphine diester from prodrugs and nanostructured lipid carriers.

Besides, for LOV release from LMH in PBS, ethanol and tween 80 media, it was found that about 48% of the LOV released within 48 hours (LOV loaded both in bilayer and aqueous core), demonstrated a controlled release profile **(Figure 3-15)**. However, this release was faster than LMH **(Figure 3-13A)** with inner core loaded, 27% and slower than LMH **(Figure 3-13B)** with bilayer loaded, 73% over the same time period in PBS and PEG-400 release media.

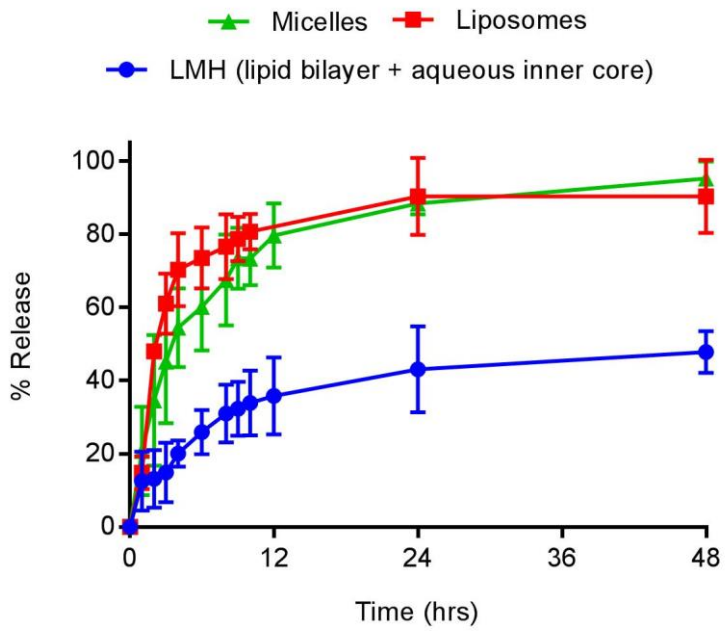


Figure 3-15: LOV release from micelles, liposomes and LMH (lipid bilayer and aqueous inner core) in release media (PBS with 0.2% of tween 80) and 20 % ethanol (mean ± SD, n = 3).

The release of LOV from LMH loaded in both the bilayer and the micellar inner core was only performed for the ethanol/tween release media. This is because, the LOV release from both bilayer and the micellar inner core gives the total drug release from LMH, which provides the greater amount of the LOV. To dissolve these LOV and keep gradient in constant ethanol/tween release media. The PEG-400/PBS was not used here due to low saturation solubility of LOV than ethanol/tween as well as simulated with the physiological system. Moreover, the use of ethanol/tween in a release media will impact on the permeability of a lipid bilayer (i.e. the liposome), potentially in a different way to the use of a micelle containing release media (the micelles provide the "sink" for the released poorly soluble drug to be solubilized in). This type of media is reported in the literature[443-444] and it was part from an evaluation of methodology and after that, came back to the general method of PEG 400/PBS as a media.

3.4.4. *In vitro* drug release kinetics

To determine the release mechanism of LOV release from micelles, liposomes, and LMH, the Korsmeyer–Peppas[445] model was used as this model is reliable compared to other models.[446-452] This model is simple and applied for a polymeric matrix. There are several simultaneous processes considered in this model such as water and drug diffusion, drug and dissolution/swelling of the matrix. Key attributes of the models include water and drug diffusion coefficients vary as functions of water concentration. The power law can only give limited insight into the exact release mechanism of the drug and the value of exponent *n* are found that would indicate a diffusion controlled drug release mechanism. All parameters are quite realistic in my kinetic analysis, that's why the Korsmeyer-Peppas model was used to fit release kinetics. Literature is also provided that have used a similar model for determining the kinetics of release from micelles and liposomes. [292] reliable compared to other models.[446-452] This model relates to the fractional release of drug with time and the model is derived according to **equation (3-2).**

$$M_t/M_\infty = Kt^n \qquad \textit{Equation (3-2)}$$

This model generally describes release from a polymeric system where M_t/M_∞ is fractional drug release (usually as %), *K* is a characteristic kinetic constant and *n*, an exponent coefficient that characterises the mechanism of release.

In order to access more details of the release mechanism, the diffusion coefficient (*D*) for each of the drug molecules in the nanocarriers matrix also derived using the non-steady-state diffusion model equation as described elsewhere[293, 453] **(equation 3-3)**

$$M_t/M_\infty = 4(Dt/\pi\lambda^2)^{1/2} \qquad \textit{Equation (3-3)}$$

Where, *Dt* drug diffusion coefficient at time t, λ is the thickness of the nanocarriers (the value is too small, so it was considered negligible and (*t*) is the time of the measurement.

The drug release data were fitted to both **equation 3-2** and **3-3** using a custom-written non-linear regression code within the MATLAB programme (Appendix A). The resulting diffusion constants (*D*) from **equation 3-3** and exponent values (*n*) from **equation 3-2** are shown in **Table 3-5** and **Teble 3-6**, respectively.

The diffusion coefficient (*D*) values of LOV from the LMH particles are less than from liposomes and micelles in release media PBS with PEG-400 0.5% (v/v), which correlates with their release rate. The LMH shows a slow release, therefore, its *D* value is small in comparison to micelles and liposomes. Similarly, the diffusion rate from micelles is smaller than that determined for liposomes. The same trend is also observed for other sink condition, Tween 80 and 20% (v/v) ethanol.

Table 3-5: The exponent value (n) used to characterise the drug release mechanism and the diffusion coefficient (*D*) for LOV, for their release from micelles-liposome and LMH (release media PEG-400, 0.5% and 0.2 % Tween 80 + ethanol). The exponent value (n) and the diffusion coefficient (*D*) was obtained by non-linear fitting (MATLAB-R2017a) of the fractional drug (M_t/M_∞) release data to Equation 3-2 as a function of time over 48 h.

Nanocarrier Type	**PEG-400, 0.5%**			**Tween 80 + ethanol**		
	n	R^2	*D* (m^2/s) x 10^{-10}	*n*	R^2	*D* (m^2/s) x 10^{-10}
LMH (lipid bilayer)	0.528	0.930	0.128	Not done		
LMH (aqueous inner core)	0.286	0.972	0.796	0.286	0.977	3.18
Liposome	0.22	0.941	1.80	0.296	0.959	5.39

Micelle	0.347	0.993	0.382	0.337	0.981	0.70

The calculated diffusion coefficient (*D*) values are also significantly varied for different sink condition, as shown in **Figure 3-16**.

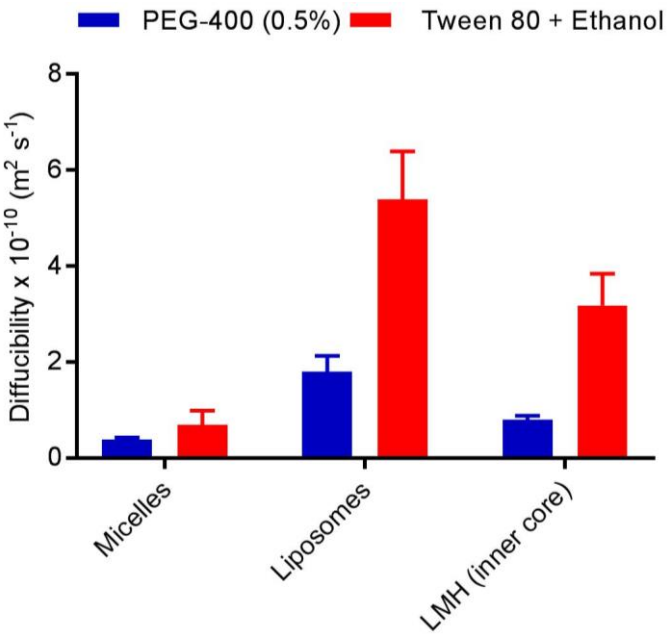


Figure 3-16: Calculated diffusion coefficients (*D*) from equation 3-2 for micelles, liposomes and LMH A) PEG-400 (0.5%) and B) Tween 80 +ethanol.

According to Korsmeyer and Peppas,[445] a value for $n < 0.5$ suggests that the overall solution-diffusion mechanism is Fickian **(Table 3-6)**. Here, it was found that the values of *n* are below 0.5 for LMH and other nanocarriers, suggesting the mechanism of the release of LOV from nanocarriers is Fickian diffusion. This mechanism follows likely due to the formation of a potential chemical gradient between the carrier and its outer release media.[445]

Table 3-6: The relationship between the diffusion exponent (*n*) and the solute (drug) release mechanism as proposed by Korsmeyer Peppas.[445]

Diffusion exponent (*n*)	**Overall solute diffusion mechanism**
$n \leq 0.50$	Fickian diffusion
$0.50 < n < 1.0$	Anomalous (non-Fickian) diffusion
1.0	Case II transport/zero-order release
$n > 1.0$	Super case II transport

3.4.5. Short–term stability test of liposomes and micelles

3.4.5.1. Physical stability of micelles and liposomes indifferent preparation (different pH) conditions

To investigate the effect of pH on the size and zeta potential of the nanocarriers, TPGS micelles and DSPG/PC/CHO liposomes were measured at four different acidic pH values; pH 2, 4, 5 and 6 and ionic strength of 1 mM NaCl. As mentioned above we prepared micelles and liposomes at 1 mM NaCl solution. Before selecting the pH of the preparation media, initially, we investigate the stability of liposomes and micelles at different pH such as 2, 4, 5 and 6 **(see Table 3-7)**. A stability study was not undertaken for drug alone because the effect of pH on lovastatin has been reported in the literature.[454]

Table 3-7: Effect of different hydrations pH on size and PDI of TPGS micelles and DSPG/PC/CHO liposomes (mean ± SD, n = 3) 24 hours after preparation.

Nanocarriers	Micelles		Liposomes		
Hydration pH	Diameter (nm.)	PDI	Diameter (nm.)	PDI	Zeta potential (mV)
1 mM NaCl	12.17 ± 1.39	0.226 ± 0.04	115 ± 7	0.232 ± 0.05	- 42 ± 3
pH 6	12.21 ± 0.16	0.214 ± 0.04	150 ± 3	0.421 ± 0.04	- 67 ± 1
pH 5	12.01 ± 0.80	0.185 ± 0.07	102 ± 1	0.228 ± 0.01	- 54 ± 1
pH 4	12.55 ± 2.09	0.161 ± 0.08	126 ± 4	0.245 ± 0.01	- 28 ± 1
pH 2	12.36 ± 0.76	0.194 ± 0.05	222 ± 14	0.428 ± 0.09	- 23 ± 3

For micelles, in 1 mM NaCl the diameter was 12.17 ± 1.39 nm and the PDI was 0.226 ± 0.04 (**Table 3-7)**. The diameters were 12.21 ± 0.16 nm, 12.01 ± 0.80 nm, 12.55 ± 2.09 nm and 12.36 ± 0.76 nm for pH 6, pH 5, pH 4 and pH 2 respectively. The obtained average particles diameters were not changed significantly with the changing of the hydration pH. All DLS spectra showed a single peak, indicating that there was no aggregation or disruption of the micelles across a range of different pHs **(Figure 3-17)**. This was achieved because of the absence of any charge on TPGS molecules. The obtained PDI values were 0.214 ± 0.04, 0.185 ± 0.07, 0.161 ± 0.08 and 0.194 ± 0.05 with similar pH conditions. The consistent size distribution of micelles with the change of the pH values was clearly visualized by DLS size distribution **(see Figure 3-17)**. The PDI was also affected at different hydration pH though the changes were not significant and the values varied from acidic to neutral for micelles (**Table 3-7)**.

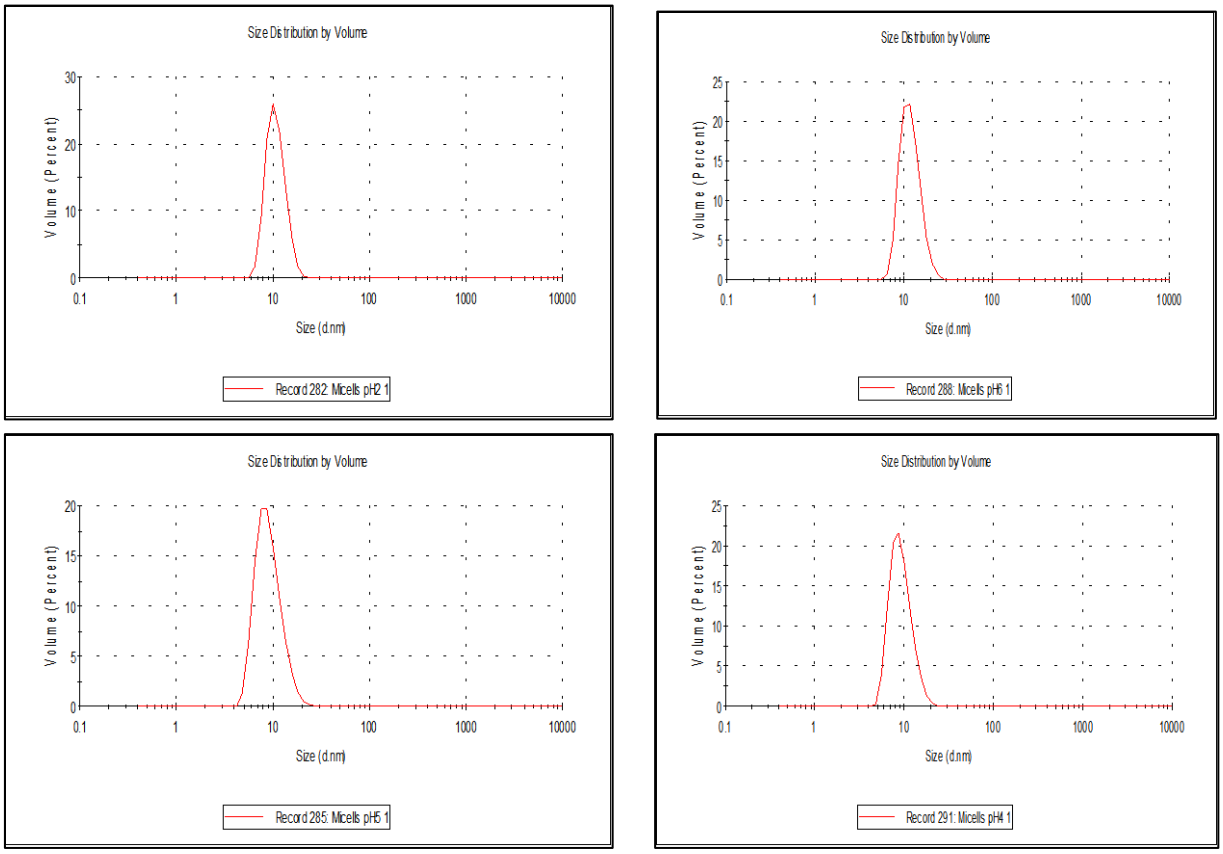


Figure 3-17: Effect of different hydration pH on LOV micelles.

For liposomes, in 1 mM NaCl solution, the diameter, PDI, and zeta potential were 115 ± 7 nm, 0.232 ± 0.05 and -42 ± 3 respectively. The change of diameters were 150 ± 3 nm, 102 ± 1 nm, 126 ± 4 nm and 222 ± 14 nm. for pH 6, pH 5, pH 4 and pH 2 respectively (**Table 3-7).** The average particles diameters and their polydispersity changed significantly with changing hydration pH. The obtained PDI values were 0.421 ± 0.04, 0.228 ± 0.01, 0.245 ± 0.01 and 0.428 ± 0.09 for pH 6, pH 5, pH 4 and pH 2 respectively also affected at different pH significantly**.** The varying diameters of the liposomes were, as shown in **Figure 3-18A**. The results showed that the obtained average particles diameter of liposomes varied in different hydration pH compared to the average particles diameter of liposomes hydrated in 1 mM NaCl solution and **Table 3-7**. In pH 2 and pH 6, the liposomes showed larger size compared to hydration in 1 mM NaCl solution (as prepared above). The obtained average particles diameter at pH 5 was slightly lower than the size of liposome prepared in 1 mM NaCl hydration media. However, at pH 4 the obtained, average particles diameter of liposomes were close to (~100 nm) to the average particles diameter of liposomes hydrated in 1 mM NaCl solution within the experimental errors **(Figure 3-18A)**. The fluctuated liposome size

with the change of pH value was clearly visualized by DLS size distribution **(see Figure 3-19)**. The size distribution showed additional peaks in pH 2, 4 and 6, indicating the degradation of the liposomes at the different condition. Particles observed above 200 n.m. may be due to aggregation of liposomes at pH 2 and pH 4 when they were partially deprotonated. The aggregation number increases with an increasing ionic strength and lowering of the pH.[455-457] This aggregation leads to a larger apparent size. Similar aggregation also observed by Hasan *et al*.[458] when he evaluated the influence of pH on the diameter of chitosan-coated liposomes at pH 6.5.

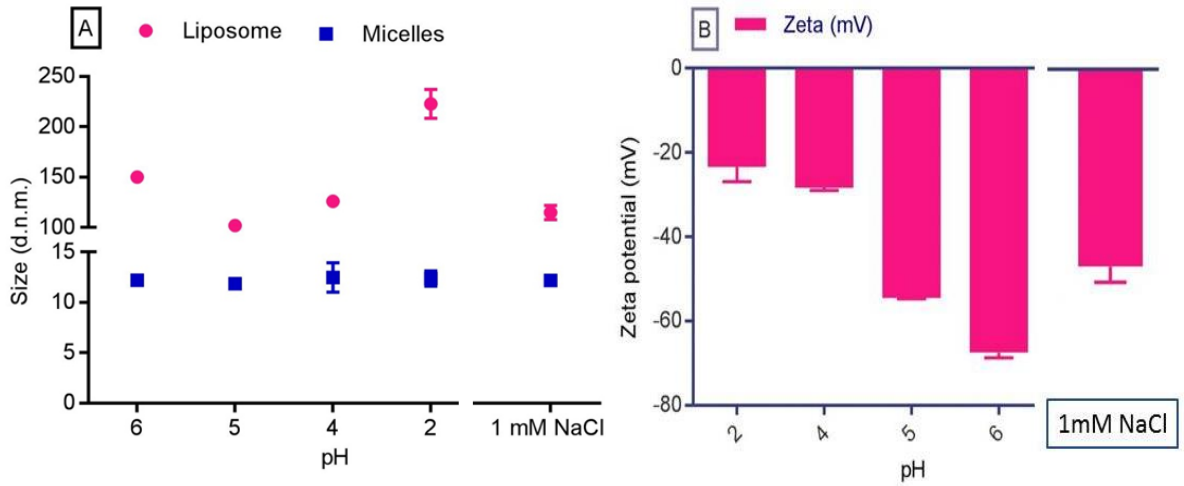
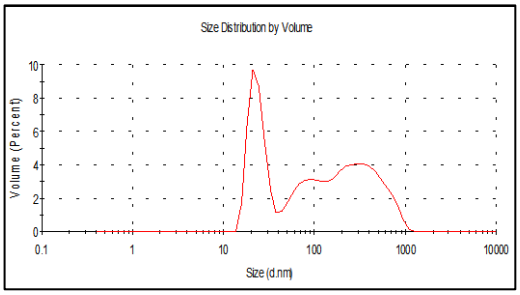


Figure 3-18: Effect of different hydration pH on (A) particle size of liposomes and micelles and (B) zeta potential for DSPG/PC liposomes (mean ± SD, n =3).

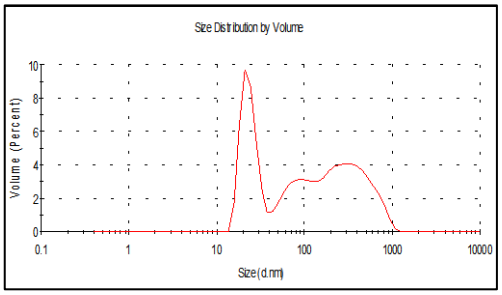
The zeta potential of the liposomes was also varied in different hydration pH. In different pH the zeta values were - 67 ± 1 mV, - 54 ± 1 mV, - 28 ± 1 mV and - 23 ± 3 mV for pH 6, pH 5, pH 4 and pH 2 respectively. The zeta potential affected drastically at different hydration pH significantly. The zeta values increased with high hydration pH (pH 5 and pH 6) compared to the zeta values of liposomes hydrated in 1 mM NaCl solution **Figure 3-18B.** The zeta showed increased value in pH 5- pH 6, and it is reported that zeta potential values above 30 mV provide good stability and above 60 mV provides excellent stability because of the enhanced stabilization of the liposomes at higher pH value.[417-418] However, zeta potential values reduced at lower pH value observed for pH 4 and pH 2. This reduced zeta was due to aggregation of liposomes at pH 2 and pH 4. The zeta potential became more anionic at higher pH and less anionic at a lower pH. This is most likely due to the extent of protonation of the

primary amines on DSPG and PC lipids. At lower pH, more of the amines are expected to be protonated, thus lowering the zeta potential value. Even a small change in pH could have a very big impact on zeta potential, as demonstrated here with the DSPG/PC/CHO liposomes. However, this effect is highly dependent upon on pH values within the range tested (pH 2–6).

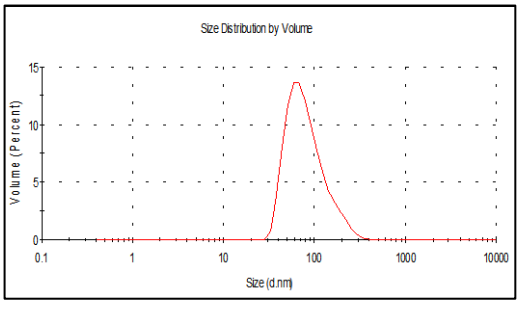
Similarly, reduced zeta potential and subsequent aggregation with pH was reported by Honary *et al.*[417-418] Clogston *et al.*[459] and Smith *et al*. also as reported that small changes in any of these parameters can potentially have dramatic effects on the zeta potential values of the liposomes.[460] Among the parameters, ionic strength (i.e. 1mM NaCl) and pH are two of the most varied parameters for zeta potential measurements, yet have the most profound impact on the output values. As highlighted in **Figure 3-18B**, small changes in pH (ionic strength was kept constant) can have a significant effect on the zeta potential distribution. Similarly high negative charge - 63 ± 2 mV in higher pH 7.6 was reported by Smith *et al.* for a DSPC/CHO/DOPS liposome.[460] They also observed reduced zeta potential value from - 63 ± 2 mV to - 45 ± 1 after addition of 0.01 mol/L NaCl in that solution of pH 7.6. It indicates that presence of NaCl in the solution has an effect on the zeta potential of liposomes.



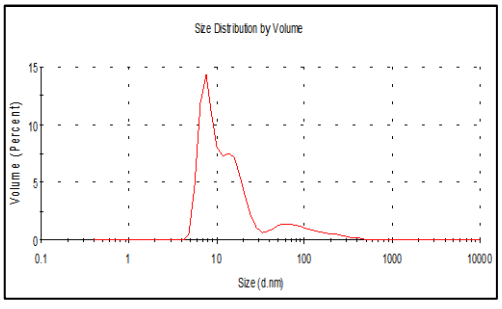
pH 2



pH 4



pH 5



pH 6

Figure 3-19: Effect of different hydration pH on LOV liposomes.

3.4.5.2. LOV content stability at different pH values

The stability of LOV in formulations was also determined at different pH for up to 3 months when stored at 4°C (**Table 3-8**) to investigate any changes in LOV loading, size and zeta potential over time. The short-term stability of the LOV content (percentage) in liposomes and micelles were also measured after 3 months stored at 4 °C in similar pHs, including 1mM NaCl solution (**Figure 3-20)**.

The liposomes formulated at pH 5 retained a higher content of LOV, with almost 75% of LOV still present after 90 days (**Figure 3-20**). Again, lower LOV content was found at pH 2 and after 14 days only 40 % drug was detected, which was further reduced to 30% after 90 days. However, for pHs 4, 6, and in 1 mM NaCl, almost similar trends were observed where 50% LOV was present after 90 days.

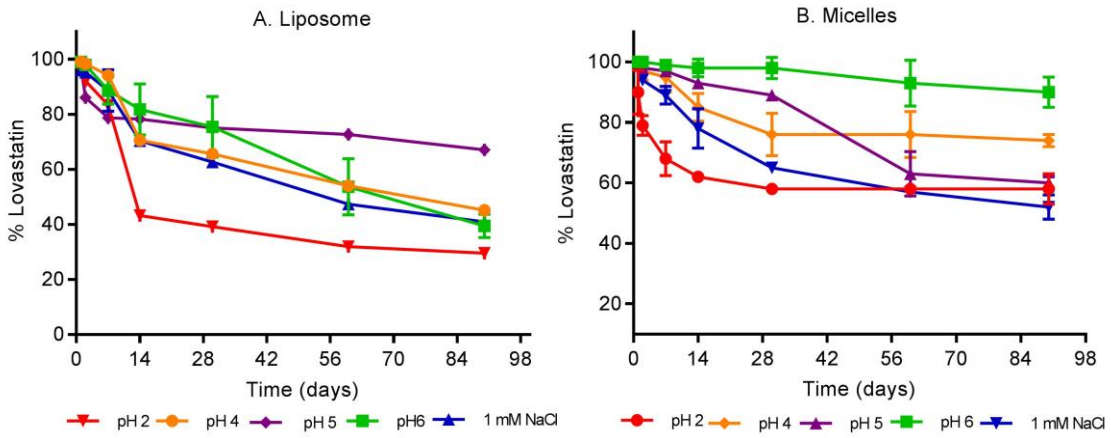


Figure 3-20: The percentage of LOV content in A) liposomes and B) micelles with i) 1 mM NaCl (ionic strength) and ii) 1 mM NaCl + different hydration pH over 3 months (mean ± SD, n = 3).

For micelles, the highest stability of LOV content was found at pH 6 (**Figure 3-20B**). The micelles retained almost 100% of its initial LOV content after 14 days and then gradually decreased to nearly 93% within 90 days after storage at 4 °C. At pH 4 the drug content decreases to 76% after 30 days and then remained constant over 90 days. However, at pH 2, 5 and in 1 mM NaCl, despite initial differences in LOV content, after 90 days approximately 60% of LOV was still present. testified

On the basis of this study, it was concluded that pH 5 was the optimal pH for long-term storage of LOV-containing hybrids. Similar pH value (pH ~ 5) was also reported by Alvarez *et al*. for the stability of a statin drug simvastatin. It has been testified that the statins exist in the lactonic form and however, it can be reversibly hydrolyzed to the hydroxy acid form at both very low and alkaline pH. Formulation of the poorly soluble simvastatin lactone form in micellar systems in this pH may enable both improvements of solubility and delay of hydrolysis, resulting in greater oral bioavailability.[461]

3.4.5.1. LMH Physical stability with storage

The stability was measured in different hydration pH for 24 hours and the changes in size and zeta potential were investigated in aqueous dispersions over the storage time of 3 months in a fridge (4 °C), as listed in **Table 3-8**.

Table 3-8: Data presented here of the size and zeta potential up to 3 months (mean ± SD, n = 3)

Nanocarriers			LMH	Liposomes	Micelles
Size (nm)	Initial		167.71 ± 2	94.27 ± 0.2	11.08 ± 0.2
	Months	1	152.17 ± 2	99.58 ±0.2	12.77 ± 0.1
		2	138.46 ± 24	110.18 ± 8	12.84 ± 0.1
		3	133.8 ± 0.7	158.5 ± 0.4	14.89 ± 2.5
Polydispercity index (PDI)	Initial		0.505 ± 0.2	0.264 ± 0.01	0.135 ± 0.02
	Months	1	0.257 ± 0.0	0.231 ± 0.03	0.261 ± 0.02
		2	0.212 ± 0.0	0.419 ± 0.1	0.147 ± 0.01
		3	0.218 ± 0.0	0.229 ± 0.02	0.189 ± 0.06
Zeta potential (mV)	Initial		-22 ± 2.7	-42.3 ± 1.1	-1.26 ± 1.6
	Months	1	-28.4 ± 0.7	-34.16 ± 6.0	Not done nearly 0
		2	-30.56 ± 0.5	-48.18 ± 3.1	
		3	-38.93 ± 0.8	-59.95 ± 8.5	

For LMH, it was observed that their size decreased by 20.4% at the conclusion of storage (3 months). The DLS spectra **(Figure 3-20)** showed a monomodal distribution for the LMH formulation, indicating no major aggregation or disruption of the LMH particles. A different trend was observed for the liposomes and micelles. Liposomes average particle size gradually increased from 94 to 158 nm and for micelles, a slight increase was observed from 11- 14 nm over the course of three months. In general, aqueous liposomal dispersions suffered a series of stability problems such as aggregation and leakage of the encapsulated drugs. In this sense,

freeze-drying may offer an alternative for storing liposomes suspension, by preserving them in a more stable dry state as has been referred to in previous studies.[462]

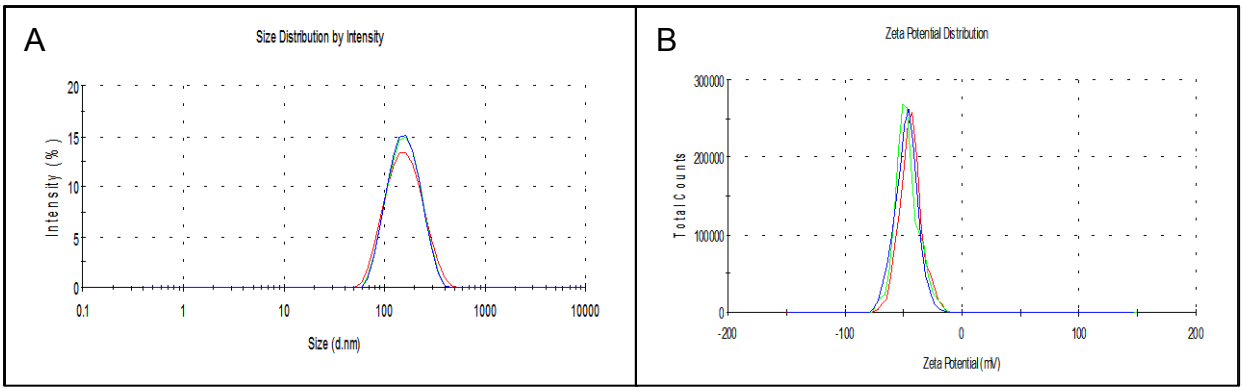


Figure 3-21: (A) The size distribution and (B) zeta potential of LMH after 3 months kept in the freezer (4°C) (mean ± SD, n = 3).

The zeta potential of LMH, however, increased with increased storage time. The zeta potential of liposomes also fluctuated over the storage period. Zeta potential was not measured for micelles as TPGS possess neutral charge, however, the changes were not significant for either liposomes or micelles.

3.5. Conclusion

A novel LMH system was developed through a combination of micelles and liposomes. The micelles were developed based on commonly used polymers and surfactants that are widely used for drug delivery, including poloxamer 407, 188, DC, TPGS, and a mixed poloxamer-DC system to rationalise their physical characteristics and influence of their chemical structure on drug loading and release capabilities. The loading of LOV within TGPS micelles was 2.05 (% w/w), which was an improvement over the other surfactant systems studied (0.181 % w/w for poloxamer micelles and 0.926 % w/w for poloxamer and DC mixed micelles). However, the LOV loading was lower than for DC micelles. The TPGS micelles demonstrated good stability and appearance over time by visual inspection of size and loading level for 3 months. Although the drug loading levels of DC-based micelles was greater, their long-term stability at room temperature was poor, rendering them unsuitable for future applications. Similarly, liposomes were also developed using different lipids: including; PC, CHO and DSPG, as well as combinations of these lipids, to optimise their

physical characteristics and drug loading. Initially, PC/CHO liposome was prepared and found unstable due to poor charge. The DSPG/PC/CHO liposome was found to be the most highly negative and have better physicochemical properties.

Finally, a combination of micelles and liposomes, a LMH was developed. Different methods of LOV incorporation were investigated to determine how to incorporate the micelles into the liposomes and also the key part of this study was to optimize the drug loading and the drug EE of LOV into LMH. LOV loading was comparatively high for RPE compare to FT and TFH methods. A significant quantity of LOV loading was achieved, with improvement in aqueous solubility of LOV. Moreover, the Cryo-TEM of LMH (PC: DSPG-TPGS) and liposomes revealed a spherical shape surrounded by a thin lipid bilayer (unilamellar) with an average diameter of > 100 nm. Some worm-like micelles were scattered inside the inner aqueous core of the LMH which was absent in liposomes. The LMH improved the release profile compared to the individual liposomes and micelles. Though LOV from micelles and micelles loaded in LMH demonstrated extended sustained for 288 hours release characteristics, however, LOV loaded in liposomes and liposomes of the LMH exhibited controlled release over 72 hours only.

A short-term stability test for LMH was performed over 3 months in 4 °C. It was observed that their size decreased by 20.4% with a monomodal size distribution for the LMH formulation, indicating no major aggregation or disruption of the LMH particles. The presence of TPGS stabilized the lipid bilayer, which provided a significant improvement in stability compared to the liposomes. From the drug content stability study, it was found that the liposomes formulated at pH 5 retained the higher content of LOV, with almost 75% of LOV still present after 90 days. However, for micelles, the highest stability of LOV content was found at pH 6. The micelles retained almost 100% of its initial LOV content after 14 days and then gradually decreased to nearly 93% within 90 days after storage at 4 °C.The LMH generated in this work could be helpful for the sustained and controlled release of LOV. Overall, this result combined together gives a unique hybrid particle system with advanced controlled drug release properties advantageous for further *in vivo* study for application in the clinic.

Chapter Four

4. Evaluation of a Liposome-Micelle Hybrid System to Improve the Intestinal Transport of Lovastatin using Caco-2 Cell Monolayers

Chapter outline

In this chapter, the cellular activity of lovastatin (LOV) encapsulated in LMH was investigated in a Caco-2 cell monolayer (CCM) *in vitro* model of the intestine. Initially, the biocompatibility of the LMH system was determined with the Caco-2 cell line and then a number of experiment was performed. The study includes cellular permeability, measurements of transepithelial electric resistance (TEER), apparent permeability (*Papp*), efflux ratio (ER), drug transportation, cellular uptake and accumulation of LMH within cell monolayers. The biocompatibility of the LMH system was evaluated by an Alamar blue assay. The *Papp* was used to trace the perviousness of LOV-LMH in comparison to free drug from the apical to the basolateral (A-B) or basolateral to apical (B-A) side and by either passive or active transport processes. From these measurements, the ER and drug transportation across the monolayer was determined. The intracellular uptake and accumulation of the LMH were also investigated within the CCM. The overall cellular activity is schematically presented in **Figure 4-1**

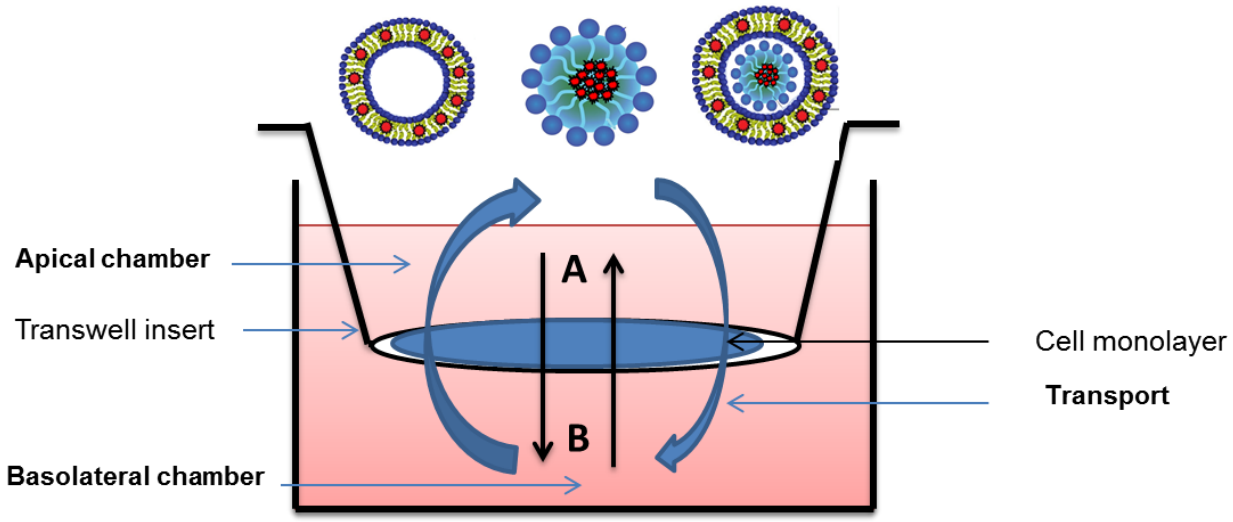


Figure 4-1: Schematic representation of Caco-2 cell monolayer (CCM) cultured on permeable supports to trace the permeability of the LMH in two directions, from the apical to the basolateral (A-B) side or basolateral to apical (B-A).

4.1. Introduction

LOV is an inhibitor of 3-hydroxy-3-methylglutaryl-coenzyme A (HMG-CoA) reductase that is currently used in the treatment of hypercholesterolemia and mixed dyslipidemia. LOV is a monocarboxylic acid with a pKa of 4.26.[349] It is a highly lipophilic and poorly water-soluble drug (0.4 mg/L).[79] According to the Biopharmaceutical Classification System (BCS), LOV is a Class II drug (high permeability and low solubility).[93] Due to its high lipophilicity, LOV undergoes extensive first-pass metabolism in the liver, resulting in low and variable bioavailability and pre-systemic metabolism; it shows < 5 % bioavailability and only 30 % of the oral dose is absorbed.[111] LOV and its β-hydroxy acid metabolite are both highly bound (> 95%) to human plasma proteins and can cross the blood-brain and placental barriers. The plasma half-life is only 1.1-1.7 hour.[109] The low bioavailability is attributed to the following aspects: (1) the limited aqueous solubility and dissolution, (2) the multidrug efflux pump, due to an increased activity of P-glycoprotein 1 (permeability glycoprotein or P-gp), and (3) high affinity to intestinal and liver cytochrome P450 metabolic enzymes.[463]

P-gp is an efflux transporter expressed in the apical membrane of many cells including tissues of gastrointestinal tract (GIT) and canalicular membrane of the liver, where it has been shown to limit the oral absorption of LOV through efflux from the intestinal mucosa to gut lumen.[464] Thus, inhibition of P-gp is a possible mechanism to increase LOV oral bioavailability by

reducing intestinal and/or hepatic efflux transport.[465-466] Two families of transporters, multidrug resistance (MDR) and multidrug resistance-associated protein (MRP),[301] mediate apical drug efflux. P-gp, also known as multidrug resistance protein 1 (MDR1), is the most studied member of the apical efflux transporters[467] and has been shown to limit intestinal absorption of a large number of hydrophobic drugs including LOV.[467-470] P-gp is present in the apical membrane of Caco-2 cells, where it is responsible for the polarized transport of various hydrophobic drugs, and possibly phospholipids, across cell monolayers against a concentration gradient.[467, 471] Phospholipids have been previously reported to be substrates of P-glycoprotein and possibly inhibit P-glycoprotein efflux or transport of drugs like LOV.[471-472]

Cell culture models, such as human epithelial colorectal adenocarcinoma (Caco-2) cell monolayers (CCM), have been widely used as an *in vitro* model to study the absorption to evaluate the behaviour of oral drugs in the intestine because of its simplicity and viable nature.[298, 303, 473-474] Caco-2 cells differentiate both structurally and functionally into cells resembling mature enterocytes, mimicking the human intestinal epithelium, including the typical membrane transporters, apical brush borders and tight junctions between adjacent cells as well as P-gp, and have also been shown to express several transport systems of different drug molecules.[475] The coexistence of enzymes and P-gp in Caco-2 cells is important for the evaluation of metabolism and efflux effect of oral drug formulations.[299-300, 476] Caco-2 cells are often used for studying drug transport as they provide the main routes of substance transport from 1) the paracellular route through tight junction complexes, 2) the passive transcellular route through the bodies of epithelial cells, and 3) the active, carrier-mediated paracellular through cells.[298]

In mechanistic studies of drug permeability, the Caco-2 monolayer model has been utilized because of its simplicity and viable nature.[473-474] Being actual epithelial barriers, the effects of formulation excipients on this layer can be easily studied.[473-474, 477] The permeability of a drug across Caco-2 cell monolayers is closely correlated to its *in vivo* oral drug absorption and bioavailability.[476, 478-481] Caco-2 cell monolayers have been utilized for studies on both active and passive drug transport in the presence of nutrients and other chemicals.[298, 303, 473] Bidirectional transport assay on Caco-2 cell monolayers is also the gold standard *in vitro* model for identifying substrates of P-gp.[480]

For drug absorption from the intestine, it must pass through or cross one or more layers of intestinal cells as a barrier in order to enter the systemic circulation.[482] The ability of the cellular membrane to allow molecules or carriers across the membrane is called cellular permeability. Drug permeation involves transport processes that contribute to the net influx of drug into the intestinal epithelial cells. The lipophilic drugs can rapidly partition from the luminal fluid into the cell membranes of the intestinal epithelium and are mainly transported via the transcellular pathway. However, hydrophilic drugs partition poorly into the cell membranes and are subsequently transported via the paracellular pathway. Apart from passive diffusion, drugs are also transported by specific transporters/carriers present in intestinal epithelium. Depending upon the intended site of action for a drug, a series of drug transport process may be required to reach the target site.[301]

Drug transport across the intestinal epithelium may occur mainly by a concentration gradient driven passive diffusion. Passive diffusion occurs through transcellular (via the cell membrane of enterocytes) or paracellular (via the tight junction between the enterocytes) pathways (**Figure 4.2**).

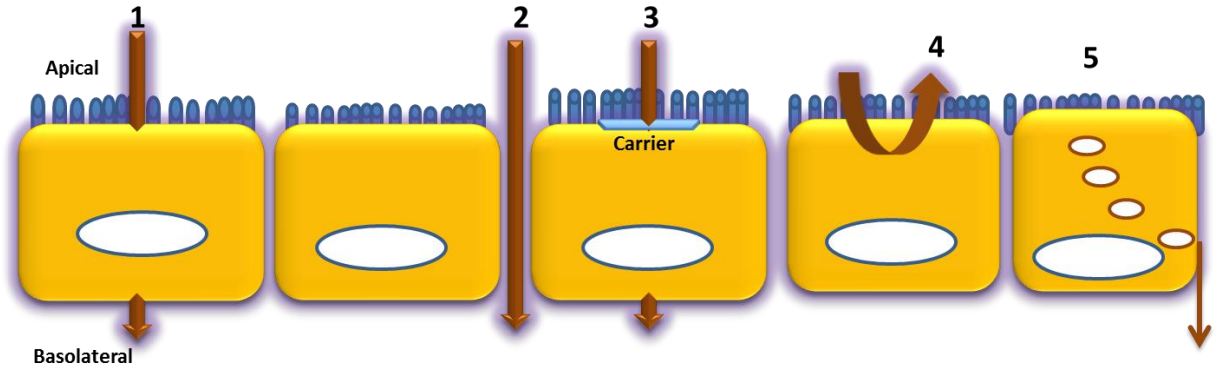


Figure 4-2: Schematic representation of routes and mechanisms of drug transport across the intestinal epithelium: (1) passive transcellular route, (2) passive paracellular route, (3) carrier-mediated transport, (4) carrier-mediated efflux, and (5) vesicular transport. Modified from Shah *et al*.[301]

The pathway used by a drug will be dependent upon the physicochemical properties of the drug and on the physiological properties of the cellular barrier.[483] Lipophilic compounds can rapidly partition from the luminal fluid into the cell membranes of the intestinal epithelium and are mainly transported via the transcellular pathway. However, hydrophilic drugs partition poorly into the cell membranes and are subsequently transported via the paracellular

pathway.[301, 484] Apart from passive diffusion, certain drugs[485-488] are transported by specific transporters or carriers present in the intestinal epithelium (**Figure 4-2**). A few substances that enter the cytoplasm of mucosal cells are extruded to the intestinal lumen through a process known as apical efflux (carrier-mediated efflux).

TEER is a widely accepted quantitative technique to measure the integrity of tight junction dynamics in cell culture models of endothelial and epithelial monolayers. TEER values are strong indicators of the integrity of the cellular barriers before they are evaluated for transport of drugs or chemicals.[489] An alternative method for assessing monolayer integrity is the measurement of permeability of hydrophilic and hydrophobic marker molecules, such as fluorescent compounds Lucifer yellow, which is passively transported across the monolayers by the paracellular and transcellular routes.[301] Apart from passive diffusion, certain nutrients, vitamins and their structural analogs within a series of xenobiotics [486-488, 490] are transported by specific transporters/carriers present in the intestinal epithelium (**Figure 4-2**). A few substances that enter the cytoplasm of mucosal cells are extruded to the intestinal lumen through a process known as apical efflux (carrier-mediated efflux) (**Figure 4-2**).

Liposomes and micelles have gained significant attention in the field of oral administration because they can improve the bioavailability of orally administered drugs.[491] They can protect encapsulated drugs against degradation by the enzymes in the GIT and reduce the first-pass effect.[492] Surfactants used in micelles have been shown to influence monolayer permeability, for example, Chen *et al.* and Ujhelyi et al. reported that paracellular permeability of the monolayer was influenced by d-α-Tocopheryl polyethylene glycol 1000 succinate (simply TPGS or Vitamin E TPGS)[493-494] Liposomal formulations, have been demonstrated to influence carrier-mediated efflux rate and passive permeation of LOV through the epithelial monolayer.[471]

The main mechanisms by which oral bioavailability could be improved by the use of LMH are, e.g. improved solubility, protection of the drug from acidic environments in the gastro-intestinal tract. Thus more drugs delivered to the gastro-intestinal tract and improve intestinal absorption from the uptake of micelles. Inhibition of P-gp activity would be the main mechanism by which oral bioavailability was improved by the use of LMH (major compound phospholipids) as phospholipids have been previously reported to be substrates of P-

glycoprotein and possibly inhibit P-glycoprotein efflux or transport of drugs like LOV.[58, 471-472 59]

4.2. Materials and equipment

1,2-Distearoyl-sn-glycero-3-phospho-1'-rac-glycerol, sodium-salt (DSPG-Na) with C18:0, < 99%, (Molecular Weight: 801.058), was purchased from Avanti Polar Lipids, (INC. Lipoid). Cholesterol (CHO) with 99% purity with a molecular weight (MW) of 386.65 was purchased from Sigma-Aldrich (USA). LOV (crystalline powder), with 98% purity was purchased from International Laboratory (USA). Poloxamer 407 (P407) and 3α,12α-Dihydroxy-5β-cholanic acid sodium salt (Sodium deoxycholate-SDC) were purchased from Sigma-Aldrich Pty. Ltd.(Australia). d-α -Tocopheryl polyethylene glycol 1000 succinate (TPGS) was purchased from Antares, Health Products, INC, (USA).

Human epithelial colorectal adenocarcinoma cells (Caco-2) were kindly donated by the School of Medical Science, University of Sydney. 24-well polystyrene plates with inserts and lids (polycarbonate transwell filter with 0.4 μm pores and a surface area of 0.7 cm^2) were purchased from Millipore Corporation Ltd., Bedford, MA, USA. Dulbecco's modified eagle`s medium (DMEM) with [+] 4.5 g/ l-D glucose, [+] l- glutamine, [-] sodium pyruvate, 1% nonessential amino acids, and 10% fetal bovine serum (FBS) and transport buffer Hank's balanced salt solution (HBSS); containing (500 mL):12.5 mL of 1 M D-glucose and 10 mL of 1 M 4-(2- hydroxymethyl)-1-piperazine ethane sulfonic acid (HEPES) buffer, 1 mL of 625 mM $CaCl_2$, 1 mL of 250 mM $MgCl_2$ were purchased from Gibco Life technologies, USA. Trypsin 0.25% (w/v) in Phosphate Buffer Solution (PBS), DMSO, HEPES and permeability marker Lucifer Yellow (LY) solution were purchased from Sigma Aldrich. A Class II cabinet with laminar flow hood and sample analysis equipment including a fluorimeter, monochromator plate reader (BioTek Instruments Inc, USA) was used and provided by UNSW cell culture facility. A TEER instrument (Millicell ERS-2 volt-ohm meter) was purchased from Millipore Co., Bedford, MA, USA.

4.3. Experimental methodology

4.3.1. Assessment of cell viability by Alamar blue method

The cytotoxicity of free drug and LOV-LMH were assessed using a modified Alamar blue assay[495] as described previously.[483, 496] Caco-2 cells were routinely maintained in DMEM with 4.5 g/ l- D glucose, l- glutamine, sodium pyruvate, 1% nonessential amino acids, and 10% (v/v) fetal bovine serum (FBS). Cells were allowed to grow in a culture flask in an incubator at 37 °C with a controlled atmosphere containing 5% CO_2 and at 95% relative humidity. Cells were passaged at 80–90% confluency at a split ratio of 1:3 using 0.25% trypsin. The cells were seeded into 96-well tissue culture plates at a density of 1×10^4 cells per well in 100 μL of DMEM medium and allowed to grow for 24 hours. The culture was maintained at 37 °C in an atmosphere of 5% CO_2 and 95% relative humidity and then used in the cell viability (biocompatibility) experiment. A total of seven doses of the LMH was prepared by dissolving 20 mg of freeze-dried dry powder of LMH (LOV 1.5 mg) dissolved with 0.1% DMSO and diluted to the final concentrations of 1.0, 0.5, 0.10, 0.05, 0.01, 0.005 and 0.0001 mg/mL with DMEM. After 24 hours, the cytotoxicity of the LMH system was determined. Alamar Blue® solution was directly added to the medium to prepare a final concentration of 10% in each well. After 4 hrs of incubation with Alamar Blue®, the absorbance was measured at 570 nm and 596 nm using a thermo multiskan Ascent plate reader. Results were expressed as cell viability (%) calculated using **equation 1**. The cells, treated with medium, were considered as a control (100% viable).

$$Cell\ viability\ (\%) = \frac{(Abs)sample}{(Abs)control}\ X\ 100 \quad \text{.....} \textit{Equation 4.1}$$

Where, $(Abs)_{sample}$, is attributed to the absorbance of cells treated with free drug or drug-loaded formulations and $(Abs)_{control,}$ is related to the absorbance of cells without any drug treatment.

4.3.2. Permeability assessment of LOV-LMH

The permeability of the cell monolayer was monitored during the differentiation period by measuring the TEER in culture medium using a commercial apparatus (Millicell ERS; Millipore Co., Bedford, MA) as previously described by Ferruzza *et al.*[497] with some modification. TEER measurement is used as an index of monolayer confluence and integrity

in cell culture experiments.[489] TEER has also been used to measure the paracellular permeability of cell monolayers.[498]

To prepare a Caco-2 monolayer suitable for permeability assessment, the cells were seeded at a cell density of approximately 40,500 cells/cm^2 on polycarbonate transwell filters (0.4 μm pores and a surface area of 0.7 cm^2) in 24-well polystyrene plates and routinely maintained in DMEM at 37 °C with controlled atmosphere containing 5% CO_2 and 90% relative humidity for 21 days. The medium was changed on alternate days, firstly the basolateral and then the apical, which contains 400 and 600 μL, respectively. Culture medium was replaced every 48–72 hours. At the end of 14 and 21 days of differentiation, the integrity of the monolayers was assessed by the TEER.

The permeability study was performed on day 21 of the experiment as reported by most previous studies.[497, 499] By day 21, the monolayers have become differentiated with regard to the expression of many transport proteins and brush border hydrolases.[497, 500] For this study, the DMEM (growth media) from the apical chamber was replaced by the transport buffer, HBSS, for both the control and sample.[501] This buffer was also used to prepare the samples for treatment (LMH, along with individual samples of liposomes and micelles, and a sample of free LOV for comparison). Each of the nanocarriers and free LOV samples contains 100 μmol of LOV.

At the end of the growth period, plates were equilibrated with transport buffer (HBSS) and equilibrated in the incubator for half an hour. The TEER value was recorded every 20 minutes of the experimental period for the first hour, then followed by every hour for each well. The resistance of a blank insert (without cells) was also determined to subtract as a background value. Only monolayers displaying TEER values above 300 Ω·cm^2 were used in the transport experiments. TEER value with 300 Ω cm^2 was chosen as the limit for the permeability study as reference by the article.[489] TEER measures the resistance to passive ion transport and reflects the tightness and confluence of cell monolayers. The final TEER values are expressed as Ω cm^2 on the basis of the following equation[489]:

$$TEER = (R - Rb)\ X\ A \quad \text{..... Equation 4.2}$$

Calculation of Resistance of a unit area of 1 cm^2

$Resistance = Total\ resistance - blank\ resistance$……..……*Equation 4.3*

$Resistance\ of\ a\ unit\ area$

= Resistance (Ω) x Effective membrane area* (cm^2)……*Equation 4.4*

Here, R =$Total\ resistance$, Rb = blank resistance and A = the effective membrane area, was 0.49 cm^2 (7 x 7 cm).

Transport of free LOV and LOV encapsulated nanocarriers; micelles, liposome, and LMH across the Caco-2 cell monolayers were studied using monolayers 21 days post-seeding. Before the experiments, the monolayers were equilibrated with transport medium and pre incubated for 30 min. LOV 100 µM/mL solution and LOV containing nanocarriers (containing 100 µM LOV) were freshly prepared by dissolving in 0.5% (v/v) of DMSO and HBSS. All media (DMEM) were replaced and equilibrated with HBSS buffer (400 µL in the apical wells and 600 µL in the basal Wells) for 30 minutes. Then samples were replaced with the buffer HBSS (pH 7.2) to the apical (400 µL) or basal (600 µL) wells. Incubation was undertaken for 2 hours. After incubation 500 µL of samples were taken from the appropriate wells, depending on the direction of transport (i.e., from the basal well for A-to-B transport or the apical well for B-to-A transport), for an ER determination. After treatment, the treating solution was withdrawn and the cells were washed three times with PBS. HBSS in the BL chamber was collected and transported samples were lysed by methanol. Samples were quantitatively analysed by HPLC for LOV content (method described in **Section 4.4.3.**). These quantitative determinations of LOV were required prior to the determination of the P_{app} value and efflux ratio.

4.3.3. Evaluation of the Caco-2 cell monolayer integrity using lucifer yellow

The integrity of the Caco-2 cell monolayers was evaluated using LY, using a modified method described previously.[306] After removing samples for LOV analysis, the remaining liquid was aspirated from the apical and basal wells. 500 µL of 0.1 mg/mL LY solution was added to the apical wells and 1,000 µL of HBSS to the basal wells, these were then incubated at 37 °C for 60 minutes. 200 µL aliquots of samples were transferred from the basal wells to a 96 well plate and absorbance measured in a spectrofluorometer with excitation wavelength at 570 nm and emission at 585 nm. The fluorescence for HBSS Buffer (as blank to deduct the

background value used as a media to prepare the samples) and a 0.1 mg/mL LY solution were also measured. The fluorescence intensity of LY was analysed with a Microplate Fluorescence Reader (Tecan i-control FL600, Bio-Tek, Winooski, USA) using a fluorescence excitation wavelength of 540–570 nm (peak excitation is 570 nm) and fluorescence emission at 580–610 nm (peak emission is 585 nm). A standard curve was prepared from 0.5 to 100 µM LY (molecular weight = 457.25 g/mol).

Analysis then proceeded to determination of the P_{app} value and ER from equations 4.5 and 4.6.[502]

a. The apparent LOV permeability (P_{app} x 10^{-6} cm/s) was calculated as follows: P_{app}

$$P_{app} = \frac{VR}{A\ X\ C0}\ X\ \frac{dMt}{dt} \quad \text{.....Equation 4.5}$$

V_R is the volume of the receiving chamber, A = monolayer filter area (cm^2), Co = mass of compound initially in the donor compartment, dMt/dt = the rate of drug permeation across the cells

b. The ER was calculated as the ratio of P_{app} determined in the A-to-B direction to P_{app} determined in the B-to-A direction:

ER = (P_{app} B-A) / (P_{app} A-B) .....*Equation 4.6*

where the ratio of the basolateral–apical (secretion) component P_{app} B-A to the apical-basolateral (absorption) component P_{app} A-B was assessed. Theoretically, an ER superior to unity suggests the presence of one or various efflux transporters in the tested formulation. For compounds with an ER in the range of 1–2, a specific P-gp inhibitor may be used to confirm the presence of the latter transporter.

c. The percent permeability of LY from the fluorescence values was calculated as follows:

$$\%\ permeability = \frac{(Sample - blank)}{(Lucifer\ yellow - blank)}\ X\ 100 \quad \text{.....Equation 4.7}$$

4.3.4. LOV assay method

Described in **Chapter 3,** Section **3.3.2.**

4.3.5. Transportation and cellular uptake of LOV

Transportation and cellular uptake of LOV were evaluated using a modified method described previously.[304, 503] For transportation and uptake studies, cells were plated at a density of 40,480 cells/cm^2 onto a 24 mm polycarbonate transwell filter with 0.4-μm pores and a surface area of 0.7 cm^2. At the beginning of each experiment, the monolayer was washed twice with PBS and pre-equilibrated for 30 min with buffer (HBSS). LOV, liposomes, micelles and LMH solutions of 400 μL (drug content 100 μmol/mL) were added to the apical chambers of the monolayers inserted in each well containing 600 μL HBSS (pH 7.4). The pH conditions were chosen in order to reproduce the physiological pH gradient existing *in vivo* across the small intestinal mucosa. The plate was placed in the incubator for 24 hours at 37 ^oC. During the interval of 1 hour, a 500 μl sample was taken from the basolateral side and replaced by the same amount of transport buffer. At the end of the transport experiment (8 hours)**,** samples (100 μl) were also taken from the apical side. LOV content was measured by HPLC assay method in **Section 4.3.4.**

4.3.6. Intracellular uptake and accumulation

Intracellular uptake and accumulation of LOV were assessed using a modified method described previously.[304, 306] At the end of the LOV transport experiment (8 hours), the treated sample solution was withdrawn and the cells were washed three times with PBS. Cells of each transwell filter were trypsinised, collected and lysed and were diluted with 1 mL of methanol and kept for 24 hours. The solution was then centrifuged at 10,000 rpm for 10 minutes and the supernatant was analysed. LOV content was measured by HPLC (**Section 4.3.4.** LOV assay method).

4.3.7. Statistics analysis method

All results are presented as mean + standard deviation of the mean. One-way analysis of variance (ANOVA) was used to determine the significance. Paired t-test was performed to

compare different individual sets of data. $p < 0.05$ was used as a parameter of analysis limit (variation limit) describe in the method.

One way analysis of variance (ANOVA) statistic methodology was used to determine whether the data of cell viability (control and LMH), a decrease of TEER value (control, LOV and nanocarriers), permeability (between A→B and B→A), LY permeability (control, LOV and nanocarriers) and were significantly different (means of three or more groups are different). ANOVA uses F-tests to statistically test the equality of means. To use the F-test to determine whether group means are equal, it's just a matter of including the correct variances in the ratio. In one-way ANOVA, the F-statistic is this ratio:

F = variation between sample means / variation within the samples

If the observations for each group are close to the group mean, the variance within the samples is low. However, if the observations for each group are further from the group mean, the variance within the samples is higher. ANOVA uses the F-test to determine whether the variability between group means is larger than the variability of the observations within the groups. If that ratio is sufficiently large, it can be conclude that not all the means are equal.

Here, *P* value was calculated from data analysis using MS Excel.

4.4. Results and discussion

4.4.1. Cell viability assessment of LOV-LMH

Intestinal permeability enhancement may be attributed to damage to the intestinal epithelial barrier by the LMH formulation. Therefore, Caco-2 cell viability in the presence of LOV-LMH was evaluated by an Alamar blue assay, as shown in **Figure 4-3**. LOV-LMH showed no toxic effect on Caco-2 cells at concentrations from 0.0001-1 mg/mL LOV; cell viability was ~100% for the 0.0001-1 mg/mL concentration range. Similar unaffected cell viability was also reported by Hossain *et al.* with different concentrations of soy, squid and starfish PC liposomes after 24 hours incubation and exposure of up to 100 μM PC liposomes encapsulated docosahexaenoic acid and eicosapentaenoic acid.[306]

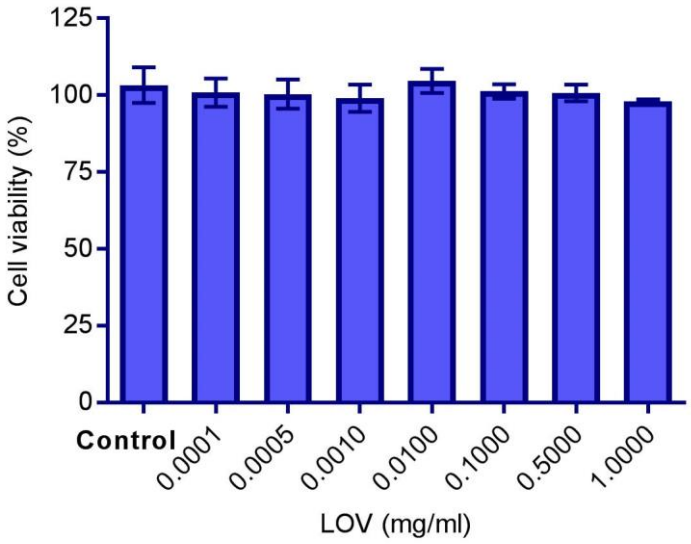


Figure 4-3: Caco-2 cell viability as a function of various levels of LOV-LMH inclusion. Viability determined after 48 hours of treatment by Alamar blue assay. Data presented as the mean ± SD (n = 4) from two individual experiments in quadruplicate. **control without the drug. A statistically significant ($p < 0.039$) difference between the control and LMH.

From the single factor ANOVA data analysis it is found that there was a statistically significant ($p < 0.039$) differences between the control and LMH for the cell viability data. There was a statistically significant difference between control and LMH.

4.4.2. Caco-2 cell monolayer permeability assessment of LOV-LMH

Prior to permeability studies, the Caco-2 cells were cultured in 24-well plates and the TEER values were measured to ensure the development of a suitable cell monolayer over 21 days. The control TEER value was taken from the media (DMEM + FBS-10%) without cells, it was < 200 Ω cm^2 and remained constant for the duration of the experiment. The average TEER value in Caco 2-cell monolayer (CCM) containing media was found to be 1435 ± 139 Ω cm^2 on the 14^{th} day and 1320 ± 196 Ω cm^2 on the 21^{st} day (see **Figure 4-4**). These indicated cells were growing and a complete monolayer was developed by 14 days. The cell resistance decreased by 8% from the 14^{th} to 21^{st} days. All the TEER values were persistently above 305 Ω cm^2, indicating the integrity of the cell monolayers, as 305 Ω cm^2 is the minimum limit reported by most previous reports of permeability studies.[504-507]

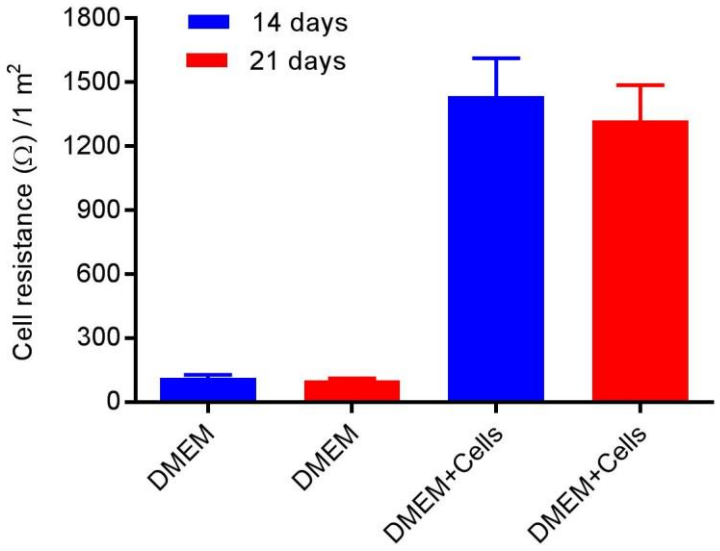


Figure 4-4: Resistance of Caco-2 Cell monolayers (CCM) measured on the 14th day and 21st day (2 days) of monolayer formation in DMEM control media. The data are presented as mean ± SD (n = 4).

The TEER across CCM typically increases with culture time, reaching a maximum after about 10-15 days, although such cultures express less well-differentiated features[497] and a few reports also suggest it to be 21-24 days for formation of all involved transporters.[505-507] In the current study, permeability analysis was performed on day 21 of the experiment as reported in the literature.[489, 499] TEER values were measured at the start (0 min) and the end of the permeation study (120 min) in the presence of LOV encapsulated in LMH, liposomes, and micelles, as well as free LOV solutions. The TEER values with Caco-2 cell monolayers at the start of the test ranged from 687 to 1497 Ω (after background resistance was subtracted) in HBSS buffer. At the end of the permeation studies, these values ranged from 446 to 663 Ω which still indicates intact cell monolayer as reported previously.[489]

The TEER values decreased immediately after addition of LOV-loaded micelles, liposomes, LMH, and free LOV, as described in **Figure 4-5**. After 2 hours of treatment, the TEER values of cell monolayers was decreased in micelles, liposomes, LMH and LOV to 55 %, 46 %, 34 % and 90 % of the initial value, respectively and greater reduction for LMH than liposomes and micelles. Compared to free LOV, this reduction from an initial value is 1.6 fold, 1.95 fold and 2.6 fold for micelles, liposomes, and LMH respectively. From this drop in resistance, we concluded that the nanocarriers were able to open the tight junction of the Caco-2 cells.

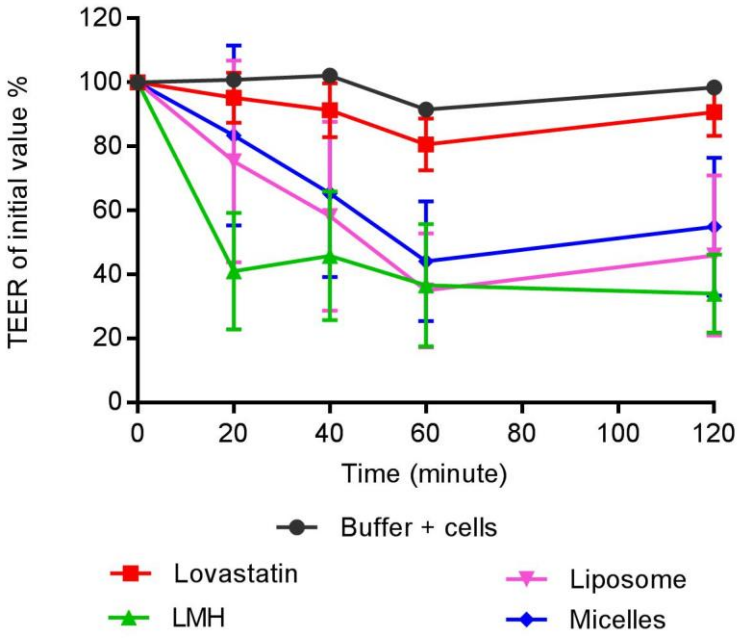


Figure 4-5: Effect of 100 µM LOV encapsulated in micelles, liposomes, LMH and free LOV on the TEER in Caco-2 cell monolayers (21 days old) in HBSS over 2 hours of the treatment period. Control without treatment (Cells with buffer and buffer only). The data are presented as mean ± SD (*n* = 4). One way ANOVA analysis indicates a statistically significant (P < 0.006) difference between control and nanoparticles.

Alternatively, an increase in TEER suggests a recovery of the tight junctions.[492] The TEER did not change significantly for the control system (no treatment) in HBSS buffer and cells. The potency of the TEER-decreasing effect of the nanocarriers is dependent on the treatment period. As shown in **Figure 4-5,** the incubation of LOV-nanocarriers on the apical side of Caco-2 cell monolayers led to a reduction in TEER after 20 minutes and this continued to 60 minutes, which has been attributed to the opening of tight junctions (TJs).[508] This indicates that the micelles, liposomes, and LMH used here were able to open the TJs and increase paracellular permeability of LOV through the TJs.[498,474, 509] As revealed in **Figure 4-5,** the reduction of TEER was more significant for the LMH than liposomes and micelles, indicating better paracellular permeability enhancement by LMH. After 60 minutes the TEER value started to increase and stayed in a steady state.

One-way analysis of variance (ANOVA) analysis indicates statistically significant (p < 0.006) differences between control and nanoparticles. The post- hoc-corrected t-tests analysis report as "true'' for micelles and LOV compared to blank implies that there is 95% of chance

of difference between blank and LOV. The effect of TEER is significantly higher for micelles and LOV compared to blank. However the analysis report as "false'' for liposome and LMH compared to blank implies that there is no significance of difference between blank and LMH. The effect of TEER is significantly lower for liposome and LMH compared to blank. However, compared to LOV the analysis report as "true'' for LMH, liposome and micelles compared to free LOV implies the effect of nanocarriers on the TEER is significantly higher compared to the free LOV.

The findings here correlate with similar decreased TEER values published in the literature for liposomes[306, 505] and micelles.[68] Sezgin *et al.* reported PEG-phosphatidyl-ethanolamine (PE) micelles were able to open tight junctions of the Caco-2 cell monolayer.[222] Hossain *et al.* reported that treatment of Caco-2 monolayers with 25, 50 and 100 μM squid meal and starfish PC liposomes resulted in decreased TEER by between 9% and 30%, in the 20-minute treatment.[306] Reduction of TEER values has also been reported in the literature for rhodamine containing chitosan-coated liposomes passing through Caco-2 monolayers.[510] Cheng *et al*. reported that tremella–alginate-liposomes were able to open tight junctions of the CCMin a similar way.[508]

The permeation coefficient, or P_{app}, was quantified by the bidirectional transport of LOV across the CCM; this is dependent on the carrier system (micelles, liposomes, LMH and LOV solution). The transepithelial fluxes of LOV across Caco-2 cell monolayers at 37°C temperature in the absorptive (apical-to-basolateral; A→B) and secretory (basolateral-to-apical; B→A) directions in the presence of nanocarriers; micelles, liposomes, and LMH were assessed (**Figure 4-6A)**.

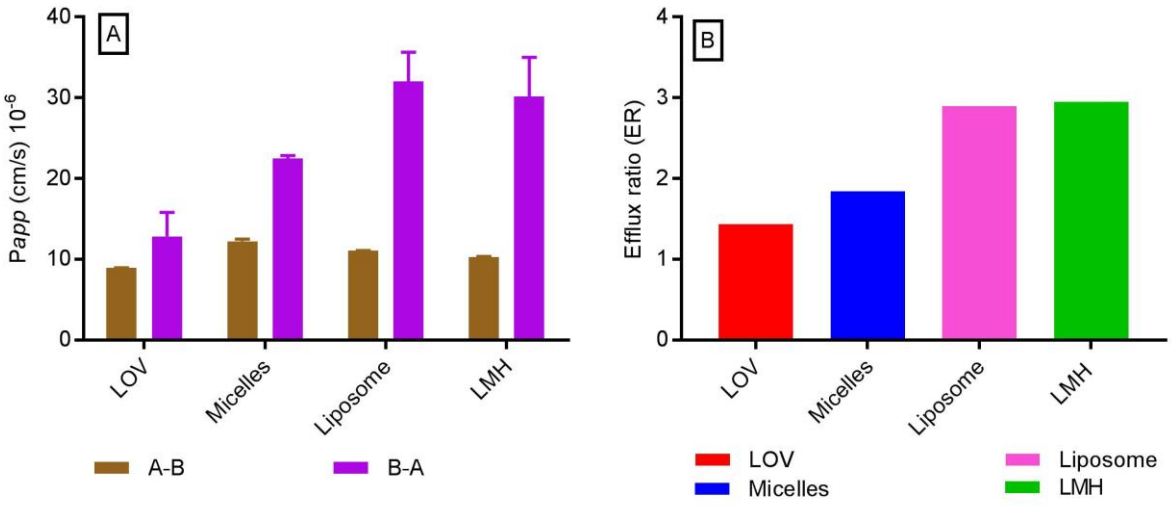


Figure 4-6: A) The A→B and B→A fluxes of LOV and LOV loaded nanocarriers (100 µM) were determined at pH 7.4 as a function of time (2 hours at 37°C) and B) Transepithelial efflux of LOV across CCM. Each point represents the mean (4 S.E.M.) of 4 determinations (CCM). One way ANOVA analysis indicates statistically significant ($p < 0.02$) differences between A→B and B→A permeability.

It was observed that the P_{app} of LOV from A→B and B→A direction increased by 1.34, 1.23 and 1.14-fold and 2.46, 3.53 and 3.33-fold for LOV encapsulated in micelles, liposomes, and LMH, respectively (**Figure 4-6A and Table 4.1**). From the single factor ANOVA data analysis it is found that a statistically significant difference ($p < 0.02$) was found for enhancement of LOV permeability for B→A direction for micelles, liposomes, and LMH compared to the A-B permeability. Thus, the nanocarriers modified the permeability of LOV through the CCM.

These results indicate a significant ($p < 0.05$) enhancement of LOV permeability for B→A direction for micelles, liposomes, and LMH compared to the A-B permeability. The P_{app} value for the B→A transport of LOV in CCM was 1.84, 2.90 and 2.95 times higher in micelles, liposomes, and LMH than the A→B P_{app} value respectively (**Table 4-1**). These results also demonstrated that the micelles, liposomes, and LMH could significantly enhance the permeability of LOV in the B→A direction which could be explained with the specific transporters (P-gp) blocking the apical transport of LOV to A→B direction. However, LOV is taken up by a basolateral transporter (other than P-gp) from the basolateral membrane and excreted by apical efflux transporters at the apical membrane (**Figure 4-7)**. Li *et al.*[511]

demonstrated similar involvement of an uptake transporter at the basolateral membrane for a statin drug rosuvastatin (basolateral transporter) in a bidirectional transport in Caco-2 cells.[511]

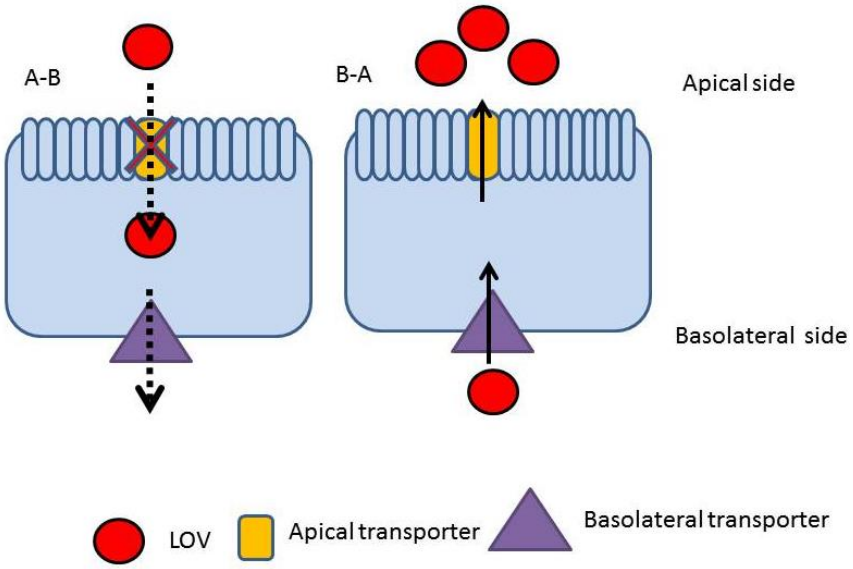


Figure 4-7: Model for the proposed LOV transport, left) blocking the apical transporter reduces LOV, A→B transport, reduced LOV transport, and right) LOV was taken up by a basolateral transporter from the basolateral membrane and excreted by apical efflux transporters at the apical membrane; Image modified from Li *et al.*[305]

The respective P_{app} values are in good agreement with previously reported values for verapamil, digoxin, and cerivastatin which also demonstrated higher B→A transport than A→B transport.[512-513] Similarly, Francis *et al*. reported higher permeability in the B→A direction compared to A→B direction for cyclosporin loaded polysaccharide based polymeric micelles.[70] The greater B→A transport was also reported for the *in vitro* permeability of cerivastatin (3 fold) by Kivisto *et al.* [513] and of atorvastatin (7 fold higher) by Wu *et al.*[302] It has also been reported by Li *et al*.[305] that statin drugs; atorvastatin, LOV, and rosuvastatin, displayed extremely low A→B transport because of their low solubility and both the drug and the other excipients such as phospholipids are the P-gp substrate which restricts diffusion and transport in the A→B direction compared to the B→A transport.[305] Wang *et al.* also reported LOV, atorvastatin and simvastatin are very potent and effective inhibitors of P-gp transport due to their similar molecular structure as well as, similar physical and chemical properties.[514] Therefore, evidence from the previous studies suggests that LOV is a P-gp substrate.

The nanocarriers significantly improved the permeability for LOV by assisting its transport for rapid absorption by intestinal epithelial cells[515] by either paracellular or transcellular mechanism (as reported in **Figure 4-5)** could be explained by two hypotheses. Firstly, nanocarriers infiltrate the mucus layer, then break and release the loaded drugs, which open up tight junctions, thus allowing the released drug to permeate through the paracellular route.[516] Alternatively, intact nanocarriers adhere to tight junctions, open them up and then encapsulated drugs are released to be transported between paracellular cells. In the latter case, the drug remains encapsulated during the mucus layer transport to reach tight junctions, which is an advantage because the nanocarriers act as a reservoir for the drug to controls the drug release.[517]

Recently, it has been shown that the mmePEG750P(CL-co-TMC) polymer micelles containing risperidone could transport across caco-2 monolayers and also the intestinal barrier after oral administration.[68] Thus having a chance to reach the bloodstream and being able to attain their pharmacological target while keeping their native structure. Batrakova *et al.* and Sezgin *et al.* reported transcellular uptake Pluronic P85 micelles[518] and Pluronic® F127 micelles[222] via endocytosis of caco-2 cells and no paracellular permeability was observed. It has been reported that the mechanism of transport of nanocarriers in caco-2 cells is size dependent.[51968, 520-521522] Desai *et al*. demonstrated that 100 nm poly(lactic-co-glycolic acid) (PLGA) particles diffused throughout the submucosal layers, whereas 10 μm particles were predominantly localized on the epithelial lining of the tissues.[521]

Many transport studies across the intestinal barrier have been performed with liposomes and it is generally accepted that liposomes do not penetrate the vesicles as intact vesicles.[142, 519] They can fuse with the lipids in the cell membrane or alternatively, liposomes can disintegrate on the cell membrane surface where the lipid molecules disrupting the packing and fluidity of the lipid bilayers and can act as a drug reservoir.[519] They cannot diffuse through cells by passive diffusion due to their size. Maitani *et al*. have shown that 100 nm liposomes are absorbed more effectively than those of 200 nm in diameter.[523] Sattler *et al.* reported, in the presence of cyclodextrin, hypericin loaded liposomes (70–100 nm) bound to the cell surface and drug transport occurred by transcellular diffusion via lipophilic domains. No intracellular uptake and no transport by enterocytes of intact liposome was reported.[524]

The ER was calculated as the ratio of the P_{app} measured in the B→A direction divided by the P_{app} in the A→B direction **(Figure 4-6B and Table 4-1)** is another important parameter used to describe possible mechanisms of drug and nanocarrier permeability. The net flux of LOV was observed in the secretory direction (P_{app} B→A) in Caco-2 cells. Theoretically, an ER superior to unity implies the presence of one or various efflux transporters in the formulations[480, 525-526] however, an ER close to 1.0, indicates intestinal absorption to be dominated by passive diffusion.[527] Micelles, liposomes, LMH and free drugs showed an ER≥ 1 (1.84, 2.90, 2.95, and 1.44 respectively), which could lead to an interpretation of transporter diffusion by slowing apical transport and acceleration of the basal pathway.

Table 4-1: The parameters determined from permeability assay of LOV through CCM using different nanocarriers.

Test compound Type (each contains 100 µM LOV)	**P_{app} (cm/s) × 10^{-6}***		**Efflux ratio (secretory (B→A) P_{app} /absorptive (A→B) P_{app})**
	Transport direction		
	Absorptive (A→B)	**Secretory (B→A)**	
Free-LOV (control)	8.94 ± 0.026	12.85 ± 2.95	1.44
Micelles	12.24 ± 0.26	22.48 ± 0.38	1.84
Liposome	11.04 ± 0.046	32 ± 3.64	2.90
LMH	10.24 ± 0.11	30.18 ± 4.84	2.95

* P_{app} values are expressed as the means ± S.D. (x10^{-6}, cm/s); n =3

4.4.3. Evaluation of the Caco-2 cell monolayer integrity using Lucifer yellow

After the permeability experiments, evaluation of permeability characteristics of Caco-2 cells can be performed by measuring the passive passage of different molecules across the monolayer. Small hydrophilic compounds such as Lucifer yellow (LY) cross the monolayer mainly via the paracellular space, such as through the tight junctions (TJs), and can be considered markers of passage by this route.[528] LY is used as a fluorescent permeability marker with very low permeability (P_{app} < 0.4 X 10^{-6} cm/s);[305] and has been used as a marker of TJ maturation,[529] to assess the barrier integrity and to determine whether the working concentration of a test compound disrupts the integrity of the monolayer. The LY assay was

performed after the permeability assay (after two hours) described above. After each Caco-2 monolayer sample treatment, the LY permeability (% Permeability) assay was performed for each membrane. LY (%) permeability tests were undertaken at the same concentration as the drug used (i.e. 100 µM in HBSS, as has been reported previously).[306, 530]

The micelles, liposomes, LMH and free LOV were able to increase LY permeability significantly compared to control (buffer and cells only) as shown in Figure **4-8**.

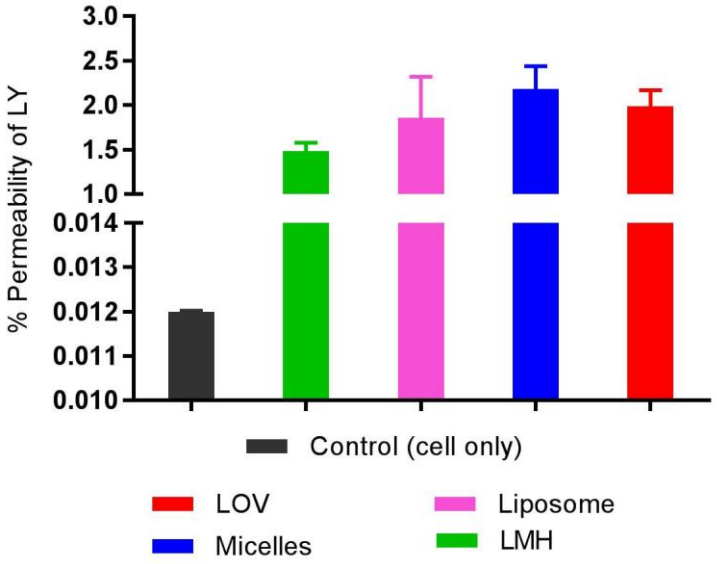


Figure 4-8: Percent permeability of LY (100 µM) from A→B; added to the apical chamber of CCM treated with 100 µM LOV and 100 µM LOV incorporated into each nanocarrier; micelles, liposomes, and LMH; were incubated for 1-hour with 100 µM LY. After 1-hour samples were collected from the basal chamber. Here the control was only the cells. LY was measured by fluorescence intensity at excitation and emission wavelengths of 485 and 520 nm, respectively. Results are means ± SD (n = 4). A statistically significant ($P < 0.014$) difference between control and nanocarriers.

The difference in LY permeability was not varied among the nanocarriers. However, they were significantly increased compared to the control. Micelles showed a greater increase than LMH, as hydrophilic molecules, such as TPGS, have been reported to have greater permeability than lipophilic drugs or molecules. Chen *et al.*[493] and Ujhelyi *et al.*[494] reported that paracellular permeability of the monolayer was enhanced by TPGS and other surfactants.

This data closely correlates with P*app* A→B as this study was performed in the A→B direction.

From the Single Factor ANOVA data analysis it is found that there is a statistically significant ($p < 0.014$) differences between A→B and B→A permeability. The post- hoc-corrected t-tests analysis reports as "true'' for LOV, LMH, liposome, and micelles compared to control implies that there is 95% of chance of difference between control and LOV. The LY permeability is significantly higher for LOV, LMH, liposome, and micelles compared to control.

Here, LOV appears to be efficient at opening the tight junctions on its own. However, the nanocarriers do increase transport of LOV (**Figure 4-6A**, A→B only); the nanocarriers may have a combined mechanism (paracellular and P-gp mediated transport) of drug transport in addition to TJ opening.

4.4.4. Transport of LOV with different nanocarriers (micelles, liposomes, and LMH) across a Caco-2 cell monolayer

To assess the capability of the nanocarriers to enhance LOV transport, Caco-2 monolayers were treated for 8 hours with LOV and LOV encapsulated in micelles, liposomes and LMH all containing 100 µM of LOV; the results are shown in **Figure 4-9**.

Monitoring the transport of LOV across CCM, after 8 hours of incubation time, the A→B permeability of LOV loaded in micelles, liposomes, and LMH increased approximately 2-fold higher compared to free LOV. The LOV transport was increased significantly by; micelles, liposomes, and LMH. In all cases, the transport was biphasic with respect to incubation time: slow or insignificant transport was detected during the first 2 hours of contact (where permeability was assessed), followed by a steeper increase in transport upon prolonged incubation. The transport data showed sigmoidal characteristics[531] over 8 hours for all LOV-nanocarriers including the free LOV. Similar sigmoidal characteristic data was reported by Hilgers *et al.*[532] for transport of different molecules.

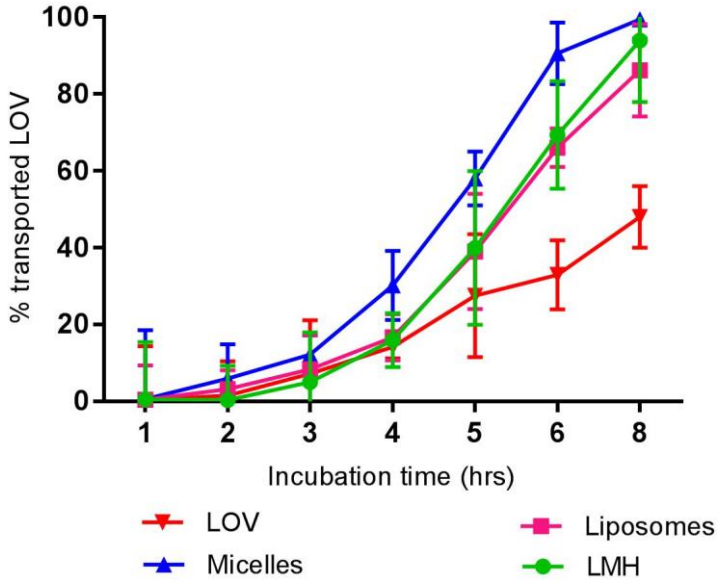


Figure 4-9: LOV transported across Caco-2 monolayers after 8 hours of incubation in the A→B direction at 37°C in the presence of micelles, liposomes and LMH containing 100 µM of LOV and LOV 100 µM, expressed as a percentage of the initial concentration of 100 µM LOV, added to the apical compartment, as a function of time, mean ± SD (n=4).

It was mentioned above that P-gp can act as a barrier to the intestinal absorption of LOV from the apical membrane (A→B direction) initially. For the first 2 hours of the transport study (**Figure 4-6**) P-gp on the apical side (A-B) has been shown to limit the transport of LOV through the apical membrane **(Figure 4-6 A)**. After 2 hours, LOV transport increased significantly which may result from saturation of the P-gp present in the apical membrane of Caco-2 cells[471] allowing LOV transport to increase across the cell monolayers i.e., or transcellular way **(Figure 4.10)**. Similar results were reported by Wu *et al.*[302] for atorvastatin transport through CCM.

However, other explanations have been proposed, such as TPGS of micelles has been described to be capable of inhibiting the biological activity of P-gp **(Figure 4.10)** as reported by Chen *et al.*[493] and Dintaman *et al.*[232] Hochman *et al.*[533] and Chen *et al.*[534] suggested that cellular uptake and excretion of statin drugs is mediated by a variety of membrane transporters. The transport of doxorubicin through sterically stabilized liposomes was also reported by Lasic *et al.* to occur through interaction with cells (enterocytes and M cells) by mechanisms such as endocytosis, fusion, adsorption and lipid exchange. The endocytotic pathway for absorption of liposomes is either by receptor-mediated endocytosis or absorptive

endocytosis which requires no ligands and depends on the diameter and surface properties of the liposomes.[196]

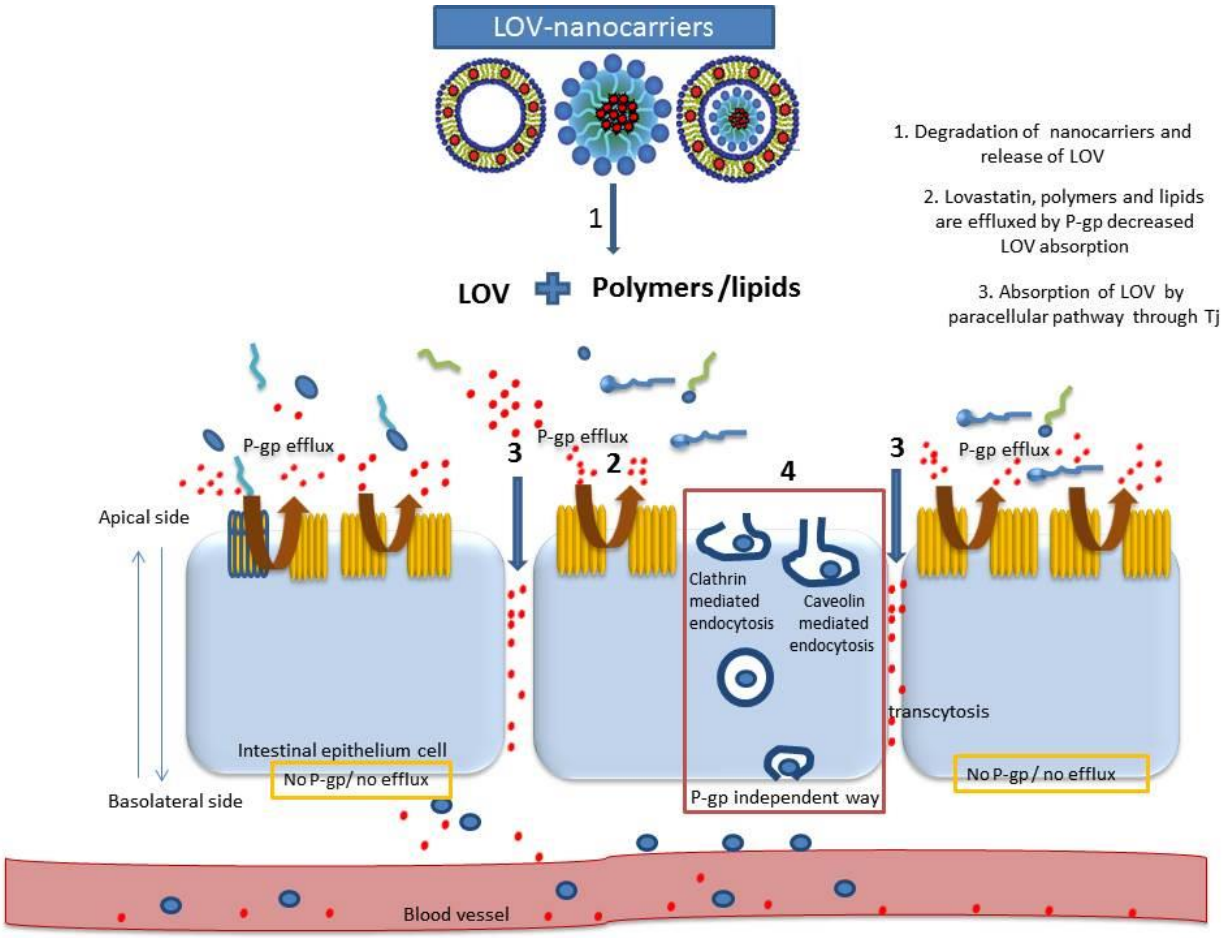


Figure 4-10: Scheme of different possible transport ways of LOV and nanocarriers: micelles, liposomes and LMH, (1) degradation of nanocarriers and release of LOV, (2) inhibition of LOV absorption by the effect of the multidrug efflux transporter P-gp in the apical membrane of intestinal epithelium cells, (3) The hypothetical paracellular way of transport of LOV and (4) Other P-gp independent transport way of nanocarriers micelles, liposomes and LMH. Modified image from Mo *et al*.[503]

4.4.5. Intracellular uptake and accumulation

It has been reported that nanocarriers such as micelles and liposomes, can enhance drug uptake of Caco-2 cells.[535-536] At the end of the LOV transport experiment at 8 hours, the intracellular uptake and accumulation of LOV were assessed to determine which carriers promoted the greater transportation and accumulation of drug molecules. The intracellular uptake and accumulation of LOV within the CCM are reported in **Figure 4-11**.

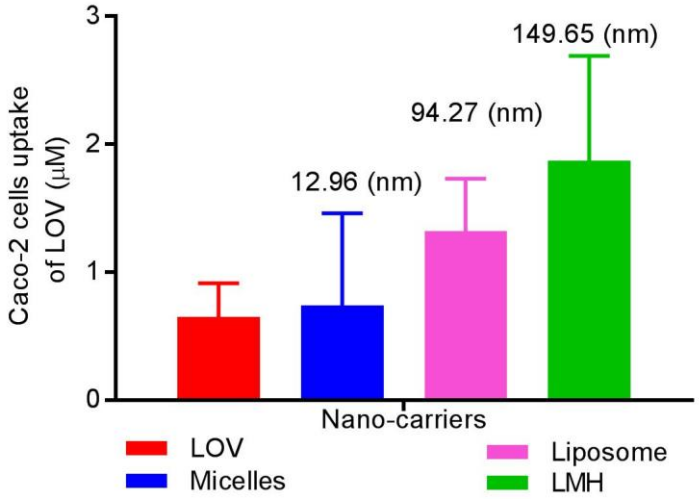


Figure 4-11: Caco-2 cell uptake of LOV and LOV loaded nanocarriers (all containing 100 μM LOV). The average particle diameter of the nanocarriers, micelles, liposomes, and LMH are shown above the standard deviation bars (also reported in Chapter 3)

As shown in **Figure 4-11**, the Caco-2 cell uptake of LOV encapsulated in micelles, liposomes and LMH were 1.14-fold, 2.03-fold, and 2.88-fold higher than that of LOV at the same concentration (100 μM) of free LOV, respectively, indicating that LOV nanocarriers had a strong influence on uptake and accumulation of LOV in the Caco-2 cell monolayers. A greater uptake was observed for LMH compared to the liposomes and micelles. It is worthy to mention that the quantity of LOV accumulation was insignificant (μg) to produce cytotoxicity as it is lower than the IC_{50} of LOV as reported *in vitro*.[537]

From the results, it was also found that the LOV accumulation depends on particle diameter and charge of the nanocarrier, i.e. the larger particle diameter liposomes and LMH assisted LOV to uptaken more by the cells than the smaller diameter micelles. The carriers may present the LOV at the correct place and in a molecular form for uptake. Similar results were reported by He *et al.* for rhodamine B containing chitosan polymeric nanoparticles (150-500 nm), where particle diameter of 150 nm tended to accumulate in tumors more efficiently,[538] and Yin Win *et al.*[539] demonstrated coumarin-6 loaded PLGA nanocarriers with diameter of 100- 200 nm could be internalized more easily compared to larger particles by a receptor-mediated endocytosis. The intracellular uptake was also influenced by the zeta potential of

the nanocarriers as the larger the negative surface charge the greater the cellular uptake was observed for LMH, liposomes, and micelles (**Table 4-3**).

Table 4-3: The average particle diameter and zeta potential of LOV loaded nanocarriers.

Nanocarrier Type	Diameter (nm)	Zeta-potential (mV)
Micelles	12.96 ± 1.61	-1.41 ± 1.95
Liposome	94.27 ± 0.273	-42.3 ± 1.13
LMH	149.65 ± 1.79	-46.3 ± 1.93

Straubinger *et al*. demonstrated that high electrostatic surface charge could promote liposome-cell interaction and negatively charged liposomes were predominantly taken up by cells.[540] A possible mechanism of cellular uptake and accumulation may be due to the transport of LOV across CCM and then blocking the basal membrane partially by basal transporter which inhibits diffusion of LOV out of the cell and increased the accumulation of LOV in cells (**Figure 4-12)** as reported by Li *et al*.[305]

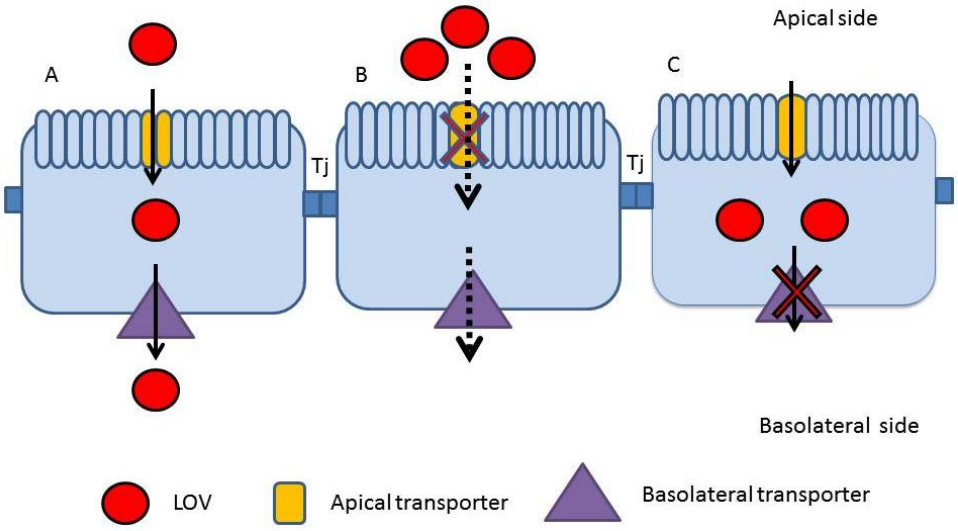


Figure 4-12: Model for the proposed LOV, A→B transport across CCM. A) LOV was taken up by an apical transporter from the apical membrane and excreted by basolateral efflux transporters at the basolateral membrane; B) blocking the apical transporter reduces LOV, A→B transport, reduced LOV transport C) blocking the basolateral efflux transporter reduces LOV, A→B transport but increases its intracellular accumulation. Image modified from Li *et al.*[511]

4.5. Conclusion

The success of colloidal nanoparticle-based therapy depends largely on the behaviour of the nanoparticle in the tissue microenvironment and their interactions with cells forming the tissue. In this study, a LOV encapsulated LMH was evaluated *in vitro* as a potential oral delivery system, i.e. to improve its permeability in comparison to individual micelles and liposomes. Importantly, the LMH system was shown to be non-toxic to the cells when evaluated by an Alamar blue assay. The TEER values indicated the good cellular integrity of the Caco-2 cell monolayers, which was decreased significantly by the LMH, leading to speculation that their greater permeability across the epithelial cells was via the paracellular route. It was also found that the P*app* of the LMH for the B→A direction was higher than the permeability in the A→B direction demonstrated that micelles, liposomes, and LMH could significantly enhance the permeability of LOV in the B→A direction. In a Caco-2 model, the LOV-LMH showed a significantly improved transport of LOV as compared to free LOV over 8 hours. Along with these, the additional loading, controlled release characteristics and stability of the LMH leads to a significant improvement of current drug delivery system in compare to liposome and micelles. The results highlight the significance of the LMH nature of intracellular trafficking of poorly soluble drugs and could open alternative opportunities for oral delivery of poorly soluble drugs.

Chapter Five

5. Development of a Temperature-Sensitive Liposome-Micelle-Hybrid (TS-LMH) System for Anticancer Drugs Paclitaxel and 5-fluorouracil

Chapter outline

In this chapter, a temperature sensitive liposome-micelle-hybrid (TS-LMH) was developed to improve control of the release of encapsulated anticancer drugs at elevated temperature; this is aligned with potential for targeted chemotherapeutic activity. The procedure used to prepare TS-LMH was similar to that used to prepare LMH (chapter 3) however; dipalmitoyl-sn-glycero-3-phosphorylglycerol (DPPG, which has a phase transition at 41.5°C) and polyethylene glycol (PEG) 1500 were additionally included in the liposome to facilitate thermoresponsive drug release. Additionally, thermoresponsive micelles were prepared with D-α Tocopheryl polyethylene glycol 1000 succinate (TPGS) using a similar procedure as described in chapter 3. TPGS has a melting point at 38°C (37-41°C), providing thermoresponsive properties to the micelles.

Two model anticancer drugs, paclitaxel (PTX) and 5-Fluorouracil (5-FU) were selected to investigate the thermosensitive LMH drug delivery system. PTX is one of the most widely used and effective antineoplastic agents isolated from natural sources, the bark of *Taxus brevifolia*.[112] It is a pseudo alkaloid that has a taxane ring as its nucleus ($C_{47}H_{51}NO_{14}$, MW 853.93).[113] It is a microtubule inhibitor and approved for chemotherapy of various types of solid tumors, e.g. ovarian, breast, pulmonary prostate, melanoma, oesophageal cancer, and Kaposi's sarcoma. However, its clinical use is limited due to its low aqueous solubility (< 0.03 mg/mL).[80] It has been a great challenge to formulation scientists due to its water-insolubility and efflux by p-glycoprotein (p-gp) expressed in the intestinal epithelial cells which are considered as a major reason for poor absorption of orally administered PTX.[114-115]

Moreover, PTX can bind to plasma proteins and decreases the ability to penetrate the tumor interstitium at an effective concentration and increases the toxicity to healthy tissues.[112, 116] Also, the excipients used in commercial formulations cause adverse effects.[117-121] Hence, to increase the solubility, reduce toxicity and selectively target to tumor tissue, PTX has been encapsulated in liposomes[71, 122-123] and micelles[76, 124] which show greater accumulation at the tumor site and enhanced permeability and retention (EPR).[121, 125-126]

PTX is a colourless to slightly yellow or (in pure form) an off-white crystalline powder. It is a highly lipophilic compound with a *log P* value of 3.96.[127]Among non-aqueous solvents, the solubility is found to be ~46 mM in ethanol, ~20 mM in methylene chloride or acetonitrile, and ~14 mM in isopropanol. It is also soluble in methanol, tertiary-butanol, and dimethyl sulfoxide.

5-FU is an effective and widely used chemotherapeutic agent for more than 50 years in the treatment of colorectal,[128] breasts,[129] and skin cancer.[130] However, 5-FU suffers from several drawbacks; e.g. a short plasma half-life after intravenous bolus administration and drug resistance by tumor cells.[131] Therefore, requiring high doses that lead to severe side effects, including gastrointestinal, haematological, neuronal, dermatological effects, pancytopenia, and cardio-toxicity.[132]

To overcome these limitations, 5-FU has been encapsulated into liposomes to prolong its circulation time, reduce the associated side effects, improve its therapeutic index and efficacy, and favour drug accumulation in tumors.[102-103]

5-FU is a white to nearly white crystalline powder; practically odourless with a *log P* value of -0.89 and *pKa* 8.02. It is soluble in methanol.[74]

Initially, only PTX was encapsulated into the micelles' core and then also within the liposomal bilayer to prepare a PTX encapsulated LMH system, as schematically represented in **Figure 5-1**.

Secondly, a combination of PTX and 5-FU were loaded into the LMH system, i.e. PTX was encapsulated into the liposomal bilayer and 5-FU was loaded in the TPGS micelles of the LMH aqueous core to distinguish their loading and release profiles **(Figure 5-2)**. PTX loaded liposomes, PTX loaded micelles and 5-FU loaded micelles were also prepared individually and their physicochemical properties (e.g. average particle size and zeta-potential) characterised. These were then combined to form the new thermosensitive PTX-PTX LMH and PTX-5FU LMH systems. The formulations were optimised with respect to size and surface charge. Microscopy studies were used to determine the morphology of the LMH. Temperature-triggered release from the LMH was studied using a dialysis method at 37°C (i.e. physiological temperature) and 42°C (i.e. the highest temperature approved for mild clinical hyperthermia).

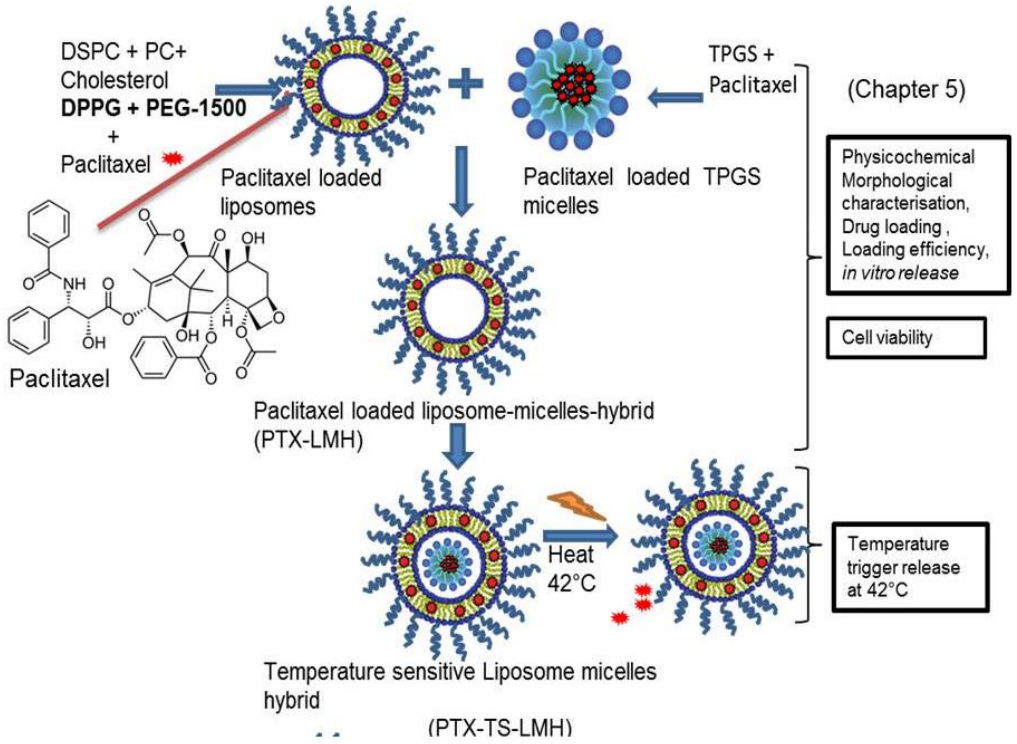


Figure 5-1: Schematic presentation of PTX encapsulated thermoresponsive liposome-micelles-LMH system (PTX-TS-LMH)

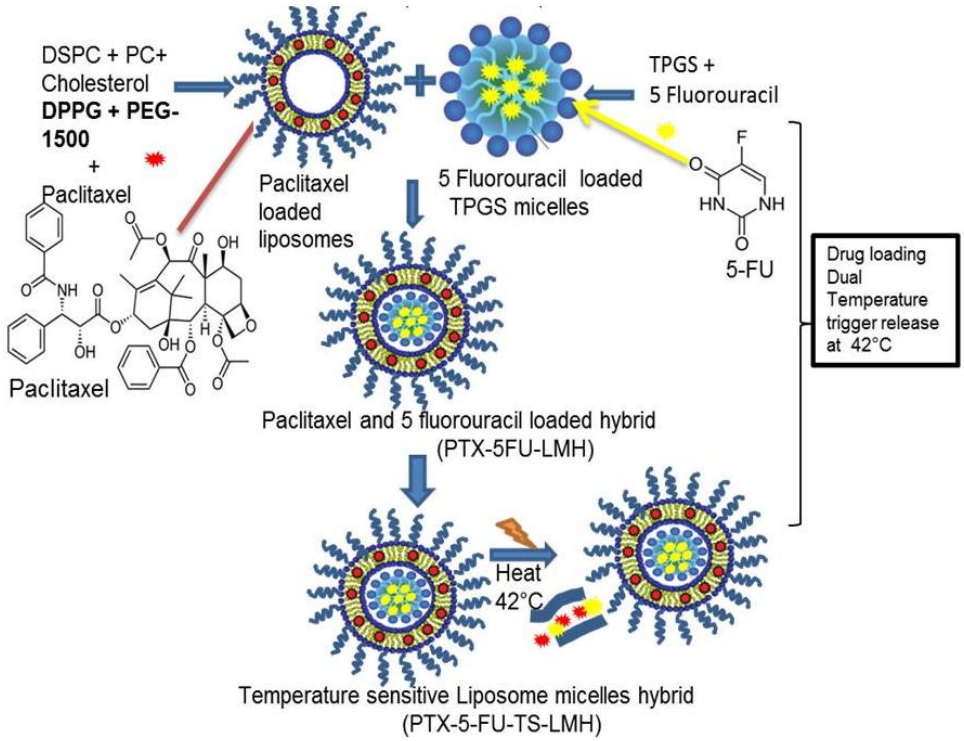


Figure 5-2: Schematic presentation of the thermoresponsive PTX-5FU encapsulated liposome-micelles-hybrid system (PTX-5FU-TS-LMH).

This chapter also includes evaluation of the chemotherapeutic activity for both free PTX and PTX encapsulated nanocarriers against multi-drug resistance (MDR) human cervical adenocarcinoma (HeLa) cells using the Alamar blue assay. Cellular permeability studies of PTX were also investigated using monolayers of the human colonic Caco-2 cell line, a well-established *in vitro* model of the human intestinal epithelium to monitor their efficacy for oral absorption. Specifically, this approach enabled studies of cellular permeability, transepithelial electric resistance (TEER), apparent permeability (*Papp*), efflux ratio (ER), drug transportation, cellular uptake and accumulation of LMH within the cell monolayers. Moreover, the effect of DPPG lipid and PEG in the LMH formulation were examined in these in vitro cell models. The overall cellular studies are schematically presented in **Figure 5-3.**

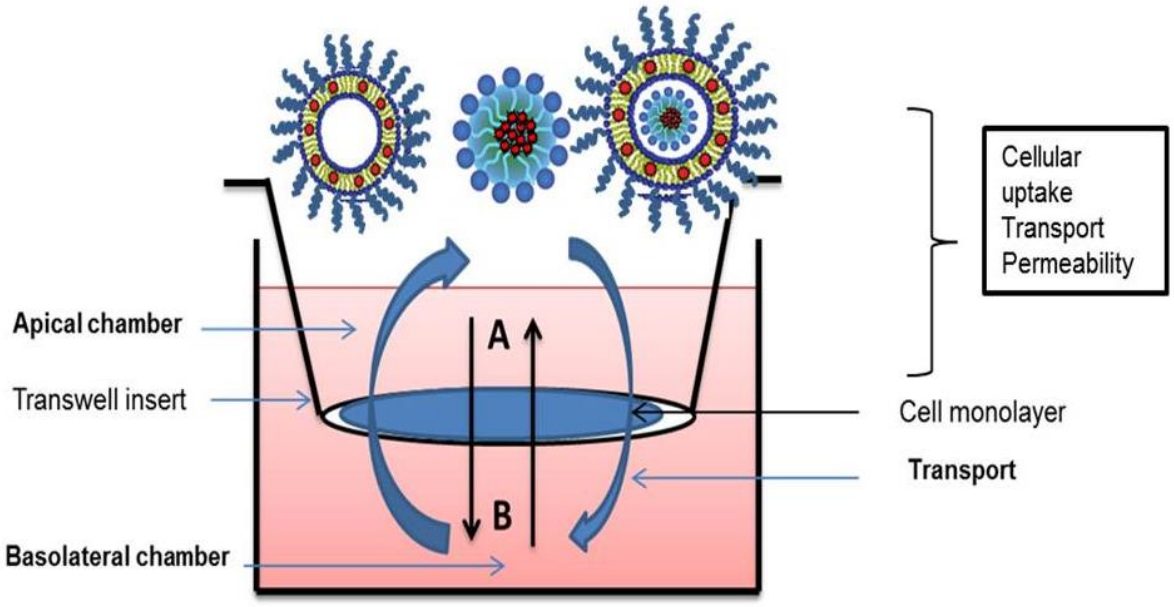


Figure 5-3: Schematically representation of Caco-2 cell monolayer (CCM) cultured on a permeable supports to monitor the permeability of the LMH in two directions, from the apical to the basolateral (A-B) side or basolateral to apical (B-A).

5.1. Introduction

The success of chemotherapy has historically been limited for the treatment of cancer due to the adverse side effect of anticancer drugs which mainly come from insolubility. Poorly water-soluble drugs generally have a tendency to distribute and accumulate in the peripheral tissues, rather than the sites of the cancerous growth.[541] As a consequence, they follow

nonspecific tissue distribution, thus coupled with toxic effects.[344, 542-544] It is also made inevitably that the dose required to achieve a therapeutic concentration at the target site is deemed to be higher and further significant detrimental systemic side effects are manifested.[344, 542-544] A drug with limited aqueous solubility is not suitable for the general delivery routes (e.g. oral or intravenous) of administration so they clearly deserve more attention in order to turn them into safe and effective clinical therapies. Other factors, including incompatibility, instability in the biological environment, proper control of release, lack of suitable route of administration and physiological barriers (e.g. the blood-brain-barrier) are major challenges to successful chemotherapeutics development.[545]

PTX is a diterpenoid centered around a bulky, complex, and fused taxane ring composed of a number of hydrophobic substituents, which makes it a highly lipophilic compound with a *log P* value of 3.69 and aqueous solubility of less than 0.03 mg/mL.[546-547] Due to the particularly low solubility and poor permeability of PTX, it is classified under class IV of the Biopharmaceutical Classification System (BCS).[112, 548] Oral delivery of PTX is appealing over intravenous routes due to factors such as patient convenience, compliance, and the relative safety of the oral route in terms of minimizing infection. Yet, orally delivered Taxol therapy is sparingly used due to its low oral bioavailability.[549] Biologically, the low bioavailability is mainly attributed to the poor aqueous solubility and dissolution of PTX in gastrointestinal fluids. Subsequent hepatic drug metabolism by cytochrome P450 metabolic enzymes (CYP450), rapid clearance by mucus, low permeability across the epithelium, and efflux by multidrug transporter P-glycoprotein (P-gp) all contribute to the insufficient bioavailability of orally delivered PTX.[503, 549-550] Different approaches have been made to improve the solubility and pharmacological properties of PTX to overcome the above problems. To improve PTX's solubility; complexes with cyclodextrins,[551-553] co-solvency[112] mixed-micellar formulations,[554] emulsions.[555-556] liposomes[122, 557], microspheres,[558-559] nanoparticles,[560] and polymeric micellar formulations using amphiphilic block copolymers have been investigated.[561-564] Water-soluble prodrugs have also been extensively studied to increase the aqueous solubility and site-specific release and tumor targeting of PTX.[565-566]

Another chemotherapeutic agent, 5-FU or 5-fluoro-2,4-pyrimidinedione is one of the most successful and widely employed chemotherapeutic agents in the treatment of breast,[567] colorectal[568] and skin cancer,[569] three of the most frequently occurring malignant tumours.[570] It acts as a competitive inhibitor of three enzymes involved in the metabolism of pyrimidines

and therefore inhibits the synthesis of DNA.[571] However, 5-FU suffers from several drawbacks, i.e. poor and erratic oral bioavailability,[572] a short plasma half-life after intravenous bolus administration (10–20 minutes), drug clearance from plasma within 1 hour as a consequence of a very rapid metabolism by the dihydropyrimidine dehydrogenase or uracil reductase enzymes,[131] low tumor selectivity and low drug retention in tumor tissue; as a consequence, its therapeutic administration results in high incidence of chemotherapy-induced multiple organ toxicity.[571]

Another major obstacle to successful chemotherapy is the development of multi drug resistance (MDR), which in the clinic causes significant toxicity and undesirable side effects.[573-575] The uptake of anticancer drugs from the gastrointestinal lumen is largely limited by P-glycoprotein (P-gp) which is over-expressed in many human cancer[549, 576] and contributes to resistance to chemotherapy treatment.[577] To overcome MDR, co-administration of different chemotherapeutic drugs in a chemotherapy regime is utilised and thus maximizing the therapeutic effect by overcoming the mechanisms of drug resistance associated with cancer management.

Recently, significant attention has been given to the co-administration approach that uses liposomes as a delivery vehicle. Liposomes co-loaded with either Doxorubicin (DOX) and verapamil[578] or PTX and tariquidar are shown to reverse the MDR.[579] Ji *et al*. also reported a nano hybrid system of non-ionic surfactant inserted in liposomes and loaded with PTX for reversal of MDR.[441] Therefore, in these examples, liposomes can enhance cellular uptake, increase intracellular drug concentration, thereby avoiding the inherent toxicity caused by the MDR, and bypassing trans-membrane protein-mediated efflux.[580-581] Incorporation of an anticancer drug into liposomes improves its performance by extending the plasma half-life,[582] increasing the solubility of the drug, enhancing accumulation in solid tumours via the enhanced permeability and retention (EPR) effect,[583-584] and shielding the drug from deactivating plasma proteases.[585] Liposomes represent a versatile technology with many advantages over other formulations including; biocompatibility, biodegradability, marked decrease in drug toxicity or an increase in therapeutic efficacy, and passive and active targeting of anticancer agents.[157] Liposome surfaces can also be modified to specifically target cancer cells.[586-589]

Surface modification of liposomes with PEG, can extend the circulation time of nanocarriers in the blood while reducing the likelihood of the mononuclear phagocytic system (MPS) recognition and removal of the drug delivery nanocarriers.[171, 587-589] PEGylated liposomes containing DOX (Doxil) were the first nanoscale drug delivery system, receiving clinical approval in 1995.[326] In addition, a variety of other modifications can be made to liposomes to further tailor the delivery of their therapeutic payloads. Lipids with lower melting points can be incorporated into a liposome to provide temperature-dependent behaviour. In recent years, the use of clinical hyperthermia to trigger thermoresponsive liposomal drug release has emerged as a viable strategy to enable the rapid release of the entire drug payload within the tumour vasculature.[320, 590]

Along with liposomes, micelle-based drug delivery systems have received increasing attention due to their potential to load insoluble drugs while offering control over release kinetics, as well as being easily modified to minimised toxicity, and enhance circulation or provide specific cell targeting capacity.[21, 147, 149, 222-223, 591] Liu *et al.* reported a slow and incomplete release of DOX from three different p(NIPAAm-co-DMAAm)-PLGA micelle formulations at 37°C, i.e. below the transition temperature, but rapidly DOX release at and above the transition temperature of 39.5°C.[592] Moreover, micelles prepared with TPGS are reported to be able to address the above-mentioned concerns, i.e. as an effective P-gp inhibitor, TPGS could act as a reversal agent for P-gp mediated MDR,[232] inhibit P-gp mediated drug efflux[593] and reduce intestinal metabolism.[594] Stimulus-coupled drug delivery can control the drug-releasing pattern temporally and spatially, and improve the accumulation of chemotherapeutic agents at targeting sites[595-599] by triggering with heat,[45-46, 598] light,[600-602] and ultrasound.[603-605] Whereas most of these systems are still under development at various preclinical stages, temperature-sensitive liposomes (TSLs) have progressed to an advanced stage of clinical development (i.e. Phase III clinical trials).[207] Based on TSLs and PEGylation, liposomes have been developed that rapidly releases their contents in response to a heat stimulus within the mild, clinically-achievable hyperthermia range of 40- 42°C with long circulation time.[599, 606-608]

Therefore, a well-designed nanocarrier is in demand which can lead to multifunctional benefits including (1) improved circulation half-life (i.e. by PEGylation), (2) active and passive targeting to the cancer cells leading to improved tumour levels (e.g. by applying hyperthermia), (3) reduced systemic side effects as a result of encapsulating in micelles and

liposomes, (4) allowing co-delivery of multiple drugs (PTX and 5-FU) in a combination of liposome and micelles using a single nanocarrier (i.e. liposome-micelle-hybrid) leading to enhanced anticancer effects by reversing MDR, (5) overcoming clinical resistance conferred by drug efflux transporters (e.g. P-glycoprotein).

The advantages of using thermal sensitive LMH for oral delivery of anticancer drugs are to improve drug release over non-thermal sensitive LMH. The TS-LMH liposomal drug delivery approach is designed to selectively target the diseased tissue (using hyperthermia-internal triggering), while minimizing uptake by normal tissues.

The aim of this research is to optimize the formulation of a PEGylated liposome in combination with micelles using into a single nanocarrier (i.e. liposome-micelle-hybrid), a temperature-sensitive LMH (TS-LMH) system with co-encapsulation of PTX and 5-FU, designed to release drug rapidly upon a temperature triggering using mild hyperthermia at 41-42°C. PEGylated lipids will confer stealth properties to the formulation, leading to a prolonged release time.[609] Encapsulation of these two anticancer agents in a single LMH carrier will lead to the co-delivery of PTX and 5-FU in targeted cancer cells and protects a labile drug from degradation. The use of multiple drugs allows for simultaneous targeting of more than one characteristic of the tumor[610] by reducing the dosage of the drugs to reduce cytotoxicity[549] The TS-LMH liposomal drug delivery approach is designed to selectively target the diseased tissue (using hyperthermia), while minimizing uptake by normal tissues.

5.2. Materials

5.2.1. Materials used for LMH preparation

1,2-Dipalmitoyl-sn-glycero-3-phosphorylglycerol (DPPG) was purchased from Avanti Polar Lipids Inc. 1,2-Distearoyl-sn-glycero-3-phospho-1'-rac-glycerol, sodium-salt (DSPG-Na) with C18:0, < 99%, (Molecular Weight: 801.058), 1,2-Dipalmitoyl-sn-Glycero-3-phosphocholine (DPPG), and phosphatidylcholine (PC) with C18:0, < 98% were purchased from Avanti polar lipids, (INC. Lipoid). Cholesterol (CHO) with 99% purity with M.W 386.65 was purchased from Sigma-Aldrich life science (USA). Polyethylene glycol (PEG) 1500 purchased from Sigma-Aldrich. PTX was purchased from Sinopharm Chemical Reagent Co. Ltd. (China). 5 Fluorouracil was supplied by Beijing Mesochem Technology Co

(Beijing, China). d-α -Tocopheryl polyethylene glycol 1000 succinate (TPGS) was purchased from Antares, Health Products, INC, (US/Canada). All reagents; NaCl, NaOH, H3PO4, Tween 20, PEG-400 and buffer (PBS tablets) solution components were an analytical grade for preparation. HPLC grade acetonitrile and analytical grade chloroform, methanol, ethanol were used as solvents.

5.2.2. Materials used for cytotoxicity study

Human cervical adenocarcinoma (HeLa) cells were purchased from American Type Culture Collection (ATCC) Manassas, VA, USA. Dulbecco's modified eagle`s medium (DMEM) with [+] 4.5 g/ L-D glucose, [+] L- glutamine, [-] sodium pyruvate, 1% nonessential amino acids, and 10% Fetal bovine serum (FBS). Trypsin 0.25% (w/v) in Phosphate Buffer Solution (PBS) were purchased from Sigma Aldrich. A Class II cabinet with a laminar flow hood, fluorimeter and monochromator plate reader (BioTek Instruments Inc, USA) were used and provided by UNSW cell culture facility in the school of medical science (Lowy children cancer centre).

5.2.3. Materials used for permeability study

Human epithelial colorectal adenocarcinoma cells (Caco-2) were kindly donated by the School of Medical Science, University of Sydney. 24-well polystyrene plates with inserts and lids (polycarbonate transwell filter with 0.4 μm pores and a surface area of 0.7 cm^2) were purchased from Millipore Corporation Ltd., Bedford, MA, USA. Dulbecco's modified eagle`s medium (DMEM) with [+] 4.5 g/ l-D glucose, [+] l- glutamine, [-] sodium pyruvate, 1% nonessential amino acids, and 10% Fetal bovine serum (FBS) and transport buffer Hank's balanced salt solution (HBSS); containing (500 mL):12.5 mL of 1 M D-glucose and 10 mL of 1 M 4-(2- hydroxymethyl)-1-piperazine ethane sulfonic acid (HEPES) buffer, 1 mL of 625 mM $CaCl_2$, 1 mL of 250 mM $MgCl_2$ were purchased from Gibco ife technologies, USA. Trypsin 0.25% (w/v) in Phosphate Buffer Solution (PBS), DMSO, HEPES and permeability marker Lucifer Yellow (LY) solution were purchased from Sigma Aldrich. A Class II cabinet with laminar flow hood and sample analysis equipment fluorimeter, monochromator plate reader (BioTek Instruments Inc, USA) was used and provided by UNSW cell culture facility. A TEER instrument (Millicell ERS-2 volt-ohm meter) was purchased from Millipore Co., Bedford, MA, USA.

5.3. Experimental Methodology for preparation and characterisation

5.3.1. Preparation of PTX encapsulated thermosensitive micelles

The method used for the PTX-loaded micelles was modified from direct dissolution[222-223, 241, 377-378] and solvent evaporation method.[377, 379-381] Different quantities of PTX (5 mg, 10 mg, and 15 mg) were weighed and mixed with 100 mg of TPGS and then dissolved in chloroform. The solvent was evaporated by rotary evaporator for 2 hours at 38 °C while rotating at 60 rpm. The film was then hydrated with 10 mL of PBS solution containing 0.9% sucrose. The hydrated solution was sonicated for 30 minutes to form micelles. A clear drug-loaded micelle solution was formed. The free drug was separated by centrifugation at 10,000 rpm for 20 minutes.

5.3.2. Formulation of PTX encapsulated thermosensitive liposome

The PTX-loaded liposomes were prepared by the thin-film hydration method accordingly to Bangham *et al*.[146] Afergan *et al*.[384] and others.[146, 379, 383, 611] The compositions of lipids used for liposome preparation were DPPG, DSPG, PC, cholesterol and PEG-1500 in a molar ratio 80:5:5:2.5:10. As a thermosensitive lipid, we have chosen dipalmitoyl-sn-glycero-3-phosphorylglycerol (DPPG)[51-53, 612] because it exhibits a phase transition temperature of 41.5 ± 0.5°C, in the adequate range for thermosensitive formulations.[207] Cholesterol (CHO) was also included to promote in vivo stability.[607, 613] The lipids (100 mg) and PTX (10, 15, 20 and 25 mg) were weighted, mixed, and dissolved in a mixture of methanol-chloroform-water (10 mL) with a ratio of 1:5:0.2. in a round bottom flask by gentle hand shaking and sonication (1-2 min) to form a clear solution. The round-bottom flask connected to a BUCHI rotavapor R-124 and BUCHI water bath B-480 with applied vacuum and temperature above the phase transition of the lipids.[385] The excipient-solvent mixture was subjected to vacuum evaporation for 3 hours until the complete evaporation of the organic solvents and remove all traces of chloroform and to form a thin drug-lipid film at 60°C, which was above the phase transition temperature (Tc) of the lipids (55°C). The rotation speed was kept at the slowest (60 rpm) to prepare a high-quality thin film.

The homogenously dry, thin lipid film was dried for an hour with N_2 gas and then kept under vacuum in a hood overnight to remove the solvent completely. The resultant film was rehydrated with 0.9 % (w/v) sucrose in phosphate buffered saline (PBS); as described in

articles for hydration of PTX liposome[614-615] for 2 hours in a water bath with controlled temperature (60°C) with constant rotation at slow speed. The hydrated solution was subsequently sonicated in an ice bath for 10 minutes by ultrasonicator. The ice bath was used to improve the rigidity of the obtained liposomes. The drug-loaded liposomes (pellets) were separated from the unencapsulated free drug (supernatant) by ultracentrifugation (32,000 rpm at 4°C). The collected pellets were suspended in the same hydration media as used before for liposome preparation, extruded through polycarbonate filters (400- 800 nm pore diameter) 8-10 times to obtain highly monodispersed (PDI < 0.25) and unilamellar liposomes.[386,157] The final liposome product appeared as a clear transparent light bluish-white suspension. The liposome suspension was kept in the fridge (4°C) prior to use.

5.3.3. Formulation of PTX encapsulated thermosensitive LMH

The PTX loaded micelles in **Section 5.3.1** were used to rehydrate the PTX encapsulated liposomal dry film for PTX LMH preparation. The ultrasonication, ultra-centrifugation, and size extrusion methods were followed as described in **Section 5.3.2.**

5.3.4. Preparation of 5-FU-PTX dual-encapsulated LMH

5.3.4.1. Preparation of 5-FU loaded micelles

5-FU was weighed in four different quantities; 10 mg, 15 mg, 20 mg and 25 mg and with100 mg of TPGS for 5-FU micelles formulation. The micelle preparation method was followed as described in **Section 5.3.1.**

5.3.4.2. Preparation of PTX loaded liposome

The film formation of PTX encapsulated liposome was followed the same procedures as described in the first paragraph of **Section 5.3.2.**

5.3.4.3. Preparation of PTX-5-FU loaded LMH

The 5-FU-loaded-micelles was used to hydrate the PTX-loaded-liposome film for PTX- 5-FU LMH preparation following by sonication-ultracentrifugation-extrusion methods were followed the same procedures as described in **Section 5.3.2.**

5.4. Encapsulation efficiency and drug loading

Samples of the PTX and 5-FU nanocarrier formulations were prepared by diluting 100 μL of each formulation with 900 μL of acetonitrile and vortexed to disrupt the carriers. The samples

were centrifuged and filtered through the 0.22 µm PTFE syringe filters before analysis. The concentration of PTX and 5-FU in the micelles, liposome, and LMH the prepared samples were analysed by HPLC, using the assay methods as described below.

5.4.1. PTX assay method

The concentration of PTX was analysed using HPLC system (Shimadzu UFLC (Model LC-20 AD) with an X-Bridge TM C18 column (156 x 10.0 mm), USA. The mobile phase was a mixture of 45% (v/v) of acetonitrile and 55% (v/v) of water. An isocratic elution method was used. The flow rate was set at 1.0 mL/min. The absorbance was measured at 227 nm. The run was for 10 minutes. The mobile phase was degassed by ultra-sonication for 30 minutes before use and was not allowed to recirculate during the analysis. The samples were injected at a volume of 50 µL at room temperature. A series of working solutions with concentrations ranging from 10 to 500 µg/mL were used for generating the linear calibration curve (n = 4) by plotting the chromatographic peak area versus PTX concentrations over the range of 10-500 µg/mL ($y = 99666x - 138531$, $R^2 = 0.9895$). The limit of quantification (LOQ) value was 10 µg/mL. The method was highly specific for the PTX peaks (average retention time 1.52 minutes). The precision and accuracy for both intra and inter-day analyses were within the acceptable analytical limits (i.e. < 10%). Repeated analysis of the samples showed excellent precision (< 3%) in the peak area results. Therefore, the selected HPLC method is highly applicable for PTX quantification for *in vitro*. All analyte were diluted suitably to meet the calibration concentration range.

5.4.2. 5-Fluorouracil assay method

5-FU solution concentrations were analysed using HPLC (Shimadzu UFLC (Model LC-20 AD) with an X-Bridge TM C18 column (156 x 10.0 mm), USA). The mobile phase was a mixture of 10% (v/v) of methanol and 90% (v/v) PBS solution. An isocratic elution method was used and the flow rate was set at 1.0 mL/min. The absorbance was measured at 254 nm. The run was for 10 minutes. The mobile phase was degassed by ultra-sonication for 30 minutes before use and was not allowed to recirculate during the analysis. The samples were injected at a volume of 50 µl at room temperature. A series of working solutions with concentrations ranging from 10 to 500 µg/mL were used for generating the linear calibration curve (n = 4) by plotting the chromatographic peak area versus 5FU concentrations over the range of 10- 500 µg/mL ($y = 33707x$, $R^2 > 0.9975$). The limit of quantification (LOQ) value

was 10 µg/mL. The method was highly specific for the in which the 5-FU peaks (average retention time 1.96 minutes) The precision and accuracy for both Intra and inter-day analyses were within the acceptable analytical limits (i.e.<10%). The high specificity and reproducibility of the assay were (102- 108%) of 5-FU calibration samples. Repeated analysis of the samples has shown excellent precision (< 3%) in the peak area results. Therefore, the selected HPLC method is highly applicable for 5-FU quantification for *in vitro*. All analyte were diluted suitably to meet the calibration concentration range.

The encapsulation efficiency (*EE*%) of the nanocarrier formulations for each drug was calculated using the following **equation 5-1**:

$$EE\% = \frac{We}{Wi} \times 100 \quad \text{.....} \textbf{\textit{Equation 5-1}}$$

Where, *We*, is the amount of the encapsulated drug in the formulation and *Wi*, is the initially added amount of the drug.

5.5. Physical characterisation of PTX-loaded LMH

5.5.1. Particle diameter and size distribution

The average particle diameter (Z-average), size distribution (polydispersity index-PDI) and zeta potential of the nanocarriers were measured by Phase Analysis Light Scattering (PALS) and Dynamic Light Scattering (DLS) techniques using Malvern Zetasizer Nano instrument and Nano ZS ZEN 3600 (red badge), respectively. Each sample was placed into a disposable sizing cuvette (for diameter) and clear disposable Zeta cell (for zeta). Zeta potential of liposome and LMH were measured in 1 mM NaCl. The diameter of micelle was analyzed without any treatment beforehand, and the liposomes or the LMH systems, they were diluted 100 times with Mili-Q water prior to the analysis. For each sample, the diameter was measured 3 times with 6 runs for 4 minutes (1 minute for equilibrium and 3 minutes for 3 measurements) at 25ºC; the attenuation was set at 7 and 9 and the material RI was set at 1.59. The correlation function and count rate were also observed (approximately 300-500).

5.5.2. Morphological characterisation of PTX loaded LMH

Transmission electron microscope (TEM) was used to characterise the micelles, liposome, and LMH morphologically. After dilution with PBS, from the sample suspensions, a droplet of the sample (6 µL) was applied on a Formvar-coated copper grid, or a carbon-coated copper

grid for 1 minute and excess sample was blotted away with filter paper. Liposomes were subsequently negatively stained with 2% uranyl acetate. Aqueous uranyl acetate (2%, 20 µL) was applied to the TEM grid for 60 s and the excess stain was blotted away with filter paper. TEM micrographs were recorded on a JEOL 1400 (100 kV) (16/11/16) and an FEI Tecnai G2 20.

5.5.2. Temperature-triggered release of PTX and 5-FU from TS-LMH

Drug release from the formulations was studied in vitro in PBS buffer (pH =7.4) in the presence of 0.5 % PEG-400 as a solubilizer and sink conditions were maintained in the release media. About 4 mL of each formulation was tightly sealed in a dialysis bag (MW cut off 12 kDa) and immersed in 40 mL of release medium. The release study was performed at 37 °C and 42 °C and mixing were achieved using a magnetic stirrer (100 rpm). At defined time intervals, an aliquot of 0.5 mL was taken from the release medium followed by the immediate replacement with an equal volume of the fresh media into the release vessel to maintain sink condition. Samples were analysed by HPLC methods as described in **Sub-section 5.4.1 and 5.4.2.**

5.5.4. Dry sample preparation (Sample drying) for cell studies

Freeze-drying or lyophilization of the formulation was performed to enhance the chemical/ physical stabilities of the LMH, liposome and micelles formulations and minimize lipid hydrolysis. Phospholipids in liposomes are known to be sensitive to hydrolysis and oxidation in an aqueous medium. The hydrolytic degradation may change the rigidity of liposomal bilayers, retention of entrapped drug, and alter liposome diameter and distribution.[616-617] So, the liquid form samples of micelles, liposome, and LMH were dried prior to reconstitution for cell studies. First, the samples were frozen using liquid nitrogen and kept in a freeze dryer (Christ Alpha 1-4 LD plus) for 48 hours at -50°C temperature and at pressure 0.001 Pa. After drying the whole dry powder was weighed and 1 mg of the dry powders were analyzed for the drug content and stored in the freezer prior to studies of cell cytotoxicity, and cell permeability and transportation.

5.5.5. Cytotoxicity assays of PTX-LMH on HeLa cells by Alamar Blue method

HeLa cells were grown in DMEM supplemented with 10% (v/v) fetal bovine serum (FBS). The cells were maintained in an incubator supplied with 5% CO_2 and 95% air humidified

atmosphere at 37°C. Suspension samples of HeLa cells in growth media were seeded into 96-well tissue culture plates at a density of 1×10^4 cells per well and allowed to grow for 24 h. The culture was maintained incubator then used in the cytotoxicity experiment. Cytotoxicity of each formulation was assessed using an Alamar Blue® assay.[496] Alamar Blue® is a dye and used as a cell viability assay reagent. This dye is a redox indicator that yields a colorimetric change and a fluorescent signal in response to metabolic activity. It is a proven safe and non-toxic dye used for quantitative analysis of cell viability and cell proliferation, for cytokine bioassays and in vitro cytotoxicity studies (Suppliers information, Thermo Fisher Scientific)

Initially, the sample was prepared with DMEM and FBS (10%) by dissolving in 0.5% (v/v) of DMSO. A total of nine concentrations of each formulation were prepared with dilution of the first sample; 0.1 µg/mL, 1 µg/mL, 2 µg/mL, 5 µg/mL, 8 µg/mL, 10 µg/mL, 20 µg/mL, 25 µg/mL and 30 µg /mL and placed in 96-well cell plate for 4 hours. After 4 hours the solutions were used to determine cytotoxicity of the nanocarriers. Alamar Blue® solution was directly added to the medium resulting in a final concentration of 10% in each well. After 4 hours of incubation with Alamar Blue®, absorbance was measured at 570 nm using a BioRad microplate reader (ELX800, Biotek, USA). Untreated cells were taken as a control with 100% viability and cells without addition of sample were used as a blank. Results were expressed as cell viability (%) by using **equation 5-2**. The cells, treated with medium, were considered as a control (100% viable).

$$Cell\ viability\ (\%) = \frac{(Abs)sample}{(Abs)control}\ X\ 100 \quad \textbf{\textit{Equation 5-2}}$$

Where, $(Abs)_{sample}$, is attributed to the absorbance of cells treated with free drug or drug-loaded formulations and $(Abs)_{control,}$ is related to the absorbance of cells without any drug treatment.

5.5.5. Permeability assessment of PTX-LMH

The cellular permeability of the nanocarriers was monitored by measuring the TEER in culture medium using a commercial apparatus (Millicell ERS; Millipore Co., Bedford, MA)

as previously described by Ferruzza *et al.*[497] with some modification. TEER measurement is used as an index of monolayer confluence and integrity in cell culture experiments.[489] TEER also has been used to measure the paracellular permeability of the cell monolayers.[498]

To prepare a Caco-2 monolayer suitable for permeability assessment, the cells were seeded at a cell density of approximately 40,000 cells/cm^2 on polycarbonate transwell filters (0.4 μm pores and a surface area of 0.7 cm^2) in 24-well polystyrene plates and routinely maintained in DMEM at the incubator for 21 days. The medium was changed on alternate days, firstly the basolateral and then the apical, which contains 400 and 600 μL, respectively. Culture medium was replaced every 48–72 hours. At the end of 14 and 21 days of differentiation, the integrity of the monolayers was assessed by the TEER.

The permeability study was performed on day 21 of the experiment as reported most of the literature.[497, 499] By 21 day, the monolayers have become differentiated with regard to the expression of many transport proteins and brush border hydrolases.[497] For this study, the DMEM (growth media) from the apical chamber was replaced by the transport buffer HBSS for both the control and sample.[501] This buffer was also used to prepare the samples for treatment (LMH, along with individual samples of liposomes, micelles, and free PTX for comparison). Each of the nanocarriers and free PTX sample contains 100 μmol of PTX.

At the end of the growth period, plates were equilibrated with transport buffer (HBSS) and incubated in the incubator for half an hour. The TEER value was recorded every 20 minutes of the experimental period for the first hour, followed by every hour for each well. The resistance of a blank insert (without cells) was also determined to subtract as a background value. Only monolayers displaying TEER values above 300 Ω·cm^2 were used in the transport experiments. TEER measures the resistance to passive ion transport and reflects the tightness and confluence of cell monolayers. The final TEER values are expressed as Ω cm^2 on the basis of the following equations[489]:

$$TEER = (R - Rb)\ X\ A \quad \text{.....} \textbf{\textit{equation 5-3}}$$

Calculation of Resistance of a unit area of 1 cm^2

$$Resistance = Total\ resistance - blank\ resistance \text{.....} \textbf{\textit{equation 5-4}}$$

$$Resistance\ of\ a\ unit\ area$$

= Resistance (Ω) *X* Effective membrane area* (cm^2)……***equation 5-5***

Here, *R* = Total resistance, *Rb* = blank resistance and *A* = the effective membrane area = 0.7 cm (= 0.7^2 = 0.49 cm).

Transport of free PTX and PTX encapsulated nanocarriers; micelles, liposome, and PTX-LMH across the Caco-2 cell monolayers were studied followed a modified method described in article,[618] using monolayers 21 days post-seeding. Before the experiments, the monolayers were equilibrated with transport medium and preincubated for 30 min in similar procedures as described above. PTX 100 µM/mL solution and PTX containing nanocarriers (containing 100 µM drugs) were freshly prepared by dissolving in 0.5% (v/v) of DMSO and HBSS. All media (DMEM) from different wells were replaced and equilibrated with HBSS buffer (400 µL in the apical wells and 600 µL in the basal Wells) for 30 minutes. Then the samples were added by replacing with the buffer HBSS (pH 7.2) to the apical (400 µL) or basal (600 µL) wells. Incubation was undertaken for 2 hours. After incubation, 500 µL of samples were taken from the appropriate wells, depending on the direction of transport (i.e., from the basal well for A-to-B transport or the apical well for B-to-A transport), for an efflux ratio determination. After treatment, the treating solution was withdrawn and the cells were washed three times with PBS. HBSS in the basolateral chamber was collected and transported samples were lysed with methanol. Samples were quantitatively analysed by HPLC for PTX content (method described in **Section 5.4.1.**). This quantitative determination of PTX was required prior to the determination of the P_{app} value and efflux ratio.

The integrity of the Caco-2 cell monolayers was evaluated using LY, followed a modified method described in Article.[306] After removing samples for PTX analysis, the remaining liquid was aspirated from the apical and basal wells. The LY solution (500 µL of 0.1 mg/mL) was added to the apical wells and 1000 µL of transport buffer (HBSS) to the basal wells. These were then incubated at 37 °C for 60 minutes. 200 µL aliquots of samples were transferred from the basal wells to a 96 well cell culture plate and absorbance measured in a spectrofluorometer with excitation wavelength at 485 nm and emission at 535 nm. The fluorescence for HBSS Buffer (as blank to deduct the background value used as a media to prepare the samples) and a 0.1 mg/mL LY solution were also measured. The fluorescence intensity of LY was analysed with by a Microplate Fluorescence Reader (Tecan i-control FL600, Bio-Tek, Winooski, USA) using a fluorescence excitation wavelength of 540–570 nm

(peak excitation is 570 nm) and fluorescence emission at 580–610 nm (peak emission is 585 nm). A standard curve was prepared from 0.5 to 100 µM (molecular weight = 457.25 g/mol). The 96 well plate containing samples for analysis was placed on a solid black plate of the fluorescence Reader.

Analysis then proceeded to determination of the P_{app} value and efflux ratio from equations 4.6 and 4.7.[502]

c. The apparent PTX permeability (P_{app} x 10^{-6} µg/s) was calculated as follows: P_{app}

$$P_{app} = \frac{VR}{A\ X\ C0}\ X\ \frac{dMt}{dt} \quad \text{.....} \textbf{\textit{Equation 5-6}}$$

V_R is the volume of the receiving chamber, A = monolayer filter area (cm^2), Co = mass of compound initially in the donor compartment, dMt/dt = the rate of drug permeation across the cells

d. The efflux ratio (ER) was calculated as the ratio of P_{app} determined in the A-to-B direction to P_{app} determined in the B-to-A direction:

ER = (P_{app} B-A) / (P_{app} A-B) ..... ***Equation 5-7***

where the ratio of the basolateral–apical (secretion) component P_{app} B–A to the apical-basolateral (absorption) component P_{app} A–B was assessed. Theoretically, an ER superior to unity suggests the implication of one or various efflux transporters in a disposition of tested compound. For compounds with an ER in the range of 1–2, a specific P-gp inhibitor is used to confirm the implication of the latter transporter.

c. The percent permeability of LY from the fluorescence values was calculated as follows:

$$\%\ permeability = \frac{(Sample - blank)}{(Lucifer\ yellow - blank)}\ X\ 100 \quad \text{.....} \textbf{\textit{Equation 5-8}}$$

5.5.6. Transport and cellular uptake of PTX study of PTX with different nanocarriers (micelles, liposome, and LMH) to the apical-to-basolateral (A→B) direction

Transportation and cellular uptake of PTX were evaluated using a modified method described in the literature.[304, 503] For this study, cells were plated at a 40,000 cells/cm^2 onto a 24 mm polycarbonate transwell filter with 0.4 µm pores and a surface area of 0.7 cm^2. At the

beginning of each experiment, the monolayer was washed twice with PBS and pre-equilibrated for 30 min with buffer (HBSS). PTX, micelles, liposome, and LMH suspensions of 400 µL (drug content 100 µmol/mL) were added to the apical chambers of the monolayers inserted in each well containing 600 µL HBSS (pH 7.4). The pH conditions were chosen in order to reproduce the physiological pH gradient existing *in vivo* across the small intestinal mucosa. The plate was placed in the incubator for 24 hours at 37^{o}C. A 500 µL samples were taken at 0 minute, 2 hours, 4 hours, 8 hours, 12 hours and 24 hours, from the basolateral side and replaced by the same amount of transport buffer. At the end of the transport experiment (24 h)**,** samples (100 µL) were also taken from the apical side. PTX content was measured by HPLC assay method in **Section 5.4.1.**

5.5.7. Statistics analysis method

One way analysis of variance (ANOVA) statistic method was used to determine whether the data of cell toxicity (control and LMH), decrease of TEER value (control, LOV and nanocarriers), permeability (between control and nanocarriers), LY permeability (control, PTX and nanocarriers) and were significantly different (means of these groups are different). ANOVA uses F-tests to statistically test the equality of means. To use the F-test to determine whether group means are equal, it's just a matter of including the correct variances in the ratio. In one-way ANOVA, the F-statistic is this ratio:

F = variation between sample means / variation within the samples

Here, *P* value was calculated from data analysis using MS Excel.

5.6. Results and discussion

5.6.1. Physical characterisation of PTX-LMH

The average particle diameter, particle size distribution (PDI) and zeta potential (ζ) of PTX loaded LMH, liposome and micelles were determined as shown in **Table 5-1**. The blank micelles and liposomes were found to have diameters of 13 nm and 154 nm whereas loaded micelles and liposomes were found to have diameters of 10 nm and 167 nm, respectively (see **Table 5-1**), in agreement with previously studied micelles and liposomes in chapter 3 and literature values.

Table 5-1: Average particle diameter, particle size distribution (PDI) and zeta potential of PTX loading micelles, liposome, and LMH (mean ± SD, n = 3).

Nanocarrier Type		Diameter (nm)	Polydispercity index (PDI)	Zetapotential (mV)
Micelle	PTX-Loaded	10 ± 0.1	0.394 ± 0.007	Not measured as TPGS molecule has no charge
	Blank	13 ± 0.4	0.242 ± 0.027	
Liposome	PTX-Loaded	167 ± 4	0.276 ± 0.024	-15.2 ± 1.19
	Blank	154 ± 2	0.121 ± 0.015	
LMH	PTX-Loaded	175 ± 1	0.217 ± 0.028	-14.4 ± 0.85
	Blank	151 ± 2	0.087 ± 0.021	

Literature also reported on the comparable diameter of blank micelles and liposomes. Zhang *et al.* prepared a PTX loaded and blank TPGS micelles with a diameter of 13 nm.[419] Muthu *et al*. also reported docetaxel-loaded TPGS micelles with a diameter ranged between 12 and 14 nm using different preparation methods.[281] Similar results were published by Mu *et al*. for TPGS micelles with the mean diameter of approximately 12 nm with or without the drug (camptothecin).[420] Yan *et al*. also reported TPGS micelles with a mean diameter of 12.7 nm (blank) and 11 nm loaded with fullerene.[381]

Jain *et al*. prepared PTX-liposomes with phosphatidylcholine and cholesterol for oral delivery of PTX with a particle diameter of 114 ± 7.57 nm (PDI, 0.262 ± 0.027) and 119 ± 6.37 (0.242 ± 6.37) blank and loaded.[619] Another PTX loaded liposome system was reported by Ji *et al*.; this was prepared with soybean lecithin and cholesterol with an average particle diameter of 139.8 ± 1.4 (PDI 0.274 ± 0.007).[441]

The PTX-loaded micelles were slightly smaller than the blank micelles. This is attributed to the thermodynamic constructed behaviour of micelles and they occurred when the concentration is greater than critical micelles concentration (CMC). At this point the hydrophobic part of the molecules preferentially interacting with other molecules'

hydrophobic sections, thereby reducing the contact with the water molecules and the disorder of the individual molecules within the system. Given this, the fact that the micelles with PTX were smaller presumably means they have a smaller aggregation number (*i.e.* they consist of fewer molecules; this is because the additional PTX within the micelle core stabilises the hydrophobic core of the micelle structure).

In contrast, incorporation of PTX into the liposomes resulted in an increase in diameter (to 167 nm), attributed to the merging of the PTX within the lipid bilayer as previously reported in literature.[441] Ji *et al.* reported a nanohybrid system composed of phosphatidylcholine, cholesterol, and non-ionic surfactants HS-15 loaded with PTX showed larger particle diameter than blank nanohybrid system, which indicated that PTX loaded into nanohybrid systems could slightly expand the particles.[441]

When the blank micelles and liposomes were combined to produce the LMH system, the diameter was 151 nm, i.e. approximately the same diameter as the blank liposomes. However, the PTX loaded LMH was found to have a diameter of 175 nm, i.e. similar to the diameter of the PTX-loaded liposomes (**Table 5-1**). A similar increase in diameter after drug loading has also been reported in the literature.[221, 235]

The diameter of the drug-loaded liposomes and LMH is an important feature in oral drug delivery since they present a large surface area for interactions with the gastrointestinal tract The size, shape and surface chemistry of nanocarriers can significantly influence cellular uptake and efficacy of the treatment.[620] This diameter nanoparticle will demonstrate passive accumulation within the tumor vasculature by the EPR effect and will enhance the drug absorption.[538, 621-622] Their diameters were also optimum and desirable for delivery to the tumor cells and for rapid accumulation in a tumour and increased permeability. Similar results have also been reported for liposome with average diameter < 200 nm.[623-624] The PDI (polydispersity index) was < 0.3 for the LMH and individual carriers, which indicates that the systems can be considered to be reasonably monodispersed. **(Table 5-1 and Figure 5-4)**.

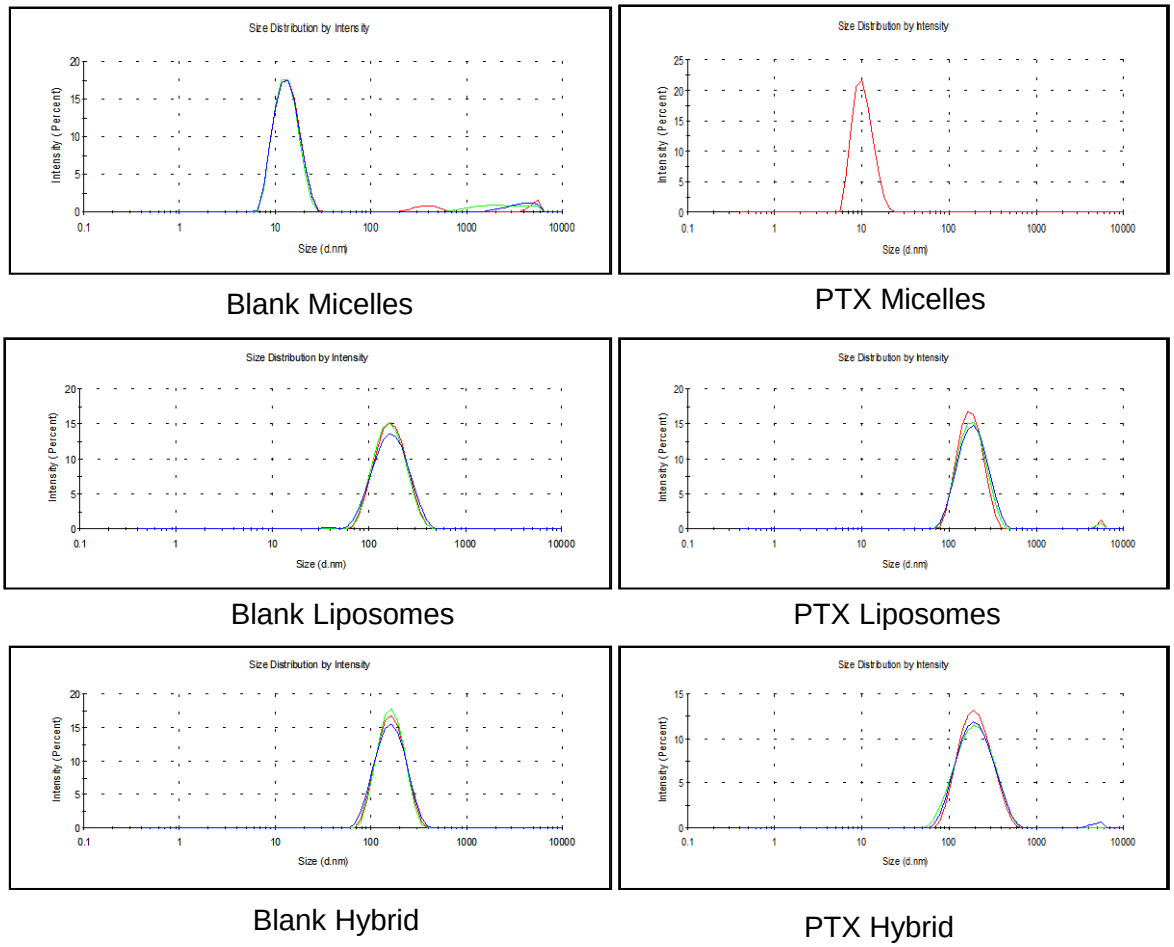


Figure 5-4: Particle size distributions of nanocarriers (mean ± SD, n=3).

The LMH displayed a negative zeta potential (ζ) potential of -14.4 ± 0.85 mV. The negative charge was due to the lipids DSPG and DPPG (The phospholipid head contains a negatively charged phosphate group) that are used to formulate the LMH. This is also true for liposomes.

5.6.3. Drug loading efficiency

Drug loading efficiency of each nanocarrier was determined by encapsulating different quantities of PTX (10 mg, 15 mg, 20 mg and 25 mg) in 100 mg of lipids used to prepare the liposome. Similarly, for PTX micelles, the same quantities of PTX were loaded in 100 mg of TPGS to determine the highest capacity of loading of each 100 mg of polymeric micelles. The same procedure was applied for the determination of 5-FU loading efficiency in micelles. The loading of 5-FU in liposomes is not reported here (already described in methodology section). The loading of drug within carriers was then investigated as a function of drug concentration with a fixed amount of polymer/lipid.

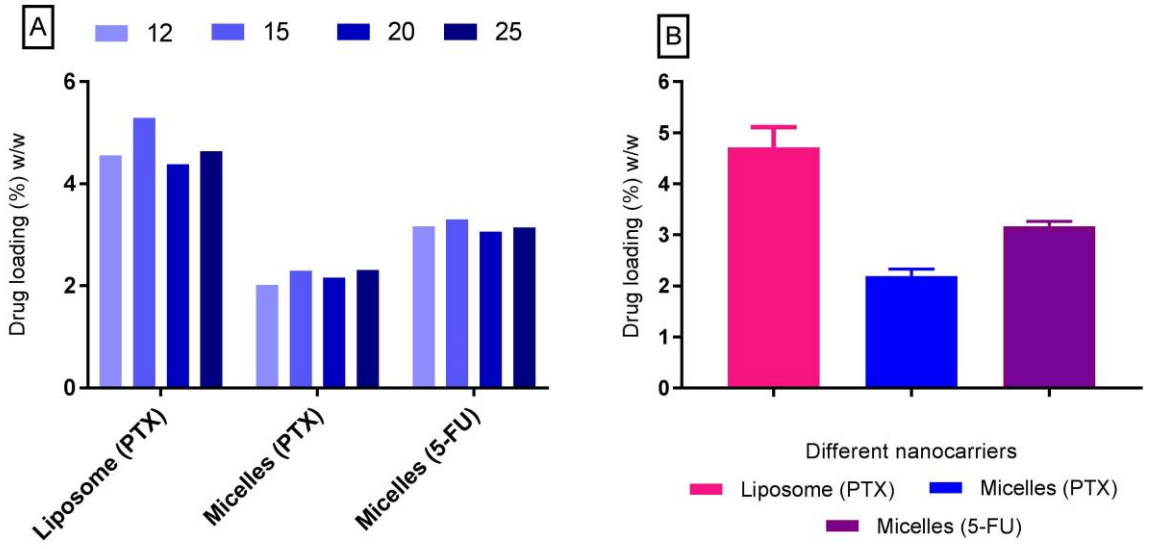


Figure 5-5: A) The relationship between added drug to the polymers/lipids and drug loading amount in different carriers and B) Average drug loading in different nanocarriers (mean ± SD, n=3). A statistically significant ($p < 6.1 \times 10^{-7}$) difference between the extent of drug loading and the increased drug quantity. The post- doc- corrected t-tests analysis says true for liposome (PTX) compared to micelles (PTX) and micelles (5-FU). This implies that there is 95% of chance of difference between PTX loading in liposome and micelles and 5-FU in micelles. The effect of PTX loading is significantly higher for liposome compared to micelles however the effect of PTX loading is significantly higher for liposome compared to 5-FU in micelles.

Keeping the polymer/lipid quantity constant (100 mg), it was also found that the average drug loading fluctuated among the different carriers. For liposomes, the average PTX loading was 4.72 ± 0.40 mg whereas the highest loading of 15 mg PTX was observed for100 mg of lipids. For micelles, the average PTX loading level was 2.20 ± 0.14 mg of PTX/100 mg of TPGS polymer whereas, for 5-FU, it was 3.16 ± 0.36 of drug/100 mg. This indicates that a greater quantity of 5-FU than PTX can be loaded within the micelles (**Figure 5-5B and Table 5-2).** This higher loading is due to the differences in *Log P*, molecular weight (MW) and aqueous solubility, indeed 5-FU has a lower MW and *Log P* compared to PTX (**Table 5-3)**. However, the extent of drug loading varying significantly with the increased drug quantity for each nanocarrier (**Figure 5-5A**).

In contrast, for LMH, the loading of PTX into the LMH's inner aqueous core (as micelles) was 1.42 mg of PTX/100 mg of (lipids + TPGS polymer). The PTX loading in micelles was lower when micelles were loaded in LMH (liposome aqueous core) compare to micelles separately (2.20 mg).

A statistically significant ($p < 6.1 \times 10^{-7}$) difference between the extent of drug loading and the increased drug quantity. The post- hoc- corrected t-tests analysis reports as "true'' for liposome (PTX) compared to micelles (PTX) and micelles (5-FU) implies that there is 95% of chance of difference between PTX loading in liposome and micelles and 5-FU in micelles. The effect of PTX loading is significantly higher for liposome compared to micelles however the effect of PTX loading is significantly higher for liposome compared to 5-FU in micelles.

A similar trend was observed for 5-FU in micelles, where the loading of 5-FU-loaded micelles into the LMH was 2.91 ± 0.417 % (2.91 mg/100 mg of lipids and polymers), which was lower than in individual micelles, i.e. 3.16 ± 0.36 of drug/100 mg of TPGS polymer (**Table 5-2)**. Significant amounts of drug were loaded into the LMH, e.g. PTX loading in LMH increased its solubility by 204-fold in comparison with pure crystalline drug and it was 2.79 and 1.30-fold higher in comparison of micelles and liposomes.

Table 5-2: Drug loading of PTX and 5-FU in individual carriers and the LMH system (mean ± SD, n=3)

Nanocarrier type	**Drug loading (%)**		**Aqueous solubility improved (fold)**	
	PTX	**5-FU**	**PTX (0.03 mg/mL)**	**5-FU (1 mg/mL)**
Micelle	2.20 ± 0.14	3.16 ± 0.36	73.40	3.20
Liposome (bilayer)	4.72 ± 0.40	X	157.33	X
LMH (core)	1.42 ± 0.03	2.91 ± 0.41	47.33	2.91
LMH (bilayer + core)	6.14 ± 0.43	X	204.66	X

The PTX and 5-FU loaded LMHs were prepared by hydration of PTX and 5-FU loaded TPGS micelles into the liposomes core by keeping empty of liposomal bilayer. This was done to determine the actual drug loading in the aqueous core of the LMH. The average drug loading in LMH for the different drugs is shown in **Figure 5-6.**

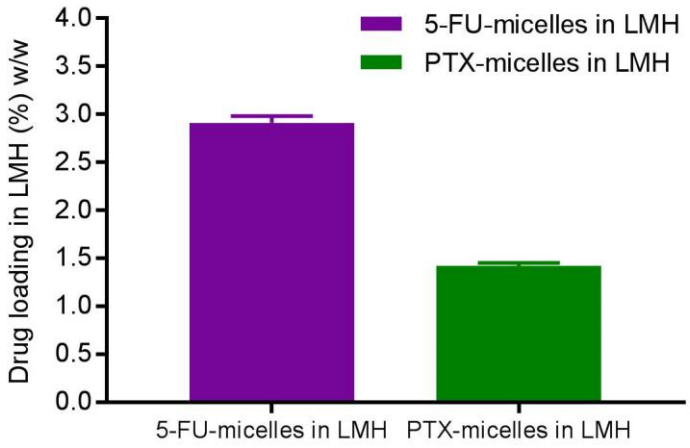


Figure 5-6: The average drug loading in LMH with different drugs, (mean ± SD, n=3).

The drug loading in LMH was higher for 5-FU compared to PTX; this was due to the properties of 5-FU as discussed above and presented in **Table 5-3**.

Table 5-3: Physiochemical properties of 5-FU and PTX.[202]

Compound	Molecular Weight (Da)	Log *P*	Aqueous solubility
5-FU	130.1	- 0.89	1 mg/mL
PTX	953.9	3	0.03 µg/mL

5.6.4. Morphological characterisation

Transmission electron microscopy (TEM) was used to characterise the morphological structure of the blank micelles, liposomes and LMH (**Figure 5-7, 5-8, 5-9)**. For micelles **(Figure 5-7)**, disk-like structures are observed of ~15 nm in diameter. Apparent diameters are slightly larger (2 nm) than determined by DLS; this may be due to flattened in the drying process. A similar structure is also found in the literature.[625] The shape of the micelles depends on their composition as reported by Arleth *et al*.[626]

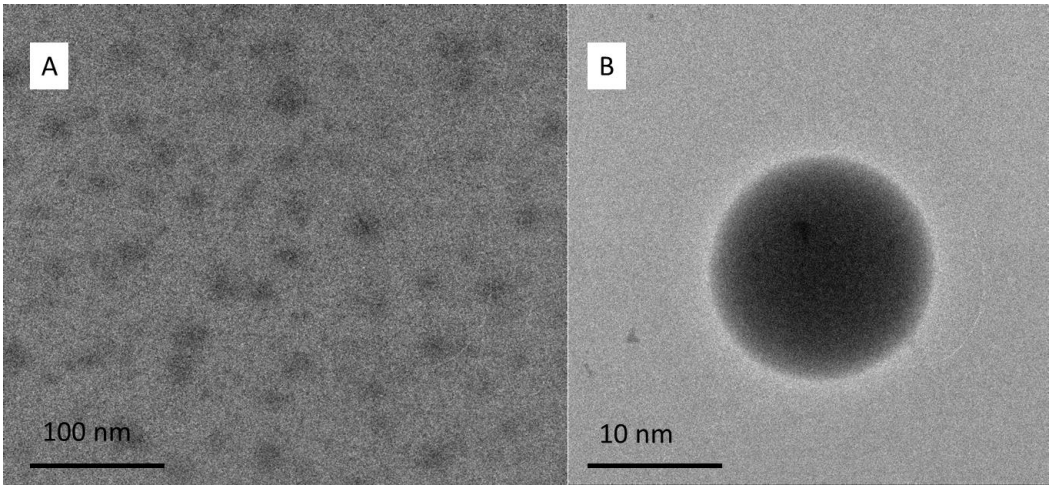


Figure 5-7: Representative transmission electron microscope image of TPGS micelles: A) low resolution view showing uniform distribution and B) a single micelle (10-15 nm in diameter).

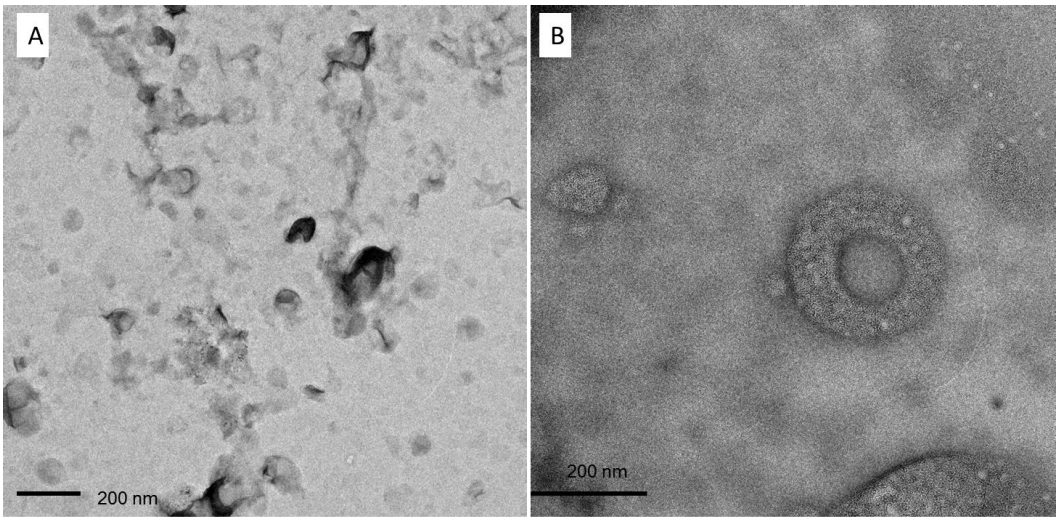


Figure 5-8: Representative transmission electron microscope image of liposomes: A) low resolution view showing uniform distribution and B) a single liposome (< 200 nm).

From TEM images of liposomes, small unilamellar liposomes are observed with a diameter < 200 nm, a disk-like spherical shape was exhibited **(Figure 5-8)**.

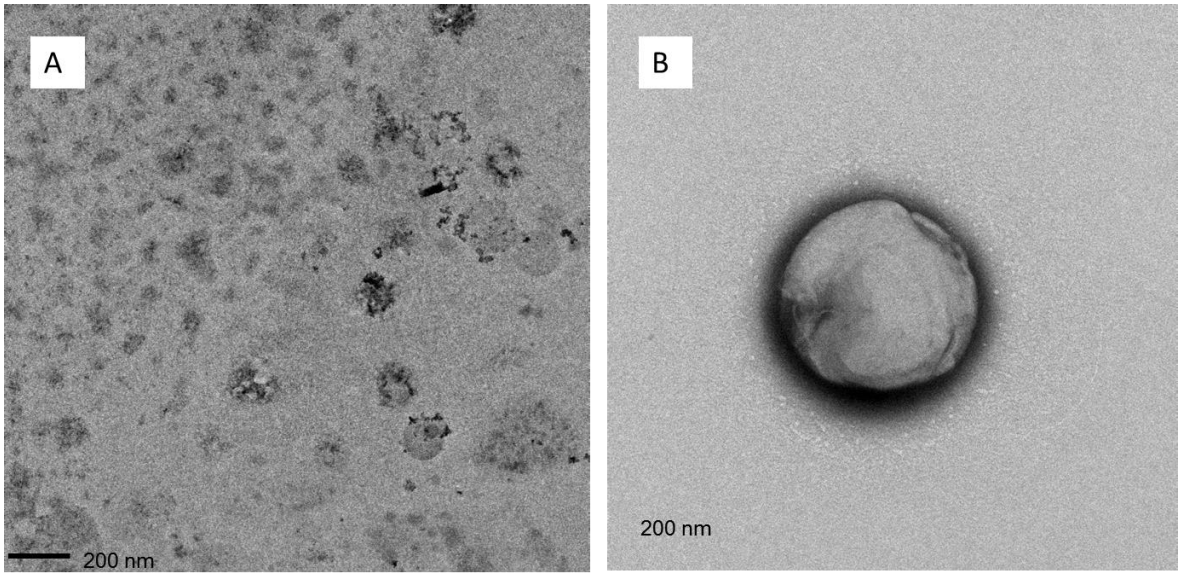


Figure 5-9: Representative transmission electron microscope image of LMH: A) low resolution view showing uniform distribution and B) a single LMH < 200 nm (mean ± SD, n=3).

LMH is observed as a roughly spherical shape with hair-like projections on the surface (**Figure 5-9**). These hair-like projections may be PEG coating around the LMH. Similar roughly spherical shapes with such hair-like projections on the surface were also reported by Lin *et al.*[627] for a curcumin encapsulated cationic liposome-PEG-polyethylenimine (PEI).

It has also been reported that spherical and round shaped particles have some advantages over the non-spherical particles, as they improved the adhesion properties of the absorptive cells and result in improved efficacy as drug carriers.[628]

5.6.5. Temperature-triggered release of PTX from micelles, liposomes, and LMH

The release of PTX and 5-FU release from micelles, liposome and LMH were determined *in vitro* at a temperature of 37°C (physiological temperature) and 42°C (hyperthermia defined as 39-43°C to the targeted site) by a dialysis method.[12,13] The micelles, liposomes and LMH nanocarriers exhibit increased (thermoresponsive) release characteristics at elevated temperature (**Figure 5-10 and 11-A, B respectively)**

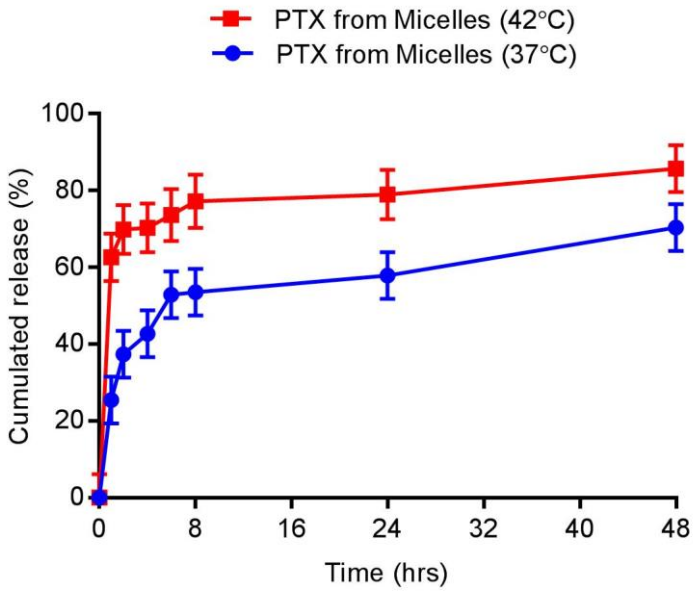


Figure 5-10: The release of PTX from TPGS micelles. Each data point represents the mean ± SD (n=3). A Statistically significant ($p < 0.04$) difference of drug release at elevated temperature 42° C and 37° C.

For TPGS micelles at 37°C temperature, PTX showed controlled release characteristics and 57% of the drug was released at 8 hours. After that, the release slowed and only 65% of PTX released over 48 hours. At elevated temperature (42°C), PTX showed moderate burst release from micelles: 60% of PTX was released in the first hour and after this time the release rate slowed and ~78% release was observed at 8 hours representing a plateau in drug release until 48 hours. With an increase in temperature from 37 to 42^{o}C an ~20% increase in the amount of PTX release was observed (**Figure 5-10**). From the Single Factor ANOVA data analysis it is found that a statistically significant ($p < 0.04$) differences between the extent of drug release at elevated temperature 42 ° C and 37° C.

In general, the drug-release mechanism from micelles is diffusion-controlled. More specifically, a drug is released from the micellar core by two major pathways, i.e. dissociation of the micelle followed by the separation of the drug from monomers. Then drug-polymer bond breakage within the micelle followed by a diffusional release of the drug from the delivery system **(Figure 5-11)**.[629]

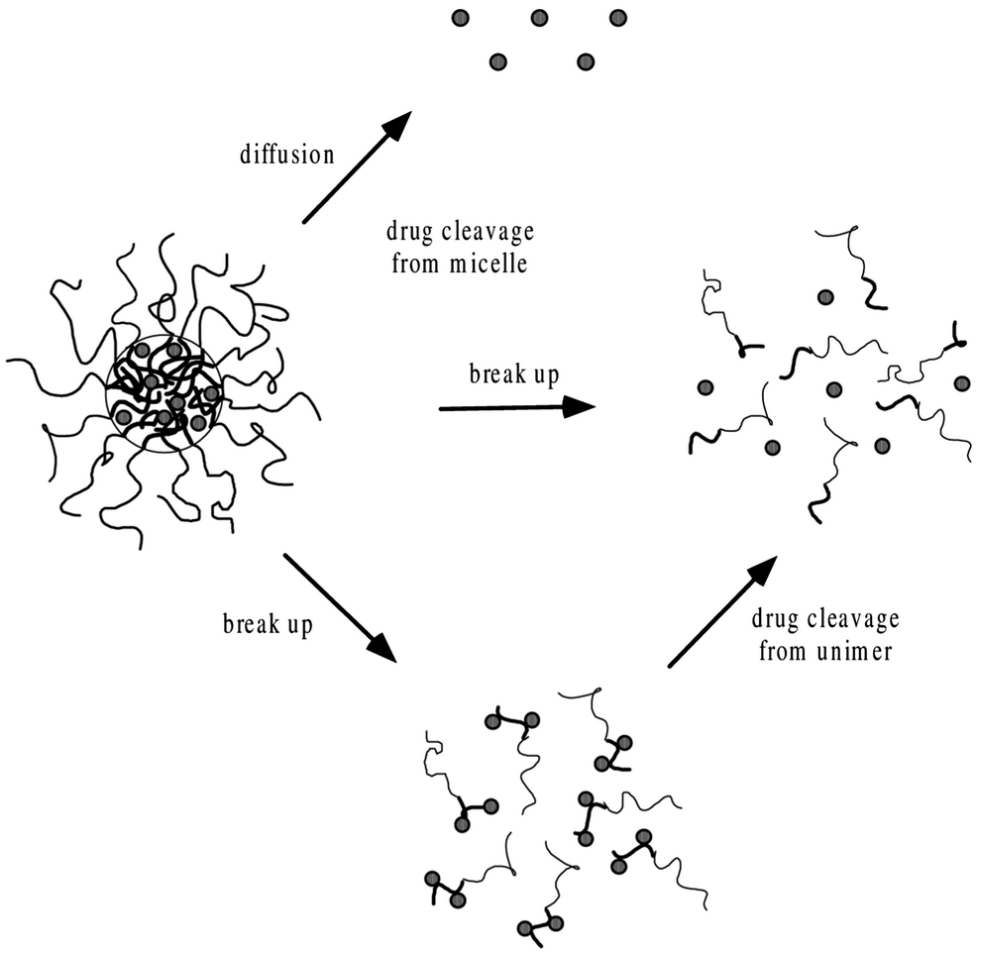


Figure 5-11: Schematic representation of drug-release mechanisms from polymer micelles. The drugs get released from the micellar core by two major pathways i.e. dissociation of the micelle followed by the separation of the drug from monomers and drug-polymer bond breakage within the micelle followed by diffusional escape from the delivery system. The image is adapted from Ahmad *et al*.[629]

However, at elevated temperature (42°C) the drug release from micelles may follow a different mechanism. The TPGS micelles consist of a hydrophobic core and a hydrophilic outer block. PTX molecules are encapsulated into the inner hydrophobic core, while the outer shell shows thermoresponsive ability (**Figure 5-12**). The micelles show thermoresponsive behavior for PTX release according to the thermally induced structural changes in the micellar outer shell structure. When temperature is increased, the hydrated shell shrinks and the hydrophobic drug becomes free from the micelles structure and released by diffusion. Similar release mechanisms from micelles at elevated temperature are reported.[630-631]

The difference in drug release mechanism from micelles at 42°C is described in **Figure 5-12** and related to the physicochemical properties of the core-forming polymers (e.g. hydrophobicity and flexibility/rigidity). At 42°C, changes in the physicochemical properties of the corona and mechanical distortion occurs, water molecules penetrate into the inner core and a channel is formed for facilitating drug release.[630]

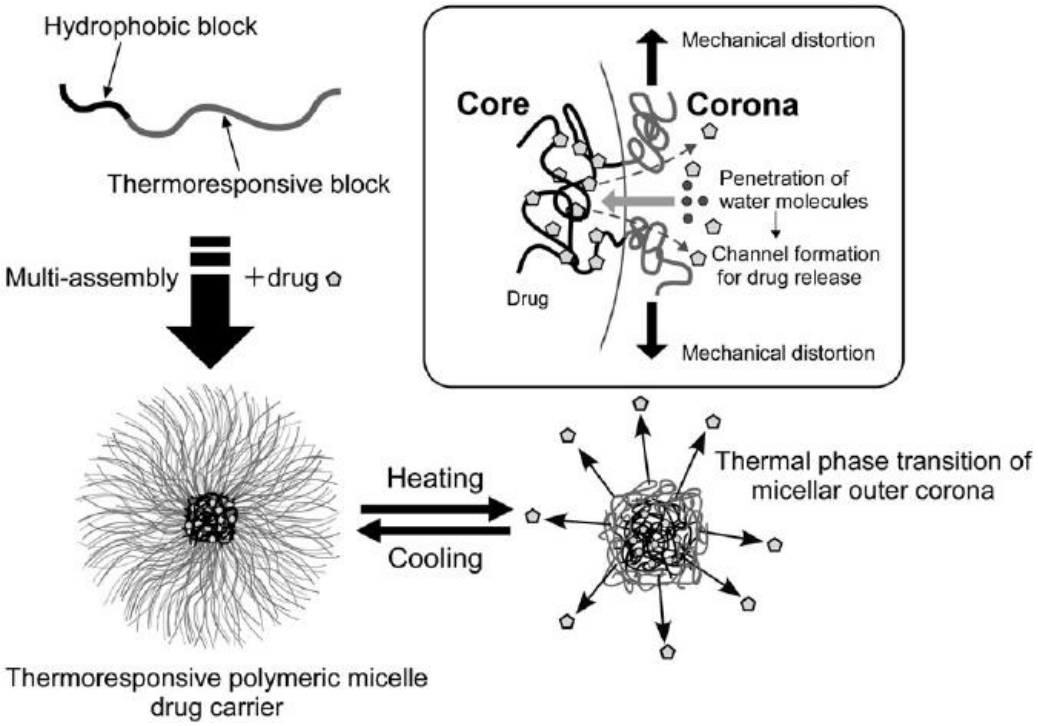


Figure 5-12: Schematic illustration of thermoresponsive polymeric micelle drug carrier system and drug release mechanism upon temperature increase. Image adapted from Nakayama *et al*.[630]

As shown in **Figure 5-12**, the formation of thermo-responsive polymeric micelles results from the assembly of block copolymers composed of a thermo-responsive block and a hydrophobic block. Drug molecules are incorporated into the hydrophobic inner core, and the thermo-responsive character is possessed by the outer shell of the polymeric micelles. When the temperature is below the phase-transition temperature of the thermoresponsive block, micelles are formed with a hydrated outer shell and hydrophobic inner core. As the temperature exceeds the phase-transition temperature, the outer shell shrinks and becomes more hydrophobic. Inter micellar aggregates may form on the basis of both a micelle

concentration and the strength of the shrunken outer shell layer's hydrophobic interactions and enhance the drug release.

For liposomes at 37°C, an initial relatively rapid release phase is observed (**Figure 5-13**) followed by a sustained release. That is, 70 % of PTX is released over 8 hours and release is then gradually slowed down until 87 % release is observed after 48 hours. A similar initial burst release phase followed by a sustained release profile was also reported by Ji *et al*.[441]

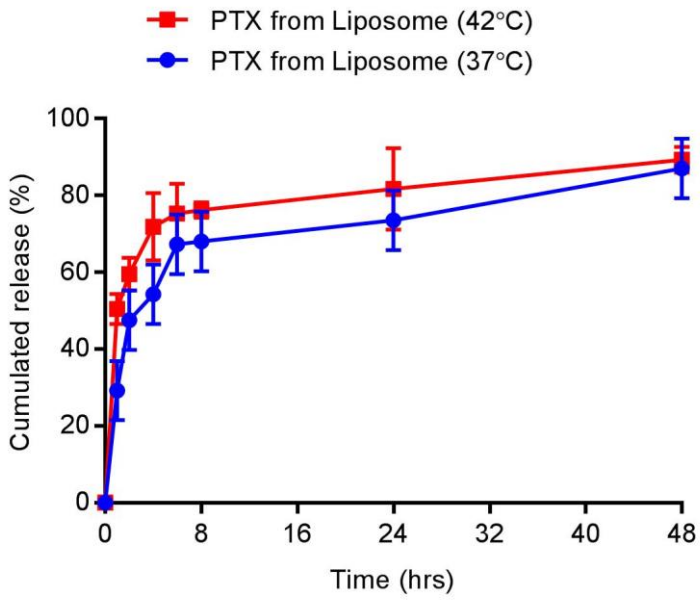


Figure 5-13: PTX release from PTX liposomes determined at 37°C and 42°C, respectively for 48 hours in sink conditions (PBS + 0.5% PEG 400). Each data represents the mean ± SD (n=3). Statistically significant ($p < 0.0134$) differences between the extent of drug release at elevated temperature 42 ° C and 37° C.

At elevated temperature (42°C), PTX also showed a faster release from the liposomes. Here 76.2% of PTX was released in the first 8 hours and release was then parallel with 37°C release and reached 81.7% after 24 hours. The drug release reached 90% over 48 hours. With an increased temperature from 37 to 42°C, an increased PTX release rate was observed (~5%) from 1 hours and continued to 24 hours and this difference was not significant at 48 hours. Elevated temperature increase the drug release rate from the liposomes (**Figure 5-13)**. From the Single Factor ANOVA data analysis it is found that a statistically significant ($p < 0.0134$) differences between the extent of drug release at elevated temperature 42 ° C and 37° C.

Literature also reports similar slow release with temperature-sensitive liposome formulations.[43, 327] Addition of the PEG in PTX-liposome covers the bilayer of the liposome forming a mushroom-brush boundary and slows the PTX release from the liposome bilayer. Similar PEGylation effects were also reported by Landon *et al.* and Kenworthy *et al.*[590, 632]

When the temperature of TSL's exceeds their Tm (Transition temperature), the phospholipid bilayer changes from a solid (ordered) gel phase to a liquid (disordered) crystalline phase, creating boundaries between the two phases through which the drug permeability is enhanced (**Figure 5-14**).[633] The existence of both solid and liquid lipid domains at the Tm leads to the formation of leaky regions at the interface between these domains. As a result, lipid membrane permeability increases. When the lipid membrane fully melts with further temperature increase, the membrane permeability is increased again as the lipid bilayer is predominantly in the fluid phase. Grain boundaries result from defects in the crystalline arrangement of lipid molecules in that region, through which the drug is released.[634]

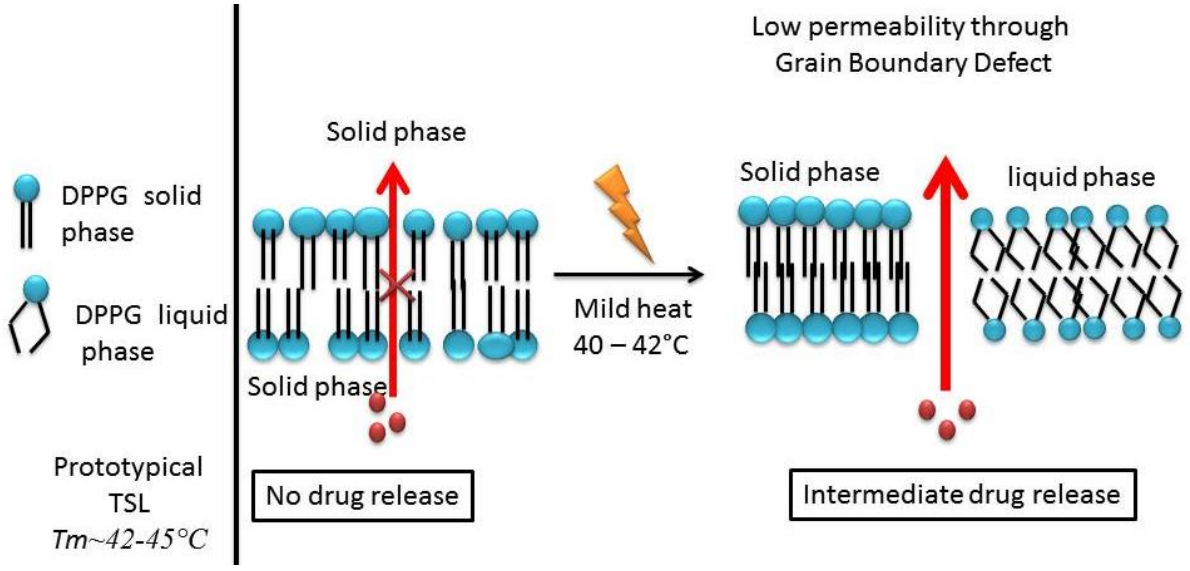


Figure 5-14: Schematic presentation of the phase transition behavior of TSL. When the lipid membrane passes through the transition temperature,[596] the bilayer permeability increases, while below that temperature, lipid membranes exist in solid phase only and therefore no drug release is expected. At the *Tm*, the existence of both the solid and the liquid phases leads to the formation of grain boundary defects in the bilayer through which drug release occurs. Image modified from Needham *et al.*[635]

For LMH (PTX release from micelles' core only) at 37°C, PTX showed a controlled release profile over 8 hours, reached PTX release of 33.1% and then gradually increased to 50% at 48 hours. At elevated temperature (42°C), PTX showed an enhanced release rate and 43.71%

of PTX was released in the first 8 hours and then 60% release after 24 hours. A gradual controlled release was observed at this temperature with a similar fashion of 37 ^{o}C and achieved 67% of PTX release at 48 hrs. With an increase in temperature from 37^{o}C to 42^{o}C an ~17% increase in the amount of PTX release was observed (**Figure 5-15**).

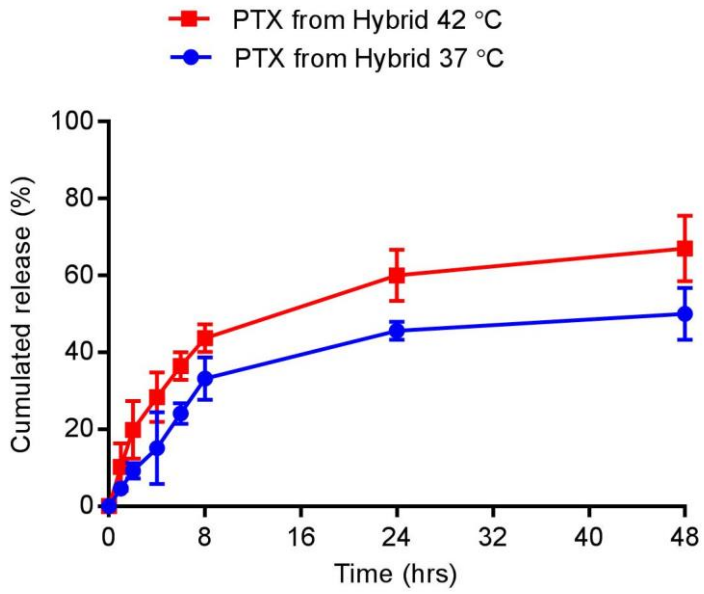


Figure 5-15: PTX release from LMH (PTX in micelles core) determined at 37 °C and 42 °C, respectively for 48 hours in sink condition (PBS + 0.5% PEG 400). Each data represents the mean ± SD (n=3). Statistically significant ($p < 8.2 \times 10^{-4}$) differences between the extent of drug release at elevated temperature 42° C and 37° C.

From the Single Factor ANOVA data analysis it is found that a statistically significant ($p < 8.2 \times 10^{-4}$) differences between the extent of drug release at elevated temperature 42 ° C and 37° C.

PTX is held in the core of the micelles and it has to pass from micelles' core (**Figure 5-16C**) through the lipid bilayer of the LMH; this retards the release of the PTX from internal micelles' core to the external release media. PTX faced greater obstacles to diffuse through the lipid bilayer acting as a physical barrier slowing drug release (**Figure 5-16 C**) in addition to the micellar environment. Therefore, in LMH, for the combination of the liposome and micelle barriers, provide better control of the release profile.

The LMH showed an obvious change in drug release profiles compared with liposomes and micelles which suggested that the modification of lipid vesicles with surfactants (insertion of

TPGS micelles into the structure of lipid bilayer) could affect the structure integrity and in vitro stability of lipid vesicles. Therefore, the different release of PTX from the micelles and liposomes is not entirely unexpected.

The release of PTX from the LMH can be as a simple diffusion-controlled drug release from the micelle or lipid bilayer which is described **in Figure 5-16 A and B**, Similar diffusion-controlled PTX release mechanism from liposome was also reported by Nie *et al*.[636] The total quantity of drug (100% of PTX) was not diffused out from the nanocarriers within the experimental period because of bigger hydrophobic PTX molecules trapped in network with a hydrophobic interaction. A similar hydrophobic interaction also reported by Sun *et al*.[637]

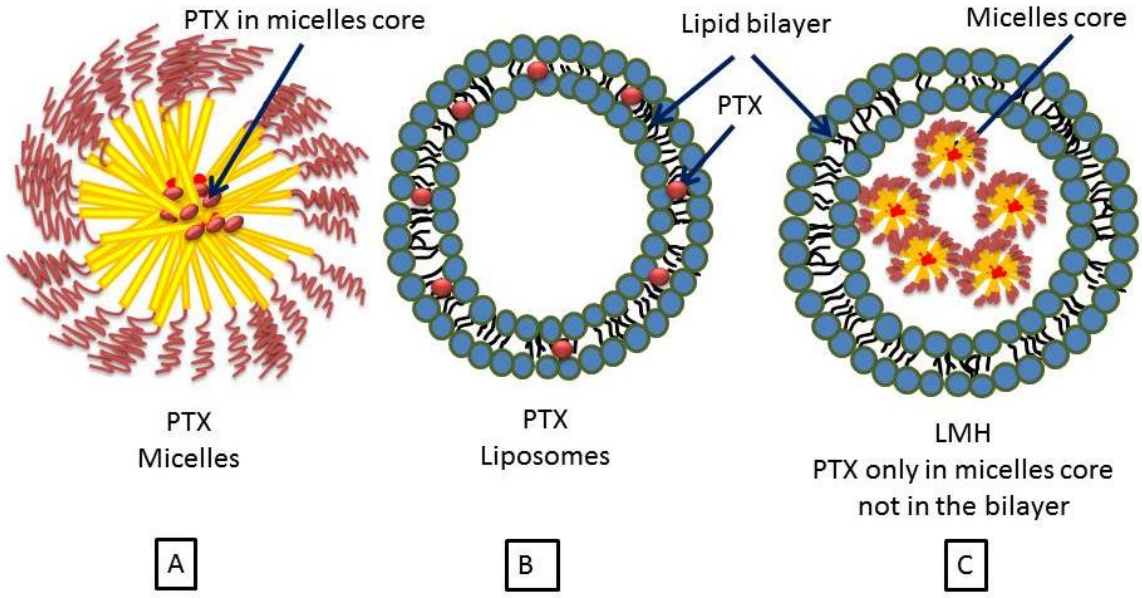


Figure 5-16: Schematic diagrams of drug release barriers from different carriers; A) PTX from micelles core, B) PTX from liposome bilayer and C) PTX from LMH (micelles' core only) drug not loaded in the bilayer.

5.6.6. Temperature-triggered release of PTX and 5-FU from PTX-5-FU-LMH and 5-FU from micelles

To further explore the controlled release of drug from the LMH system, we included another small drug molecule 5-FU into micelles' core of LMH keeping PTX in bilayer. The release of PTX and 5-FU from combination loaded LMH (PTX-5-FU-LMH) was then investigated in a similar dialysis procedure as discussed above, with two different temperature at 37°C and 42 °C and for 0-8 days.

For PTX-5-FU-LMH at 37°C the release of PTX (larger molecules with MW 854 g/M) from the bilayer of LMH showed very slow and control release characteristics and only 20% of PTX was released from LMH lipid bilayer after 24 hours (inset graph) and 45% release after 192 hours (8 days) **(Figure 5-17A)**.

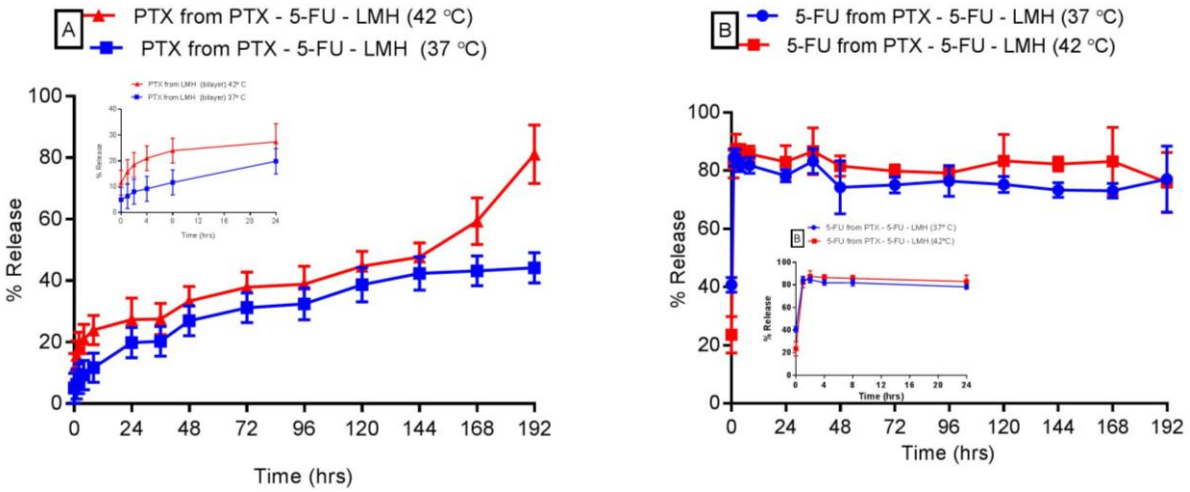


Figure 5-17: The % release of A) PTX from liposome bilayer of PTX-5-FU-LMH for 24 hours (inset graph) and 192 hours, statistically significant ($p < 9.1x\ 10^{-4}$) differences between the extent of PTX release at elevated temperature 42 ° C and 37° C and B) 5-FU from PTX-5-FU-LMH micelles for 24 hours (inset graph) and 192 hours at 37°C and 42°C in release media PBS + PEG-400 (0.5%) pH: 7.4). For 5-FU statistically significant ($p< 7.8\ x\ 10^{-6}$) differences between the extent of 5-FU release at elevated temperature 42° C and 37° C. Each data represents the (mean ± SD, n = 3).

At elevated temperature (42°C) PTX showed similar release kinetics to that at 37°C. However, the release amount was ~8% higher than at 37°C (inset graph) and continued until 144 hours with the same trend. After 144 hours, the release at elevated temperature was sharply deviated from the release of 37°C and reached to 81% at 192 hours which is 35% higher than the 37°C release **(Figure 5-17A)**. A spike in the release at the end of the experiment was appeared at the higher temperature due to a sharp decreased of bilayer stability or defects in the lipid bilayer as they became more hydrated for being a long time in the release media. This hydrated and deformed lipid bilayer increased the drug release sharply and make the spike in the release profile. A similar anomalous peak was reported by Garbuzenko *et al.* for a PEG-DSPE liposome at 48°C. The diameter and specific turbidity of

the liposomes decreased with increase in temperature and this effect was attributed mainly to the change in the spatial structure of the PEG-DSPE molecule as reported.[638]

It is noteworthy that the release of PTX from PTX-5-FU-LMH **(Figure 5-17)** was slow in comparison to that from PTX-LMH **(Figure 5-17,** at 48 hours**)** as described above. This is considered due to the structural changes due to encapsulation of 5-FU molecules in the LMH core that reduce PTX release. The encapsulation in of 5-FU in the core of the liposomes may responsible for changes in the dynamics of specific regions. These drug compounds affected the membrane hydration degree, ordered the lipid phosphate region and increased the disorder of the acyl chain methylenes. These physicochemical changes may effects LMH to reduce PTX release as reported in article.[639] Confocal microscopy also confirmed the structural changes due to encapsulation of drugs in the core of liposome.[640]

The release of 5-FU at 37°C from the inner core of PTX-5-FU-LMH was rapid, i.e. 85% released within 2 hours and it then remained in a steady state over 24 hours (**Figure 5-17B inset graph**). At 42°C 91% of 5-FU released in 96 hours, i.e. ~10% higher release than at 37°C **(Figure 5-17B inset graph)**. The temperature effect seem significant for PTX-5-FU-LMH.

The release of 5-FU from micelles at 37°C and 42°C (**Figure 5-18**, **inset graph**) fairly correlate with the release of 5-FU from the inner core of PTX-5-FU-LMH (**Figure 5-17B inset graph**). The drug release amount, rate and variation of the release of 5-FU from micelles at 37°C and 42°C temperature were very similar with the release from the inner core of PTX-5-FU-LMH except at 120 hours they mixed together to reach 100%.

The rapid release of 5-FU is due to its lower molecular weight and higher solubility compared to PTX (**Table 5-3); this** accounts for the increased release from LMH and micelles (compared to the PTX release data shown previously). The smaller molecule may more easily diffuse out from the micelle core and bilayer of LMH.

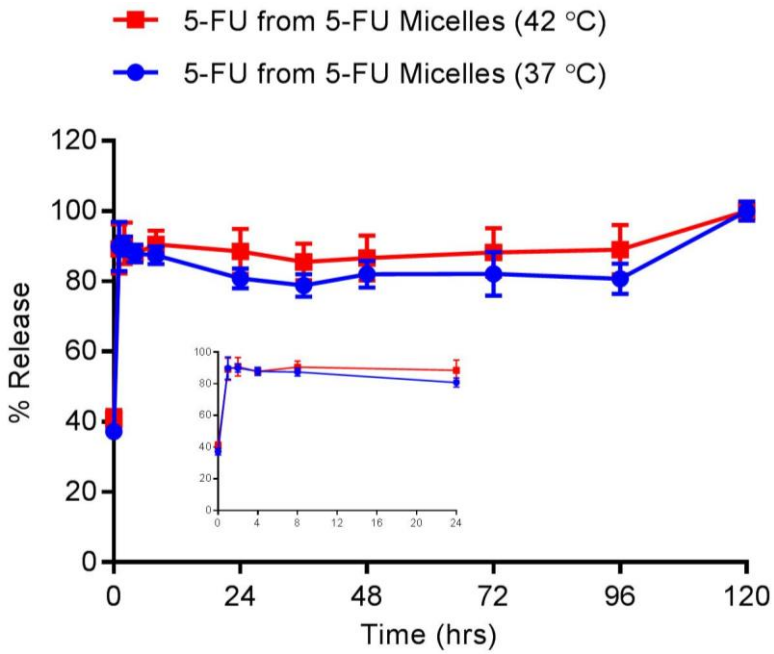


Figure 5-18: The release of 5-FU from micelles for 24 hours (inset graph) and 120 hours at 37°C and 42°C in release media (PBS + PEG-400 0.5% with pH 7.4). Each data represents the (mean ± SD, n = 3). A statistically significant ($p < 2.9 \times 10^{-6}$) differences between the extent of drug release at elevated temperature 42 ° C and 37° C.

5.6.7. Release kinetics of PTX and 5-FU from LMH

To further probe release mechanisms, the release kinetics data for PTX and 5-FU from the micelles, liposomes, and LMH (at 37ºC and 42ºC), were fitted with the Korsmeyer–Peppas[445] model as described in **equation (5-9).**

$$M_t/M_\infty = Kt^n \qquad \textit{equation (5-9)}$$

This model is generally used to describe drug release from polymeric systems where M_t/M_∞ is the fractional drug release (usually as %), K is a characteristic kinetic constant and n, an exponent coefficient that characterises the mechanism of release.

In order to elucidate more details of the release mechanism, the Korsmeyer-Peppas model can be extended to incorporate the diffusion coefficient (D) for the drug molecule in the nanocarrier matrix.[293, 453] **(equation 5-10)**

$$M_t/M_\infty = 4(Dt/\pi\lambda^2)^{1/2} \qquad \textit{equation 5-10}$$

Where *Dt* is the diffusion coefficient at time t, λ is the thickness of the nanocarriers

Drug release data were fitted to both **equations 5-9** and **5-10** using a custom-written non-linear regression code within the MATLAB programme (Appendix A). The resulting *D* from **equation 5-10** and exponent values (*n*) from **equation 5-9** are shown in **Tables 5-4**.

Table 5-4: The exponent value (*n*) used to characterise the drug release mechanism and the diffusion coefficient (*D*) for PTX, for its release from micelles, liposomes and LMH at temperatures 37ºC and 42ºC. The exponent value (*n*) and the diffusion coefficient (*D*) was obtained by non-linear fitting (MATLAB-R2017a) of the fractional drug (M_t/M_∞) release data (**Figure 5-10, Figure 5-13, and Figure 5-15**) to **equation 5-9** as a function of time over 48 hours.

Nanocarrier Type	**37°C**		**42°C**	
	n	*D* (m^2/s) x 10^{-10}	*n*	*D* (m^2/s) x10^{-10}
LMH (PTX in micelles' core)	0.433	0.599	0.36	1.14
LMH (PTX in bilayer)	0.408	0.104	0.357	0.196
Liposome	0.204	1.49	Non-fit	Non-fit
Micelle	0.205	2.34	Non-fit	Non-fit

According to Korsmeyer and Peppas, a value for *n* less than 0.5 suggests that the overall solution-diffusion mechanism is Fickian[445] (**Table 5-5)**.

Table 5-5: The relationship between the diffusion exponent (*n*) and the solute (drug) release mechanism.[445]

Diffusion exponent (*n*)	**Overall solute diffusion mechanism**
$n \leq 0.50$	Fickian diffusion
$0.50 < n < 1.0$	Anomalous (non-Fickian) diffusion
1.0	Case II transport/zero-order release
$n > 1.0$	Super case II transport

Here, the results showed that the *n* is < 0.5 for the PTX in nanocarriers at 37ºC. This is applicable for LMH core and bilayer at 42ºC, suggesting the mechanism of the PTX release from nanocarriers was Fickian diffusion **(Table 5-5)**. This mechanism is likely due to the formation of a potential chemical gradient. The release data of PTX from micelles and liposomes at 42ºC and 5-FU are not well fitted by the model because of burst release. The *D* value for PTX micelles, liposomes and LMH at 37ºC and 42ºC is summarised in **Figure 5-19.**

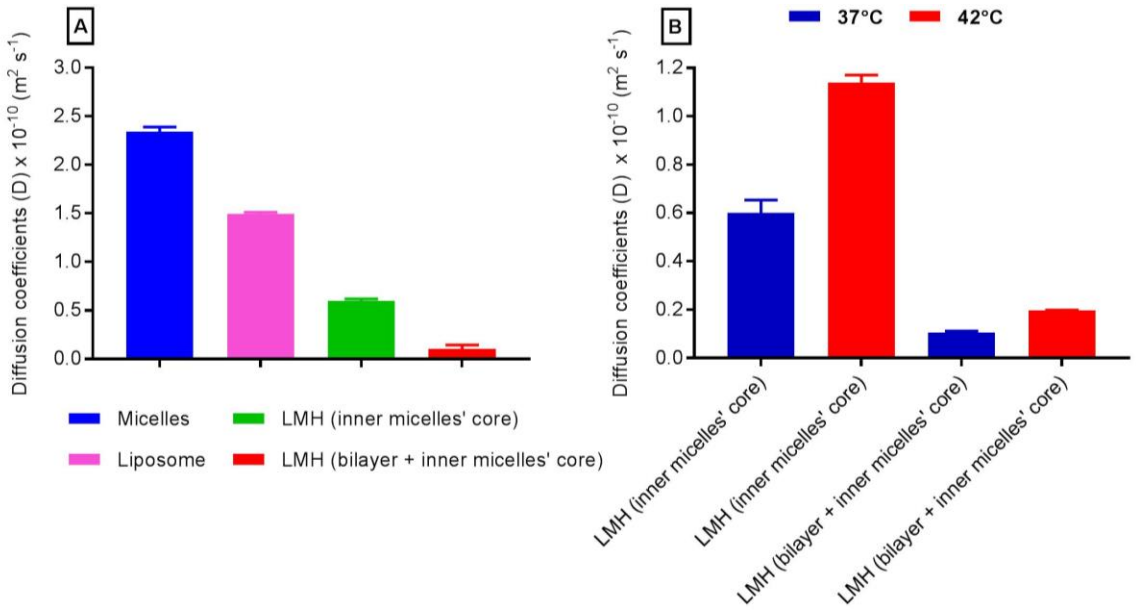


Figure 5-19: Calculated diffusion coefficient values (*D*) from **equation (5-10)** for PTX from A) micelles, liposomes, LMH inner micelles' core, and both LMH bilayer and inner micelles' core at 37ºC and B) inner micelles' core of LMH and both lipid bilayer and inner micelles' core of LMH at temperatures 37ºC and 42ºC. A statistically significant ($p < 4.7 \times 10^{-13}$) differences of diffusion coefficient between the micelles, liposome and LMH (micelles core and bilayer). A statistically significant ($p < 6.3 \times 10^{-13}$) differences of diffusion coefficient between the PTX release kinetics from LMH (bilayer) at different temperatures 42°C and 37°C.

The calculated diffusion coefficient (*D*) for PTX was getting lower from micelles to LMH at 37ºC **(Figure 5-19A)** which is likely correlated with their release kinetics. For micelles, *D* was higher as drug passes easily through the network of micelles. However, for liposome, this is lower than micelles as it has to pass the double layer of the liposome makes their rate of diffusion slow. Similarly, the *D* value of PTX from micelles'core of the LMH was further decreased in compared to the micelles and liposome as it has to pass both the micelles' core and a bilayer of the LMH. However, the drug in the bilayer of LMH released slowly compared to others, therefore their diffusion coefficient *D* value is minimum. This may be explained by blocking the diffusion channel of the bilayer of LMH by some of the TPGS polymers.

The relative change of diffusion coefficient *D* in different temperature appear to correlate well with their release; the higher temperature, the greater diffusion coefficient **(Figure 5-19B)**.Temperature also affects the diffusion rate of the PTX from the nanocarriers. The higher the temperature, the greater the *D* value from micelles and LMH. The changes with temperature can be explained according to kinetic theory (e.g. the Einstein relationship:

Diffusion = mobility x Boltzmann's constant x absolute temperature), the diffusion of particles (Brownian motion) correlates directly to temperature (T in Kelvin).[641]

From one-way ANOVA analysis a statistically significant ($p < 4.7 \times 10^{-13}$) differences of diffusion coefficient between the micelles, liposome and LMH (micelles core and bilayer) and a statistically significant ($p < 6.3 \times 10^{-13}$) differences of diffusion coefficient between the PTX release kinetics from LMH (bilayer) at different temperatures 42°C and 37°C. The post-hoc-corrected t-tests analysis reports as "true'' for micelles compared to liposome, H-core and H-bilayer implies that there is 95% of chance of difference between micelles, liposome, H-core and H-bilayer. The release kinetics of PTX is significantly higher for micelles compared to liposomes and LMH (H-core and H-bilayer).

5.6.8. Assessment of cytotoxicity

To evaluate the cytotoxicity of PTX encapsulated micelles, liposomes, LMH and free PTX against tumor cells (human cervical adenocarcinoma (HeLa) cells), a standard cell viability assay was utilised. Cell viability was investigated for 4 hours using the Alamar Blue assay in the presence of a range of PTX concentrations from 1-30 μg/mL in loaded nanocarriers **(Figure 5-20A, B, and C)**.

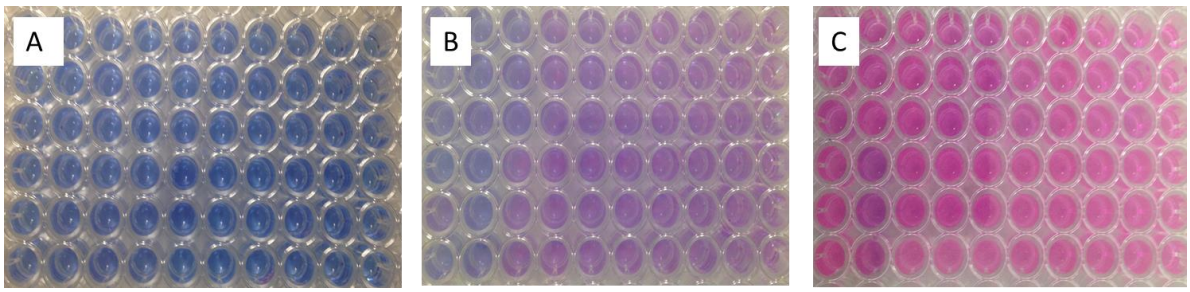


Figure 5-20: Hela cells treatment of 96-well plate, A) initial image after Alamar blue treatment, B) image after 2 hours and C) 4 hours.

For PTX loaded micelles, initially both loaded micelles and free PTX show similar toxicity and 60% of the cells survived. However, at a higher concentration (25-30 μg/mL) greater toxicity of PTX micelles was observed which is similar to free PTX.

Liposomes showed an enhanced cytotoxic effect in comparison to micelles and cell viability was ~ 40%. However, the PTX-LMH formulation exhibited superior toxicity than micelles and liposomes, i.e. 30% of cells survived in the lower concentration range (0.5-8.0 µg/mL). Most importantly, cell viability is gradually reduced to close to zero at the maximum concentration investigated (i.e. 30µg/mL), which demonstrated the dominant chemotherapeutic efficacy of LMH compared to micelles, liposomes and free PTX (**Figure 5-21C)**.

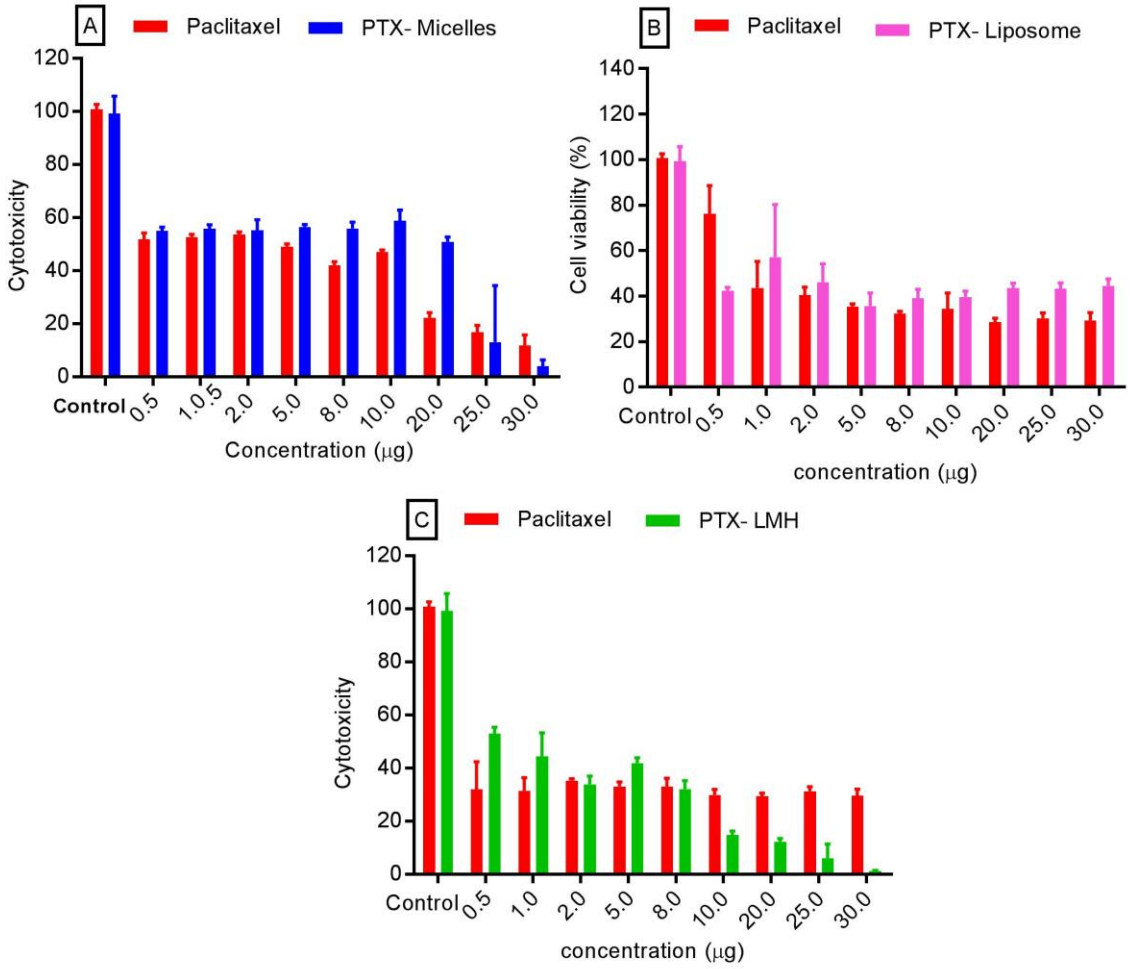


Figure 5-21: The effect of (A) free PTX and PTX- micelles B) free PTX and PTX-liposome and C) free PTX and PTX-LMH on cells viability using HeLa cell lines after 4 hours of treatment (mean ± SD, n = 4), three different 96 well plates are cultured for different nanocarriers formulations separately with the control free PTX. A statistically significant ($p < 0.048$) difference between free PTX and nanocarriers.

Statistical analysis was performed on this cytotoxic data via one way ANOVA analysis (n =3) comparing the observed changes between the three nanocarriers and free drug analysed

as a function of time. The ANOVA results confirm a statistically significant difference (p < 0.048) in cell viability upon treatment with nanocarriers compared to free drug within a 4 hour period. The post-hoc-corrected t-tests analysis reports as "false'' for micelles vs liposome and true for liposome vs hybrid implies that there is no significant difference between micelles and liposome. However for liposome vs hybrid implies that there is 95% of chance of difference between liposome and hybrid. The cytotoxicity of micelles is significantly different from liposome yet it is significantly lower for hybrid compared to micelles.

5.6.9. Measurements of permeation co-efficient or apparent permeability

Prior to permeability studies, the Caco-2 cells were cultured in 24-well plates and the TEER values were measured to ensure the development of a suitable cell monolayer over 21 days. The control TEER value was taken from the media (DMEM + FBS-10%) without cells, it was < 200 Ω cm^2 and remained constant for the duration of the experiment. The average TEER value in a Caco2-cell monolayer (CCM) containing media was found to be 1036 ± 327 Ω cm^2 on the 14th day and 1363 ± 262 Ω cm^2 on the 21st day (see **Figure 5-22**).

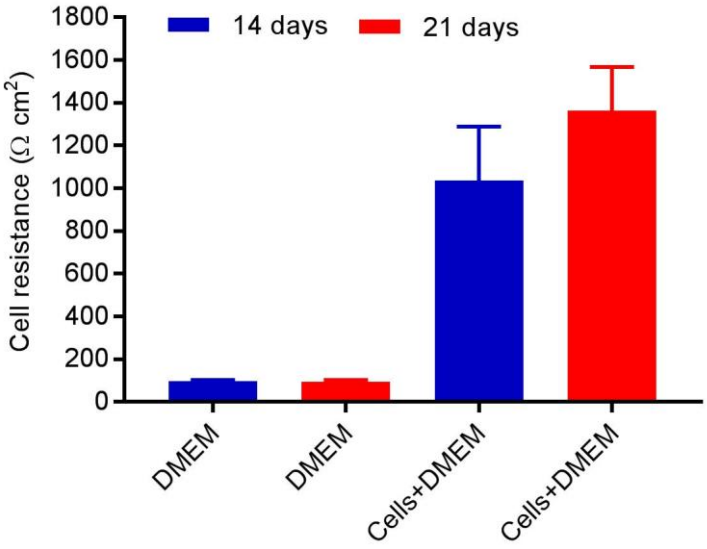


Figure 5-22: Resistance of Caco-2 Cell monolayers (CCM) measured on the 14th day and 21st day (2 days) of monolayer formation in DMEM control media. The data are presented as mean ± SD (n = 4).

These findings indicated the cells were growing and a complete monolayer was developed by 14 days. All the TEER values were persistently above 305 Ω cm^2, indicating the integrity of the cell monolayers, as 305 Ω cm^2 is the minimum limit reported previously.[504-507]

The TEER across a CCM typically increases with culture time,[642] reaching a maximum after about 10-15 days,[497] such cultures express less well-differentiated features,[643] and a few reports suggest the requirement of 21-24 days for formation of all involved transporters.[505-507] Therefore, in the current study, permeability study was performed on day 21 of the cultured monolayer formation, as reported most of the literature.[489, 499]

Firstly, after sample treatment, the TEER values were measured at the start (0 minute) and the end of the permeation study (120 minutes) in the presence of PTX loaded micelles, liposomes and LMH as well as the free PTX solutions. Each of the nanocarriers and free PTX sample contains 100 µM of PTX. The TEER values with Caco-2 cell monolayers at the start of the test ranged from 330 to 1452 Ω cm^2 (after background resistance was subtracted) in HBSS buffer. At the end of the permeation studies, these values ranged from 347 to1382 Ω cm^2 which indicates intact cell monolayers as reported previously.[489] The TEER values decreased immediately after addition of PTX-loaded micelles, liposomes, LMH, and free PTX, as described in **Figure 5-23**.

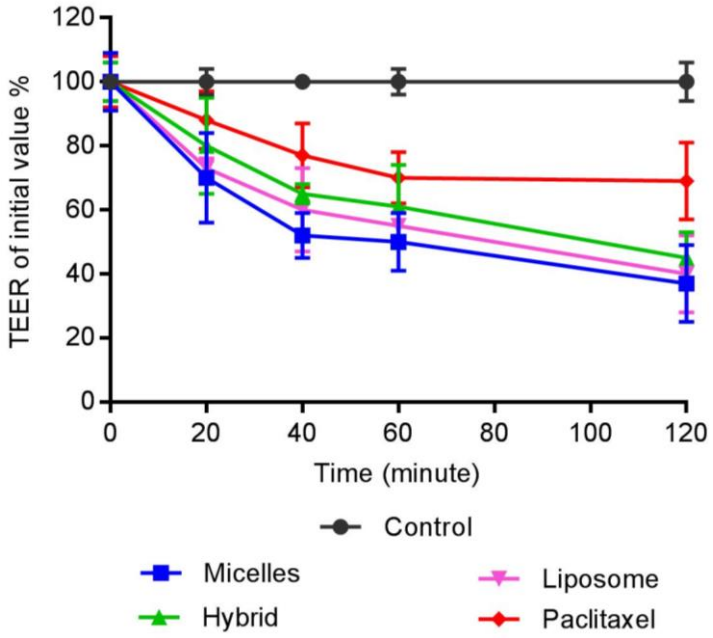


Figure 5-23: Effect of 100 µM PTX encapsulated LMH, liposome, micelles and free PTX on the TEER in Caco-2 cell monolayers (21 days old) in HBSS over 2 hours of the treatment period. Control without treatment (Cells with buffer only). The data are presented as mean ± SD (n = 4).

The average TEER values with Caco-2 cell monolayers at the start of the test (0 minutes) for the micelles, liposome, LMH, and PTX were 836 ± 611 Ω cm^2, 1331 ± 65 Ω cm^2, 754 ± 622 Ω cm^2 and 1154 ± 419 Ω cm^2 (after background resistance subtracted) in HBSS buffer. At the end of the permeation studies, the values decreased to 381 ± 69 Ω cm^2, 718 ± 369 Ω cm^2, 736 ± 367 Ω cm^2 and 660 ± 476 Ω cm^2. After 2 hours of treatment, the TEER values of Caco-2 cell monolayers decreased in presence of PTX in micelles, liposome, and LMH, and free PTX by 37 %, 40 %, 45 % and 69 % of the initial value, respectively. In compared to free PTX, this reduction from an initial value is 1.8-fold, 1.7-fold, and 1.53-fold higher for micelles, liposome, and LMH respectively. From this drop in resistance, we concluded that the nanocarriers were able to open the tight junction of the Caco-2 cells. After 40 minutes a slow decrease of TEER was observed which indicates a transient recovery of the tight junctions.[492] As shown in **Figure 5-23,** the incubation of PTX-nanocarriers on the apical side of Caco-2 cell monolayers led to the immediate reduction in TEER, which might be attributed to the effect of nanocarriers on the tight junctions (TJs). This indicates that the micelles, liposomes, and LMH used here were able to open the TJs[508] and increase paracellular permeability of PTX through the TJs.[474, 498, 509]

A similar reduction of TEER values has also been reported in **Chapter 4** for LOV**.** These findings demonstrated that all of the nanocarriers could transiently open the tight junctions between Caco-2 cells and enhance the possibility of paracellular permeability as described earlier in **Chapter 4**. The findings here correlate well with similar decreased TEER values published in the literature for liposomes[306, 505] and micelles.[68] Vander Merwe *et al*. reported N-trimethyl chitosan chloride, a polymer showed a pronounced reduction in the TEER in *in vitro* studies performed on Caco-2 cell monolayers and transport via the paracellular route was confirmed by confocal laser scanning microscopy.[498] The TJs serve as a barrier to paracellular diffusion and measurement of TEER is a good indication of the tightness of the junctions between epithelial cells.[644]

The TEER reduction was similar for all nanocarriers though slightly higher for the TPGS micelles. However, here it is observed that the Pegylated DSPG: PC: DPPG liposome and

TS-LMH showed a slower reduction of TEER values (40 % and 45 %) in comparison to DSPG: PC liposome and LMH (33% and 42 % in **chapter 4**) as shown in **Figure 5-23**. It is assumed that PEGylation prohibited the TEER reduction that resulted in less ability to open the TJ compared to non-Pegylated liposomes and LMH.

The permeation coefficient or apparent permeability (P_{app}) was quantified by the bidirectional transport of PTX across the CCM; this is dependent on the carrier system (micelles, liposomes, LMH and PTX solution). The transepithelial fluxes of 100 µM of PTX across CCMs at 37°C in the absorptive (apical-to-basolateral; A→B) and secretory (basolateral-to-apical; B→A) directions versus time of incubation in the presence of micelles, liposomes, and LMH were assessed **(Figure 5-24)**.

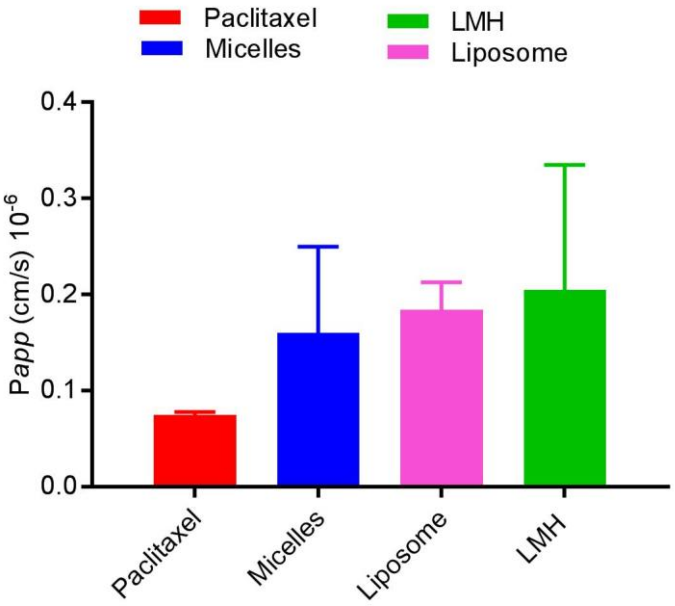


Figure 5-24: The B→A fluxes of PTX and PTX loaded nanocarriers (100 µM) were determined at pH 7.4 as a function of time (2 hours at 37°C). Each point represents the mean (4 S.E.M.) of 4 determinations (CCM). The P*app* values, expressed in centimeters per second. A statistically significant difference ($p < 5.98 \times 10^{-7}$) among the free PTX and nanocarriers.

The B→A permeability is higher for the nanocarriers than for free PTX, which indicates the nanocarriers are helping to improve the PTX uptake by Caco-2 cells. Similar results were found in **Chapter 4.** The A→B permeability was not able to be determined here as the concentration present in the permeation samples were below the quantification limits for the HPLC analysis method used for PTX (data not shown). This data showed that very little of

the drug is permeating A-B. When the permeability samples were analyzed there was no peak found in the HPLC analysis.

The permeability enhancement compared to free PTX (as a control) was calculated from the P_{app} measured in the B→A direction of the individual nanocarriers divided by the P_{app} of the PTX (as a control) **Table 5-6**. These results indicate a significant enhancement of PTX permeability for B→A direction for micelles, liposome and LMH in compared to free PTX. The P_{app} value for the B→A transport of PTX in CCM was 2.13-fold, 2.4-fold and 2.6-fold higher in micelles, liposome, and LMH in comparison to free PTX (**Table 5-6**).

Table 5-6: Parameters from permeability assay of PTX through CCM using different carriers

Test compound type (each contains 100 µM PTX)	**P*app* (cm/s) x 10^{-6} mean ± SD**	**Permeability enhancement compared to free PTX (fold)**
	Absorptive (B-A) direction	
Free-PTX (as a control)	0.075 ± 0.28	-
Micelles	0.16 ± 0.90	2.13
Liposome	0.18 ± 0.29	2.4
LMH	0.20 ± 1.3	2.6

* P_{app} values are expressed as the means ± S.D. (x10^{-6}, cm/s); n =3

Statistical analysis was performed on the B-A permeability data via one way ANOVA analysis (n=3) comparing the observed changes between the three nanocarriers and free drug. The ANOVA results suggest a statistically significant difference ($p < 5.98 \times 10^{-7}$) in cell permeability between the nanocarriers and free drug within 2 hours period. This implies that there is 95% of chance of difference between LMH and liposome. The post-hoc-corrected t-tests analysis reports as "true'' for micelles, liposome and LMH compared to free PTX implies that the permeability of PTX is significantly lower for micelles, liposomes and LMH compared to free PTX.

5.6.10. Evaluation of the Caco-2 cell monolayer integrity using Lucifer yellow

After permeability experiments, evaluation of permeability characteristics of Caco-2 cell monolayers can be performed by measuring the passive passage of different molecules across the monolayer. The Lucifer yellow (LY) assay was performed after the permeability assay (after two hours) described above. After each Caco-2 monolayer sample treatment, the LY permeability (% Permeability) assay was performed for each membrane. LY (%)

permeability tests were undertaken at the same concentration as the drug used (i.e. 100 µM in HBSS, as has been reported previously).[306, 530]

The percent permeability of LY for micelles, liposome, and free PTX are 0.43 ± 0.26 %, 0.30 ± 0.005 %, 0.29 ± 0.1% and 0.79 ± 0.02 % which was more than 20-fold higher for the nanocarriers compared to the control (cells only) (**Figure 5-25**). It is noted that free PTX showed a greater increase of LY permeability due to deterioration of the cell monolayer with direct exposure of PTX.

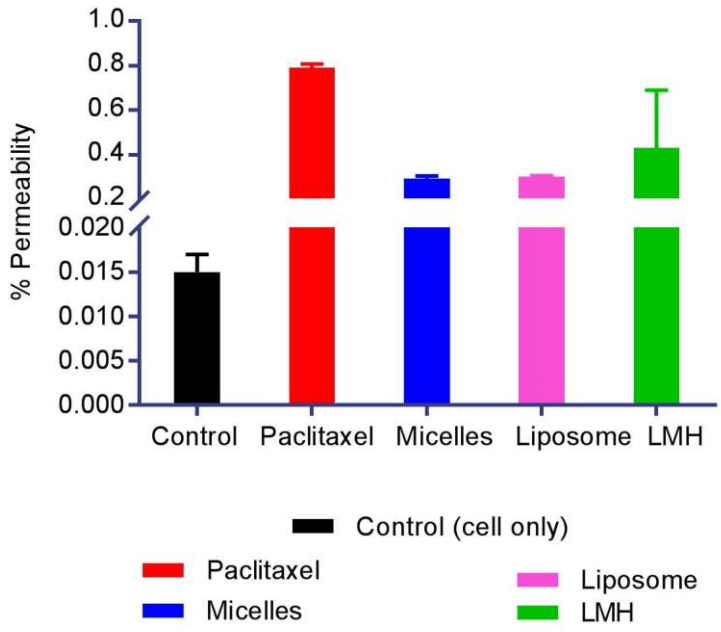


Figure 5-25: Percent permeability of LY (100 µM) from A→B; added to the apical chamber of CCM treated with 100 µM PTX and 100 µM PTX incorporated into each nanocarrier; micelles, liposomes, and LMH; were incubated for 1-hour with 100 µM LY. After 1-hour samples were collected from the basal chamber. Here the control was only the cells. LY was measured by fluorescence intensity at excitation and emission wavelengths of 485 and 520 nm, respectively. Results are means ± SD (n = 4). A statistically significant ($P < 0.000767$) difference between control, PTX and nanocarriers.

The average LY P_{app} value was 0.34 ± 0.08, which is close to the reported value of 0.3 %,[645] that indicates the cell monolayer has sufficiently developed its tight junctions for reliable permeability assays.[645]

From the Single Factor ANOVA data analysis it is found that a statistically significant ($p < 0.000767$) differences within control, PTX and nanocarriers permeability. The post- hoc-

corrected t-tests analysis reports as "true'' for micelles, liposome and LMH compared to free PTX implies that there is 95% of chance of difference between LMH and liposome. The LY permeability of PTX is significantly lower for micelles, liposomes and LMH compared to free PTX.

5.6.11. Transport studies of PTX with different nanocarriers (micelles, liposome, and LMH) in the apical-to-basolateral (A→B) direction

To assess the capability of PTX-nanocarriers to enhance PTX transport, Caco-2 monolayers were treated for 24 hours with PTX and PTX encapsulated in micelles, liposome and LMH containing 100 µM of PTX, and the results are shown in **Figure 5-26**.

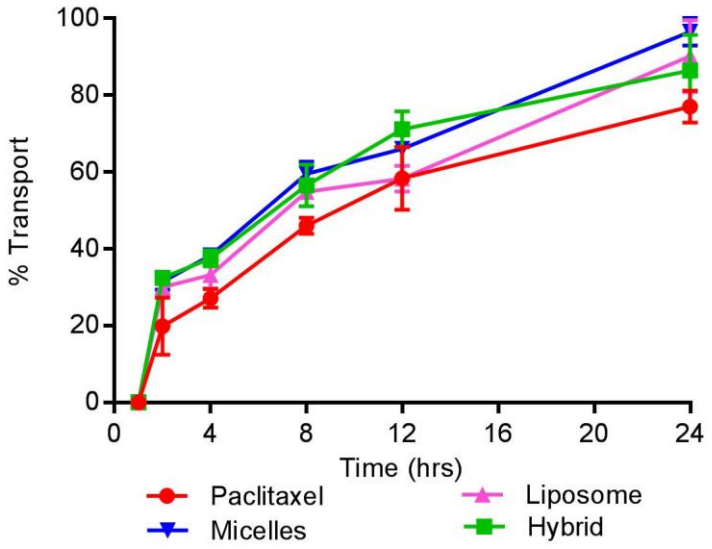


Figure 5-26: PTX transported across Caco-2 monolayers after 24 hours of incubation in the A→B direction at 37°C in the presence of micelles, liposome, and LMH containing 100 µM of PTX and PTX 100 µM, expressed as a percentage of the initial concentration of 100 µM PTX, added to the apical compartment, as a function of time, mean ± SD (n=4). A statistically significant ($p < 0.000729$) difference between PTX and nanocarriers was found.

Monitoring the transport of PTX across Caco-2 cell monolayers, after 24 hours of incubation time, the A→B permeability of PTX loaded in micelles, liposomes, and LMH increased 1.25, 1.17, and 1.12-fold higher compared to free PTX. PTX transport increased more than one fold higher by; micelles, liposomes, and LMH. In all cases, the transport increased gradually

with respect to incubation time. It is noticeable that for the PTX containing nanocarriers transport was higher than for free PTX and LMH transport was most effective over 16 hours.

The transport of pegylated DPPG: DSPG: PC showed the controlled manner in compared to the transport of DSPG: PC liposome and LMH **(biphasic** behaviour, **Chapter 4)**. We assumed that the controlled release was due to the presence of PEG in the PTX-formulations as PEGylation increased the PTX release compared to the non-PEGylated liposome reported by Yoshizawa *et al*.[557]

Although the precise mechanism of transport remains unclear at this point, evidence also suggests that the transport of PTX could be mediated by a variety of membrane transporters and P-gp efflux has been widely reported.[646-647] From the Single Factor ANOVA data analysis it is found that a statistically significant ($p < 0.000729$) differences between PTX and nano-carriers. The post-hoc-corrected t-tests analysis reports as "true'' for micelles, liposome and LMH compared to free PTX implies that there is 95% of chance of difference between LMH and liposome. The transport of free PTX was significantly lower compared to PTX-nanocarriers.

5.7. Conclusion

Developing a suitable carrier system for the chemotherapy drug PTX has proved to be a challenge and the commercially available solution dosage form of PTX remains far from ideal due to toxicities resulting from the existing formulations. Therefore, novel temperature-sensitive LMH system for PTX (PTX-TSH) and 5-FU (5-FU-TSH) were developed. The average particle diameter of PTX loaded LMH, liposome and micelles were found within range with optimum particle size distribution and higher stability was observed. Significant amounts of drug was loaded into the LMH, where, PTX loading in LMH increased its solubility by 204-fold higher in comparison with pure PTX. Loading in LMH was also 2.79 and 1.30-fold higher in comparison with micelles and liposomes, respectively. Similar enhancement of loading was also observed for 5-FU. The microscopic structure of the PTX TS-LMH was observed to be roughly spherical in shape with hair-like projections on the surface (PEG coating around the LMH offers improved adhesion properties and may also impact on targeting, cellular uptake, transport, and degradation).

Release of PTX and 5-FU from loaded nanocarriers exhibited thermoresponsive characteristics at 42 °C i.e. ~5-20% greater release than at body temperature. The PTX showed controlled released characteristics in LMH and liposomes, while the 5-FU exhibited burst release properties either from micelles or micelles in the core of LMH. The PTX nanocarriers follow Fickian diffusion release mechanism which governed by the potential drug concentration gradient between the reserver and release media.

Moreover, it has been demonstrated by clinical oncologists that to achieve the maximal anticancer effect, therapies that hit as many potential targets or pathways as possible are desirable because cancer cells are a population of highly heterogeneous cells. Co-delivery of anticancer agents enables an early detection of drug response or resistance and an early evaluation of benefit/risk ratio of the current therapy which makes prompt regimen adjustment and individualized medication possible.

The PTX loaded LMH particles showed better cellular activity against HeLa cells compared to liposomes and micelles. A significant increase in the permeability and transport of PTX was observed in Caco-2 cell monolayers in the presence of PEG and DPPG when compared to the LOV-LMH. The paracellular permeability of PTX was enhanced by 2.6-fold, 2.4-fold and 2.13-fold for LMH, liposomes, and micelles, respectively. Transport of PTX across Caco-2 cell monolayers was also observed slow and controlled fashion, over a longer period of time (for 24 hours) which is differed from the previous LMH system (biphasic for 8 hours) due to the PEGylation.

Finally, LMH containing high PTX concentrations inside the lipid bilayer and in the inner aqueous core demonstrated improved and controlled drug release ability at elevated temperature. LMH is potentially better options for delivery of PTX as they can minimize detrimental toxicities while enhancing the therapeutic efficacy. Based on these results, it can be concluded that the formulations developed in this work may be considered as effective anticancer drug delivery systems for cancer chemotherapy.

Chapter Six

6. Conclusions and Future Direction

6.1. Summary of research findings

The principal objective of this thesis was to improve the solubility of insoluble drugs by designing and constructing hybrid nanoparticles through the combination of liposomes and micelles for improved drug delivery and to overcome current challenges with liposome and micelle-based delivery systems. The investigations focused on loading and release of the widely-used cardiovascular drug lovastatin (LOV) in liposome-micelle hybrid (LMH) systems. Also, the anticancer drugs paclitaxel (PTX) and 5-fluorouracil (5-FU, a sparingly water-soluble drug) were used to evaluate temperature sensitive release in hyperthermia of the thermoresponsive liposome-micelle hybrid (TS-LMH). Systemic investigations were undertaken in this research to reveal a number of advantages offered by the novel LMH

formulations. These studies and results have enabled us to gain further understanding of the mechanism of LMH formation, physical and microscopic characterisatics and cellular activities of LMH nanoparticles. This knowledge can be translated into further applications to improve the oral bioavailability of poorly water-soluble and lipophilic bioactives and other new delivery approaches through other administration routes. In terms of advancing the knowledge on the drug delivery properties of LMH, several milestones are worth highlighting in this thesis.

6.1.1. Liposome-micelles-hybrid system for oral delivery of poorly water-soluble drugs

For LMH system development and optimisation, the micelles were based on polymers and surfactants that are widely used for drug delivery, including poloxamer 407, poloxamer 188, deoxycholate, d-α-tocopherol polyethylene glycol 1000 succinate (vitamin E, or TPGS). Their physical characteristics and influence of their chemical structure on the drug loading was rationalised. The loading of LOV within TGPS micelles was found to be higher (2.05 % w/w) comparable to other micellar system with an acceptable appearance (clear), and stable diameter and drug content over 3 months. Liposomes were also developed using different lipids: including; phosphatidylcholine (PC), cholesterol (CHO) and distearoyl phosphatidyl glycerol-Na (DSPG) to optimise their physical properties and drug loading. Initially, PC/CHO liposomes were prepared and found to be unstable due to their low negative charge. Incorporation of another lipid (DSPG) to make DSPG/PC/CHO liposomes increased the negative charge and improved their stability properties.

LMH systems were prepared by combining micelles and liposomes using three different liposome preparation methods, i.e. thin film hydration, reverse phase evaporation and freeze-thawing. The extent of LOV loading in the LMH systems was dependent on the method of preparation and in general, reverse phase evaporation increased LOV loading in comparison with the other methods. Importantly, LOV loading in LMH was significantly enhanced compared to the loading levels for individual liposome or micelle formulations.

In current study, we didn't formulate poloxamer micelle-liposome hybrids, but rather TPGS micelles-liposome hybrids. It is reported that polymeric micelles may be adsorbed on the surface of liposomes. This would influence the way the drug is associated with the carrier, i.e. either encapsulation inside or adsorbed on its surface.[648] Here, it was observed that the TPGS/polymer micelles encapsulated mostly inside the liposome carrier (confirm from

CryTEM). However, to remove free micelles, we used high-speed ultra-centrifugation (32000 rpm 4 hours) so that free micelles migrate into the supernatant, as they are hydrophilic and too small to undergo centrifugation.[649] Nevertheless, there may be some surface-bound encapsulated micelles present which were not possible to remove by ultracentrifugation. These would require a dialysis or column separation step to remove them, but this was not desirable in the current study.

The LMH system with an average particle size of ~200 nm, a low polydispersity and highly negative zeta-potential value was stable against aggregation. Cryo-TEM images of LMH (PC: CHO: DSPG-TPGS) confirmed a spherical shaped morphology surrounded by a thin lipid bilayer (unilamellar) with worm-like/spherical micelles within the inner aqueous core; these were not observed for empty liposomes. LOV loading in LMH increased its solubility by 166-fold in comparison with pure crystalline drug and it was 3.32 and 1.32-fold higher in comparison of micelles and liposomes. Moreover, LMH systems exhibited controlled release characteristics compared to the individual liposomes and micelles.
The physicochemical stability of LMH was investigated at different pH values (2 to 6) and pH 5 was found to be optimum to retain their physical properties and active drug content. For LMH stored for 3 months at pH 5 and 4 °C the size and zeta potential were stable.

6.1.2. Cell permeability, transportation and cell viability studies of lovastatin loaded liposome-micelle-hybrid system

The success of a nanocarrier-based therapy depends largely on its behaviour in the tissue microenvironment and the nature of interactions with cells forming the tissue; these control properties such as distribution and bioavailability.

In Caco-2 cell monolayer model studies, LOV-LMH and liposomes were more rapidly and effectively up taken by intestinal epithelial cells than micelles; this is considered via a paracellular route. The apparent permeability (*Papp*) of the LMH carriers for the basolateral-apical (B-A) direction was higher than for the apical-to-basolateral (A-B) direction; this demonstrated LMH significantly enhances the permeability of LOV in the former direction compared to micelles and liposomes. Initially, the recorded standard TEER values indicated good cellular integrity, which was decreased significantly by the treatment of LMH, demonstrating greater permeability across the monolayer of the cells than liposome and micelles. Monitoring the transport across cell monolayers, after 8 hours of incubation time,

the LMH increased LOV transport approximately 2-fold compared to free LOV. The observed transport kinetics of the LOV-LMH was biphasic, i.e. slow for 2 hours but then gradually increased over 8 hours' time. The results highlight the significance of the LMH nature on cells for intracellular trafficking of poorly soluble drugs and could open an innovative avenue for the oral delivery of the poorly water-soluble drug LOV.

6.1.3. Development of a temperature sensitive liposome-micelle-hybrid system for anticancer drugs

A temperature sensitive liposome-micelle hybrid (TS-LMH) system was developed to enable controlled release of encapsulated anticancer drugs at an elevated temperature. Initially, only PTX was encapsulated into both the micelle cores and liposomal bilayers to prepare a PTX encapsulated LMH system. Then, a combination of PTX and 5-FU were loaded into the LMH system, i.e. PTX was encapsulated into the liposomal bilayer and 5-FU was loaded in the TPGS micelles of the LMH aqueous inner core. A thin film evaporation procedure was used to prepare TS-LMH i.e. similar to LOV LMH, TPGS micelles, and 1, 2-Dipalmitoyl-sn-glycero-3-phosphorylglycerol (DPPG) and PEG-1500 were additionally included in DSPG-PC-CHOL liposomes to introduce thermosensitivity.

The average particle diameter of PTX loaded LMH, was 175 nm and possessed a low (< 0.2) particle size distribution. Addition of PEG and DPPG had no significant effect on the size of the TS-LMH, however, they did show some effect on the zeta potential of the TS-LMH, which was reduced from -33.02 ± 8.97 (mV) to -14.4 ± 0.85 (mV). The microscopic structure (determined using TEM) of the TS-LMH was observed to be roughly spherical in shape with hair-like projections on the surface (PEG coating around the LMH). Significant amounts of drug was loaded into the LMH, where, PTX loading in LMH increased its solubility by 204-fold in comparison with pure crystalline drug and it was 2.79 and 1.30-fold higher in comparison of micelles and liposomes.

Release of PTX and 5-FU from loaded nanocarriers exhibited thermoresponsive characteristics at 42°C i.e. ~5-20% greater release than at body temperature. The PTX showed controlled released characteristics in LMH and liposomes, while the 5-FU exhibited burst release properties either from micelles or micelles in the core of LMH. This is due to the small molecular size of 5-FU and its fast diffusion.

The PTX-encapsulated LMH showed better cell killing ability against HeLa cancer cells compared to liposomes and micelles. A significant increase in the permeability and transport of PTX was observed in Caco-2 cells in the presence of PEG and DPPG when compared to the LOV-LMH. The paracellular permeability of PTX was enhanced by 2.6-fold, 2.4-fold and 2.13-fold for LMH, liposomes, and micelles, respectively. Correspondingly, a more significant reduction of TEER values was evident for the LMH than for liposomes and micelles. Additionally, the reduced TEER value for TS-LMH compared to the LMH is likely due to the presence of the PEG/DPPG. Transport of PTX across Caco-2 cell monolayers was also observed released more slowly, over a longer period of time (for 24 hours) from the previous LMH system (biphasic for 8 hours) due to the PEGylation.

In conclusion, a LMH system has been successfully developed, containing greater drug levels inside the lipid bilayer and improved controlled drug release ability from the inner aqueous core at both physiological and elevated temperature. LMH can be engineered as TS-LMH for potential delivery of anticancer drugs and offers better cellular activity against cancer cells and improved permeability and transport across Caco-2 cells. The formulations developed in this work may be considered as effective drug delivery systems for cardiovascular and cancer chemotherapy.

6.2. Future direction

In this study, we have developed various liposome-micelle hybrid formulations for the improvement of aqueous solubility of poorly soluble drugs and demonstrated the feasibility of improved oral administration of these drugs. Further studies should be considered for improved understanding of properties such as the phase transition temperature of TS-LMH, specific role of transporters, dual delivery of anticancer drugs to cancer cells and safety profiles. These additional studies would help to translate LMH applications in the clinic. Suggestions for more specific studies follow.

Differential scanning calorimetry (DSC) could be carried out on the thermosensitive hybrids and liposomes in order to measure the temperature-dependence of the excess heat capacity of a system due to thermal phase transitions. Heat capacity curves of liposomes that undergo such transitions contain information on the enthalpy and entropy of these transitions.

The cellular activity of the nanocarriers speculated that a number of different inhibitors also could affect cellular uptake. Examples of such inhibitors are; P-gp inhibitor, sodium azide (NaN_3), cyclosporin A (CyA), and endocytosis inhibitor chlorpromazine (CPZ,)[650] which bind on the cells surface and potentiate the uptake of LMH systems by Caco-2 cells. Further studies are required to investigate the effect of these inhibitors on drug transport mechanisms using LMH.

We investigated the cell viability of PTX-LMH, however further work should be undertaken to include 5-FU with PTX-LMH in the cell studies for investigation of the MDR effect against cancer resistance cells.

Finally, to gain further mechanistic insight and to demonstrate the safety and efficacy of these novel liposome-micelle hybrid formulations, further *in vivo* studies in animal models are required. The establishment of a proper *in vitro-in vivo* correlation will also enable a precise control in designing new formulations for challenging drugs and their clinical applications.

7. Reference

1. Rasenack, N.; Müller, B. W., Poorly water-soluble drugs for oral delivery - A challenge for pharmaceutical development. Part I: Physicochemical and biopharmaceutical background/strategies in pharmaceutical development. *Pharmazeutische Industrie* **2005,** *67* (3), 323-326.

2. Pouton, C. W., Formulation of poorly water-soluble drugs for oral administration: Physicochemical and physiological issues and the lipid formulation classification system. *European Journal of Pharmaceutical Sciences* **2006,** *29* (3-4 SPEC. ISS.), 278-287.

3. Porter, C. J. H.; Pouton, C. W.; Cuine, J. F.; Charman, W. N., Enhancing intestinal drug solubilisation using lipid-based delivery systems. *Advanced drug delivery reviews* **2008,** *60* (6), 673-691.

4. Savjani, K. T.; Gajjar, A. K.; Savjani, J. K., Drug solubility: importance and enhancement techniques. *ISRN pharmaceutics* **2012,** *2012*.

5. Lipinski, C., Adv Drug Del Rev 1997; 23: 3.(b) Lipinski CA, Lombardo F, Dominy BW, Feeney PJ. *Adv Drug Del Rev* **2001,** *46*, 3.

6. Giliyar, C.; Fikstad, D.; Tyavanagimatt, S., Challenges and opportunities in oral delivery of poorly water-soluble drugs. *Drug Deliv. Technol* **2006,** *6*, 57-63.

7. Narvekar, M.; Xue, H. Y.; Eoh, J. Y.; Wong, H. L., Nanocarrier for Poorly Water-Soluble Anticancer Drugs—Barriers of Translation and Solutions. *AAPS PharmSciTech* **2014,** *15* (4), 822-833.

8. Trevaskis, N. L.; Charman, W. N.; Porter, C. J., Lipid-based delivery systems and intestinal lymphatic drug transport: a mechanistic update. *Advanced drug delivery reviews* **2008,** *60* (6), 702-716.

9. Fahr, A.; Liu, X., Drug delivery strategies for poorly water-soluble drugs. *Expert opinion on drug delivery* **2007,** *4* (4), 403-416.

10. Rajesh Babu, V.; Aleem, M. A.; Nikhat, S. R.; Aslam, S.; Khan, M., Nanosuspension technology for poorly water soluble drugs: An overview. *Research Journal of Pharmacy and Technology* **2011,** *4* (4), 515-520.

11. Pande, V. V.; Abhale, V. N., Nanocrystal technology: A particle engineering formulation strategy for the poorly water soluble drugs. *Der Pharmacia Lettre* **2016,** *8* (5), 384-392.

12. Nkansah, P.; Antipas, A.; Lu, Y.; Varma, M.; Rotter, C.; Rago, B.; El-Kattan, A.; Taylor, G.; Rubio, M.; Litchfield, J., Development and evaluation of novel solid nanodispersion system for oral delivery of poorly water-soluble drugs. *Journal of Controlled Release* **2013,** *169* (1-2), 150-161.

13. Vasconcelos, T.; Sarmento, B.; Costa, P., Solid dispersions as strategy to improve oral bioavailability of poor water soluble drugs. *Drug discovery today* **2007,** *12* (23), 1068-1075.

14. Varshosaz, J., Lipid-based nanoparticles for enhancing oral bioavailability of drugs. In *Biocompatible Nanomaterials: Synthesis, Characterization and Applications*, 2011; pp 267-284.

15. Carino, G. P.; Jacob, J. S.; Mathiowitz, E., Nanosphere based oral insulin delivery. *Journal of Controlled Release* **2000,** *65* (1), 261-269.

16. Lee, C. H.; Lo, L. W.; Mou, C. Y.; Yang, C. S., Synthesis and characterization of positive-charge functionalized mesoporous silica nanoparticles for oral drug delivery of an anti-inflammatory drug. *Advanced Functional Materials* **2008,** *18* (20), 3283-3292.

17. Tang, F.; Li, L.; Chen, D., Mesoporous silica nanoparticles: synthesis, biocompatibility and drug delivery. *Advanced Materials* **2012,** *24* (12), 1504-1534.

18. Liu, J.; Cui, L.; Losic, D., Graphene and graphene oxide as new nanocarriers for drug delivery applications. *Acta biomaterialia* **2013,** *9* (12), 9243-9257.

19. Goenka, S.; Sant, V.; Sant, S., Graphene-based nanomaterials for drug delivery and tissue engineering. *Journal of Controlled Release* **2014,** *173*, 75-88.

20. Croy, S.; Kwon, G., Polymeric micelles for drug delivery. *Current pharmaceutical design* **2006,** *12* (36), 4669-4684.

21. Torchilin, V. P., Micellar nanocarriers: pharmaceutical perspectives. *Pharmaceutical research* **2007,** *24* (1), 1.

22. Torchilin, V. P., Structure and design of polymeric surfactant-based drug delivery systems. *Journal of controlled release* **2001,** *73* (2), 137-172.

23. Bala, I.; Hariharan, S.; Kumar, M. R., PLGA nanoparticles in drug delivery: the state of the art. *Critical Reviews™ in Therapeutic Drug Carrier Systems* **2004,** *21* (5).

24. Guo, Y.; Luo, J.; Tan, S.; Otieno, B. O.; Zhang, Z., The applications of Vitamin E TPGS in drug delivery. *European Journal of Pharmaceutical Sciences* **2013,** *49* (2), 175-186.

25. Torchilin, V. P., Recent advances with liposomes as pharmaceutical carriers. *Nature Reviews Drug Discovery* **2005,** *4* (2), 145-160.

26. Lian, T.; Ho, R. J., Trends and developments in liposome drug delivery systems. *Journal of pharmaceutical sciences* **2001,** *90* (6), 667-680.

27. MuÈller, R. H.; MaÈder, K.; Gohla, S., Solid lipid nanoparticles (SLN) for controlled drug delivery–a review of the state of the art. *European journal of pharmaceutics and biopharmaceutics* **2000,** *50* (1), 161-177.

28. Almeida, A. J.; Souto, E., Solid lipid nanoparticles as a drug delivery system for peptides and proteins. *Advanced drug delivery reviews* **2007,** *59* (6), 478-490.

29. Ahmed, K.; Li, Y.; McClements, D. J.; Xiao, H., Nanoemulsion-and emulsion-based delivery systems for curcumin: encapsulation and release properties. *Food Chemistry* **2012,** *132* (2), 799-807.

30. Kuentz, M.; Holm, R.; Elder, D. P., Methodology of oral formulation selection in the pharmaceutical industry. *European Journal of Pharmaceutical Sciences* **2016,** *87*, 136-163.

31. Humberstone, A. J.; Charman, W. N., Lipid-based vehicles for the oral delivery of poorly water soluble drugs. *Advanced drug delivery reviews* **1997,** *25* (1), 103-128.

32. Wais, U.; Jackson, A. W.; He, T.; Zhang, H., Nanoformulation and encapsulation approaches for poorly water-soluble drug nanoparticles. *Nanoscale* **2016,** *8* (4), 1746-1769.

33. Bindu, M. B.; Kusum, B.; Banji, D., Novel strategies for poorly water soluble drugs. *International Journal of Pharmaceutical Sciences Review and Research* **2010,** *4* (3), 76-84.

34. Vyas, A.; Gidwani, B., Technologies to counter poor solubility issues: A review. *Research Journal of Pharmacy and Technology* **2013,** *6* (11), 1258-1270.

35. Mura, S.; Nicolas, J.; Couvreur, P., Stimuli-responsive nanocarriers for drug delivery. *Nature Materials* **2013,** *12* (11), 991-1003.

36. Gil, E. S.; Hudson, S. M., Stimuli-reponsive polymers and their bioconjugates. *Progress in polymer science* **2004,** *29* (12), 1173-1222.

37. Jhaveri, A.; Deshpande, P.; Torchilin, V., Stimuli-sensitive nanopreparations for combination cancer therapy. *Journal of Controlled Release* **2014,** *190*, 352-370.

38. Tagami, T.; Foltz, W. D.; Ernsting, M. J.; Lee, C. M.; Tannock, I. F.; May, J. P.; Li, S.-D., MRI monitoring of intratumoral drug delivery and prediction of the therapeutic effect with a multifunctional thermosensitive liposome. *Biomaterials* **2011,** *32* (27), 6570-6578.

39. Kono, K.; Nakai, R.; Morimoto, K.; Takagishi, T., Thermosensitive polymer-modified liposomes that release contents around physiological temperature. *Biochimica et Biophysica Acta (BBA) - Biomembranes* **1999,** *1416* (1–2), 239-250.

40. Hossann, M.; Wiggenhorn, M.; Schwerdt, A.; Wachholz, K.; Teichert, N.; Eibl, H.; Issels, R. D.; Lindner, L. H., In vitro stability and content release properties of phosphatidylglyceroglycerol containing thermosensitive liposomes. *Biochimica et Biophysica Acta (BBA)-Biomembranes* **2007,** *1768* (10), 2491-2499.

41. Gupta, B.; Torchilin, V. P., Monoclonal antibody 2C5-modified doxorubicin-loaded liposomes with significantly enhanced therapeutic activity against intracranial human brain U-87 MG tumor xenografts in nude mice. *Cancer Immunology, Immunotherapy* **2007,** *56* (8), 1215-1223.

42. Park, J.; Kirpotin, D.; Hong, K.; Shalaby, R.; Shao, Y.; Nielsen, U.; Marks, J.; Papahadjopoulos, D.; Benz, C., Tumor targeting using anti-her2 immunoliposomes. *Journal of Controlled Release* **2001,** *74* (1), 95-113.

43. Yatvin, M. B.; Weinstein, J. N.; Dennis, W. H.; Blumenthal, R., Design of liposomes for enhanced local release of drugs by hyperthermia. *Science* **1978,** *202* (4374), 1290-1293.

44. Yarmolenko, P. S.; Zhao, Y.; Landon, C.; Spasojevic, I.; Yuan, F.; Needham, D.; Viglianti, B. L.; Dewhirst, M. W., Comparative effects of thermosensitive doxorubicin-containing liposomes and hyperthermia in human and murine tumours. *International Journal of Hyperthermia* **2010,** *26* (5), 485-498.

45. Ta, T.; Porter, T. M., Thermosensitive liposomes for localized delivery and triggered release of chemotherapy. *Journal of Controlled Release* **2013,** *169* (1-2), 112-125.

46. Li, L.; ten Hagen, T. L.; Schipper, D.; Wijnberg, T. M.; van Rhoon, G. C.; Eggermont, A. M.; Lindner, L. H.; Koning, G. A., Triggered content release from optimized stealth thermosensitive liposomes using mild hyperthermia. *Journal of Controlled Release* **2010,** *143* (2), 274-279.

47. Soga, O.; van Nostrum, C. F.; Fens, M.; Rijcken, C. J.; Schiffelers, R. M.; Storm, G.; Hennink, W. E., Thermosensitive and biodegradable polymeric micelles for paclitaxel delivery. *Journal of Controlled Release* **2005,** *103* (2), 341-353.

48. Park, K. M.; Bae, J. W.; Joung, Y. K.; Shin, J. W.; Park, K. D., Nanoaggregate of thermosensitive chitosan-Pluronic for sustained release of hydrophobic drug. *Colloids and Surfaces B: Biointerfaces* **2008,** *63* (1), 1-6.

49. Li, W.; Li, J.; Gao, J.; Li, B.; Xia, Y.; Meng, Y.; Yu, Y.; Chen, H.; Dai, J.; Wang, H., The fine-tuning of thermosensitive and degradable polymer micelles for enhancing intracellular uptake and drug release in tumors. *Biomaterials* **2011,** *32* (15), 3832-3844.

50. Unezaki, S.; Maruyama, K.; Takahashi, N.; Koyama, M.; Yuda, T.; Suginaka, A.; Iwatsuru, M., Enhanced Delivery and Antitumor Activity of Doxorubicin Using Long-Circulating Thermosensitive Liposomes Containing Amphipathic Polyethylene Glycol in Combination with Local Hyperthermia. *Pharmaceutical Research* **1994,** *11* (8), 1180-1185.

51. Maruyama, K.; Unezaki, S.; Takahashi, N.; Iwatsuru, M., Enhanced delivery of doxorubicin to tumor by long-circulating thermosensitive liposomes and local hyperthermia. *Biochimica et Biophysica Acta (BBA)-Biomembranes* **1993,** *1149* (2), 209-216.

52. Iga, K.; Hamaguchi, N.; Igari, Y.; Ogawa, Y.; Gotoh, K.; Ootsu, K.; Toguchi, H.; Shimamoto, T., Enhanced antitumor activity in mice after administration of thermosensitive liposome encapsulating cisplatin with hyperthermia. *Journal of Pharmacology and Experimental Therapeutics* **1991,** *257* (3), 1203-1207.

53. Bassett, J.; Anderson, R.; Tacker, J., Use of temperature-sensitive liposomes in the selective delivery of methotrexate and cis-platinum analogues to murine bladder tumor. *The Journal of urology* **1986,** *135* (3), 612-615.

54. Gaber, M. H.; Hong, K.; Huang, S. K.; Papahadjopoulos, D., Thermosensitive sterically stabilized liposomes: formulation and in vitro studies on mechanism of doxorubicin release by bovine serum and human plasma. *Pharmaceutical research* **1995,** *12* (10), 1407-1416.

55. Liu, R.; Fraylich, M.; Saunders, B. R., Thermoresponsive copolymers: from fundamental studies to applications. *Colloid and Polymer Science* **2009,** *287* (6), 627-643.

56. Nakayama, M.; Okano, T., Multi-targeting cancer chemotherapy using temperature-responsive drug carrier systems. *Reactive and Functional Polymers* **2011,** *71* (3), 235-244.

57. Ganta, S.; Devalapally, H.; Shahiwala, A.; Amiji, M., A review of stimuli-responsive nanocarriers for drug and gene delivery. *Journal of controlled release* **2008,** *126* (3), 187-204.

58. Li, Y.; Chen, Z.; Cui, Y.; Zhai, G.; Li, L., The construction and characterization of hybrid paclitaxel-in-micelle-in-liposome systems for enhanced oral drug delivery. *Colloids and Surfaces B: Biointerfaces* **2017,** *160*, 572-580.

59. Zhang, W.; Li, C.; Jin, Y.; Liu, X.; Wang, Z.; Shaw, J. P.; Baguley, B. C.; Wu, Z.; Liu, J., Multiseed liposomal drug delivery system using micelle gradient as driving force to improve amphiphilic drug retention and its anti-tumor efficacy. *Drug Delivery* **2018,** *25* (1), 611-622.

60. Weng, K. C.; Noble, C. O.; Papahadjopoulos-Sternberg, B.; Chen, F. F.; Drummond, D. C.; Kirpotin, D. B.; Wang, D.; Hom, Y. K.; Hann, B.; Park, J. W., Targeted Tumor Cell Internalization

and Imaging of Multifunctional Quantum Dot-Conjugated Immunoliposomes in Vitro and in Vivo. *Nano Letters* **2008,** *8* (9), 2851-2857.

61. Zhang, W.; Song, Y.; Eldi, P.; Guo, X.; Hayball, J. D.; Garg, S.; Albrecht, H., Targeting prostate cancer cells with hybrid elastin-like polypeptide/liposome nanoparticles. *International Journal of Nanomedicine* **2018,** *13*, 293-305.

62. Lin, Y.; Wu, J.; Gu, W.; Huang, Y.; Tong, Z.; Huang, L.; Tan, J., Exosome–Liposome Hybrid Nanoparticles Deliver CRISPR/Cas9 System in MSCs. *Advanced Science* **2018,** *5* (4).

63. Coimbra, M.; Isacchi, B.; Van Bloois, L.; Torano, J. S.; Ket, A.; Wu, X.; Broere, F.; Metselaar, J. M.; Rijcken, C. J. F.; Storm, G.; Bilia, R.; Schiffelers, R. M., Improving solubility and chemical stability of natural compounds for medicinal use by incorporation into liposomes. *International Journal of Pharmaceutics* **2011,** *416* (2), 433-442.

64. Elorza, M. A.; Elorza, B.; Chantres, J. R., Stability of liposomal formulations: action of amphiphilic molecules. *International Journal of Pharmaceutics* **1997,** *158* (2), 173-183.

65. Torchilin, V., Micellar Nanocarriers: Pharmaceutical Perspectives. *Pharmaceutical Research* **2007,** *24* (1), 1-16.

66. Niu, M.; Tan, Y.; Guan, P.; Hovgaard, L.; Lu, Y.; Qi, J.; Lian, R.; Li, X.; Wu, W., Enhanced oral absorption of insulin-loaded liposomes containing bile salts: A mechanistic study. *International Journal of Pharmaceutics* **2014,** *460* (1-2), 119-130.

67. Batrakova, E.; Han, H.-Y.; Alakhov, V.; Miller, D.; Kabanov, A., Effects of Pluronic Block Copolymers on Drug Absorption in Caco-2 Cell Monolayers. *Pharmaceutical Research* **1998,** *15* (6), 850-855.

68. Mathot, F.; van Beijsterveldt, L.; Préat, V.; Brewster, M.; Ariën, A., Intestinal uptake and biodistribution of novel polymeric micelles after oral administration. *Journal of Controlled Release* **2006,** *111* (1–2), 47-55.

69. Guan, P.; Lu, Y.; Qi, J.; Niu, M.; Lian, R.; Hu, F.; Wu, W., Enhanced oral bioavailability of cyclosporine A by liposomes containing a bile salt. *International journal of nanomedicine* **2011,** *6*, 965-974.

70. Francis, M. F.; Cristea, M.; Yang, Y.; Winnik, F. M., Engineering polysaccharide-based polymeric micelles to enhance permeability of cyclosporin A across Caco-2 cells. *Pharmaceutical research* **2005,** *22* (2), 209-219.

71. Koudelka, Š.; Turánek, J., Liposomal paclitaxel formulations. *Journal of Controlled Release* **2012,** *163* (3), 322-334.

72. lovastatin physicochemical properties.

73. Paclitaxel physicochemical properties.

74. https://cameochemicals.noaa.gov/chemical/5005, 5 Fluorouracil chemical and physical properties

75. Daugherty, A. L.; Mrsny, R. J., Transcellular uptake mechanisms of the intestinal epithelial barrier Part one. *Pharmaceutical science & technology today* **1999,** *2* (4), 144-151.

76. Bromberg, L., Polymeric micelles in oral chemotherapy. *Journal of Controlled Release* **2008,** *128* (2), 99-112.

77. Gaucher, G.; Satturwar, P.; Jones, M. C.; Furtos, A.; Leroux, J. C., Polymeric micelles for oral drug delivery. *European Journal of Pharmaceutics and Biopharmaceutics* **2010,** *76* (2), 147-158.

78. Ruenraroengsak, P.; Cook, J. M.; Florence, A. T., Nanosystem drug targeting: Facing up to complex realities. *Journal of Controlled Release* **2010,** *141* (3), 265-276.

79. Seenivasan, A.; Gummadi, S. N.; Panda, T.; Théodore, T., Quantification of Lovastatin Produced by Monascus purpureus. *Open Biotechnology Journal* **2015,** *9*, 6-13.

80. Singh, S.; Dash, A. K., Paclitaxel in cancer treatment: perspectives and prospects of its delivery challenges. *Critical Reviews™ in Therapeutic Drug Carrier Systems* **2009,** *26* (4).

81. Merisko-Liversidge, E. M.; Liversidge, G. G., Drug nanoparticles: Formulating poorly water-soluble compounds. *Toxicologic Pathology* **2008,** *36* (1), 43-48.

82. Wu, C. Y.; Benet, L. Z., Predicting drug disposition via application of BCS: transport/absorption/elimination interplay and development of a biopharmaceutics drug disposition classification system. *Pharmaceutical Research* **2005,** *22* (1), 11-23.

83. Williams, H. D.; Trevaskis, N. L.; Charman, S. A.; Shanker, R. M.; Charman, W. N.; Pouton, C. W.; Porter, C. J. H., Strategies to Address Low Drug Solubility in Discovery and Development. *Pharmacological Reviews* **2013,** *65* (1), 315-499.

84. Lawrence, X. Y.; Amidon, G. L.; Polli, J. E.; Zhao, H.; Mehta, M. U.; Conner, D. P.; Shah, V. P.; Lesko, L. J.; Chen, M.-L.; Lee, V. H., Biopharmaceutics classification system: the scientific basis for biowaiver extensions. *Pharmaceutical research* **2002,** *19* (7), 921-925.

85. Amidon, G. L.; Lennernäs, H.; Shah, V. P.; Crison, J. R., A theoretical basis for a biopharmaceutic drug classification: the correlation of in vitro drug product dissolution and in vivo bioavailability. *Pharmaceutical research* **1995,** *12* (3), 413-420.

86. Wu, C.-Y.; Benet, L. Z., Predicting drug disposition via application of BCS: transport/absorption/elimination interplay and development of a biopharmaceutics drug disposition classification system. *Pharmaceutical research* **2005,** *22* (1), 11-23.

87. Butler, J. M.; Dressman, J. B., The developability classification system: application of biopharmaceutics concepts to formulation development. *Journal of pharmaceutical sciences* **2010,** *99* (12), 4940-4954.

88. Chen, M.-L.; Amidon, G. L.; Benet, L. Z.; Lennernas, H.; Lawrence, X. Y., The BCS, BDDCS, and regulatory guidances. *Pharmaceutical research* **2011,** *28* (7), 1774-1778.

89. Yu, L. X.; Amidon, G. L.; Polli, J. E.; Zhao, H.; Mehta, M. U.; Conner, D. P.; Shah, V. P.; Lesko, L. J.; Chen, M. L.; Lee, V. H. L., Biopharmaceutics classification system: the scientific basis for biowaiver extensions. *Pharmaceutical Research* **2002,** *19* (7), 921-925.

90. Dahan, A.; Miller, J. M.; Amidon, G. L., Prediction of solubility and permeability class membership: provisional BCS classification of the world's top oral drugs. *The AAPS journal* **2009,** *11* (4), 740-746.

91. Leuner, C.; Dressman, J., Improving drug solubility for oral delivery using solid dispersions. *European journal of Pharmaceutics and Biopharmaceutics* **2000,** *50* (1), 47-60.

92. Stella, V. J.; Nti-Addae, K. W., Prodrug strategies to overcome poor water solubility. *Advanced drug delivery reviews* **2007,** *59* (7), 677-694.

93. Brenner, G.; Ellison, D.; Kaufman, M., Analytical profiles of drug substances and excipients. *New York: Academic Press Inc;* **1992,** *21*, 277-315.

94. Zabaleta, V.; Ponchel, G.; Salman, H.; Agüeros, M.; Vauthier, C.; Irache, J. M., Oral administration of paclitaxel with pegylated poly(anhydride) nanoparticles: Permeability and pharmacokinetic study. *European Journal of Pharmaceutics and Biopharmaceutics* **2012,** *81* (3), 514-523.

95. Dai, X. L.; Li, S.; Chen, J. M.; Lu, T. B., Improving the Membrane Permeability of 5-Fluorouracil via Cocrystallization. *Crystal Growth and Design* **2016,** *16* (8), 4430-4438.

96. Williams, A. C.; Barry, B. W., Terpenes and the lipid–protein–partitioning theory of skin penetration enhancement. *Pharmaceutical research* **1991,** *8* (1), 17-24.

97. Mazzaferro, S.; Bouchemal, K.; Ponchel, G., Oral delivery of anticancer drugs II: the prodrug strategy. *Drug Discovery Today* **2013,** *18* (1–2), 93-98.

98. Dai, X.-L.; Li, S.; Chen, J.-M.; Lu, T.-B., Improving the Membrane Permeability of 5-Fluorouracil via Cocrystallization. *Crystal Growth & Design* **2016,** *16* (8), 4430-4438.

99. Naguib, Y. W.; Kumar, A.; Cui, Z., The effect of microneedles on the skin permeability and antitumor activity of topical 5-fluorouracil. *Acta Pharmaceutica Sinica B* **2014,** *4* (1), 94-99.

100. Pangeni, R.; Choi, S. W.; Jeon, O. C.; Byun, Y.; Park, J. W., Multiple nanoemulsion system for an oral combinational delivery of oxaliplatin and 5-fluorouracil: Preparation and in vivo evaluation. *International Journal of Nanomedicine* **2016,** *11*, 6379-6399.

101. Shishu; Kamalpreet; Maheshwari, M., Development and evaluation of novel microemulsion based oral formulations of 5-fluorouracil using non-everted rat intestine sac model. *Drug Development and Industrial Pharmacy* **2012,** *38* (3), 294-300.

102. Fresta, M.; Villari, A.; Puglisi, G.; Cavallaro, G., 5-Fluorouracil: various kinds of loaded liposomes: encapsulation efficiency, storage stability and fusogenic properties. *International journal of pharmaceutics* **1993,** *99* (2), 145-156.

103. Ozer, A.; Talsma, H., Preparation and stability of liposomes containing 5-fluorouracil. *International journal of pharmaceutics* **1989,** *55* (2-3), 185-191.

104. Petaccia, M.; Condello, M.; Giansanti, L.; La Bella, A.; Leonelli, F.; Meschini, S.; Gradella Villalva, D.; Pellegrini, E.; Ceccacci, F.; Galantini, L.; Mancini, G., Inclusion of new 5-fluorouracil amphiphilic derivatives in liposome formulation for cancer treatment. *MedChemComm* **2015,** *6* (9), 1639-1642.

105. Zou, W.; Sun, W.; Zhang, N.; Xu, W., Enhanced oral bioavailability and absorption mechanism study of N3-O-toluyl-fluorouracil-loaded liposomes. *Journal of Biomedical Nanotechnology* **2008,** *4* (1), 90-98.

106. Lee, D. A.; Leong, K. W.; Panek, W. C.; Eng, C. T.; Glasgow, B. J., The use of bioerodible polymers and 5-fluorouracil in glaucoma filtration surgery. *Investigative Ophthalmology & Visual Science* **1988,** *29* (11), 1692-1697.

107. Yun, Q.; Wang, S. S.; Xu, S.; Yang, J. P.; Fan, J.; Yang, L. L.; Chen, Y.; Fu, S. Z.; Wu, J. B., Use of 5-Fluorouracil Loaded Micelles and Cisplatin in Thermosensitive Chitosan Hydrogel as an Efficient Therapy against Colorectal Peritoneal Carcinomatosis. *Macromolecular Bioscience* **2016**.

108. Henwood, J. M.; Heel, R. C., Lovastatin. A preliminary review of its pharmacodynamic properties and therapeutic use in hyperlipidaemia. *Drugs* **1988,** *36* (4), 429-454.

109. Merck and Co Inc. TABLETS MEVACOR® (LOVASTATIN) 2012. http://www.merck.com/product/usa/pi_circulars/m/mevacor/mevacor_pi.pdf (accessed 7 september 2012).

110. Sun, J. X.; Niecestro, R.; Phillips, G.; Shen, J.; Lukacsko, P.; Friedhoff, L., Comparative pharmacokinetics of lovastatin extended-release tablets and lovastatin immediate-release tablets in humans. *The Journal of Clinical Pharmacology* **2002,** *42* (2), 198-204.

111. Romana, B.; Batger, M.; Prestidge, C. A.; Colombo, G.; Sonvico, F., Expanding the therapeutic potential of Statins by means of nanotechnology enabled drug delivery systems. *Current Topics in Medicinal Chemistry* **2014,** *14* (9), 1182-1193.

112. Singla, A. K.; Garg, A.; Aggarwal, D., Paclitaxel and its formulations. *International journal of pharmaceutics* **2002,** *235* (1), 179-192.

113. Mastropaolo, D.; Camerman, A.; Luo, Y.; Brayer, G. D.; Camerman, N., Crystal and molecular structure of paclitaxel (taxol). *Proceedings of the National Academy of Sciences* **1995,** *92* (15), 6920-6924.

114. Feng, L.; Mumper, R. J., A critical review of lipid-based nanoparticles for taxane delivery. *Cancer letters* **2013,** *334* (2), 157-175.

115. Ceruti, M.; Crosasso, P.; Brusa, P.; Arpicco, S.; Dosio, F.; Cattel, L., Preparation, characterization, cytotoxicity and pharmacokinetics of liposomes containing water-soluble prodrugs of paclitaxel. *Journal of controlled release* **2000,** *63* (1), 141-153.

116. Marupudi, N. I.; Han, J. E.; Li, K. W.; Renard, V. M.; Tyler, B. M.; Brem, H., Paclitaxel: a review of adverse toxicities and novel delivery strategies. *Expert opinion on drug safety* **2007,** *6* (5), 609-621.

117. Szebeni, J.; Alving, C. R.; Muggia, F. M., Complement activation by Cremophor EL as a possible contributor to hypersensitivity to paclitaxel: an in vitro study. *Journal of the national cancer institute* **1998,** *90* (4), 300-306.

118. van Zuylen, L.; Karlsson, M. O.; Verweij, J.; Brouwer, E.; de Bruijn, P.; Nooter, K.; Stoter, G.; Sparreboom, A., Pharmacokinetic modeling of paclitaxel encapsulation in Cremophor EL micelles. *Cancer Chemother Pharmacol* **2001,** *47* (4), 309-318.

119. Gianni, L.; Kearns, C. M.; Giani, A.; Capri, G.; Viganó, L.; Lacatelli, A.; Bonadonna, G.; Egorin, M. J., Nonlinear pharmacokinetics and metabolism of paclitaxel and its pharmacokinetic/pharmacodynamic relationships in humans. *Journal of Clinical Oncology* **1995,** *13* (1), 180-190.

120. Weiss, R. B.; Donehower, R.; Wiernik, P.; Ohnuma, T.; Gralla, R.; Trump, D.; Baker Jr, J.; Van Echo, D.; Von Hoff, D.; Leyland-Jones, B., Hypersensitivity reactions from taxol. *Journal of Clinical Oncology* **1990,** *8* (7), 1263-1268.

121. Terwogt, J. M.; Nuijen, B.; Huinink, W. T. B.; Beijnen, J., Alternative formulations of paclitaxel. *Cancer treatment reviews* **1997,** *23* (2), 87-95.

122. Yang, T.; Choi, M.-K.; Cui, F.-D.; Kim, J. S.; Chung, S.-J.; Shim, C.-K.; Kim, D.-D., Preparation and evaluation of paclitaxel-loaded PEGylated immunoliposome. *Journal of Controlled Release* **2007,** *120* (3), 169-177.

123. Zhang, Q.; Huang, X.-E.; Gao, L.-L., A clinical study on the premedication of paclitaxel liposome in the treatment of solid tumors. *Biomedicine & Pharmacotherapy* **2009,** *63* (8), 603-607.

124. Huh, K. M.; Min, H. S.; Lee, S. C.; Lee, H. J.; Kim, S.; Park, K., A new hydrotropic block copolymer micelle system for aqueous solubilization of paclitaxel. *Journal of Controlled Release* **2008,** *126* (2), 122-129.

125. Shieh, M.-F.; Chu, I.-M.; Lee, C.-J.; Kan, P.; Hau, D.-M.; Shieh, J.-J., Liposomal delivery system for taxol. *Journal of fermentation and bioengineering* **1997,** *83* (1), 87-90.

126. Straubinger, R. M.; Sharma, A.; Mayhew, E., Taxol formulation. Google Patents: 1995.

127. Surapaneni, M. S.; Das, S. K.; Das, N. G., Designing Paclitaxel Drug Delivery Systems Aimed at Improved Patient Outcomes: Current Status and Challenges. *ISRN Pharmacology* **2012,** *2012*, 623139.

128. Wilson, P. M.; El-Khoueiry, A.; Iqbal, S.; Fazzone, W.; LaBonte, M. J.; Groshen, S.; Yang, D.; Danenberg, K. D.; Cole, S.; Kornacki, M., A phase I/II trial of vorinostat in combination with 5-fluorouracil in patients with metastatic colorectal cancer who previously failed 5-FU-based chemotherapy. *Cancer Chemother Pharmacol* **2010,** *65* (5), 979-988.

129. Bunnell, C. A.; Winer, E. P., Oral 5-FU analogues in the treatment of breast cancer. *Oncology (Williston Park, NY)* **1998,** *12* (10 Suppl 7), 39-43.

130. Neubert, T.; Lehmann, P., Bowen's disease—a review of newer treatment options. *Ther Clin Risk Manag* **2008,** *4* (5), 1085-1095.

131. MacMillan, W. E.; Wolberg, W. H.; Welling, P. G., Pharmacokinetics of fluorouracil in humans. *Cancer research* **1978,** *38* (10), 3479-3482.

132. Okeda, R.; Shibutani, M.; Matsuo, T.; Kuroiwa, T.; Shimokawa, R.; Tajima, T., Experimental neurotoxicity of 5-fluorouracil and its derivatives is due to poisoning by the monofluorinated organic metabolites, monofluoroacetic acid and α-fluoroβ-alanine. *Acta neuropathologica* **1990,** *81* (1), 66-73.

133. Van den Mooter, G., The use of amorphous solid dispersions: A formulation strategy to overcome poor solubility and dissolution rate. *Drug Discovery Today: Technologies* **2012,** *9* (2), e79-e85.

134. Newman, A.; Knipp, G.; Zografi, G., Assessing the performance of amorphous solid dispersions. *Journal of pharmaceutical sciences* **2012,** *101* (4), 1355-1377.

135. Challa, R.; Ahuja, A.; Ali, J.; Khar, R., Cyclodextrins in drug delivery: an updated review. *Aaps Pharmscitech* **2005,** *6* (2), E329-E357.

136. Loftsson, T.; Brewster, M. E., Cyclodextrins as Functional Excipients: Methods to Enhance Complexation Efficiency. *Journal of Pharmaceutical Sciences 101* (9), 3019-3032.

137. Vallet-Regí, M.; Balas, F.; Arcos, D., Mesoporous materials for drug delivery. *Angewandte Chemie International Edition* **2007,** *46* (40), 7548-7558.

138. Pouton, C. W., Formulation of poorly water-soluble drugs for oral administration: Physicochemical and physiological issues and the lipid formulation classification system. *European Journal of Pharmaceutical Sciences* **2006,** *29* (3), 278-287.

139. Mu, H.; Holm, R.; Müllertz, A., Lipid-based formulations for oral administration of poorly water-soluble drugs. *International journal of pharmaceutics* **2013,** *453* (1), 215-224.

140. Tang, B. C.; Dawson, M.; Lai, S. K.; Wang, Y. Y.; Suk, J. S.; Yang, M.; Zeitlin, P.; Boyle, M. P.; Fu, J.; Hanes, J., Biodegradable polymer nanoparticles that rapidly penetrate the human mucus barrier. *Proceedings of the National Academy of Sciences* **2009,** *106* (46), 19268-19273.

141. Cone, R. A., Barrier properties of mucus. *Advanced drug delivery reviews* **2009,** *61* (2), 75-85.

142. Roger, E.; Lagarce, F.; Garcion, E.; Benoit, J. P., Biopharmaceutical parameters to consider in order to alter the fate of nanocarriers after oral delivery. *Nanomedicine* **2010,** *5* (2), 287-306.

143. Farokhzad, O. C.; Langer, R., Impact of nanotechnology on drug delivery. *Acs Nano* **2009,** *3* (1), 16-20.

144. Shin, D. H.; Tam, Y. T.; Kwon, G. S., Polymeric micelle nanocarriers in cancer research. *Frontiers of Chemical Science and Engineering* **2016,** *10* (3), 348-359.

145. Sapra, P.; Allen, T., Ligand-targeted liposomal anticancer drugs. *Progress in lipid research* **2003,** *42* (5), 439-462.

146. Bangham, A.; Standish, M.; Watkins, J., Diffusion of univalent ions across the lamellae of swollen phospholipids. *Journal of molecular biology* **1965,** *13* (1), 238.

147. Fielding, R., Liposomal drug delivery. Advantages and limitations from a clinical pharmacokinetic and therapeutic perspective. *Clinical pharmacokinetics* **1991,** *21* (3), 155.

148. Nee Ling, S. S.; Magosso, E.; Khan, N. A. K.; Kah, H. Y.; Barker, S. A., Enhanced oral unavailability and intestinal lymphatic transport of a hydrophilic drug using liposomes. *Drug development and industrial pharmacy* **2006,** *32* (3), 335-345.

149. Akbarieh, M.; Besner, J.; Galal, A.; Tawashi, R., Liposomal delivery system for the targeting and controlled release of praziquantel. *Drug development and industrial pharmacy* **1992,** *18* (3), 303-317.

150. Barenholz, Y. C., Doxil®—the first FDA-approved nano-drug: lessons learned. *Journal of controlled release* **2012,** *160* (2), 117-134.

151. Beloqui, A.; del Pozo-Rodríguez, A.; Isla, A.; Rodríguez-Gascón, A.; Solinís, M. Á., Nanostructured lipid carriers as oral delivery systems for poorly soluble drugs. *Journal of Drug Delivery Science and Technology* **2017**.

152. Aungst, B. J., Novel formulation strategies for improving oral bioavailability of drugs with poor membrane permeation or presystemic metabolism. *Journal of pharmaceutical sciences* **1993,** *82* (10), 979-987.

153. Amarnath, S.; Sharma, U., Liposomes in drug delivery: progress and limitations. *Int J Pharm* **1997,** *154*, 123 - 140.

154. Barenholz, Y.; Crommelin, D., Liposomes as pharmaceutical dosage forms. *Encyclopedia of pharmaceutical technology* **1994,** *9*, 1-39.

155. Himanshu, A.; Sitasharan, P.; Singhai, A., Liposomes as drug carriers. *IJPLS* **2011,** *2* (7), 945 - 951.

156. Mozafari, M. R., Liposomes: an overview of manufacturing techniques. *Cellular and Molecular Biology Letters* **2005,** *10* (4), 711.

157. Lasic, D. D., Novel applications of liposomes. *Trends in Biotechnology* **1998,** *16* (7), 307-321.

158. Bergstrand, N. Liposomes for drug delivery: From physico-chemical studies to applications. Acta Universitatis Upsaliensis, 2003.

159. Lasic, D. D., *Liposomes: from physics to applications*. Elsevier Science Ltd: 1993.

160. Sahoo, S. K.; Labhasetwar, V., Nanotech approaches to drug delivery and imaging. *Drug discovery today* **2003,** *8* (24), 1112-1120.

161. Gabizon, A.; Goren, D.; Cohen, R.; Barenholz, Y., Development of liposomal anthracyclines: from basics to clinical applications. *J Control Release* **1998,** *53*, 275 - 279.

162. Allen, T., Liposomes. Opportunities in drug delivery. *Drugs* **1997,** *54* (Suppl 4), 8 - 14.

163. Chapman, D., Physiochemical Properties of Phospholipids and Lipid Water Systems. *Liposome Technology, Gregoriadis, G., ed* **1984,** *1*, 1-19.

164. Mastrobattista, E.; Crommelin, D. J.; Wilschut, J.; Storm, G., Targeted liposomes for delivery of protein-based drugs into the cytoplasm of tumor cells. *Journal of liposome research* **2002,** *12* (1-2), 57-65.

165. Fendler, J. H., Optimizing drug entrapment in liposomes: chemical and biophysical considerations. *Liposomes in biological systems. John Wiley and Sons, Chichester, UK* **1980**, 87-100.

166. Ho, R. J.; Gibaldi, M., *Biotechnology and biopharmaceuticals: transforming proteins and genes into drugs*. John Wiley & Sons: 2004.

167. Noriyuki, M.; Yasuko, N.; Mariko, K.; Shozo, M.; Hitoshi, S., Mechanism for the inducement of the intestinal absorption of poorly absorbed drugs by mixed micelles II. Effect of the incorporation of various lipids on the permeability of liposomal membranes. *International Journal of Pharmaceutics* **1980,** *4* (4), 281-290.

168. Storm, G.; Crommelin, D. J., Liposomes: quo vadis? *Pharmaceutical Science & Technology Today* **1998,** *1* (1), 19-31.

169. Hatziantonioy, S.; Demetzos, C., Lipids of membranes: chemistry, biological role and applications as drug carriers. *Studies in Natural Products Chemistry* **2008,** *34*, 173-202.

170. Sercombe, L.; Veerati, T.; Moheimani, F.; Wu, S. Y.; Sood, A. K.; Hua, S., Advances and Challenges of Liposome Assisted Drug Delivery. *Frontiers in Pharmacology* **2015,** *6*, 286.

171. Immordino, M. L.; Dosio, F.; Cattel, L., Stealth liposomes: review of the basic science, rationale, and clinical applications, existing and potential. *International journal of nanomedicine* **2006,** *1* (3), 297.

172. Kozubek½, A.; Gubernator, J.; Przeworska, E.; Stasiuk, M., Liposomal drug delivery, a novel approach: PLARosomes. **2000**.

173. Allen, T.; Chonn, A., Large unilamellar liposomes with low uptake into the reticuloendothelial system. *FEBS letters* **1987,** *223* (1), 42-46.

174. Drummond, D. C.; Meyer, O.; Hong, K.; Kirpotin, D. B.; Papahadjopoulos, D., Optimizing liposomes for delivery of chemotherapeutic agents to solid tumors. *Pharmacological reviews* **1999,** *51* (4), 691-744.

175. Gabizon, A.; Shmeeda, H.; Barenholz, Y., Pharmacokinetics of pegylated liposomal doxorubicin. *Clinical pharmacokinetics* **2003,** *42* (5), 419-436.

176. Dhoot, N. O.; Wheatley, M. A., Microencapsulated liposomes in controlled drug delivery: strategies to modulate drug release and eliminate the burst effect. *Journal of pharmaceutical sciences* **2003,** *92* (3), 679-689.

177. Takeuchi, H.; Matsui, Y.; Yamamoto, H.; Kawashima, Y., Mucoadhesive properties of carbopol or chitosan-coated liposomes and their effectiveness in the oral administration of calcitonin to rats. *Journal of controlled release* **2003,** *86* (2), 235-242.

178. Gabizon, A. A., Stealth liposomes and tumor targeting: one step further in the quest for the magic bullet. AACR: 2001.

179. Romberg, B.; Hennink, W. E.; Storm, G., Sheddable coatings for long-circulating nanoparticles. *Pharmaceutical research* **2008,** *25* (1), 55-71.

180. Medina, O. P.; Zhu, Y.; Kairemo, K., Targeted liposomal drug delivery in cancer. *Current pharmaceutical design* **2004,** *10* (24), 2981-2989.

181. Hauser, H., Methods of preparation of lipid vesicles: assessment of their suitability for drug encapsulation. *Trends in Pharmacological Sciences* **1982,** *3* (C), 274-277.

182. Riaz, M., Liposome preparation method. *Pak J Pharm Sci* **1996,** *9* (1), 65 - 77.

183. Akbarzadeh, A.; Rezaei-Sadabady, R.; Davaran, S.; Joo, S. W.; Zarghami, N.; Hanifehpour, Y.; Samiei, M.; Kouhi, M.; Nejati-Koshki, K., Liposome: classification, preparation, and applications. *Nanoscale Research Letters* **2013,** *8* (1), 102.

184. Bangham, A. D., Liposomes: The Babraham connection. *Chemistry and Physics of Lipids* **1993,** *64* (1-3), 275-285.

185. Szoka, F.; Papahadjopoulos, D., Procedure for preparation of liposomes with large internal aqueous space and high capture by reverse-phase evaporation. *Proceedings of the National Academy of Sciences* **1978,** *75* (9), 4194-4198.

186. Gruner, S. M.; Lenk, R. P.; Janoff, A. S.; Ostro, N. J., Novel multilayered lipid vesicles: comparison of physical characteristics of multilamellar liposomes and stable plurilamellar vesicles. *Biochemistry* **1985,** *24* (12), 2833-2842.

187. Kan, P.; Tsao, C.-W.; Wang, A.-J.; Su, W.-C.; Liang, H.-F., A liposomal formulation able to incorporate a high content of Paclitaxel and exert promising anticancer effect. *Journal of drug delivery* **2010,** *2011*.

188. Kim, S.; Turker, M. S.; Chi, E. Y.; Sela, S.; Martin, G. M., Preparation of multivesicular liposomes. *Biochimica et Biophysica Acta (BBA)-Biomembranes* **1983,** *728* (3), 339-348.

189. OHSAWA, T.; MIURA, H.; HARADA, K., Improvement of encapsulation efficiency of water-soluble drugs in liposomes formed by the freeze-thawing method. *Chemical and pharmaceutical bulletin* **1985,** *33* (9), 3945-3952.

190. Pick, U., Liposomes with a large trapping capacity prepared by freezing and thawing of sonicated phospholipid mixtures. *Archives of biochemistry and biophysics* **1981,** *212* (1), 186-194.

191. Hope, M. J.; Bally, M. B.; Mayer, L. D.; Janoff, A. S.; Cullis, P. R., Generation of multilamellar and unilamellar phospholipid vesicles. *Chemistry and Physics of Lipids* **1986,** *40* (2), 89-107.

192. Ostro, M. J., *Liposomes: from biophysics to therapeutics*. Courier Corporation: 1987.

193. Kreuter, J., *Colloidal drug delivery systems*. CRC Press: 1994; Vol. 66.

194. Bittman, R.; Clejan, S.; Lund-Katz, S.; Phillips, M. C., Influence of cholesterol on bilayers of ester-and ether-linked phospholipids Permeability and 13C-nuclear magnetic resonance measurements. *Biochimica et Biophysica Acta (BBA)-Biomembranes* **1984,** *772* (2), 117-126.

195. Vemuri, S.; Rhodes, C., Preparation and characterization of liposomes as therapeutic delivery systems: a review. *Pharmaceutica Acta Helvetiae* **1995,** *70* (2), 95-111.

196. Lasic, D., Recent developments in medical applications of liposomes: sterically stabilized liposomes in cancer therapy and gene delivery in vivo. *Journal of Controlled Release* **1997,** *48* (2-3), 203-222.

197. Maestrelli, F.; González-Rodríguez, M. L.; Rabasco, A. M.; Mura, P., Effect of preparation technique on the properties of liposomes encapsulating ketoprofen–cyclodextrin complexes aimed for transdermal delivery. *International journal of pharmaceutics* **2006,** *312* (1), 53-60.

198. Zawada, Z., A single-step method of liposome preparation. *Cell Mol Biol Lett* **2004,** *9* (4A), 603-12.

199. Mohammed, A. R.; Weston, N.; Coombes, A. G. A.; Fitzgerald, M.; Perrie, Y., Liposome formulation of poorly water soluble drugs: optimisation of drug loading and ESEM analysis of stability. *International Journal of Pharmaceutics* **2004,** *285* (1), 23-34.

200. Mohammed, A.; Weston, N.; Coombes, A.; Fitzgerald, M.; Perrie, Y., Liposome formulation of poorly water soluble drugs: optimisation of drug loading and ESEM analysis of stability. *International Journal of Pharmaceutics* **2004,** *285* (1), 23-34.

201. Wishart, D. S.; Knox, C.; Guo, A. C.; Shrivastava, S.; Hassanali, M.; Stothard, P.; Chang, Z.; Woolsey, J., DrugBank: a comprehensive resource for in silico drug discovery and exploration. *Nucleic acids research* **2006,** *34* (suppl 1), D668-D672.

202. Ali, M. H.; Moghaddam, B.; Kirby, D. J.; Mohammed, A. R.; Perrie, Y., The role of lipid geometry in designing liposomes for the solubilisation of poorly water soluble drugs. *International Journal of Pharmaceutics* (0).

203. Arora, S.; Gupta, A.; Sharma, S.; Sharma, A., Preparation, characterization, in vitro & in vivo evaluation of elastic liposomal formulation of lovastatin. *Journal of Pharmacy Research* **2011,** *4* (11).

204. NOUNOU, M.; EL-KHORDAGUI, L. K.; KHALAFALLAH, N. A.; KHALIL, S. A., In vitro drug release of hydrophilic and hydrophobic drug entities from liposomal dispersions and gels. *Acta pharmaceutica* **2006,** *56* (3), 311-324.

205. Mamot, C.; Drummond, D. C.; Noble, C. O.; Kallab, V.; Guo, Z.; Hong, K.; Kirpotin, D. B.; Park, J. W., Epidermal growth factor receptor–targeted immunoliposomes significantly enhance the efficacy of multiple anticancer drugs in vivo. *Cancer research* **2005,** *65* (24), 11631-11638.

206. Sawant, R. R.; Torchilin, V. P., Challenges in development of targeted liposomal therapeutics. *The AAPS journal* **2012,** *14* (2), 303-315.

207. Al-Ahmady, Z.; Kostarelos, K., Chemical Components for the Design of Temperature-Responsive Vesicles as Cancer Therapeutics. *Chemical Reviews* **2016,** *116* (6), 3883-3918.

208. Muthu, M. S.; Kulkarni, S. A.; Raju, A.; Feng, S.-S., Theranostic liposomes of TPGS coating for targeted co-delivery of docetaxel and quantum dots. *Biomaterials* **2012,** *33* (12), 3494-3501.

209. Muthu, M. S.; Kulkarni, S. A.; Xiong, J.; Feng, S.-S., Vitamin E TPGS coated liposomes enhanced cellular uptake and cytotoxicity of docetaxel in brain cancer cells. *International journal of pharmaceutics* **2011,** *421* (2), 332-340.

210. Wang, T.; Yin, X.; Lu, Y.; Shan, W.; Xiong, S., Formulation, antileukemia mechanism, pharmacokinetics, and biodistribution of a novel liposomal emodin. *Int J Nanomedicine* **2012,** *7*, 2325-37.

211. Zhang, Z.; Tan, S.; Feng, S.-S., Vitamin E TPGS as a molecular biomaterial for drug delivery. *Biomaterials* **2012,** *33* (19), 4889-4906.

212. Anderson, K. E.; Eliot, L. A.; Stevenson, B. R.; Rogers, J. A., Formulation and evaluation of a folic acid receptor-targeted oral vancomycin liposomal dosage form. *Pharmaceutical Research* **2001,** *18* (3), 316-322.

213. Xu, H.; He, L.; Nie, S.; Guan, J.; Zhang, X.; Yang, X.; Pan, W., Optimized preparation of vinpocetine proliposomes by a novel method and in vivo evaluation of its pharmacokinetics in New Zealand rabbits. *Journal of Controlled Release* **2009,** *140* (1), 61-68.

214. Chen, Y.; Lu, Y.; Chen, J.; Lai, J.; Sun, J.; Hu, F.; Wu, W., Enhanced bioavailability of the poorly water-soluble drug fenofibrate by using liposomes containing a bile salt. *International Journal of Pharmaceutics* **2009,** *376* (1–2), 153-160.

215. Gregoriadis, G., Drug entrapment in liposomes. *Febs Letters* **1973,** *36* (3), 292-296.

216. Anderson, M.; Omri, A., The Effect of Different Lipid Components on the in Vitro Stability and Release Kinetics of Liposome Formulations. *Drug Delivery: Journal of Delivery and Targeting of Therapeutic Agents* **2004,** *11* (1), 33-39.

217. Adeyeye, M. C.; Brittain, H. G., *Preformulation in solid dosage form development*. Informa Healthcare New York: 2008.

218. Gutman, H.; Arvidsson, G.; Fontell, K.; Lindblom, G., In KL Mittal, B Lindman (eds) Surfactants in Solution. Plenum Press, New York: 1984.

219. Zhang, L.; Eisenberg, A., Multiple morphologies of" crew-cut" aggregates of polystyrene-b-poly (acrylic acid) block copolymers. *Science* **1995,** *268* (5218), 1728.

220. Lu, Y.; Park, K., Polymeric micelles and alternative nanonized delivery vehicles for poorly soluble drugs. *International Journal of Pharmaceutics* **2013,** *453* (1), 198-214.

221. Kwon, G. S., Polymeric Micelles for Delivery of Poorly Water-Soluble Compounds. *Critical reviews in therapeutic drug carrier systems* **2003,** *20* (5), 357-403.

222. Sezgin, Z.; Yüksel, N.; Baykara, T., Preparation and characterization of polymeric micelles for solubilization of poorly soluble anticancer drugs. *European Journal of Pharmaceutics and Biopharmaceutics* **2006,** *64* (3), 261-268.

223. Torchilin, V. P., Structure and design of polymeric surfactant-based drug delivery systems. *Journal of Controlled Release* **2001,** *73* (2-3), 137-172.

224. Oliveira, C. P.; Ribeiro, M. E. N. P.; Ricardo, N. M. P. S.; Souza, T. V. D. P.; Moura, C. L.; Chaibundit, C.; Yeates, S. G.; Nixon, K.; Attwood, D., The effect of water-soluble polymers, PEG and PVP, on the solubilisation of griseofulvin in aqueous micellar solutions of Pluronic F127. *International Journal of Pharmaceutics* **2011,** *421* (2), 252-257.

225. Gaucher, G.; Satturwar, P.; Jones, M.-C.; Furtos, A.; Leroux, J.-C., Polymeric micelles for oral drug delivery. *European Journal of Pharmaceutics and Biopharmaceutics* **2010,** *76* (2), 147-158.

226. Kadam, Y.; Yerramilli, U.; Bahadur, A., Solubilization of poorly water-soluble drug carbamezapine in Pluronic® micelles: Effect of molecular characteristics, temperature and added salt on the solubilizing capacity. *Colloids and Surfaces B: Biointerfaces* **2009,** *72* (1), 141-147.

227. Kadam, Y.; Yerramilli, U.; Bahadur, A.; Bahadur, P., Micelles from PEO-PPO-PEO block copolymers as nanocontainers for solubilization of a poorly water soluble drug hydrochlorothiazide. *Colloids and Surfaces B: Biointerfaces* **2011,** *83* (1), 49-57.

228. Bernabeu, E.; Gonzalez, L.; Cagel, M.; Gergic, E. P.; Moretton, M. A.; Chiappetta, D. A., Novel Soluplus®—TPGS mixed micelles for encapsulation of paclitaxel with enhanced in vitro cytotoxicity on breast and ovarian cancer cell lines. *Colloids and Surfaces B: Biointerfaces* **2016,** *140*, 403-411.

229. Bernabeu, E.; Helguera, G.; Legaspi, M. J.; Gonzalez, L.; Hocht, C.; Taira, C.; Chiappetta, D. A., Paclitaxel-loaded PCL–TPGS nanoparticles: In vitro and in vivo performance compared with Abraxane®. *Colloids and Surfaces B: Biointerfaces* **2014,** *113*, 43-50.

230. Gao, Z.; Lukyanov, A. N.; Singhal, A.; Torchilin, V. P., Diacyllipid-polymer micelles as nanocarriers for poorly soluble anticancer drugs. *Nano letters* **2002,** *2* (9), 979-982.

231. Valle, J. W.; Armstrong, A.; Newman, C.; Alakhov, V.; Pietrzynski, G.; Brewer, J.; Campbell, S.; Corrie, P.; Rowinsky, E. K.; Ranson, M., A phase 2 study of SP1049C, doxorubicin in P-glycoprotein-targeting pluronics, in patients with advanced adenocarcinoma of the esophagus and gastroesophageal junction. *Investigational New Drugs* **2011,** *29* (5), 1029-1037.

232. Dintaman, J. M.; Silverman, J. A., Inhibition of P-Glycoprotein by D-α-Tocopheryl Polyethylene Glycol 1000 Succinate (TPGS). *Pharmaceutical Research* **1999,** *16* (10), 1550-1556.

233. Zhou, Q.; Zhang, Z.; Chen, T.; Guo, X.; Zhou, S., Preparation and characterization of thermosensitive pluronic F127-b-poly(e{open}-caprolactone) mixed micelles. *Colloids and Surfaces B: Biointerfaces* **2011,** *86* (1), 45-57.

234. Cao, N.; Feng, S.-S., Doxorubicin conjugated to d-α-tocopheryl polyethylene glycol 1000 succinate (TPGS): Conjugation chemistry, characterization, in vitro and in vivo evaluation. *Biomaterials* **2008,** *29* (28), 3856-3865.

235. Kwon, S. H.; Kim, S. Y.; Ha, K. W.; Kang, M. J.; Huh, J. S.; Tae Jong, I.; Kim, Y. M.; Park, Y. M.; Kang, K. H.; Lee, S., Pharmaceutical evaluation of genistein-loaded pluronic micelles for oral delivery. *Archives of pharmacal research* **2007,** *30* (9), 1138-1143.

236. Jones, M.-C.; Leroux, J.-C., Polymeric micelles – a new generation of colloidal drug carriers. *European Journal of Pharmaceutics and Biopharmaceutics* **1999,** *48* (2), 101-111.

237. Fan, Z.; Chen, C.; Pang, X.; Yu, Z.; Qi, Y.; Chen, X.; Liang, H.; Fang, X.; Sha, X., Adding vitamin E-TPGS to the formulation of Genexol-PM: specially mixed micelles improve drug-loading ability and cytotoxicity against multidrug-resistant tumors significantly. *PloS one* **2015,** *10* (4), e0120129.

238. Persidis, A., Cancer multidrug resistance. *Nature biotechnology* **1999,** *17* (1), 94-95.

239. Liu, J.; Lee, H.; Allen, C., Formulation of drugs in block copolymer micelles: Drug loading and release. *Current Pharmaceutical Design* **2006,** *12* (36), 4685-4701.

240. Allen, C.; Maysinger, D.; Eisenberg, A., Nano-engineering block copolymer aggregates for drug delivery. *Colloids and Surfaces B: Biointerfaces* **1999,** *16* (1), 3-27.

241. Allen, C.; Maysinger, D.; Eisenberg, A., Nano-engineering block copolymer aggregates for drug delivery. *Colloids and Surfaces B: Biointerfaces* **1999,** *16* (1-4), 3-27.

242. Yokoyama, M., Polymeric micelles as a new drug carrier system and their required considerations for clinical trials. *Expert Opinion on Drug Delivery* **2010,** *7* (2), 145-158.

243. Croy, S. R.; Kwon, G. S., The effects of Pluronic block copolymers on the aggregation state of nystatin. *Journal of Controlled Release* **2004,** *95* (2), 161-171.

244. Batrakova, E. V.; Li, S.; Miller, D. W.; Kabanov, A. V., Pluronic P85 Increases Permeability of a Broad Spectrum of Drugs in Polarized BBMEC and Caco-2 Cell Monolayers. *Pharmaceutical Research* **1999,** *16* (9), 1366-1372.

245. Lim Soo, P.; Luo, L.; Maysinger, D.; Eisenberg, A., Incorporation and release of hydrophobic probes in biocompatible polycaprolactone-block-poly (ethylene oxide) micelles: implications for drug delivery. *Langmuir* **2002,** *18* (25), 9996-10004.

246. Kang, N.; Leroux, J.-C., Triblock and star-block copolymers of N-(2-hydroxypropyl)methacrylamide or N-vinyl-2-pyrrolidone and d,l-lactide: synthesis and self-assembling properties in water. *Polymer* **2004,** *45* (26), 8967-8980.

247. Liu, J.; Xiao, Y.; Allen, C., Polymer–drug compatibility: a guide to the development of delivery systems for the anticancer agent, ellipticine. *Journal of pharmaceutical sciences* **2004,** *93* (1), 132-143.

248. Lin, W.-J.; Juang, L.-W.; Lin, C.-C., Stability and Release Performance of a Series of Pegylated Copolymeric Micelles. *Pharmaceutical Research* **2003,** *20* (4), 668-673.

249. Yokoyama, M.; Fukushima, S.; Uehara, R.; Okamoto, K.; Kataoka*, K.; Sakurai, Y.; Okano, T., Characterization of physical entrapment and chemical conjugation of adriamycin in polymeric micelles and their design for in vivo delivery to a solid tumor. *Journal of Controlled Release* **1998,** *50* (1), 79-92.

250. Kohori, F.; Yokoyama, M.; Sakai, K.; Okano, T., Process design for efficient and controlled drug incorporation into polymeric micelle carrier systems. *Journal of Controlled Release* **2002,** *78* (1), 155-163.

251. Fukushima, S.; Machida, M.; Akutsu, T.; Shimizu, K.; Tanaka, S.; Okamoto, K.; Mashiba, H.; Yokoyama, M.; Okano, T.; Sakurai, Y.; Kataoka, K., Roles of adriamycin and adriamycin dimer in antitumor activity of the polymeric micelle carrier system. *Colloids and Surfaces B: Biointerfaces* **1999,** *16* (1), 227-236.

252. Rapoport, N. Y.; Herron, J. N.; Pitt, W. G.; Pitina, L., Micellar delivery of doxorubicin and its paramagnetic analog, ruboxyl, to HL-60 cells: effect of micelle structure and ultrasound on the intracellular drug uptake. *Journal of Controlled Release* **1999,** *58* (2), 153-162.

253. Zhao, Y.; Liu, G.; Shen, J. X.; Aubry, A.-F., Reasons for calibration standard curve slope variation in LC–MS assays and how to address it. *Bioanalysis* **2014,** *6* (11), 1439-1443.

254. Kwon, G. S.; Naito, M.; Yokoyama, M.; Okano, T.; Sakurai, Y.; Kataoka, K., Physical Entrapment of Adriamycin in AB Block Copolymer Micelles. *Pharmaceutical Research* **1995,** *12* (2), 192-195.

255. Yu, B. G.; Okano, T.; Kataoka, K.; Kwon, G., Polymeric micelles for drug delivery: solubilization and haemolytic activity of amphotericin B. *Journal of Controlled Release* **1998,** *53* (1), 131-136.

256. Aliabadi, H. M.; Lavasanifar, A., Polymeric micelles for drug delivery. *Expert Opinion on Drug Delivery* **2006,** *3* (1), 139-162.

257. Dalwadi, G.; Benson, H. A. E.; Chen, Y., Comparison of Diafiltration and Tangential Flow Filtration for Purification of Nanoparticle Suspensions. *Pharmaceutical Research* **2005,** *22* (12), 2152-2162.

258. Allen, C.; Han, J.; Yu, Y.; Maysinger, D.; Eisenberg, A., Polycaprolactone–b-poly(ethylene oxide) copolymer micelles as a delivery vehicle for dihydrotestosterone. *Journal of Controlled Release* **2000,** *63* (3), 275-286.

259. Kataoka, K.; Matsumoto, T.; Yokoyama, M.; Okano, T.; Sakurai, Y.; Fukushima, S.; Okamoto, K.; Kwon, G. S., Doxorubicin-loaded poly(ethylene glycol)–poly(β-benzyl-l-aspartate) copolymer micelles: their pharmaceutical characteristics and biological significance. *Journal of Controlled Release* **2000,** *64* (1), 143-153.

260. Djordjevic, J.; Michniak, B.; Uhrich, K. E., Amphiphilic star-like macromolecules as novel carriers for topical delivery of nonsteroidal anti-inflammatory drugs. *AAPS PharmSci* **2003,** *5* (4), 1-12.

261. Burt, H. M.; Zhang, X.; Toleikis, P.; Embree, L.; Hunter, W. L., Development of copolymers of poly(d,l-lactide) and methoxypolyethylene glycol as micellar carriers of paclitaxel. *Colloids and Surfaces B: Biointerfaces* **1999,** *16* (1), 161-171.

262. Zhang, X.; Jackson, J. K.; Burt, H. M., Development of amphiphilic diblock copolymers as micellar carriers of taxol. *International Journal of Pharmaceutics* **1996,** *132* (1), 195-206.

263. Letchford, K.; Zastre, J.; Liggins, R.; Burt, H., Synthesis and micellar characterization of short block length methoxy poly(ethylene glycol)-block-poly(caprolactone) diblock copolymers. *Colloids and Surfaces B: Biointerfaces* **2004,** *35* (2), 81-91.

264. Lavasanifar, A.; Samuel, J.; Kwon, G. S., The effect of fatty acid substitution on the in vitro release of amphotericin B from micelles composed of poly(ethylene oxide)-block-poly(N-hexyl stearate-l-aspartamide). *Journal of Controlled Release* **2002,** *79* (1), 165-172.

265. Zhang, X.; Burt, H. M.; Hoff, D. V.; Dexter, D.; Mangold, G.; Degen, D.; Oktaba, A. M.; Hunter, W. L., An investigation of the antitumour activity and biodistribution of polymeric micellar paclitaxel. *Cancer Chemother Pharmacol* **1997,** *40* (1), 81-86.

266. Shuai, X.; Merdan, T.; Schaper, A. K.; Xi, F.; Kissel, T., Core-Cross-Linked Polymeric Micelles as Paclitaxel Carriers. *Bioconjugate Chemistry* **2004,** *15* (3), 441-448.

267. Liu, J.; Zeng, F.; Allen, C., Influence of serum protein on polycarbonate-based copolymer micelles as a delivery system for a hydrophobic anti-cancer agent. *Journal of Controlled Release* **2005,** *103* (2), 481-497.

268. Shuai, X.; Ai, H.; Nasongkla, N.; Kim, S.; Gao, J., Micellar carriers based on block copolymers of poly(ε-caprolactone) and poly(ethylene glycol) for doxorubicin delivery. *Journal of Controlled Release* **2004,** *98* (3), 415-426.

269. Song, R.; Zhou, Y.; Li, Y.; Yang, Z.; Li, F.; Huang, Q.; Shi, T.; Zhang, G., Preparation and characterization of mPEG-g-α-zein biohybrid micelles as a nano-carrier. *Journal of Applied Polymer Science* **2015,** *132* (38), n/a-n/a.

270. Jette, K. K.; Law, D.; Schmitt, E. A.; Kwon, G. S., Preparation and Drug Loading of Poly(Ethylene Glycol)-block-Poly(ε-Caprolactone) Micelles Through the Evaporation of a Cosolvent Azeotrope. *Pharmaceutical Research* **2004,** *21* (7), 1184-1191.

271. Le Garrec, D.; Gori, S.; Luo, L.; Lessard, D.; Smith, D. C.; Yessine, M. A.; Ranger, M.; Leroux, J. C., Poly(N-vinylpyrrolidone)-block-poly(d,l-lactide) as a new polymeric solubilizer for hydrophobic anticancer drugs: in vitro and in vivo evaluation. *Journal of Controlled Release* **2004,** *99* (1), 83-101.

272. Nishiyama, N.; Yokoyama, M.; Aoyagi, T.; Okano, T.; Sakurai, Y.; Kataoka, K., Preparation and Characterization of Self-Assembled Polymer−Metal Complex Micelle from cis-Dichlorodiammineplatinum(II) and Poly(ethylene glycol)−Poly(α,β-aspartic acid) Block Copolymer in an Aqueous Medium. *Langmuir* **1999,** *15* (2), 377-383.

273. Nishiyama, N.; Okazaki, S.; Cabral, H.; Miyamoto, M.; Kato, Y.; Sugiyama, Y.; Nishio, K.; Matsumura, Y.; Kataoka, K., Novel Cisplatin-Incorporated Polymeric Micelles Can Eradicate Solid Tumors in Mice. *Cancer Research* **2003,** *63* (24), 8977-8983.

274. Yuan, X.; Harada, A.; Yamasaki, Y.; Kataoka, K., Stabilization of Lysozyme-Incorporated Polyion Complex Micelles by the ω-End Derivatization of Poly(ethylene glycol)−Poly(α,β-aspartic acid) Block Copolymers with Hydrophobic Groups. *Langmuir* **2005,** *21* (7), 2668-2674.

275. Wakebayashi, D.; Nishiyama, N.; Itaka, K.; Miyata, K.; Yamasaki, Y.; Harada, A.; Koyama, H.; Nagasaki, Y.; Kataoka, K., Polyion Complex Micelles of pDNA with Acetal-poly(ethylene glycol)-poly(2-(dimethylamino)ethyl methacrylate) Block Copolymer as the Gene Carrier System: Physicochemical Properties of Micelles Relevant to Gene Transfection Efficacy. *Biomacromolecules* **2004,** *5* (6), 2128-2136.

276. Jette, K. K.; Law, D.; Schmitt, E. A.; Kwon, G. S., Preparation and drug loading of poly (ethylene glycol)-block-poly (ε-caprolactone) micelles through the evaporation of a cosolvent azeotrope. *Pharmaceutical research* **2004,** *21* (7), 1184-1191.

277. Shuai, X.; Ai, H.; Nasongkla, N.; Kim, S.; Gao, J., Micellar carriers based on block copolymers of poly (ε-caprolactone) and poly (ethylene glycol) for doxorubicin delivery. *Journal of Controlled Release* **2004,** *98* (3), 415-426.

278. Choucair, A.; Eisenberg, A., Interfacial solubilization of model amphiphilic molecules in block copolymer micelles. *Journal of the American Chemical Society* **2003,** *125* (39), 11993-12000.

279. Le Garrec, D.; Gori, S.; Luo, L.; Lessard, D.; Smith, D.; Yessine, M.-A.; Ranger, M.; Leroux, J.-C., Poly (N-vinylpyrrolidone)-block-poly (D, L-lactide) as a new polymeric solubilizer for hydrophobic anticancer drugs: in vitro and in vivo evaluation. *Journal of Controlled Release* **2004,** *99* (1), 83-101.

280. Yokoyama, M.; Opanasopit, P.; Okano, T.; Kawano, K.; Maitani, Y., Polymer design and incorporation methods for polymeric micelle carrier system containing water-insoluble anti-cancer agent camptothecin. *Journal of drug targeting* **2004,** *12* (6), 373-384.

281. Muthu, M. S.; Kulkarni, S. A.; Liu, Y.; Feng, S.-S., Development of docetaxel-loaded vitamin E TPGS micelles: formulation optimization, effects on brain cancer cells and biodistribution in rats. *Nanomedicine* **2012,** *7* (3), 353-364.

282. Huh, K. M.; Lee, S. C.; Cho, Y. W.; Lee, J.; Jeong, J. H.; Park, K., Hydrotropic polymer micelle system for delivery of paclitaxel. *Journal of Controlled Release* **2005,** *101* (1), 59-68.

283. Berens, A. R.; Hopfenberg, H. B., Diffusion of organic vapors at low concentrations in glassy PVC, polystyrene, and PMMA. *Journal of Membrane Science* **1982,** *10* (2), 283-303.

284. Baker, R. W.; Tuttle, M. E.; Lonsdale, H. K.; Ayres, J. W., Development of an estriol-releasing intrauterine device. *Journal of Pharmaceutical Sciences* **1979,** *68* (1), 20-26.

285. Rapoport, N., Stabilization and activation of Pluronic micelles for tumor-targeted drug delivery. *Colloids and Surfaces B: Biointerfaces* **1999,** *16* (1), 93-111.

286. Li, Y.; Kwon, G. S., Methotrexate Esters of Poly(Ethylene Oxide)-Block-Poly(2-Hydroxyethyl-L-Aspartamide). Part I: Effects of the Level of Methotrexate Conjugation on the Stability of Micelles and on Drug Release. *Pharmaceutical Research* **2000,** *17* (5), 607-611.

287. Nishiyama, N.; Koizumi, F.; Okazaki, S.; Matsumura, Y.; Nishio, K.; Kataoka, K., Differential Gene Expression Profile between PC-14 Cells Treated with Free Cisplatin and Cisplatin-Incorporated Polymeric Micelles. *Bioconjugate Chemistry* **2003,** *14* (2), 449-457.

288. Matsuya, T.; Tashiro, S.; Hoshino, N.; Shibata, N.; Nagasaki, Y.; Kataoka, K., A Core−Shell-Type Fluorescent Nanosphere Possessing Reactive Poly(ethylene glycol) Tethered Chains on the Surface for Zeptomole Detection of Protein in Time-Resolved Fluorometric Immunoassay. *Analytical Chemistry* **2003,** *75* (22), 6124-6132.

289. Lee, J.; Cho, E. C.; Cho, K., Incorporation and release behavior of hydrophobic drug in functionalized poly(d,l-lactide)-block–poly(ethylene oxide) micelles. *Journal of Controlled Release* **2004,** *94* (2), 323-335.

290. Son, S.; Shin, E.; Kim, B.-S., Light-Responsive Micelles of Spiropyran Initiated Hyperbranched Polyglycerol for Smart Drug Delivery. *Biomacromolecules* **2014,** *15* (2), 628-634.

291. Yan, Q.; Hu, J.; Zhou, R.; Ju, Y.; Yin, Y.; Yuan, J., Visible light-responsive micelles formed from dialkoxyanthracene-containing block copolymers. *Chemical Communications* **2012,** *48* (13), 1913-1915.

292. Singhvi, G.; Singh, M., Review: in-vitro drug release characterization models. *Int J Pharm Stud Res* **2011,** *2* (1), 77-84.

293. Nagai, Y.; Unsworth, L. D.; Koutsopoulos, S.; Zhang, S., Slow release of molecules in self-assembling peptide nanofiber scaffold. *Journal of controlled release* **2006,** *115* (1), 18-25.

294. Kim, S. Y.; Kim, J. H.; Kim, D.; An, J. H.; Lee, D. S.; Kim, S. C., Drug-releasing kinetics of MPEG/PLLA block copolymer micelles with different PLLA block lengths. *Journal of applied polymer science* **2001,** *82* (10), 2599-2605.

295. Zuleger, S.; Lippold, B. C., Polymer particle erosion controlling drug release. I. Factors influencing drug release and characterization of the release mechanism. *International journal of pharmaceutics* **2001,** *217* (1), 139-152.

296. Baker, R. W., *Controlled release of biologically active agents*. John Wiley & Sons: 1987.

297. Saxena, V.; Hussain, M. D., Poloxamer 407/TPGS mixed micelles for delivery of gambogic acid to breast and multidrug-resistant cancer. *Int J Nanomedicine* **2012,** *7*, 713-721.

298. Artursson, P.; Palm, K.; Luthman, K., Caco-2 monolayers in experimental and theoretical predictions of drug transport1. *Advanced drug delivery reviews* **2001,** *46* (1-3), 27-43.

299. Sarmento, B.; Andrade, F.; Silva, S. B. d.; Rodrigues, F.; das Neves, J.; Ferreira, D., Cell-based in vitro models for predicting drug permeability. *Expert opinion on drug metabolism & toxicology* **2012,** *8* (5), 607-621.

300. Kamuhabwa, A. R.; Augustijns, P.; De Witte, P. A., In vitro transport and uptake of protohypericin and hypericin in the Caco-2 model. *International Journal of Pharmaceutics* **1999,** *188* (1), 81-86.

301. Shah, P.; Jogani, V.; Bagchi, T.; Misra, A., Role of Caco-2 Cell Monolayers in Prediction of Intestinal Drug Absorption. *Biotechnology progress* **2006,** *22* (1), 186-198.

302. Wu, X.; Whitfield, L. R.; Stewart, B. H., Atorvastatin transport in the Caco-2 cell model: Contributions of P- glycoprotein and the proton-monocarboxylic acid co-transporter. *Pharmaceutical Research* **2000,** *17* (2), 209-215.

303. Artursson, P.; Palm, K.; Luthman, K., Caco-2 monolayers in experimental and theoretical predictions of drug transport. *Advanced drug delivery reviews* **1996,** *22* (1–2), 67-84.

304. Sattler, S.; Schaefer, U.; Schneider, W.; Hoelzl, J.; Lehr, C. M., Binding, uptake, and transport of hypericin by Caco-2 cell monolayers. *Journal of Pharmaceutical Sciences* **1997,** *86* (10), 1120-1126.

305. Li, J.; Volpe, D. A.; Wang, Y.; Zhang, W.; Bode, C.; Owen, A.; Hidalgo, I. J., Use of transporter knockdown caco-2 cells to investigate the in vitro efflux of statin drugs. *Drug Metabolism and Disposition* **2011,** *39* (7), 1196-1202.

306. Hossain, Z.; Kurihara, H.; Hosokawa, M.; Takahashi, K., Docosahexaenoic acid and eicosapentaenoic acid-enriched phosphatidylcholine liposomes enhance the permeability, transportation and uptake of phospholipids in Caco-2 cells. *Molecular and cellular biochemistry* **2006,** *285* (1), 155-163.

307. Jung, T.; Kamm, W.; Breitenbach, A.; Kaiserling, E.; Xiao, J.; Kissel, T., Biodegradable nanoparticles for oral delivery of peptides: is there a role for polymers to affect mucosal uptake? *European Journal of Pharmaceutics and Biopharmaceutics* **2000,** *50* (1), 147-160.

308. Walker, W. A.; Isselbacher, K. J., Uptake and transport of macromolecules by the intestine. Possible role in clinical disorders. *Gastroenterology* **1974,** *67* (3), 531.

309. Martins, S.; Sarmento, B.; Ferreira, D. C.; Souto, E. B., Lipid-based colloidal carriers for peptide and protein delivery–liposomes versus lipid nanoparticles. *International journal of nanomedicine* **2007,** *2* (4), 595.

310. Mohanraj, V.; Chen, Y., Nanoparticles-a review. *Tropical Journal of Pharmaceutical Research* **2006,** *5* (1), 561-573.

311. Lasic, D. D., *Liposomes in gene delivery*. CRC press: 1997.

312. Florence, A. T.; Hussain, N., Transcytosis of nanoparticle and dendrimer delivery systems: evolving vistas. *Advanced drug delivery reviews* **2001,** *50,* S69-S89.

313. Ponchel, G.; Irache, J.-M., Specific and non-specific bioadhesive particulate systems for oral delivery to the gastrointestinal tract. *Advanced drug delivery reviews* **1998,** *34* (2–3), 191-219.

314. Torchilin, V. P.; Lukyanov, A. N., Peptide and protein drug delivery to and into tumors: challenges and solutions. *Drug discovery today* **2003,** *8* (6), 259-266.

315. Lasic, D., Applications of liposomes. *Handbook of biological physics* **1995,** *1,* 491-519.

316. Gregoriadis, G.; Florence, A. T., Liposomes in drug delivery. *Drugs* **1993,** *45* (1), 15-28.

317. Qi, R.; Zhang, H.; Xu, L.; Shen, W.; Chen, C.; Wang, C.; Cao, Y.; Wang, Y.; van Dongen, M. A.; He, B.; Wang, S.; Liu, G.; Banaszak Holl, M. M.; Zhang, Q., G5 PAMAM dendrimer versus liposome: A comparison study on the in vitro transepithelial transport and in vivo oral absorption of simvastatin. *Nanomedicine: Nanotechnology, Biology and Medicine* **2015,** *11* (5), 1141-1151.

318. Gill, K. K.; Kaddoumi, A.; Nazzal, S., Mixed micelles of PEG 2000-DSPE and vitamin-E TPGS for concurrent delivery of paclitaxel and parthenolide: Enhanced chemosenstization and antitumor efficacy against non-small cell lung cancer (NSCLC) cell lines. *European journal of pharmaceutical sciences* **2012,** *46* (1), 64-71.

319. Mekhail, G. M.; Kamel, A. O.; Awad, G. A. S.; Mortada, N. D., Anticancer effect of atorvastatin nanostructured polymeric micelles based on stearyl-grafted chitosan. *International Journal of Biological Macromolecules* **2012,** *51* (4), 351-363.

320. Kono, K., Thermosensitive polymer-modified liposomes. *Advanced Drug Delivery Reviews* **2001,** *53* (3), 307-319.

321. Zhu, L.; Torchilin, V. P., Stimulus-responsive nanopreparations for tumor targeting. *Integrative Biology* **2013,** *5* (1), 96-107.

322. Karino, T.; Koga, S.; Maeta, M., Experimental studies of the effects of local hyperthermia on blood flow, oxygen pressure and pH in tumors. *Surgery Today* **1988,** *18* (3), 276-283.

323. Horsman, M.; Overgaard, J., Hot Topic: Can mild hyperthermia improve tumour oxygenation? *International journal of hyperthermia* **1997,** *13* (2), 141-147.

324. Kong, G.; Dewhirst, M., Review hyperthermia and liposomes. *International Journal of Hyperthermia* **1999,** *15* (5), 345-370.

325. Dou, Y.; Hynynen, K.; Allen, C., To heat or not to heat: Challenges with clinical translation of thermosensitive liposomes. *Journal of Controlled Release* **2017,** *249,* 63-73.

326. Barenholz, Y., Doxil® — The first FDA-approved nano-drug: Lessons learned. *Journal of Controlled Release* **2012,** *160* (2), 117-134.

327. Mills, J. K.; Needham, D., Lysolipid incorporation in dipalmitoylphosphatidylcholine bilayer membranes enhances the ion permeability and drug release rates at the membrane phase transition. *Biochimica et Biophysica Acta (BBA)-Biomembranes* **2005,** *1716* (2), 77-96.

328. Needham, D.; Park, J.-Y.; Wright, A. M.; Tong, J., Materials characterization of the low temperature sensitive liposome (LTSL): effects of the lipid composition (lysolipid and DSPE–PEG2000) on the thermal transition and release of doxorubicin. *Faraday discussions* **2013,** *161*, 515-534.

329. Wang, Z.-Y.; Zhang, H.; Yang, Y.; Xie, X.-Y.; Yang, Y.-F.; Li, Z.; Li, Y.; Gong, W.; Yu, F.-L.; Yang, Z., Preparation, characterization, and efficacy of thermosensitive liposomes containing paclitaxel. *Drug delivery* **2016,** *23* (4), 1222-1231.

330. Al Sabbagh, C.; Tsapis, N.; Novell, A.; Calleja-Gonzalez, P.; Escoffre, J.-M.; Bouakaz, A.; Chacun, H.; Denis, S.; Vergnaud, J.; Gueutin, C., Formulation and pharmacokinetics of thermosensitive stealth® liposomes encapsulating 5-Fluorouracil. *Pharmaceutical research* **2015,** *32* (5), 1585-1603.

331. Lindner, L. H.; Hossann, M.; Vogeser, M.; Teichert, N.; Wachholz, K.; Eibl, H.; Hiddemann, W.; Issels, R. D., Dual role of hexadecylphosphocholine (miltefosine) in thermosensitive liposomes: active ingredient and mediator of drug release. *Journal of Controlled Release* **2008,** *125* (2), 112-120.

332. Kono, K.; Yoshino, K.; Takagishi, T., Effect of poly (ethylene glycol) grafts on temperature-sensitivity of thermosensitive polymer-modified liposomes. *Journal of controlled release* **2002,** *80* (1), 321-332.

333. Hossann, M.; Wiggenhorn, M.; Schwerdt, A.; Wachholz, K.; Teichert, N.; Eibl, H.; Issels, R. D.; Lindner, L. H., In vitro stability and content release properties of phosphatidylglyceroglycerol containing thermosensitive liposomes. *Biochimica et Biophysica Acta (BBA) - Biomembranes* **2007,** *1768* (10), 2491-2499.

334. Kim, S. Y.; Lee, Y. M.; Shin, H. J.; Kang, J. S., Indomethacin-loaded methoxy poly(ethylene glycol)/poly(ε-caprolactone) diblock copolymeric nanosphere: Pharmacokinetic characteristics of indomethacin in the normal Sprague-Dawley rats. *Biomaterials* **2001,** *22* (14), 2049-2056.

335. Tian, Y.; Mao, S., Amphiphilic polymeric micelles as the nanocarrier for peroral delivery of poorly soluble anticancer drugs. *Expert Opinion on Drug Delivery* **2012,** *9* (6), 687-700.

336. Guissi, F.; Lü, L. W.; Han, Z. H.; Gu, Y. Q., Nanoparticles in photothermal therapy and photothermal. *Chinese Journal of Pharmaceutical Biotechnology* **2015,** *22* (6), 549-552.

337. Dicheva, B. M.; Koning, G. A., Targeted thermosensitive liposomes: An attractive novel approach for increased drug delivery to solid tumors. *Expert Opinion on Drug Delivery* **2014,** *11* (1), 83-100.

338. Gottesman, M. M.; Fojo, T.; Bates, S. E., Multidrug resistance in cancer: role of ATP–dependent transporters. *Nature Reviews Cancer* **2002,** *2*, 48.

339. Iyer, A. K.; Singh, A.; Ganta, S.; Amiji, M. M., Role of integrated cancer nanomedicine in overcoming drug resistance. *Advanced Drug Delivery Reviews* **2013,** *65* (13), 1784-1802.

340. Hu, C.-M. J.; Zhang, L., Nanoparticle-based combination therapy toward overcoming drug resistance in cancer. *Biochemical Pharmacology* **2012,** *83* (8), 1104-1111.

341. Xu, X.; Ho, W.; Zhang, X.; Bertrand, N.; Farokhzad, O., Cancer nanomedicine: from targeted delivery to combination therapy. *Trends in Molecular Medicine* **2015,** *21* (4), 223-232.

342. Dai, Y.; Xu, C.; Sun, X.; Chen, X., Nanoparticle design strategies for enhanced anticancer therapy by exploiting the tumour microenvironment. *Chemical Society Reviews* **2017,** *46* (12), 3830-3852.

343. Bertrand, N.; Wu, J.; Xu, X.; Kamaly, N.; Farokhzad, O. C., Cancer nanotechnology: The impact of passive and active targeting in the era of modern cancer biology. *Advanced Drug Delivery Reviews* **2014,** *66* (Supplement C), 2-25.

344. Kydd, J.; Jadia, R.; Velpurisiva, P.; Gad, A.; Paliwal, S.; Rai, P., Targeting strategies for the combination treatment of cancer using drug delivery systems. *Pharmaceutics* **2017,** *9* (4).

345. Zhang, L.; Chan, J. M.; Gu, F. X.; Rhee, J.-W.; Wang, A. Z.; Radovic-Moreno, A. F.; Alexis, F.; Langer, R.; Farokhzad, O. C., Self-Assembled Lipid−Polymer Hybrid Nanoparticles: A Robust Drug Delivery Platform. *ACS Nano* **2008,** *2* (8), 1696-1702.

346. Hallan, S. S.; Kaur, P.; Kaur, V.; Mishra, N.; Vaidya, B., Lipid polymer hybrid as emerging tool in nanocarriers for oral drug delivery. *Artificial Cells, Nanomedicine, and Biotechnology* **2016,** *44* (1), 334-349.

347. Kawabata, Y.; Wada, K.; Nakatani, M.; Yamada, S.; Onoue, S., Formulation design for poorly water-soluble drugs based on biopharmaceutics classification system: Basic approaches and practical applications. *International Journal of Pharmaceutics* **2011,** *420* (1), 1-10.

348. Kumar, S.; Bhargava, D.; Thakkar, A.; Arora, S., Drug carrier systems for solubility enhancement of BCS class II drugs: A critical review. *Critical Reviews in Therapeutic Drug Carrier Systems* **2013,** *30* (3), 217-256.

349. Schachter, M., Chemical, pharmacokinetic and pharmacodynamic properties of statins: an update. *Fundamental & clinical pharmacology* **2005,** *19* (1), 117-125.

350. Lennernäs, H.; Fager, G., Pharmacodynamics and Pharmacokinetics of the HMG-CoA Reductase Inhibitors. *Clinical Pharmacokinetics* **1997,** *32* (5), 403-425.

351. Yadava, S. K.; Naik, J. B.; Patil, J. S.; Mokale, V. J.; Singh, R., Enhanced solubility and bioavailability of lovastatin using stabilized form of self-emulsifying drug delivery system. *Colloids and Surfaces A: Physicochemical and Engineering Aspects* **2015,** *481*, 63-71.

352. Singh, S. K.; Verma, P. R. P.; Razdan, B., Development and characterization of a lovastatin-loaded self-microemulsifying drug delivery system. *Pharmaceutical Development and Technology* **2010,** *15* (5), 469-483.

353. Goyal, U.; Arora, R.; Aggarwal, G., Formulation design and evaluation of a self-microemulsifying drug delivery system of lovastatin. *Acta Pharmaceutica* **2012,** *62* (3), 357-370.

354. Bakhle, S. S.; Avari, J. G., Development and evaluation of liquid and solid self-microemulsifying drug delivery system of lovastatin. *Asian Journal of Pharmaceutics* **2016,** *10* (1), 22-35.

355. Qureshi, M. J.; Mallikarjun, C.; Kian, W. G., Enhancement of solubility and therapeutic potential of poorly soluble lovastatin by SMEDDS formulation adsorbed on directly compressed spray dried magnesium aluminometasilicate liquid loadable tablets: A study in diet induced hyperlipidemic rabbits. *Asian Journal of Pharmaceutical Sciences* **2015,** *10* (1), 40-56.

356. Beg, S.; Sandhu, P. S.; Batra, R. S.; Khurana, R. K.; Singh, B., QbD-based systematic development of novel optimized solid self-nanoemulsifying drug delivery systems (SNEDDS) of lovastatin with enhanced biopharmaceutical performance. *Drug Delivery* **2015,** *22* (6), 765-784.

357. Zhang, Y.; Zhang, H.; Che, E.; Zhang, L.; Han, J.; Yang, Y.; Wang, S.; Zhang, M.; Gao, C., Development of novel mesoporous nanomatrix-supported lipid bilayers for oral sustained delivery of the water-insoluble drug, lovastatin. *Colloids and Surfaces B: Biointerfaces* **2015,** *128*, 77-85.

358. Gu, X.; Zhang, W.; Liu, J.; Shaw, J. P.; Shen, Y.; Xu, Y.; Lu, H.; Wu, Z., Preparation and characterization of a lovastatin-loaded protein-free nanostructured lipid carrier resembling high-density lipoprotein and evaluation of its targeting to foam cells. *AAPS PharmSciTech* **2011,** *12* (4), 1200-1208.

359. Suresh, G.; Manjunath, K.; Venkateswarlu, V.; Satyanarayana, V., Preparation, characterization, and in vitro and in vivo evaluation of lovastatin solid lipid nanoparticles. *AAPS PharmSciTech* **2007,** *8* (1).

360. Yasmin, R.; Rao, S.; Bremmell, K. E.; Prestidge, C. A., Porous Silica-Supported Solid Lipid Particles for Enhanced Solubilization of Poorly Soluble Drugs. *AAPS Journal* **2016,** *18* (4), 876-885.

361. Seenivasan, A.; Panda, T.; Théodore, T., Lovastatin nanoparticle synthesis and characterization for better drug delivery. *Open Biotechnol J* **2011,** *5* (1), 28-32.

362. Mandal, S., Microemulsion drug delivery system: design and development for oral bioavailability enhancement of lovastatin. *SA Pharmaceutical Journal* **2011,** *78* (3), 44-50.

363. Ge, Z.; ZHANG, X. x.; Gan, L.; Gan, Y., Redispersible, dry emulsion of lovastatin protects against intestinal metabolism and improves bioavailability. *Acta Pharmacologica Sinica* **2008,** *29* (8), 990-997.

364. Guan, Q.; Chen, W.; Hu, X., Development of lovastatin-loaded poly(lactic acid) microspheres for sustained oral delivery: In vitro and ex vivo evaluation. *Drug Design, Development and Therapy* **2015,** *9*, 791-798.

365. Rao, S.; Tan, A.; Boyd, B. J.; Prestidge, C. A., Synergistic role of self-emulsifying lipids and nanostructured porous silica particles in optimizing the oral delivery of lovastatin. *Nanomedicine* **2014,** *9* (18), 2745-2759.

366. Zhou, J.; Zhou, D., Improvement of oral bioavailability of lovastatin by using nanostructured lipid carriers. *Drug Design, Development and Therapy* **2015,** *9*, 5269-5275.

367. Su, T. C., EVALUATION OF THE PERMEABILITY OF DIFFERENT LIPOSOME-ENCAPSULATED LOVASTATIN BY APPLICATION OF THE CACO-2 MODEL Keyword CACO-2 Liposome Permeability of different.

368. Yanamandra, S.; Venkatesan, N.; Kadajji, V. G.; Wang, Z.; Issar, M.; Betageri, G. V., Proliposomes as a drug delivery system to decrease the hepatic first-pass metabolism: Case study using a model drug. *European Journal of Pharmaceutical Sciences* **2014,** *64*, 26-36.

369. Shi, B.; Fang, C.; You, M. X.; Zhang, Y.; Fu, S.; Pei, Y., Stealth MePEG-PCL micelles: effects of polymer composition on micelle physicochemical characteristics, in vitro drug release, in vivo pharmacokinetics in rats and biodistribution in S180 tumor bearing mice. *Colloid and Polymer Science* **2005,** *283* (9), 954-967.

370. Liu, X.; Li, X.; Zhou, L.; Li, S.; Sun, J.; Wang, Z.; Gao, Y.; Jiang, Y.; Lu, H.; Wang, Q.; Dai, J., Effects of simvastatin-loaded polymeric micelles on human osteoblast-like MG-63 cells. *Colloids and Surfaces B: Biointerfaces* **2013,** *102* (0), 420-427.

371. Mezei, M.; Gulasekharam, V., Liposomes - a selective drug delivery system for the topical route of administration I. Lotion dosage form. *Life Sciences* **1980,** *26* (18), 1473-1477.

372. Tsukioka, Y.; Matsumura, Y.; Hamaguchi, T.; Koike, H.; Moriyasu, F.; Kakizoe, T., Pharmaceutical and Biomedical Differences between Micellar Doxorubicin (NK911) and Liposomal Doxorubicin (Doxil). *Japanese Journal of Cancer Research* **2002,** *93* (10), 1145-1153.

373. Gonzalez-Lopez, J.; Alvarez-Lorenzo, C.; Taboada, P.; Sosnik, A.; Sandez-Macho, I.; Concheiro, A., Self-Associative Behavior and Drug-Solubilizing Ability of Poloxamine (Tetronic) Block Copolymers. *Langmuir* **2008,** *24* (19), 10688-10697.

374. Yanamandra, S.; Venkatesan, N.; Kadajji, V. G.; Wang, Z.; Issar, M.; Betageri, G. V., Proliposomes as a drug delivery system to decrease the hepatic first-pass metabolism: Case study using a model drug. *European Journal of Pharmaceutical Sciences* **2014,** *64* (Supplement C), 26-36.

375. Kumar, R.; Rana, A. C.; Bala, R.; Seth, N., Formulation and evaluation of elastic liposomes of Clotrimazole. *International Journal of Drug Development and Research* **2012,** *4* (3), 348-355.

376. Yuk, S. H.; Oh, K. S.; Koo, H.; Jeon, H.; Kim, K.; Kwon, I. C., Multi-core vesicle nanoparticles based on vesicle fusion for delivery of chemotherapic drugs. *Biomaterials* **2011,** *32* (31), 7924-7931.

377. Bowey, K.; Tanguay, J. F.; Tabrizian, M., Liposome technology for cardiovascular disease treatment and diagnosis. *Expert Opinion on Drug Delivery* **2012,** *9* (2), 249-265.

378. Abe, K.; Higashi, K.; Watabe, K.; Kobayashi, A.; Limwikrant, W.; Yamamoto, K.; Moribe, K., Effects of the PEG molecular weight of a PEG-lipid and cholesterol on PEG chain flexibility on liposome surfaces. *Colloids and Surfaces A: Physicochemical and Engineering Aspects* **2015,** *474*, 63-70.

379. Varma, M. V.; Kaushal, A. M.; Garg, A.; Garg, S., Factors affecting mechanism and kinetics of drug release from matrix-based oral controlled drug delivery systems. *American Journal of drug delivery* **2004,** *2* (1), 43-57.

380. Shin, S. C.; Lee, H. J., Controlled release of triprolidine using ethylene-vinyl acetate membrane and matrix systems. *European Journal of Pharmaceutics and Biopharmaceutics* **2002,** *54* (2), 201-206.

381. Yan, A.; Von Dem Bussche, A.; Kane, A. B.; Hurt, R. H., Tocopheryl polyethylene glycol succinate as a safe, antioxidant surfactant for processing carbon nanotubes and fullerenes. *Carbon* **2007,** *45* (13), 2463-2470.

382. Shen, J.; Burgess, D. J., Accelerated in-vitro release testing methods for extended-release parenteral dosage forms. *Journal of Pharmacy and Pharmacology* **2012,** *64* (7), 986-996.

383. Mohanraj, V. J.; Barnes, T. J.; Prestidge, C. A., Silica nanoparticle coated liposomes: A new type of hybrid nanocapsule for proteins. *International Journal of Pharmaceutics* **2010,** *392* (1-2), 285-293.

384. Afergan, E.; David, M. B.; Epstein, H.; Koroukhov, N.; Gilhar, D.; Rohekar, K.; Danenberg, H. D.; Golomb, G., Liposomal simvastatin attenuates neointimal hyperplasia in rats. *AAPS Journal* **2010,** *12* (2), 181-187.

385. Bhardwaj, U.; Burgess, D. J., Physicochemical properties of extruded and non-extruded liposomes containing the hydrophobic drug dexamethasone. *International journal of pharmaceutics* **2010,** *388* (1), 181-189.

386. Hope, M. J.; Nayar, R.; Mayer, L. D.; Cullis, P., Reduction of liposome size and preparation of unilamellar vesicles by extrusion techniques. *Liposome technology* **1993,** *1*, 123-139.

387. Mayer, L. D.; Hope, M. J.; Cullis, P. R.; Janoff, A. S., Solute distributions and trapping efficiencies observed in freeze-thawed multilamellar vesicles. *Biochimica et Biophysica Acta (BBA) - Biomembranes* **1985,** *817* (1), 193-196.

388. Tivol, W. F.; Briegel, A.; Jensen, G. J., An Improved Cryogen for Plunge Freezing. *Microscopy and Microanalysis* **2008,** *14* (5), 375-379.

389. Dobro, M. J.; Melanson, L. A.; Jensen, G. J.; McDowall, A. W., Chapter Three - Plunge Freezing for Electron Cryomicroscopy. In *Methods in Enzymology*, Jensen, G. J., Ed. Academic Press: 2010; Vol. 481, pp 63-82.

390. Xiangyang, X.; Ling, L.; Jianping, Z.; Shiyue, L.; Jie, Y.; Xiaojin, Y.; Jinsheng, R., Preparation and characterization of N-succinyl-N′-octyl chitosan micelles as doxorubicin carriers for effective anti-tumor activity. *Colloids and Surfaces B: Biointerfaces* **2007,** *55* (2), 222-228.

391. Maarten, Handbook of biodegradable polymers.

392. Liu, T.; Nace, V. M.; Chu, B., Cloud-Point Temperatures of BnEmBn and PnEmPn Type Triblock Copolymers in Aqueous Solution. *The Journal of Physical Chemistry B* **1997,** *101* (41), 8074-8078.

393. Lim, E.-K.; Yang, J.; Park, M.-y.; Park, J.; Suh, J.-S.; Yoon, H.-G.; Huh, Y.-M.; Haam, S., Synthesis of water soluble PEGylated magnetic complexes using mPEG-fatty acid for biomedical applications. *Colloids and Surfaces B: Biointerfaces* **2008,** *64* (1), 111-117.

394. Baines, F. L.; Armes, S. P.; Billingham, N. C.; Tuzar, Z., Micellization of Poly(2-(dimethylamino)ethyl methacrylate-block-methyl methacrylate) Copolymers in Aqueous Solution. *Macromolecules* **1996,** *29* (25), 8151-8159.

395. Mittal, K. L.; Shah, D. O., *Surfactants in solution*. Springer Science & Business Media: 2013; Vol. 11.

396. Zhao, L.; Du, J.; Duan, Y.; Zang, Y. n.; Zhang, H.; Yang, C.; Cao, F.; Zhai, G., Curcumin loaded mixed micelles composed of Pluronic P123 and F68: Preparation, optimization and in vitro characterization. *Colloids and Surfaces B: Biointerfaces* **2012,** *97* (0), 101-108.

397. Wei, Z.; Hao, J.; Yuan, S.; Li, Y.; Juan, W.; Sha, X.; Fang, X., Paclitaxel-loaded Pluronic P123/F127 mixed polymeric micelles: Formulation, optimization and in vitro characterization. *International Journal of Pharmaceutics* **2009,** *376* (1), 176-185.

398. Zhang, W.; Shi, Y.; Chen, Y.; Ye, J.; Sha, X.; Fang, X., Multifunctional Pluronic P123/F127 mixed polymeric micelles loaded with paclitaxel for the treatment of multidrug resistant tumors. *Biomaterials* **2011,** *32* (11), 2894-2906.

399. Hu, F.-Q.; Ren, G.-F.; Yuan, H.; Du, Y.-Z.; Zeng, S., Shell cross-linked stearic acid grafted chitosan oligosaccharide self-aggregated micelles for controlled release of paclitaxel. *Colloids and Surfaces B: Biointerfaces* **2006,** *50* (2), 97-103.

400. Matsuoka, K.; Suzuki, M.; Honda, C.; Endo, K.; Moroi, Y., Micellization of conjugated chenodeoxy- and ursodeoxycholates and solubilization of cholesterol into their micelles: comparison with other four conjugated bile salts species. *Chemistry and Physics of Lipids* **2006,** *139* (1), 1-10.

401. Funasaki, N.; Nomura, M.; Ishikawa, S.; Neya, S., Hydrophobic Self-Association of Sodium Taurochenodeoxycholate and Tauroursodeoxycholate. *The Journal of Physical Chemistry B* **2000,** *104* (32), 7745-7751.

402. Ninomiya, R.; Matsuoka, K.; Moroi, Y., Micelle formation of sodium chenodeoxycholate and solubilization into the micelles: comparison with other unconjugated bile salts. *Biochimica et Biophysica Acta (BBA) - Molecular and Cell Biology of Lipids* **2003,** *1634* (3), 116-125.

403. Sugioka, H.; Matsuoka, K.; Moroi, Y., Temperature effect on formation of sodium cholate micelles. *Journal of Colloid and Interface Science* **2003,** *259* (1), 156-162.

404. Coello, A.; Meijide, F.; Núñez, E. R.; Tato, J. V., Aggregation behavior of bile salts in aqueous solution. *Journal of Pharmaceutical Sciences* **1996,** *85* (1), 9-15.

405. Garidel, P.; Hildebrand, A.; Neubert, R.; Blume, A., Thermodynamic Characterization of Bile Salt Aggregation as a Function of Temperature and Ionic Strength Using Isothermal Titration Calorimetry. *Langmuir* **2000,** *16* (12), 5267-5275.

406. Small, D. M., Size and Structure of Bile Salt Micelles. In *Molecular Association in Biological and Related Systems*, AMERICAN CHEMICAL SOCIETY: 1968; Vol. 84, pp 31-52.

407. NICOLA, Bile salts: definition, functions, enterohepatic circulation, synthesis. **2016**.

408. Singh, J.; Unlu, Z.; Ranganathan, R.; Griffiths, P., Aggregate Properties of Sodium Deoxycholate and Dimyristoylphosphatidylcholine Mixed Micelles. *The Journal of Physical Chemistry B* **2008,** *112* (13), 3997-4008.

409. Balmbra, R. R.; Clunie, J. S.; Corkill, J. M.; Goodman, J. F., Variations in the micelle size of non-ionic detergents. *Transactions of the Faraday Society* **1964,** *60*, 979-985.

410. Letchford, K.; Liggins, R.; Burt, H., Solubilization of hydrophobic drugs by methoxy poly(ethylene glycol)‐block‐polycaprolactone diblock copolymer micelles: Theoretical and experimental data and correlations. *Journal of Pharmaceutical Sciences 97* (3), 1179-1190.

411. Moriarty, R. M.; David, N. E.; Mahmood, N. A.; Prasad, A. R.; Swaringen, R. A.; Reid, J. G.; Sahoo, A. K., Synthetic Bile Acid Composition, Method, and Preparation. Google Patents: 2012.

412. Letchford, K.; Burt, H., A review of the formation and classification of amphiphilic block copolymer nanoparticulate structures: micelles, nanospheres, nanocapsules and polymersomes. *European Journal of Pharmaceutics and Biopharmaceutics* **2007,** *65* (3), 259-269.

413. Madenci, D.; Egelhaaf, S. U., Self-assembly in aqueous bile salt solutions. *Current Opinion in Colloid & Interface Science* **2010,** *15* (1), 109-115.

414. Kumar, K.; Patial, B. S.; Chauhan, S., Conductivity and fluorescence studies on the micellization properties of sodium cholate and sodium deoxycholate in aqueous medium at different temperatures: Effect of selected amino acids. *The Journal of Chemical Thermodynamics* **2015,** *82* (Supplement C), 25-33.

415. Gao, Y.; Li, L. B.; Zhai, G., Preparation and characterization of Pluronic/TPGS mixed micelles for solubilization of camptothecin. *Colloids and Surfaces B: Biointerfaces* **2008,** *64* (2), 194-199.

416. Arafat, M.; Kirchhoefer, C.; Mikov, M., Mixed Micelles Loaded with Bile Salt: An Approach to Enhance Intestinal Transport of the BCS Class III Drug Cefotaxime in Rats. *European Journal of Drug Metabolism and Pharmacokinetics* **2017,** *42* (4), 635-645.

417. Honary, S.; Zahir, F., Effect of zeta potential on the properties of nano-drug delivery systems - A review (Part 1). *Tropical Journal of Pharmaceutical Research* **2013,** *12* (2), 255-264.

418. Honary, S.; Zahir, F., Effect of zeta potential on the properties of nano-drug delivery systems - A review (Part 2). *Tropical Journal of Pharmaceutical Research* **2013,** *12* (2), 265-273.

419. Zhang, T.; Luo, J.; Fu, Y.; Li, H.; Ding, R.; Gong, T.; Zhang, Z., Novel oral administrated paclitaxel micelles with enhanced bioavailability and antitumor efficacy for resistant breast cancer. *Colloids and Surfaces B: Biointerfaces* **2017,** *150*, 89-97.

420. Mu, L.; Elbayoumi, T. A.; Torchilin, V. P., Mixed micelles made of poly(ethylene glycol)–phosphatidylethanolamine conjugate and d-α-tocopheryl polyethylene glycol 1000 succinate as pharmaceutical nanocarriers for camptothecin. *International Journal of Pharmaceutics* **2005,** *306* (1), 142-149.

421. Jhaveri, A. M.; Torchilin, V. P., Multifunctional polymeric micelles for delivery of drugs and siRNA. *Frontiers in Pharmacology* **2014,** *5*, 77.

422. Xiang, Y.; Liang, L.; Wang, X.; Wang, J.; Zhang, X.; Zhang, Q., Chloride channel-mediated brain glioma targeting of chlorotoxin-modified doxorubicine-loaded liposomes. *Journal of Controlled Release* **2011,** *152* (3), 402-410.

423. Nava, G.; Piñón, E.; Mendoza, L.; Mendoza, N.; Quintanar, D.; Ganem, A., Formulation and in vitro, ex vivo and in vivo evaluation of elastic liposomes for transdermal delivery of ketorolac tromethamine. *Pharmaceutics* **2011,** *3* (4), 954-970.

424. Sharma, A.; Straubinger, N. L.; Straubinger, R. M., Modulation of human ovarian tumor cell sensitivity to N-(phosphonacetyl)-L-aspartate (PALA) by liposome drug carriers. *Pharmaceutical research* **1993,** *10* (10), 1434-1441.

425. Mura, P.; Maestrelli, F.; González-Rodríguez, M. L.; Michelacci, I.; Ghelardini, C.; Rabasco, A. M., Development, characterization and in vivo evaluation of benzocaine-loaded liposomes. *European Journal of Pharmaceutics and Biopharmaceutics* **2007,** *67* (1), 86-95.

426. Cereda, S.; De Araujo, D. R.; De Paula, E., Liposomal prilocaine: preparation, characterization, and in vivo evaluation. *Journal of Pharmacy and Pharmaceutical Sciences* **2004**.

427. de Paula, E.; Schreier, S., Use of a novel method for determination of partition coefficients to compare the effect of local anesthetics on membrane structure. *Biochimica et Biophysica Acta (BBA)-Biomembranes* **1995,** *1240* (1), 25-33.

428. Maurer, N.; Fenske, D. B.; Cullis, P. R., Developments in liposomal drug delivery systems. *Expert opinion on biological therapy* **2001,** *1* (6), 923-947.

429. Sriwongsitanont, S.; Ueno, M., Effect of freeze-thawing process on the size and lamellarity of PEG-lipid liposomes. *The Open Colloid Science Journal* **2010,** *4* (1).

430. MacDonald, R. C., Method of preparing giant size liposomes. Google Patents: 1985.

431. Ashley, C. E.; Carnes, E. C.; Phillips, G. K.; Padilla, D.; Durfee, P. N.; Brown, P. A.; Hanna, T. N.; Liu, J.; Phillips, B.; Carter, M. B., The targeted delivery of multicomponent cargos to cancer cells by nanoporous particle-supported lipid bilayers. *Nature materials* **2011,** *10* (5), 389-397.

432. Johnsson, M.; Edwards, K., Liposomes, Disks, and Spherical Micelles: Aggregate Structure in Mixtures of Gel Phase Phosphatidylcholines and Poly(Ethylene Glycol)-Phospholipids. *Biophysical Journal* **2003,** *85* (6), 3839-3847.

433. Urbán, P.; Estelrich, J.; Adeva, A.; Cortés, A.; Fernàndez-Busquets, X., Study of the efficacy of antimalarial drugs delivered inside targeted immunoliposomal nanovectors. *Nanoscale research letters* **2011,** *6* (1), 620.

434. Cautela, J.; Giustini, M.; Pavel, N. V.; Palazzo, G.; Galantini, L., Wormlike reverse micelles in lecithin/bile salt/water mixtures in oil. *Colloids and Surfaces A: Physicochemical and Engineering Aspects* **2017,** *532* (Supplement C), 411-419.

435. Cai, S.; Vijayan, K.; Cheng, D.; Lima, E. M.; Discher, D. E., Micelles of Different Morphologies—Advantages of Worm-like Filomicelles of PEO-PCL in Paclitaxel Delivery. *Pharmaceutical Research* **2007,** *24* (11), 2099-2109.

436. Du, Y.-Z.; Wang, L.; Yuan, H.; Wei, X.-H.; Hu, F.-Q., Preparation and characteristics of linoleic acid-grafted chitosan oligosaccharide micelles as a carrier for doxorubicin. *Colloids and Surfaces B: Biointerfaces* **2009,** *69* (2), 257-263.

437. Tan, S.; Li, X.; Guo, Y.; Zhang, Z., Lipid-enveloped hybrid nanoparticles for drug delivery. *Nanoscale* **2013,** *5* (3), 860-872.

438. Rudra, A.; Deepa, R. M.; Ghosh, M. K.; Ghosh, S.; Mukherjee, B., Doxorubicin-loaded phosphatidylethanolamine-conjugated nanoliposomes: in vitro characterization and their accumulation in liver, kidneys, and lungs in rats. *International journal of nanomedicine* **2010,** *5*, 811-823.

439. Tilcock, C. P. S.; Fisher, D., The interaction of phospholipid membranes with poly(ethylene glycol). Vesicle aggregation and lipid exchange. *Biochimica et Biophysica Acta (BBA) - Biomembranes* **1982,** *688* (2), 645-652.

440. Malinin, V. S.; Frederik, P.; Lentz, B. R., Osmotic and Curvature Stress Affect PEG-Induced Fusion of Lipid Vesicles but Not Mixing of Their Lipids. *Biophysical Journal* **2002,** *82* (4), 2090-2100.

441. Ji, X.; Gao, Y.; Chen, L.; Zhang, Z.; Deng, Y.; Li, Y., Nanohybrid systems of non-ionic surfactant inserting liposomes loading paclitaxel for reversal of multidrug resistance. *International Journal of Pharmaceutics* **2012,** *422* (1), 390-397.

442. Zhang, L.; Granick, S., How to Stabilize Phospholipid Liposomes (Using Nanoparticles). *Nano Letters* **2006,** *6* (4), 694-698.

443. Kuo-Sheng, L.; Chih-Jen, W.; Tzu-Chen, Y.; Sung, K. C.; Ming-Chuan, K.; Jhi-Joung, W.; Jia-You, F., Combined strategies of apomorphine diester prodrugs and nanostructured lipid carriers for efficient brain targeting. *Nanotechnology* **2012,** *23* (9), 095103.

444. Williams, A. C.; Barry, B. W., Penetration enhancers. *Advanced Drug Delivery Reviews* **2004,** *56* (5), 603-618.

445. Korsmeyer, R. W.; Gurny, R.; Doelker, E.; Buri, P.; Peppas, N. A., Mechanisms of solute release from porous hydrophilic polymers. *International journal of pharmaceutics* **1983,** *15* (1), 25-35.

446. Biswas, G. R.; Majee, S. B., Modeling of drug-diffusion kinetics of amoxicillin trihydrate from buccal tablets. *International Journal of Pharma and Bio Sciences* **2015,** *6* (2), B859-B866.

447. Chavda, H.; Patel, C., Preparation and in vitro evaluation of a stomach specific drug delivery system based on superporous hydrogel composite. *Indian Journal of Pharmaceutical Sciences* **2011,** *73* (1), 30-37.

448. Chopra, S.; Venkatesan, N.; Betageri, G. V., Formulation of lipid bearing pellets as a delivery system for poorly soluble drugs. *International Journal of Pharmaceutics* **2013,** *446* (1-2), 136-144.

449. Haghiralsadat, F.; Amoabediny, G.; Helder, M. N.; Naderinezhad, S.; Sheikhha, M. H.; Forouzanfar, T.; Zandieh-doulabi, B., A comprehensive mathematical model of drug release kinetics from nano-liposomes, derived from optimization studies of cationic PEGylated liposomal doxorubicin formulations for drug-gene delivery. *Artificial Cells, Nanomedicine and Biotechnology* **2017**, 1-9.

450. Kunasekaran, V.; Krishnamoorthy, K., Kinetic modeling of Rasagiline mesylate from nanoscale solid lipid particles. *International Journal of Pharmacy and Pharmaceutical Sciences* **2015,** *7* (11), 300-305.

451. Sareen, R.; Bhardwaj, V.; Mehta, V.; Sharma, A., Topical gel incorporated with non-ionic surfactant based solid lipid microspheres of ketoprofen: Physicochemical analysis and anti-inflammatory evaluation. *International Journal of Pharmacy and Pharmaceutical Sciences* **2015,** *7* (10), 199-206.

452. Simi, S. P.; Saraswathi, R.; Sankar, C.; Krishnan, P. N.; Dilip, C.; Ameena, K., Formulation and evaluation of Albendazole microcapsules for colon delivery using chitosan. *Asian Pacific Journal of Tropical Medicine* **2010,** *3* (5), 374-378.

453. Panda, J. J.; Mishra, A.; Basu, A.; Chauhan, V. S., Stimuli responsive self-assembled hydrogel of a low molecular weight free dipeptide with potential for tunable drug delivery. *Biomacromolecules* **2008,** *9* (8), 2244-2250.

454. Piecha, M.; Sarakha, M.; Trebše, P.; Kočar, D., Stability studies of cholesterol lowering statin drugs in aqueous samples using HPLC and LC-MS. *Environmental Chemistry Letters* **2010,** *8* (2), 185-191.

455. Mukhopadhyay, S.; Maitra, U., Chemistry and biology of bile acids. *Current Science* **2004,** *87* (12), 1666-1683.

456. Rich, A.; Blow, D. M., Formation of a Helical Steroid Complex. *Nature* **1958,** *182*, 423.

457. Blow, D. M.; Rich, A., Studies on the Formation of Helical Deoxycholate Complexes. *Journal of the American Chemical Society* **1960,** *82* (14), 3566-3571.

458. Hasan, M.; Ben Messaoud, G.; Michaux, F.; Tamayol, A.; Kahn, C. J. F.; Belhaj, N.; Linder, M.; Arab-Tehrany, E., Chitosan-coated liposomes encapsulating curcumin: study of lipid-polysaccharide interactions and nanovesicle behavior. *RSC Advances* **2016,** *6* (51), 45290-45304.

459. Clogston, J. D.; Patri, A. K., Importance of Physicochemical Characterization Prior to Immunological Studies. In *Handbook of Immunological Properties of Engineered Nanomaterials*, WORLD SCIENTIFIC: 2012; pp 25-52.

460. Smith, M. C.; Crist, R. M.; Clogston, J. D.; McNeil, S. E., Zeta potential: a case study of cationic, anionic, and neutral liposomes. *Analytical and Bioanalytical Chemistry* **2017,** *409* (24), 5779-5787.

461. Alvarez-Lorenzo, C.; Concheiro, A., Polymeric micelles as drug stabilizers: the camptothecin and simvastatin cases. *Journal of Drug Delivery Science and Technology* **2010,** *20* (4), 249-257.

462. Ola, H.; Yahiya, S. A.; El-Gazayerly, O. N., Effect of formulation design and freeze-drying on properties of fluconazole multilamellar liposomes. *Saudi Pharmaceutical Journal* **2010,** *18* (4), 217-224.

463. Jacobsen, W.; Kirchner, G.; Hallensleben, K.; Mancinelli, L.; Deters, M.; Hackbarth, I.; Benet, L. Z.; Sewing, K.-F.; Christians, U., Comparison of Cytochrome P-450-Dependent Metabolism and Drug Interactions of the 3-Hydroxy-3-methylglutaryl-CoA Reductase Inhibitors Lovastatin and Pravastatin in the Liver. *Drug Metabolism and Disposition* **1999,** *27* (2), 173-179.

464. Staud, F.; Ceckova, M.; Micuda, S.; Pavek, P., Expression and Function of P-Glycoprotein in Normal Tissues: Effect on Pharmacokinetics. In *Multi-Drug Resistance in Cancer*, Zhou, J., Ed. Humana Press: Totowa, NJ, 2010; pp 199-222.

465. Hunter, J.; Jepson, M. A.; Tsuruo, T.; Simmons, N. L.; Hirst, B. H., Functional expression of P-glycoprotein in apical membranes of human intestinal Caco-2 cells. Kinetics of vinblastine secretion and interaction with modulators. *Journal of Biological Chemistry* **1993,** *268* (20), 14991-14997.

466. Karlsson, J.; Kuo, S.-M.; Ziemniak, J.; Artursson, P., Transport of celiprolol across human intestinal epithelial (Caco-2) cells: mediation of secretion by multiple transporters including P-glycoprotein. *British Journal of Pharmacology* **1993,** *110* (3), 1009-1016.

467. Zaman, G. J. R.; Flens, M. J.; Van Leusden, M. R.; De Haas, M.; Mülder, H. S.; Lankelma, J.; Pinedo, H. M.; Scheper, R. J.; Baas, F.; Broxterman, H. J.; Borst, P., The human multidrug resistance-associated protein MRP is a plasma membrane drug-efflux pump. *Proceedings of the National Academy of Sciences of the United States of America* **1994,** *91* (19), 8822-8826.

468. Stephens, R. H.; O'Neill, C. A.; Warhurst, A.; Carlson, G. L.; Rowland, M.; Warhurst, G., Kinetic Profiling of P-glycoprotein-Mediated Drug Efflux in Rat and Human Intestinal Epithelia. *Journal of Pharmacology and Experimental Therapeutics* **2001,** *296* (2), 584-591.

469. Huisman, M. T.; Smit, J. W.; Wiltshire, H. R.; Hoetelmans, R. M. W.; Beijnen, J. H.; Schinkel, A. H., P-Glycoprotein Limits Oral Availability, Brain, and Fetal Penetration of Saquinavir Even with High Doses of Ritonavir. *Molecular Pharmacology* **2001,** *59* (4), 806-813.

470. Sparreboom, A.; van Asperen, J.; Mayer, U.; Schinkel, A. H.; Smit, J. W.; Meijer, D. K. F.; Borst, P.; Nooijen, W. J.; Beijnen, J. H.; van Tellingen, O., Limited oral bioavailability and active epithelial excretion of paclitaxel (Taxol) caused by P-glycoprotein in the intestine. *Proceedings of the National Academy of Sciences* **1997,** *94* (5), 2031-2035.

471. Lo, Y.-L., Phospholipids as multidrug resistance modulators of the transport of epirubicin in human intestinal epithelial Caco-2 cell layers and everted gut sacs of rats. *Biochemical Pharmacology* **2000,** *60* (9), 1381-1390.

472. Sugawara, T.; Kushiro, M.; Zhang, H.; Nara, E.; Ono, H.; Nagao, A., Lysophosphatidylcholine Enhances Carotenoid Uptake from Mixed Micelles by Caco-2 Human Intestinal Cells. *The Journal of Nutrition* **2001,** *131* (11), 2921-2927.

473. Hovgaard, L.; Brøndsted, H.; Nielsen, H. M., Drug delivery studies in Caco-2 monolayers. II. Absorption enhancer effects of lysophosphatidylcholines. *International Journal of Pharmaceutics* **1995,** *114* (2), 141-149.

474. Ward, P. D.; Tippin, T. K.; Thakker, D. R., Enhancing paracellular permeability by modulating epithelial tight junctions. *Pharmaceutical Science & Technology Today* **2000,** *3* (10), 346-358.

475. Antunes, F.; Andrade, F.; Ferreira, D.; Nielsen, H. M.; Sarmento, B., Models to predict intestinal absorption of therapeutic peptides and proteins. *Current Drug Metabolism* **2013,** *14* (1), 4-20.

476. Sarmento, B.; Andrade, F.; Da Silva, S. B.; Rodrigues, F.; Das Neves, J.; Ferreira, D., Cell-based in vitro models for predicting drug permeability. *Expert Opinion on Drug Metabolism and Toxicology* **2012,** *8* (5), 607-621.

477. Johansson, F.; Hjertberg, E.; Eirefelt, S.; Tronde, A.; Hultkvist Bengtsson, U., Mechanisms for absorption enhancement of inhaled insulin by sodium taurocholate. *European Journal of Pharmaceutical Sciences* **2002,** *17* (1), 63-71.

478. Sun, H.; Chow, E. C. Y.; Liu, S.; Du, Y.; Pang, K. S., The Caco-2 cell monolayer: usefulness and limitations. *Expert Opinion on Drug Metabolism & Toxicology* **2008,** *4* (4), 395-411.

479. Balimane, P. V.; Han, Y.-H.; Chong, S., Current industrial practices of assessing permeability and P-glycoprotein interaction. *The AAPS Journal* **2006,** *8* (1), E1-E13.

480. Marsousi, N.; Doffey-Lazeyras, F.; Rudaz, S.; Desmeules, J. A.; Daali, Y., Intestinal permeability and P-glycoprotein-mediated efflux transport of ticagrelor in Caco-2 monolayer cells. *Fundamental and Clinical Pharmacology* **2016,** *30* (6), 577-584.

481. Zhou, S. F., Structure, function and regulation of P-glycoprotein and its clinical relevance in drug disposition. *Xenobiotica* **2008,** *38* (7-8), 802-832.

482. Murakami, T., Absorption sites of orally administered drugs in the small intestine. *Expert Opinion on Drug Discovery* **2017,** *12* (12), 1219-1232.

483. Haghiralsadat, F.; Amoabediny, G.; Sheikhha, M. H.; Zandieh-doulabi, B.; Naderinezhad, S.; Helder, M. N.; Forouzanfar, T., New liposomal doxorubicin nanoformulation for osteosarcoma: Drug release kinetic study based on thermo and pH sensitivity. *Chemical Biology and Drug Design* **2017,** *90* (3), 368-379.

484. Deli, M. A., Potential use of tight junction modulators to reversibly open membranous barriers and improve drug delivery. *Biochimica et Biophysica Acta (BBA) - Biomembranes* **2009,** *1788* (4), 892-910.

485. Hidalgo, I. J.; Raub, T. J.; Borchardt, R. T., Characterization of the human colon carcinoma cell line (Caco-2) as a model system for intestinal epithelial permeability. *Gastroenterology* **1989,** *96* (3), 736-749.

486. Hidalgo, I. J., Assessing the absorption of new pharmaceuticals. *Current topics in medicinal chemistry* **2001,** *1* (5), 385-401.

487. Hidalgo, I. J.; Borchardt, R. T., Transport of bile acids in a human intestinal epithelial cell line, Caco-2. *Biochimica et Biophysica Acta (BBA) - General Subjects* **1990,** *1035* (1), 97-103.

488. Artursson, P., Cell cultures as models for drug absorption across the intestinal mucosa. *Critical reviews in therapeutic drug carrier systems* **1991,** *8* (4), 305-330.

489. Srinivasan, B.; Kolli, A. R.; Esch, M. B.; Abaci, H. E.; Shuler, M. L.; Hickman, J. J., TEER measurement techniques for in vitro barrier model systems. *Journal of laboratory automation* **2015,** *20* (2), 107-126.

490. Raeissi, S. D.; Hidalgo, I. J.; Segura-Aguilar, J.; Artursson, P., Interplay Between CYP3A-Mediated Metabolism and Polarized Efflux of Terfenadine and Its Metabolites in Intestinal Epithelial Caco-2 (TC7) Cell Monolayers. *Pharmaceutical Research* **1999,** *16* (5), 625-632.

491. Roger, E.; Lagarce, F.; Garcion, E.; Benoit, J.-P., Biopharmaceutical parameters to consider in order to alter the fate of nanocarriers after oral delivery. *Nanomedicine* **2010,** *5* (2), 287-306.

492. Niu, M.; Lu, Y.; Hovgaard, L.; Guan, P.; Tan, Y.; Lian, R.; Qi, J.; Wu, W., Hypoglycemic activity and oral bioavailability of insulin-loaded liposomes containing bile salts in rats: the effect of cholate type, particle size and administered dose. *European Journal of Pharmaceutics and Biopharmaceutics* **2012,** *81* (2), 265-272.

493. Chen, W.; Miao, Y.-Q.; Fan, D.-J.; Yang, S.-S.; Lin, X.; Meng, L.-K.; Tang, X., Bioavailability Study of Berberine and the Enhancing Effects of TPGS on Intestinal Absorption in Rats. *AAPS PharmSciTech* **2011,** *12* (2), 705-711.

494. Ujhelyi, Z.; Fenyvesi, F.; Váradi, J.; Fehér, P.; Kiss, T.; Veszelka, S.; Deli, M.; Vecsernyés, M.; Bácskay, I., Evaluation of cytotoxicity of surfactants used in self-micro emulsifying drug delivery systems and their effects on paracellular transport in Caco-2 cell monolayer. *European Journal of Pharmaceutical Sciences* **2012,** *47* (3), 564-573.

495. van Meerloo, J.; Kaspers, G. J.; Cloos, J., Cell sensitivity assays: the MTT assay. *Cancer cell culture: methods and protocols* **2011**, 237-245.

496. Sahebkar, A.; Badiee, A.; Ghayour-Mobarhan, M.; Goldouzian, S. R.; Jaafari, M. R., A simple and effective approach for the treatment of dyslipidemia using anionic nanoliposomes. *Colloids and Surfaces B: Biointerfaces* **2014,** *122*, 645-652.

497. Ferruzza, S.; Rossi, C.; Scarino, M. L.; Sambuy, Y., A protocol for differentiation of human intestinal Caco-2 cells in asymmetric serum-containing medium. *Toxicology in Vitro* **2012,** *26* (8), 1252-1255.

498. van der Merwe, S. M.; Verhoef, J. C.; Verheijden, J. H. M.; Kotzé, A. F.; Junginger, H. E., Trimethylated chitosan as polymeric absorption enhancer for improved peroral delivery of peptide drugs. *European Journal of Pharmaceutics and Biopharmaceutics* **2004,** *58* (2), 225-235.

499. Buckley, S. T.; Fischer, S. M.; Fricker, G.; Brandl, M., In vitro models to evaluate the permeability of poorly soluble drug entities: challenges and perspectives. *European journal of pharmaceutical sciences : official journal of the European Federation for Pharmaceutical Sciences* **2012,** *45* (3), 235-50.

500. Ménard, D.; Beaulieu, J.-F., Human Intestinal Brush Border Membrane Hydrolases. In *Membrane Physiopathology*, Bkaily, G., Ed. Springer US: Boston, MA, 1994; pp 319-341.

501. Wolf, K., Physiological salines for fresh-water teleosts. *The Progressive Fish-Culturist* **1963,** *25* (3), 135-140.

502. Zidan, A. S.; Spinks, C. B.; Habib, M. J.; Khan, M. A., Formulation and transport properties of tenofovir loaded liposomes through Caco-2 cell model. *Journal of liposome research* **2013,** *23* (4), 318-326.

503. Mo, R.; Jin, X.; Li, N.; Ju, C.; Sun, M.; Zhang, C.; Ping, Q., The mechanism of enhancement on oral absorption of paclitaxel by N-octyl-O-sulfate chitosan micelles. *Biomaterials* **2011,** *32* (20), 4609-4620.

504. Liang, E.; Chessic, K.; Yazdanian, M., Evaluation of an accelerated Caco-2 cell permeability model. *Journal of Pharmaceutical Sciences* **2000,** *89* (3), 336-345.

505. Souza, V. M.; Shertzer, H. G.; Menon, A. G.; Pauletti, G. M., High glucose concentration in isotonic media alters caco-2 cell permeability. *Aaps Pharmsci* **2003,** *5* (3), 17.

506. Bravo, S. A.; Nielsen, C. U.; Amstrup, J.; Frokjaer, S.; Brodin, B., In-depth evaluation of Gly-Sar transport parameters as a function of culture time in the Caco-2 cell model. *European journal of pharmaceutical sciences* **2004,** *21* (1), 77-86.

507. Anderle, P.; Niederer, E.; Rubas, W.; Hilgendorf, C.; Spahn-Langguth, H.; Wunderli-Allenspach, H.; Merkle, H. P.; Langguth, P., P-glycoprotein (P-gp) mediated efflux in Caco-2 cell monolayers: The influence of culturing conditions and drug exposure on P-gp expression levels. *Journal of pharmaceutical sciences* **1998,** *87* (6), 757-762.

508. Cheng, H. C.; Chang, C. Y.; Hsieh, F. I.; Yeh, J. J.; Chien, M. Y.; Pan, R. N.; Deng, M. C.; Liu, D. Z., Effects of tremella-alginate-liposome encapsulation on oral delivery of inactivated H5N3 vaccine. *Journal of Microencapsulation* **2011,** *28* (1), 55-61.

509. Boulenc, X.; Breul, T.; Gautier, J.-C.; Saudemon, P.; Joyeux, H.; Roques, C.; Berger, Y.; Fabre, G., Sodium lauryl sulphate increases tiludronate paracellular transport using human epithelial caco-2 monolayers. *International Journal of Pharmaceutics* **1995,** *123* (1), 71-83.

510. Yeh, T.-H.; Hsu, L.-W.; Tseng, M. T.; Lee, P.-L.; Sonjae, K.; Ho, Y.-C.; Sung, H.-W., Mechanism and consequence of chitosan-mediated reversible epithelial tight junction opening. *Biomaterials* **2011,** *32* (26), 6164-6173.

511. Li, J.; Wang, Y.; Zhang, W.; Huang, Y.; Hein, K.; Hidalgo, I. J., The Role of a Basolateral Transporter in Rosuvastatin Transport and Its Interplay with Apical Breast Cancer Resistance Protein in Polarized Cell Monolayer Systems. *Drug Metabolism and Disposition* **2012,** *40* (11), 2102-2108.

512. Pauli-Magnus, C.; von Richter, O.; Burk, O.; Ziegler, A.; Mettang, T.; Eichelbaum, M.; Fromm, M. F., Characterization of the Major Metabolites of Verapamil as Substrates and Inhibitors of P-glycoprotein. *Journal of Pharmacology and Experimental Therapeutics* **2000,** *293* (2), 376-382.

513. Kivistö, K. T.; Zukunft, J.; Hofmann, U.; Niemi, M.; Rekersbrink, S.; Schneider, S.; Luippold, G.; Schwab, M.; Eichelbaum, M.; Fromm, M. F., Characterisation of cerivastatin as a P-glycoprotein substrate: studies in P-glycoprotein-expressing cell monolayers and mdr1a/b knock-out mice. *Naunyn-Schmiedeberg's Archives of Pharmacology* **2004,** *370* (2), 124-130.

514. Wang, E.-j.; Casciano, C. N.; Clement, R. P.; Johnson, W. W., HMG-CoA Reductase Inhibitors (Statins) Characterized as Direct Inhibitors of P-Glycoprotein. *Pharmaceutical Research* **2001,** *18* (6), 800-806.

515. Artursson, P.; Karlsson, J., Correlation between oral drug absorption in humans and apparent drug permeability coefficients in human intestinal epithelial (Caco-2) cells. *Biochemical and biophysical research communications* **1991,** *175* (3), 880-885.

516. Lin, Y.-H.; Sonaje, K.; Lin, K. M.; Juang, J.-H.; Mi, F.-L.; Yang, H.-W.; Sung, H.-W., Multi-ion-crosslinked nanoparticles with pH-responsive characteristics for oral delivery of protein drugs. *Journal of Controlled Release* **2008,** *132* (2), 141-149.

517. Yoncheva, K.; Gómez, S.; Campanero, M. A.; Gamazo, C.; Irache, J. M., Bioadhesive properties of pegylated nanoparticles. *Expert Opinion on Drug Delivery* **2005,** *2* (2), 205-218.

518. Batrakova, E. V.; Han, H. Y.; Miller, D. W.; Kabanov, A. V., Effects of pluronic P85 unimers and micelles on drug permeability in polarized BBMEC and Caco-2 cells. *Pharmaceutical Research* **1998,** *15* (10), 1525-1532.

519. Barua, S.; Mitragotri, S., Challenges associated with penetration of nanoparticles across cell and tissue barriers: A review of current status and future prospects. *Nano Today* **2014,** *9* (2), 223-243.

520. Round, A. N.; Rigby, N. M.; Garcia De La Torre, A.; MacIerzanka, A.; Mills, E. N. C.; MacKie, A. R., Lamellar structures of MUC2-rich mucin: A potential role in governing the barrier and lubricating functions of intestinal mucus. *Biomacromolecules* **2012,** *13* (10), 3253-3261.

521. Desai, M. P.; Labhasetwar, V.; Walter, E.; Levy, R. J.; Amidon, G. L., The Mechanism of Uptake of Biodegradable Microparticles in Caco-2 Cells Is Size Dependent. *Pharmaceutical Research* **1997,** *14* (11), 1568-1573.

522. Damgé, C.; Michel, C.; Aprahamian, M.; Couvreur, P.; Devissaguet, J. P., Nanocapsules as carriers for oral peptide delivery. *Journal of Controlled Release* **1990,** *13* (2), 233-239.

523. Maitani, Y.; Igarashi, S.; Sato, M.; Hattori, Y., Cationic liposome (DC-Chol/DOPE = 1:2) and a modified ethanol injection method to prepare liposomes, increased gene expression. *International Journal of Pharmaceutics* **2007,** *342* (1-2), 33-39.

524. Sattler, S.; Schaefer, U.; Schneider, W.; Hoelzl, J.; Lehr, C.-M., Binding, uptake, and transport of hypericin by Caco-2 cell monolayers. *Journal of Pharmaceutical Sciences* **1997,** *86* (10), 1120-1126.

525. Zhang, Y.; Li, X.; Zhou, Y.; Fan, Y.; Wang, X.; Huang, Y.; Liu, Y., Cyclosporin A-loaded poly(ethylene glycol)- b -poly(d, l -lactic acid) micelles: Preparation, in vitro and in vivo characterization and transport mechanism across the intestinal barrier. *Molecular Pharmaceutics* **2010,** *7* (4), 1169-1182.

526. Zastre, J.; Jackson, J. K.; Wong, W.; Burt, H. M., Methoxypolyethylene glycol-block-polycaprolactone diblock copolymers reduce P-glycoprotein efflux in the absence of a membrane fluidization effect while stimulating P-glycoprotein ATPase activity. *Journal of Pharmaceutical Sciences* **2007,** *96* (4), 864-875.

527. Wang, Q.; Kuang, Y.; Song, W.; Qian, Y.; Qiao, X.; Guo, D.-a.; Ye, M., Permeability through the Caco-2 cell monolayer of 42 bioactive compounds in the TCM formula Gegen-Qinlian Decoction by liquid chromatography tandem mass spectrometry analysis. *Journal of Pharmaceutical and Biomedical Analysis* **2017,** *146* (Supplement C), 206-213.

528. Fenyvesi, F.; Kiss, T.; Fenyvesi, É.; Szente, L.; Veszelka, S.; Deli, M. A.; Váradi, J.; Fehér, P.; Ujhelyi, Z.; Tósaki, Á., Randomly methylated β-cyclodextrin derivatives enhance taxol permeability through human intestinal epithelial Caco-2 cell monolayer. *Journal of pharmaceutical sciences* **2011,** *100* (11), 4734-4744.

529. Thiel-Demby, V. E.; Humphreys, J. E.; St. John Williams, L. A.; Ellens, H. M.; Shah, N.; Ayrton, A. D.; Polli, J. W., Biopharmaceutics Classification System: Validation and Learnings of an in Vitro Permeability Assay. *Molecular Pharmaceutics* **2009,** *6* (1), 11-18.

530. Wu, X.; Whitfield, L. R.; Stewart, B. H., Atorvastatin Transport in the Caco-2 Cell Model: Contributions of P-Glycoprotein and the Proton-Monocarboxylic Acid Co-Transporter. *Pharmaceutical Research* **2000,** *17* (2), 209-215.

531. Yasutaka, I.; Kibat, P. G.; Langer, R., Optimization of a microencapsulated liposome system for enzymatically controlled release of macromolecules. *Journal of Controlled Release* **1990,** *14* (3), 263-267.

532. Hilgers, A. R.; Conradi, R. A.; Burton, P. S., Caco-2 Cell Monolayers as a Model for Drug Transport Across the Intestinal Mucosa. *Pharmaceutical Research* **1990,** *7* (9), 902-910.

533. Hochman, J. H.; Pudvah, N.; Qiu, J.; Yamazaki, M.; Tang, C.; Lin, J. H.; Prueksaritanont, T., Interactions of Human P-glycoprotein with Simvastatin, Simvastatin Acid, and Atorvastatin. *Pharmaceutical Research* **2004,** *21* (9), 1686-1691.

534. Chen, C.; Lin, J.; Smolarek, T.; Tremaine, L., P-glycoprotein has differential effects on the disposition of statin acid and lactone forms in mdr1a/b knockout and wild-type mice. *Drug Metabolism and Disposition* **2007,** *35* (10), 1725-1729.

535. Dabholkar, R. D.; Sawant, R. M.; Mongayt, D. A.; Devarajan, P. V.; Torchilin, V. P., Polyethylene glycol–phosphatidylethanolamine conjugate (PEG–PE)-based mixed micelles: some properties, loading with paclitaxel, and modulation of P-glycoprotein-mediated efflux. *International journal of pharmaceutics* **2006,** *315* (1), 148-157.

536. Roger, E.; Lagarce, F.; Garcion, E.; Benoit, J.-P., Lipid nanocarriers improve paclitaxel transport throughout human intestinal epithelial cells by using vesicle-mediated transcytosis. *Journal of Controlled Release* **2009,** *140* (2), 174-181.

537. Masters, B. A.; Palmoski, M. J.; Flint, O. P.; Gregg, R. E.; Wangiverson, D.; Durham, S. K., In Vitro Myotoxicity of the 3-Hydroxy-3-methylglutaryl Coenzyme A Reductase Inhibitors, Pravastatin, Lovastatin, and Simvastatin, Using Neonatal Rat Skeletal Myocytes. *Toxicology and Applied Pharmacology* **1995,** *131* (1), 163-174.

538. He, C.; Hu, Y.; Yin, L.; Tang, C.; Yin, C., Effects of particle size and surface charge on cellular uptake and biodistribution of polymeric nanoparticles. *Biomaterials* **2010,** *31* (13), 3657-3666.

539. Yin Win, K.; Feng, S.-S., Effects of particle size and surface coating on cellular uptake of polymeric nanoparticles for oral delivery of anticancer drugs. *Biomaterials* **2005,** *26* (15), 2713-2722.

540. Straubinger, R. M.; Hong, K.; Friend, D. S.; Papahadjopoulos, D., Endocytosis of liposomes and intracellular fate of encapsulated molecules: encounter with a low pH compartment after internalization in coated vesicles. *Cell* **1983,** *32* (4), 1069-1079.

541. Narvekar, M.; Xue, H. Y.; Eoh, J. Y.; Wong, H. L., Nanocarrier for poorly water-soluble anticancer drugs - Barriers of translation and solutions. *AAPS PharmSciTech* **2014,** *15* (4), 822-833.

542. Chou, A. J.; Gorlick, R., Chemotherapy resistance in osteosarcoma: current challenges and future directions. *Expert Review of Anticancer Therapy* **2006,** *6* (7), 1075-1085.

543. Ozols, R. F., Challenges for chemotherapy in ovarian cancer. *Annals of Oncology* **2006,** *17* (suppl_5), v181-v187.

544. Gupta, S.; Gupta, P. K.; Dharanivasan, G.; Verma, R. S., Current prospects and challenges of nanomedicine delivery in prostate cancer therapy. *Nanomedicine* **2017,** *12* (23), 2675-2692.

545. Panchagnula, R.; Thomas, N. S., Biopharmaceutics and pharmacokinetics in drug research. *International journal of pharmaceutics* **2000,** *201* (2), 131-150.

546. Couvreur, P.; Tulkenst, P.; Roland, M.; Trouet, A.; Speiser, P., Nanocapsules: A new type of lysosomotropic carrier. *FEBS Letters* **1977,** *84* (2), 323-326.

547. Couvreur, P.; Kante, B.; Lenaerts, V.; Scailteur, V.; Roland, M.; Speiser, P., Tissue distribution of antitumor drugs associated with polyalkylcyanoacrylate nanoparticles. *Journal of Pharmaceutical Sciences* **1980,** *69* (2), 199-202.

548. Kasim, N. A.; Whitehouse, M.; Ramachandran, C.; Bermejo, M.; Lennernäs, H.; Hussain, A. S.; Junginger, H. E.; Stavchansky, S. A.; Midha, K. K.; Shah, V. P.; Amidon, G. L., Molecular Properties of WHO Essential Drugs and Provisional Biopharmaceutical Classification. *Molecular Pharmaceutics* **2004,** *1* (1), 85-96.

549. Malingré, M. M.; Beijnen, J. H.; Schellens, J. H. M., Oral Delivery of Taxanes. *Investigational New Drugs* **2001,** *19* (2), 155-162.

550. Choi, J.-S.; Jo, B.-W.; Kim, Y.-C., Enhanced paclitaxel bioavailability after oral administration of paclitaxel or prodrug to rats pretreated with quercetin. *European Journal of Pharmaceutics and Biopharmaceutics* **2004,** *57* (2), 313-318.

551. Sharma, U. S.; Balasubramanian, S. V.; Straubinger, R. M., Pharmaceutical and physical properties of paclitaxel (taxol) complexes with cyclodextrins. *Journal of Pharmaceutical Sciences* **1995,** *84* (10), 1223-1230.

552. Cserháti, T.; Holló, J., Interaction of taxol and other anticancer drugs with hydroxypropyl-β-cyclodextrin. *International Journal of Pharmaceutics* **1994,** *108* (1), 69-75.

553. Cserháti, T.; Forgács, E.; Holló, J., Interaction of taxol and other anticancer drugs with α-cyclodextrin. *Journal of Pharmaceutical and Biomedical Analysis* **1995,** *13* (4), 533-541.

554. Sharma, A.; Straubinger, R. M., Novel Taxol Formulations: Preparation and Characterization of Taxol-Containing Liposomes. *Pharmaceutical Research* **1994,** *11* (6), 889-896.

555. Tarr, B. D.; Sambandan, T. G.; Yalkowsky, S. H., A New Parenteral Emulsion for the Administration of Taxol. *Pharmaceutical Research* **1987,** *4* (2), 162-165.

556. Tarr, B. D.; Yalkowsky, S. H., A New Parenteral Vehicle for the Administration of Some Poorly Water Soluble Anti-Cancer Drugs. *PDA Journal of Pharmaceutical Science and Technology* **1987,** *41* (1), 31-33.

557. Yoshizawa, Y.; Kono, Y.; Ogawara, K.-i.; Kimura, T.; Higaki, K., PEG liposomalization of paclitaxel improved its in vivo disposition and anti-tumor efficacy. *International Journal of Pharmaceutics* **2011,** *412* (1), 132-141.

558. Liggins, R. T.; Burt, H. M., Paclitaxel-loaded poly(l-lactic acid) microspheres 3: blending low and high molecular weight polymers to control morphology and drug release. *International Journal of Pharmaceutics* **2004,** *282* (1), 61-71.

559. Mu, L.; Feng, S. S., Fabrication, characterization and in vitro release of paclitaxel (Taxol®) loaded poly (lactic-co-glycolic acid) microspheres prepared by spray drying technique with lipid/cholesterol emulsifiers. *Journal of Controlled Release* **2001,** *76* (3), 239-254.

560. Zhang, Z.; Feng, S.-S., The drug encapsulation efficiency, in vitro drug release, cellular uptake and cytotoxicity of paclitaxel-loaded poly(lactide)–tocopheryl polyethylene glycol succinate nanoparticles. *Biomaterials* **2006,** *27* (21), 4025-4033.

561. Burt, H. M.; Jackson, J. K.; Bains, S. K.; Liggins, R. T.; Oktaba, A. M. C.; Arsenault, A. L.; Hunter, W. L., Controlled delivery of taxol from microspheres composed of a blend of ethylene-vinyl acetate copolymer and poly (d,l-lactic acid). *Cancer Letters* **1995,** *88* (1), 73-79.

562. Ramaswamy, M.; Zhang, X.; Burt, H. M.; Wasan, K. M., Human plasma distribution of free paclitaxel and paclitaxel associated with diblock copolymers. *Journal of Pharmaceutical Sciences* **1997,** *86* (4), 460-464.

563. Kang Moo, H.; Hyun Su, M.; Sang Cheon, L.; Hong Jae, L.; Sungwon, K.; Kinam, P., A new hydrotropic block copolymer micelle system for aqueous solubilization of paclitaxel. *Journal of Controlled Release* **2008,** *126* (2), 122-129.

564. Saadat, E.; Amini, M.; Khoshayand, M. R.; Dinarvand, R.; Dorkoosh, F. A., Synthesis and optimization of a novel polymeric micelle based on hyaluronic acid and phospholipids for delivery of paclitaxel, in vitro and in-vivo evaluation. *International Journal of Pharmaceutics* **2014,** *475* (1), 163-173.

565. Skwarczynski, M.; Hayashi, Y.; Kiso, Y., Paclitaxel Prodrugs: Toward Smarter Delivery of Anticancer Agents. *Journal of Medicinal Chemistry* **2006,** *49* (25), 7253-7269.

566. Greenwald, R. B.; Pendri, A.; Bolikal, D.; Gilbert, C. W., Highly water soluble taxol derivatives: 2′-polyethyleneglycol esters as potential prodrugs. *Bioorganic & Medicinal Chemistry Letters* **1994,** *4* (20), 2465-2470.

567. Bunnell, C. A.; Winer, E. P., Oral 5-FU analogues in the treatment of breast cancer. *Oncology (Williston Park)* **1998,** *12* (10 Suppl 7), 39-43.

568. Cunningham, D.; James, R. D., Integrating the oral fluoropyrimidines into the management of advanced colorectal cancer. *European Journal of Cancer* **2001,** *37* (7), 826-834.

569. Neubert, T.; Lehmann, P., Bowen's disease – a review of newer treatment options. *Therapeutics and Clinical Risk Management* **2008,** *4* (5), 1085-1095.

570. Ferlay, J.; Steliarova-Foucher, E.; Lortet-Tieulent, J.; Rosso, S.; Coebergh, J. W. W.; Comber, H.; Forman, D.; Bray, F., Cancer incidence and mortality patterns in Europe: Estimates for 40 countries in 2012. *European Journal of Cancer 49* (6), 1374-1403.

571. Tian, Z.-Y.; Du, G.-J.; Xie, S.-Q.; Zhao, J.; Gao, W.-Y.; Wang, C.-J., Synthesis and Bioevaluation of 5-Fluorouracil Derivatives. *Molecules* **2007,** *12* (11), 2450.

572. Grem, J. L., 5-Fluorouracil: Forty-plus and still ticking. A review of its preclinical and clinical development. *Investigational New Drugs* **2000,** *18* (4), 299-313.

573. Wu, Q.; Yang, Z.; Nie, Y.; Shi, Y.; Fan, D., Multi-drug resistance in cancer chemotherapeutics: Mechanisms and lab approaches. *Cancer Letters* **2014,** *347* (2), 159-166.

574. Eric K. Rowinsky, M., THE DEVELOPMENT AND CLINICAL UTILITY OF THE TAXANE CLASS OF ANTIMICROTUBULE CHEMOTHERAPY AGENTS. *Annual Review of Medicine* **1997,** *48* (1), 353-374.

575. Zhang, N.; Yin, Y.; Xu, S.-J.; Chen, W.-S., 5-Fluorouracil: Mechanisms of Resistance and Reversal Strategies. *Molecules* **2008,** *13* (8), 1551.

576. Malingré, M. M.; Richel, D. J.; Beijnen, J. H.; Rosing, H.; Koopman, F. J.; Huinink, W. W. T. B.; Schot, M. E.; Schellens, J. H. M., Coadministration of cyclosporine strongly enhances the oral bioavailability of docetaxel. *Journal of clinical oncology* **2001,** *19* (4), 1160-1166.

577. Juliano, R. L.; Ling, V., A surface glycoprotein modulating drug permeability in Chinese hamster ovary cell mutants. *Biochimica et Biophysica Acta (BBA) - Biomembranes* **1976,** *455* (1), 152-162.

578. Wang, J.; Goh, B.; Lu, W.; Zhang, Q.; Chang, A.; Liu, X. Y.; Tan, T. M. C.; Lee, H., In Vitro Cytotoxicity of Stealth Liposomes Co-encapsulating Doxorubicin and Verapamil on Doxorubicin-Resistant Tumor Cells. *Biological and Pharmaceutical Bulletin* **2005,** *28* (5), 822-828.

579. Patel, N. R.; Rathi, A.; Mongayt, D.; Torchilin, V. P., Reversal of multidrug resistance by co-delivery of tariquidar (XR9576) and paclitaxel using long-circulating liposomes. *International Journal of Pharmaceutics* **2011,** *416* (1), 296-299.

580. Leonard, G. D.; Polgar, O.; Bates, S. E., ABC transporters and inhibitors: new targets, new agents. *Curr Opin Investig Drugs* **2002,** *3* (11), 1652-1659.

581. Jabr-Milane, L. S.; van Vlerken, L. E.; Yadav, S.; Amiji, M. M., Multi-functional nanocarriers to overcome tumor drug resistance. *Cancer Treatment Reviews* **2008,** *34* (7), 592-602.

582. Allen, T. M.; Hansen, C.; Martin, F.; Redemann, C.; Yau-Young, A., Liposomes containing synthetic lipid derivatives of poly(ethylene glycol) show prolonged circulation half-lives in vivo. *Biochimica et Biophysica Acta (BBA) - Biomembranes* **1991,** *1066* (1), 29-36.

583. Huang, S. K.; Lee, K.-D.; Hong, K.; Friend, D. S.; Papahadjopoulos, D., Microscopic Localization of Sterically Stabilized Liposomes in Colon Carcinoma-bearing Mice. *Cancer Research* **1992,** *52* (19), 5135-5143.

584. Huang, S. K.; Martin, F. J.; Jay, G.; Vogel, J.; Papahadjopoulos, D.; Friend, D. S., Extravasation and transcytosis of liposomes in Kaposi's sarcoma-like dermal lesions of transgenic mice bearing the HIV tat gene. *The American Journal of Pathology* **1993,** *143* (1), 10-14.

585. Immordino, M. L.; Brusa, P.; Rocco, F.; Arpicco, S.; Ceruti, M.; Cattel, L., Preparation, characterization, cytotoxicity and pharmacokinetics of liposomes containing lipophilic gemcitabine prodrugs. *Journal of Controlled Release* **2004,** *100* (3), 331-346.

586. Therapeutic PEG-ceramide nanomicelles synergize with salinomycin to target both liver cancer cells and cancer stem cells. *Nanomedicine* **2017,** *12* (9), 1025-1042.

587. Yao, X.-L.; Yoshioka, Y.; Ruan, G.-X.; Chen, Y.-Z.; Mizuguchi, H.; Mukai, Y.; Okada, N.; Gao, J.-Q.; Nakagawa, S., Optimization and Internalization Mechanisms of PEGylated Adenovirus Vector with Targeting Peptide for Cancer Gene Therapy. *Biomacromolecules* **2012,** *13* (8), 2402-2409.

588. Balalaeva, I. V.; Zdobnova, T. A.; Krutova, I. V.; Brilkina, A. A.; Lebedenko, E. N.; Deyev, S. M., Passive and active targeting of quantum dots for whole-body fluorescence imaging of breast cancer xenografts. *Journal of Biophotonics* **2012,** *5* (11-12), 860-867.

589. Sykes, E. A.; Chen, J.; Zheng, G.; Chan, W. C. W., Investigating the Impact of Nanoparticle Size on Active and Passive Tumor Targeting Efficiency. *ACS Nano* **2014,** *8* (6), 5696-5706.

590. Landon, C. D.; Park, J.-Y.; Needham, D.; Dewhirst, M. W., Nanoscale drug delivery and hyperthermia: the materials design and preclinical and clinical testing of low temperature-sensitive liposomes used in combination with mild hyperthermia in the treatment of local cancer. *The open nanomedicine journal* **2011,** *3*, 38.

591. Lasic, D., Mixed micelles in drug delivery. *Nature* **1992,** *355*, 279 - 280.

592. Liu, S. Q.; Tong, Y. W.; Yang, Y.-Y., Incorporation and in vitro release of doxorubicin in thermally sensitive micelles made from poly(N-isopropylacrylamide-co-N,N-dimethylacrylamide)-b-poly(d,l-lactide-co-glycolide) with varying compositions. *Biomaterials* **2005,** *26* (24), 5064-5074.

593. Varma, M. V. S.; Panchagnula, R., Enhanced oral paclitaxel absorption with vitamin E-TPGS: Effect on solubility and permeability in vitro, in situ and in vivo. *European Journal of Pharmaceutical Sciences* **2005,** *25* (4), 445-453.

594. Chang, T.; Benet, L. Z.; Hebert, M. F., The effect of water-soluble vitamin E on cyclosporine pharmacokinetics in healthy volunteers. *Clinical Pharmacology & Therapeutics* **1996,** *59* (3), 297-303.

595. Ponce, A.; Wright, A.; Dewhirst, M.; Needham, D., Targeted bioavailability of drugs by triggered release from liposomes. *Future Lipidology* **2006,** *1* (1), 25-34.

596. Bibi, S.; Lattmann, E.; Mohammed, A. R.; Perrie, Y., Trigger release liposome systems: local and remote controlled delivery? *Journal of Microencapsulation* **2012,** *29* (3), 262-276.

597. Kaasgaard, T.; Andresen, T. L., Liposomal cancer therapy: exploiting tumor characteristics. *Expert Opinion on Drug Delivery* **2010,** *7* (2), 225-243.

598. Koning, G. A.; Eggermont, A. M. M.; Lindner, L. H.; ten Hagen, T. L. M., Hyperthermia and Thermosensitive Liposomes for Improved Delivery of Chemotherapeutic Drugs to Solid Tumors. *Pharmaceutical Research* **2010,** *27* (8), 1750-1754.

599. Needham, D.; Anyarambhatla, G.; Kong, G.; Dewhirst, M. W., A New Temperature-sensitive Liposome for Use with Mild Hyperthermia: Characterization and Testing in a Human Tumor Xenograft Model. *Cancer Research* **2000,** *60* (5), 1197-1201.

600. Lajunen, T.; Viitala, L.; Kontturi, L. S.; Laaksonen, T.; Liang, H.; Vuorimaa-Laukkanen, E.; Viitala, T.; Le Guével, X.; Yliperttula, M.; Murtomäki, L.; Urtti, A., Light induced cytosolic drug delivery from liposomes with gold nanoparticles. *Journal of Controlled Release* **2015,** *203*, 85-98.

601. Matsuki, D.; Adewale, O.; Horie, S.; Okajima, J.; Komiya, A.; Oluwafemi, O.; Maruyama, S.; Mori, S.; Kodama, T., Treatment of tumor in lymph nodes using near-infrared laser light-activated thermosensitive liposome-encapsulated doxorubicin and gold nanorods. *Journal of Biophotonics* **2017**.

602. Spring, B. Q.; Bryan Sears, R.; Zheng, L. Z.; Mai, Z.; Watanabe, R.; Sherwood, M. E.; Schoenfeld, D. A.; Pogue, B. W.; Pereira, S. P.; Villa, E.; Hasan, T., A photoactivable multi-inhibitor nanoliposome for tumour control and simultaneous inhibition of treatment escape pathways. *Nature Nanotechnology* **2016,** *11* (4), 378-387.

603. Moussa, H. G.; Martins, A. M.; Husseini, G. A., Review on triggered liposomal drug delivery with a focus on ultrasound. *Current Cancer Drug Targets* **2015,** *15* (4), 282-313.

604. Li, Y.; An, H.; Wang, X.; Wang, P.; Qu, F.; Jiao, Y.; Zhang, K.; Liu, Q., Ultrasound-triggered release of sinoporphyrin sodium from liposome-microbubble complexes and its enhanced sonodynamic toxicity in breast cancer. *Nano Research* **2017**, 1-19.

605. Ibsen, S.; Benchimol, M.; Simberg, D.; Schutt, C.; Steiner, J.; Esener, S., A novel nested liposome drug delivery vehicle capable of ultrasound triggered release of its payload. *Journal of Controlled Release* **2011,** *155* (3), 358-366.

606. Kong, G.; Anyarambhatla, G.; Petros, W. P.; Braun, R. D.; Colvin, O. M.; Needham, D.; Dewhirst, M. W., Efficacy of Liposomes and Hyperthermia in a Human Tumor Xenograft Model: Importance of Triggered Drug Release. *Cancer Research* **2000,** *60* (24), 6950-6957.

607. Needham, D.; Dewhirst, M. W., The development and testing of a new temperature-sensitive drug delivery system for the treatment of solid tumors. *Advanced Drug Delivery Reviews* **2001,** *53* (3), 285-305.

608. Mills, J. K.; Needham, D., Lysolipid incorporation in dipalmitoylphosphatidylcholine bilayer membranes enhances the ion permeability and drug release rates at the membrane phase transition. *Biochimica et Biophysica Acta (BBA) - Biomembranes* **2005,** *1716* (2), 77-96.

609. Li, L.; ten Hagen, T. L. M.; Schipper, D.; Wijnberg, T. M.; van Rhoon, G. C.; Eggermont, A. M. M.; Lindner, L. H.; Koning, G. A., Triggered content release from optimized stealth thermosensitive liposomes using mild hyperthermia. *Journal of Controlled Release* **2010,** *143* (2), 274-279.

610. Murugan, C.; Rayappan, K.; Thangam, R.; Bhanumathi, R.; Shanthi, K.; Vivek, R.; Thirumurugan, R.; Bhattacharyya, A.; Sivasubramanian, S.; Gunasekaran, P.; Kannan, S., Combinatorial nanocarrier based drug delivery approach for amalgamation of anti-tumor agents in breast cancer cells: an improved nanomedicine strategy. *Scientific Reports* **2016,** *6*, 34053.

611. ARIKAN, Ş., A Comparison of the Effect of Methyl-b-Cyclodextrin on the Osmotic Fragility of Ovine, Bovine and Human Erythrocytes. *Turkish Journal of Veterinary and Animal Sciences* **2003,** *27* (2), 383-387.

612. Yatvin, M.; Mühlensiepen, H.; Porschen, W.; Weinstein, J.; Feinendegen, L., Selective delivery of liposome-associated cis-dichlorodiammineplatinum (II) by heat and its influence on tumor drug uptake and growth. *Cancer research* **1981,** *41* (5), 1602-1607.

613. Semple, S. C.; Chonn, A.; Cullis, P. R., Influence of Cholesterol on the Association of Plasma Proteins with Liposomes. *Biochemistry* **1996,** *35* (8), 2521-2525.

614. Wang, Z.-Y.; Zhang, H.; Yang, Y.; Xie, X.-Y.; Yang, Y.-F.; Li, Z.; Li, Y.; Gong, W.; Yu, F.-L.; Yang, Z.; Li, M.-Y.; Mei, X.-G., Preparation, characterization, and efficacy of thermosensitive liposomes containing paclitaxel. *Drug Delivery* **2016,** *23* (4), 1222-1231.

615. Kan, P.; Tsao, C.-W.; Wang, A.-J.; Su, W.-C.; Liang, H.-F., A Liposomal Formulation Able to Incorporate a High Content of Paclitaxel and Exert Promising Anticancer Effect. *Journal of Drug Delivery* **2011,** *2011*.

616. Zhang, J. A.; Anyarambhatla, G.; Ma, L.; Ugwu, S.; Xuan, T.; Sardone, T.; Ahmad, I., Development and characterization of a novel Cremophor® EL free liposome-based paclitaxel (LEP-ETU) formulation. *European journal of pharmaceutics and biopharmaceutics* **2005,** *59* (1), 177-187.

617. Kensil, C. R.; Dennis, E. A., Alkaline hydrolysis of phospholipids in model membranes and the dependence on their state of aggregation. *Biochemistry* **1981,** *20* (21), 6079-6085.

618. Yu, Y.; Huo, M.; Fu, Y.; Xu, W.; Cai, H.; Yao, L.; Chen, Q.; Mu, Y.; Zhou, J.; Yin, T., N-Deoxycholic acid-N,O-hydroxyethyl Chitosan with a Sulfhydryl Modification to Enhance the Oral Absorptive Efficiency of Paclitaxel. *Molecular Pharmaceutics* **2017,** *14* (12), 4539-4550.

619. Jain, S.; Kumar, D.; Swarnakar, N. K.; Thanki, K., Polyelectrolyte stabilized multilayered liposomes for oral delivery of paclitaxel. *Biomaterials* **2012,** *33* (28), 6758-6768.

620. Banerjee, A.; Qi, J.; Gogoi, R.; Wong, J.; Mitragotri, S., Role of nanoparticle size, shape and surface chemistry in oral drug delivery. *Journal of Controlled Release* **2016,** *238*, 176-185.

621. Dahmani, F. Z.; Yang, H.; Zhou, J.; Yao, J.; Zhang, T.; Zhang, Q., Enhanced oral bioavailability of paclitaxel in pluronic/LHR mixed polymeric micelles: Preparation, in vitro and in vivo evaluation. *European Journal of Pharmaceutical Sciences* **2012,** *47* (1), 179-189.

622. Yang, T.; Cui, F.-D.; Choi, M.-K.; Cho, J.-W.; Chung, S.-J.; Shim, C.-K.; Kim, D.-D., Enhanced solubility and stability of PEGylated liposomal paclitaxel: in vitro and in vivo evaluation. *International journal of Pharmaceutics* **2007,** *338* (1), 317-326.

623. Dicheva, B. M.; Hagen, T. L. t.; Li, L.; Schipper, D.; Seynhaeve, A. L.; Rhoon, G. C. v.; Eggermont, A. M.; Lindner, L. H.; Koning, G. A., Cationic thermosensitive liposomes: a novel dual targeted heat-triggered drug delivery approach for endothelial and tumor cells. *Nano letters* **2012,** *13* (6), 2324-2331.

624. Dua, J.; Rana, A.; Bhandari, A., Liposome: methods of preparation and applications. *Int J Pharm Stud Res* **2012,** *3*, 14-20.

625. Almgren, M.; Edwards, K.; Karlsson, G., Cryo transmission electron microscopy of liposomes and related structures. *Colloids and Surfaces A: Physicochemical and Engineering Aspects* **2000,** *174* (1–2), 3-21.

626. Arleth, L.; Ashok, B.; Onyuksel, H.; Thiyagarajan, P.; Jacob, J.; Hjelm, R. P., Detailed structure of hairy mixed micelles formed by phosphatidylcholine and PEGylated phospholipids in aqueous media. *Langmuir* **2005,** *21* (8), 3279-3290.

627. Lin, Y.-L.; Liu, Y.-K.; Tsai, N.-M.; Hsieh, J.-H.; Chen, C.-H.; Lin, C.-M.; Liao, K.-W., A Lipo-PEG-PEI complex for encapsulating curcumin that enhances its antitumor effects on curcumin-sensitive and curcumin-resistance cells. *Nanomedicine: Nanotechnology, Biology and Medicine* **2012,** *8* (3), 318-327.

628. Doshi, N.; Prabhakarpandian, B.; Rea-Ramsey, A.; Pant, K.; Sundaram, S.; Mitragotri, S., Flow and adhesion of drug carriers in blood vessels depend on their shape: a study using model synthetic microvascular networks. *Journal of Controlled Release* **2010,** *146* (2), 196-200.

629. Ahmad, Z.; Shah, A.; Siddiq, M.; Kraatz, H.-B., Polymeric micelles as drug delivery vehicles. *RSC Advances* **2014,** *4* (33), 17028-17038.

630. Nakayama, M.; Akimoto, J.; Okano, T., *Polymeric micelles with stimuli-triggering systems for advanced cancer drug targeting*. 2014; Vol. 22.

631. Nakayama, M.; Okano, T.; Miyazaki, T.; Kohori, F.; Sakai, K.; Yokoyama, M., Molecular design of biodegradable polymeric micelles for temperature-responsive drug release. *Journal of Controlled Release* **2006,** *115* (1), 46-56.

632. Kenworthy, A. K.; Hristova, K.; Needham, D.; McIntosh, T. J., Range and magnitude of the steric pressure between bilayers containing phospholipids with covalently attached poly (ethylene glycol). *Biophysical journal* **1995,** *68* (5), 1921-1936.

633. Yatvin, M.; Weinstein, J.; Dennis, W.; Blumenthal, R., Design of liposomes for enhanced local release of drugs by hyperthermia. *Science* **1978,** *202* (4374), 1290-1293.

634. Papahadjopoulos, D.; Jacobson, K.; Nir, S.; Isac, I., Phase transitions in phospholipid vesicles Fluorescence polarization and permeability measurements concerning the effect of temperature and cholesterol. *Biochimica et Biophysica Acta (BBA) - Biomembranes* **1973,** *311* (3), 330-348.

635. Needham, D.; Park, J.-Y.; Wright, A. M.; Tong, J., Materials characterization of the low temperature sensitive liposome (LTSL): effects of the lipid composition (lysolipid and DSPE-PEG2000) on the thermal transition and release of doxorubicin. *Faraday Discussions* **2013,** *161* (0), 515-534.

636. Nie, S.; Hsiao, W. L. W.; Pan, W.; Yang, Z., Thermoreversible Pluronic(®) F127-based hydrogel containing liposomes for the controlled delivery of paclitaxel: in vitro drug release, cell cytotoxicity, and uptake studies. *International Journal of Nanomedicine* **2011,** *6*, 151-166.

637. Sun, T.; Zhang, Y. S.; Pang, B.; Hyun, D. C.; Yang, M.; Xia, Y., Engineered Nanoparticles for Drug Delivery in Cancer Therapy. *Angewandte Chemie International Edition* **2014,** *53* (46), 12320-12364.

638. Garbuzenko, O.; Barenholz, Y.; Priev, A., Effect of grafted PEG on liposome size and on compressibility and packing of lipid bilayer. *Chemistry and Physics of Lipids* **2005,** *135* (2), 117-129.

639. Pagnussatt, F. A.; De Lima, V. R.; Dora, C. L.; Costa, J. A. V.; Putaux, J. L.; Badiale-Furlong, E., Assessment of the encapsulation effect of phenolic compounds from Spirulina sp. LEB-18 on their antifusarium activities. *Food Chemistry* **2016,** *211*, 616-623.

640. Schaefer, J. J.; Ma, C.; Harris, J. M., Confocal Raman microscopy probing of temperature-controlled release from individual, optically-trapped phospholipid vesicles. *Analytical Chemistry* **2012,** *84* (21), 9505-9512.

641. Arnold, J. H., STUDIES IN DIFFUSION. II. A KINETIC THEORY OF DIFFUSION IN LIQUID SYSTEMS. *Journal of the American Chemical Society* **1930,** *52* (10), 3937-3955.

642. Engle, M. J.; Goetz, G. S.; Alpers, D. H., Caco-2 cells express a combination of colonocyte and enterocyte phenotypes. *Journal of Cellular Physiology* **1998,** *174* (3), 362-369.

643. Lenaerts, K.; Bouwman, F. G.; Lamers, W. H.; Renes, J.; Mariman, E. C., Comparative proteomic analysis of cell lines and scrapings of the human intestinal epithelium. *BMC Genomics* **2007,** *8* (1), 91.

644. Kotzé, A. F.; Lueßen, H. L.; de Leeuw, B. J.; de Boer, B. G.; Coos Verhoef, J.; Junginger, H. E., Comparison of the effect of different chitosan salts and N-trimethyl chitosan chloride on the permeability of intestinal epithelial cells (Caco-2). *Journal of Controlled Release* **1998,** *51* (1), 35-46.

645. Uchida, M.; Fukazawa, T.; Yamazaki, Y.; Hashimoto, H.; Miyamoto, Y., A modified fast (4 day) 96-well plate Caco-2 permeability assay. *Journal of Pharmacological and Toxicological Methods* **2009,** *59* (1), 39-43.

646. Constantinides, P. P.; Wasan, K. M., Lipid formulation strategies for enhancing intestinal transport and absorption of P-glycoprotein (P-gp) substrate drugs: In vitro/In vivo case studies. *Journal of Pharmaceutical Sciences* **2007,** *96* (2), 235-248.

647. Bansal, T.; Akhtar, N.; Jaggi, M.; Khar, R. K.; Talegaonkar, S., Novel formulation approaches for optimising delivery of anticancer drugs based on P-glycoprotein modulation. *Drug Discovery Today* **2009,** *14* (21), 1067-1074.

648. Brigger, I.; Dubernet, C.; Couvreur, P., Nanoparticles in cancer therapy and diagnosis. *Advanced Drug Delivery Reviews* **2012,** *64*, 24-36.

649. McPhail, D.; Tetley, L.; Dufes, C.; Uchegbu, I. F., Liposomes encapsulating polymeric chitosan based vesicles — a vesicle in vesicle system for drug delivery. *International Journal of Pharmaceutics* **2000,** *200* (1), 73-86.

650. Vercauteren, D.; Vandenbroucke, R. E.; Jones, A. T.; Rejman, J.; Demeester, J.; De Smedt, S. C.; Sanders, N. N.; Braeckmans, K., The Use of Inhibitors to Study Endocytic Pathways of Gene Carriers: Optimization and Pitfalls. *Molecular Therapy* **2010,** *18* (3), 561-569.

APPENDIX

APPENDIX A

HPLC method validation

Drug qt given (mg)	Area 1	Area 2	Area 3	C(ug/ml) 1	C(ug/ml) 2	C(ug/ml) 3	Mean	% Bias	STD	% RSD
0.1	5746	5219	6021	0.10	0.09	0.11	**0.10**	-0.52	0.01	9.85
1	39492	37840	32746	0.91	0.87	0.75	**0.85**	-15.42	0.08	10.00
2.5	106963	93132	101671	2.54	2.20	2.41	**2.38**	-4.69	0.17	7.04
5	212868	206004	206718	5.08	4.92	4.94	**4.98**	-0.42	0.09	1.82
10	433123	414930	436687	10.38	9.94	10.47	**10.26**	2.64	0.28	2.73
25	1042825	1E+06	1053774	25.05	25.99	25.31	**25.45**	1.79	0.49	1.91
100	4442539	4E+06	4821445	106.82	97.70	115.93	**106.82**	6.82	9.12	8.53
0.1	5187	6021		0.09	0.11		**0.10**	-1.91	0.01	14.46
1	31438	32746		0.72	0.75		**0.74**	-26.48	0.02	3.03
2.5	98717	101671		2.34	2.41		**2.37**	-5.07	0.05	2.12
5	206004	206718		4.92	4.94		**4.93**	-1.46	0.01	0.25
10	414930	436687		9.94	10.47		**10.20**	2.05	0.37	3.63
20	753814	761496		18.09	18.28		**18.19**	-9.07	0.13	0.72
25	1081962	1E+06		25.99	25.31		**25.65**	2.59	0.48	1.87
100	4821445	5E+06		115.93	115.93		**115.93**	15.93	0.00	0.00

Number of sample	Area
1	277994
2	273131
3	269986
4	277356
5	287418
	6588.972

$$\%RSD = \frac{\text{standard deviation}}{\text{mean}} \times 100$$

$$\%Bias = \frac{\text{Concentration(detected)} - \text{Concentration(added)}}{\text{Concentration(added)}} \times 100$$

Repetibility	
1	514846
2	518609
3	514115
4	514885
5	526142
Average	517719.4
Std	5025.27435
Std Rel	10302.3112
% RSD	0.97065599

Drug qt given (mg)	Area 1	Area 2	Area 3	C(ug/ml) 1	C(ug/ml) 2	C(ug/ml) 3	Mean	% Bias	STD	% RSD
1	35213	40475	37840	0.81	0.94	0.87	**0.87**	-12.65	0.09	10.25
2.5	90605	101300	93132	2.14	2.40	2.20	**2.27**	-9.15	0.18	8.01
5	194738	206212	204137	4.65	4.92	4.87	**4.79**	-4.30	0.20	4.08
10	406876	407054	374277	9.75	9.75	8.97	**9.75**	-2.48	0.00	0.03
20	872029	835891	862872	20.94	20.07	20.72	**20.50**	2.52	0.61	3.00
25	1081962	1067487	1065352	25.99	25.64	25.59	**25.81**	3.25	0.25	0.95
1	37840	40475		0.87	0.94		**0.91**	-9.49	0.04	4.95
2.5	93132	101300		2.20	2.40		**2.30**	-7.94	0.14	6.04
5	204137	206212		4.87	4.92		**4.90**	-2.04	0.04	0.72
10	374277	407054		8.97	9.75		**9.36**	-6.40	0.56	5.96
20	862872	835891		20.72	20.07		**20.39**	1.96	0.46	2.25
25	1065352	1067487		25.59	25.64		**25.61**	2.45	0.04	0.14

Number of sample	Area
1	277994
2	273131
3	269986
4	277356
5	287418
	6588.972

$$\%RSD = \frac{\text{standard deviation}}{\text{mean}} \times 100$$

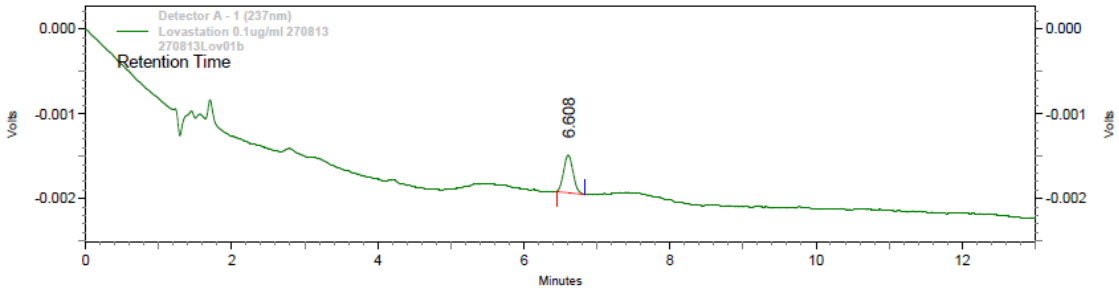
$$\%Bias = \frac{\text{Concentration(detected)} - \text{Concentration(added)}}{\text{Concentration(added)}} \times 100$$

Repetibility	
1	514846
2	518609
3	514115
4	514885
5	526142
Average	517719.4
Std	5025.27435
Std Rel	10302.3112
% RSD	0.97065599

The limit of quantification (LOQ): 0.1 µg/ml of LOV

Shimadzu CLASS-VP V6.14 SP1 *Area % Report*
Page 1 of 1

Method Name: C:\CLASS-VP\Methods\Fabio\Lovastatin_Analysis.met
Data Name: C:\CLASS-VP\Data\Fabio Sonvico & Co\Lovastatin\270813Lov01b
User: System
Acquired: 27/08/2013 11:27:39 PM
Printed: 27/08/2013 11:48:24 PM



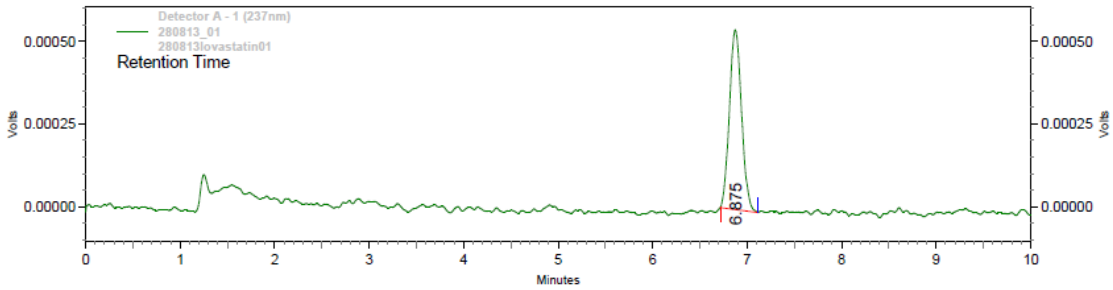
Detector A - 1 (237nm)

Pk #	Retention Time	Area	Area %	Height	Height %
1	6.608	4014	100.000	445	100.000

Totals				
	4014	100.000	445	100.000

Shimadzu CLASS-VP V6.14 SP1 *Area % Report*
Page 1 of 1

Method Name: C:\CLASS-VP\Methods\Fabio\Lovastatin_Analysis.met
Data Name: C:\CLASS-VP\Data\Fabio Sonvico & Co\Simvastatin\280813lovastatin01
User: System
Acquired: 28/08/2013 10:17:00 PM
Printed: 28/08/2013 10:31:01 PM



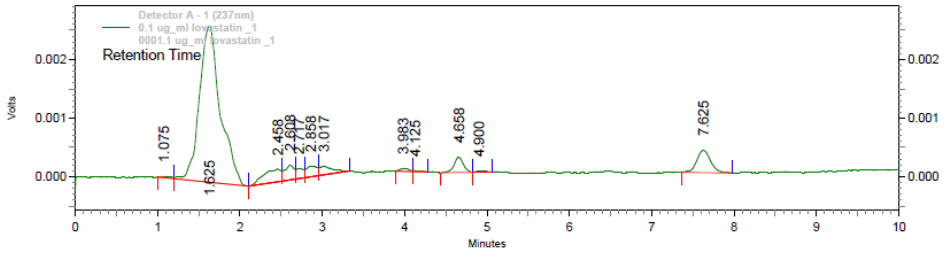
Detector A - 1 (237nm)

Pk #	Retention Time	Area	Area %	Height	Height %
1	6.875	4844	100.000	544	100.000

Totals				
	4844	100.000	544	100.000

Shimadzu CLASS-VP V6.14 SP1 *Area % Report*
Page 1 of 1

Method Name: C:\CLASS-VP\Methods\Fabio\Lovastatin_Analysis 2 .met
Data Name: C:\CLASS-VP\Data\Fabio Sonvico & Co\Lovastatin\Romana\lov solubility\calibration\0001.1 ug_ml lovastatin _1
User: System
Acquired: 4/09/2014 3:06:53 PM
Printed: 4/09/2014 3:21:58 PM



Detector A - 1 (237nm)

Pk #	Retention Time	Area	Area %	Height	Height %
1	1.075	212	0.332	22	0.503
2	1.625	46850	73.327	2662	60.860
3	2.458	3294	5.156	214	4.893
4	2.608	2039	3.191	251	5.738
5	2.717	1046	1.637	174	3.978
6	2.858	1614	2.526	183	4.184
7	3.017	1691	2.647	147	3.361
8	3.983	373	0.584	51	1.166
9	4.125	133	0.208	17	0.389
10	4.658	2046	3.202	258	5.898
11	4.900	155	0.243	18	0.412
12	7.625	4439	6.948	377	8.619
Totals		63892	100.000	4374	100.000

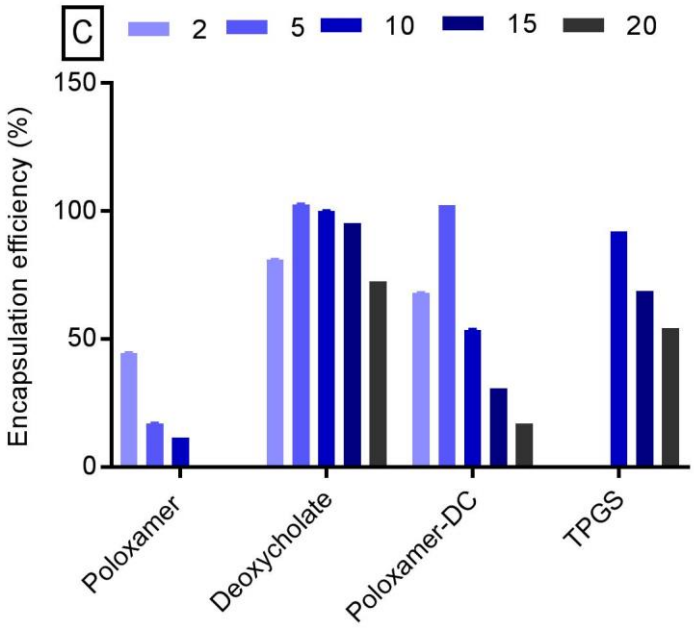
APPENDIX B

The non-entrapped drug was quantified and was a mass balance determined. The amount of drug entrapped and amount non entrapped were total equal to 100%

Drug quantity	TPGS qt	Sample	Area	C(ug/ml)	dil fact	mass(ug)	mass(mg)	LE	EE
10.5	502.6	Sample 1	4190885	100.76	1007.64	10076.39	10.08	1.96	95.97
		ppt	451633	10.83	10.83	58.46	0.06		
11	501.5	Sample 2	4417719	106.22	1062.20	10621.98	10.62	2.07	96.56
		ppt	704307	16.90	16.90	91.28	0.09		
11	500.08	Sample 3	4488002	107.91	1079.10	10791.02	10.79	2.11	98.10
		ppt	797197	19.14	19.14	99.52	0.10		
							10.50	2.05	96.88
							0.37	0.08	1.10

APPENDIX C

Figure 3-6: C) The relationship between added LOV to the polymers/surfactants and encapsulation efficiency (%) in different polymeric/surfactant micelles



However, the relationship between EE and the drug added is inversely proportional, i.e. the EE decreased with increased added drug. We investigated drug loading maxima with definite amount of polymer (500 mg). Increasing the added drug quantity from 2, 5, 10, 15 and 20 mg into fixed weight of polymeric micelles, the loading was varied based upon the polymers. The loading also varied for each polymer that is stated in **Figure 3-6A**. However, it was found that the encapsulation efficiency was decreased in each micelle with increasing amount of added LOV after certain amount (highest loading) as shown in **Figure 3-6C**.

APPENDIX D

Page 4-13, **Figure 4-3:** Caco-2 cell viability as a function of various levels of LOV-LMH inclusion. Viability determined after 48 hours of treatment by Alamar blue assay. Data presented as the mean ± SD (n = 4) from two individual experiments in quadruplicate. **control without the drug

Anova: Two-Factor Without Replication						
SUMMARY	*Count*	*Sum*	*Average*	*Variance*		
Blank	2	213.0841	106.5421	3.930367		
0.0001	2	196.542	98.271	1.009052		
0.0005	2	195.4205	97.71025	0.982662		
0.001	2	197.0093	98.50465	36.96366		
0.01	2	204.9533	102.4767	0.528495		
0.1	2	204.6729	102.3365	3.930367		
0.5	2	201.6822	100.8411	14.69124		
1	2	195.4112	97.70561	0.726748		
Column 1	8	793.4672	99.18341	11.60814		
Column 2	8	815.3083	101.9135	12.64869		
ANOVA						
Source of Variation	*SS*	*df*	*MS*	*F*	*P-value*	*F crit*
Rows	136.85	7	19.54995	4.153497	0.039945	3.787044
Columns	29.815	1	29.81452	6.334261	0.039997	5.591448
Error	32.948	7	4.706867			
Total	199.61	15				

From the single factor ANOVA data analysis it is found that there was a statistically significant ($p < 0.039$) differences between the control and LMH for the cell viability data. There was a statistically significant difference between control and LMH.

Page 4-16, **Figure 4-6:** A) The A→B and B→A fluxes of LOV and LOV loaded nanocarriers (100 µM) were determined at pH 7.4 as a function of time (2 hours at 37°C) and B) Transepithelial efflux of LOV across CCM. Each point represents the mean (4 S.E.M.) of 4 determinations (CCM).

Anova: Single Factor

SUMMARY

Groups	*Count*	*Sum*	*Average*	*Variance*
A-B	4	42.47496	10.61874	1.929377
B-A	4	97.51969	24.37992	76.0186

ANOVA

Source of Variation	*SS*	*df*	*MS*	*F*	*P-value*	*F crit*
Between Groups	378.7404	1	378.7404	9.717773	0.020655	5.987378
Within Groups	233.8439	6	38.97399			
Total	612.5843	7				

From the single factor ANOVA data analysis it is found that a statistically significant difference ($p < 0.02$) was found for enhancement of LOV permeability for B→A direction for micelles, liposomes, and LMH compared to the A-B permeability.

Page 4-20, **Figure 4-8:** Percent permeability of LY (100 µM) from A→B; added to the apical chamber of CCM treated with 100 µM LOV and 100 µM LOV incorporated into each nanocarrier; micelles, liposomes, and LMH; were incubated for 1-hour with 100 µM LY. After 1-hour samples were collected from the basal chamber. Here the control was only the cells. LY was measured by fluorescence intensity at excitation and emission wavelengths of 485 and 520 nm, respectively. Results are means ± SD ($n = 4$).

Anova: Single Factor

SUMMARY

Groups	*Count*	*Sum*	*Average*	*Variance*
Blank	8	0.44316	0.055395	0
Lovastatin	8	-47.3377	-5.917215	61.02815
Hybrid	8	31.97823	3.9972784	65.90346
Liposome	8	5.103583	0.6379478	7.418003
Micelles	8	-3.62986	-0.453733	7.562836

ANOVA

Source of Variation	*SS*	*df*	*MS*	*F*	*P-value*	*F crit*
Between Groups	408.34311	4	102.08578	3.596787	0.014728	2.641465
Within Groups	993.387145	35	28.38249			
Total	1401.73025	39				

From the Single Factor ANOVA data analysis it is found that there is a statistically significant ($p < 0.014$) differences between A→B and B→A permeability.

t-Test: Two-Sample Assuming Equal Variances				
	Control	*LOV*		
Mean	0.05539499	-5.917215046		
Variance	0	61.02814743		
Observations	8	8		
Pooled Variance	30.51407372			
Hypothesized Mean Difference	0			
df	14			
t Stat	2.162439968			
P(T<=t) one-tail	0.024190982			
t Critical one-tail	1.761310136			
P(T<=t) two-tail	0.048381964		0.009676	TRUE
t Critical two-tail	2.144786688			

The post- hoc- corrected t-tests analysis reports as "true'' for LOV compared to control implies that there is 95% of chance of difference between control and LOV. The LY permeability is significantly higher for LOV compared to control.

t-Test: Two-Sample Assuming Equal Variances				
	Control	*LMH*		
Mean	0.05539499	3.9972784		
Variance	0	65.903463		
Observations	8	8		
Pooled Variance	32.9517314			
Hypothesized Mean Difference	0			
df	14			
t Stat	-1.3733924			
P(T<=t) one-tail	0.09561291			
t Critical one-tail	1.76131014			
P(T<=t) two-tail	0.19122582		0.009676	TRUE
t Critical two-tail	2.14478669			

The post- hoc- corrected t-tests analysis reports as "true'' for LMH compared to control implies that there is 95% of chance of difference between control and LMH. The LY permeability is significantly higher for LMH compared to control.

t-Test: Two-Sample Assuming Equal Variances				
	Control	*Liposome*		
Mean	0.055395	0.637948		
Variance	0	7.418003		
Observations	8	8		
Pooled Variance	3.709002			
Hypothesized Mean Difference	0			
df	14			
t Stat	-0.60497			
P(T<=t) one-tail	0.277438			
t Critical one-tail	1.76131			
P(T<=t) two-tail	0.554876		0.009676	TRUE
t Critical two-tail	2.144787			

The post- hoc- corrected t-tests analysis reports as "true'' for liposome compared to control implies that there is 95% of chance of difference between control and liposome. The LY permeability is significantly higher for liposome compared to control.

t-Test: Two-Sample Assuming Equal Variances				
	Control	*Micelles*		
Mean	0.055395	-0.45373		
Variance	0	7.562836		
Observations	8	8		
Pooled Variance	3.7814178			
Hypothesized Mean Difference	0			
df	14			
t Stat	0.5236362			
P(T<=t) one-tail	0.3043607			
t Critical one-tail	1.7613101			
P(T<=t) two-tail	0.6087214		0.009676	TRUE
t Critical two-tail	2.1447867			

The post- hoc- corrected t-tests analysis reports as "true'' for micelles compared to control implies that there is 95% of chance of difference between control and micelles. The LY permeability is significantly higher for micelles compared to control.

The post- hoc- corrected t-tests analysis reports as "true'' for LOV, LMH, liposome and micelles compared to control implies that there is 95% of chance of difference between control and nanocarriers. The LY permeability is significantly higher for LOV, LMH, liposome and micelles compared to control.

Page 4-15, Figure 4-5: Effect of 100 µM LOV encapsulated in micelles, liposomes, LMH and free LOV on the TEER in Caco-2 cell monolayers (21 days old) in HBSS over 2 hours of

the treatment period. Control without treatment (Cells with buffer and buffer only). The data are presented as mean ± SD (n = 4).

Anova: Single Factor						
SUMMARY						
Groups	*Count*	*Sum*	*Average*	*Variance*		
Buffer + cells	5	493	98.6	17.14649		
LOV	5	457.9706	91.59412	51.07491		
LMH	5	257.6699	51.53397	754.3411		
Liposome	5	314.5803	62.91606	653.0341		
Micelles	5	347.8635	69.57269	498.3269		
ANOVA						
Source of Variation	*SS*	*df*	*MS*	*F*	*P-value*	*F crit*
Between Groups	7791.669	4	1947.917	4.934126	0.006225	2.866081
Within Groups	7895.694	20	394.7847			
Total	15687.36	24				

A statistically significant differences seen between the control and the micelles/liposomes/LMHs

t-Test: Two-Sample Assuming Equal Variances	Blank vs LOV			
	Variable 1	*Variable 2*		
Mean	98.600002	91.594118		
Variance	17.14649147	51.0749084		
Observations	5	5		
Pooled Variance	34.11069994			
Hypothesized Mean Difference	0			
df	8			
t Stat	1.896651903			
P(T<=t) one-tail	0.047226834			
t Critical one-tail	1.859548038			
P(T<=t) two-tail	0.094453668		0.018891	TRUE
t Critical two-tail	2.306004135			

The post- hoc- corrected t-tests analysis reports as "true'' for LOV compared to blank implies that there is 95% of chance of difference between blank and LOV. The effect of TEER is significantly higher for LOV compared to blank.

t-Test: Two-Sample Assuming Equal Variances		Blank vs LMH		
	Variable 1	*Variable 2*		
Mean	98.600002	51.533971		
Variance	17.14649147	754.341084		
Observations	5	5		
Pooled Variance	385.7437878			
Hypothesized Mean Difference	0			
df	8			
t Stat	3.789030582			
P(T<=t) one-tail	0.002659588			
t Critical one-tail	1.859548038			
P(T<=t) two-tail	0.005319176		0.018891	FALSE
t Critical two-tail	2.306004135			

The post- hoc- corrected t-tests analysis reports as false for LMH compared to blank implies that there is no significance of difference between blank and LMH. The effect of TEER is significantly lower for LMH compared to blank.

t-Test: Two-Sample Assuming Equal Variances			Blank vs liposome	
	Variable 1	*Variable 2*		
Mean	98.600002	62.9160635		
Variance	17.14649147	653.034062		
Observations	5	5		
Pooled Variance	335.0902767			
Hypothesized Mean Difference	0			
df	8			
t Stat	3.082207504			
P(T<=t) one-tail	0.007533207			
t Critical one-tail	1.859548038			
P(T<=t) two-tail	0.015066414		0.018891	FALSE
t Critical two-tail	2.306004135			

The post- hoc- corrected t-tests analysis reports as false for liposome compared to blank implies that there is no significance of difference between blank and liposome. The effect of TEER is significantly lower for liposome compared to blank.

t-Test: Two-Sample Assuming Equal Variances	Blank vs Micelles			
	Variable 1	*Variable 2*		
Mean	98.600002	69.572692		
Variance	17.14649147	498.326921		
Observations	5	5		
Pooled Variance	257.7367063			
Hypothesized Mean Difference	0			
df	8			
t Stat	2.858832155			
P(T<=t) one-tail	0.010594703			
t Critical one-tail	1.859548038			
P(T<=t) two-tail	0.021189405		0.018891	TRUE
t Critical two-tail	2.306004135			

The post- hoc- corrected t-tests analysis reports as "true'' for LOV and micelles compared to Blank implies that there is 95% of chance of difference between blank and nanocarriers. The effect of TEER is significantly higher for LOV and micelles compared to blank. However for Liposome and LMH it is significantly lower compared to the blank.

t-Test: Two-Sample Assuming Equal Variances	LOV vs LMH			
	Variable 1	*Variable 2*		
Mean	91.594118	51.533971		
Variance	51.07490841	754.341084		
Observations	5	5		
Pooled Variance	402.7079962			
Hypothesized Mean Difference	0			
df	8			
t Stat	3.156366435			
P(T<=t) one-tail	0.006734271			
t Critical one-tail	1.859548038			
P(T<=t) two-tail	0.013468542		0.003367	TRUE
t Critical two-tail	2.306004135			

The post- hoc- corrected t-tests analysis reports as "true'' for LMH compared to LOV implies that there is 95% of chance of difference between LOV and LMH. The effect of TEER is significantly higher for LMH compared to LOV.

t-Test: Two-Sample Assuming Equal Variances	LOV vs Liposome			
	Variable 1	*Variable 2*		
Mean	91.594118	62.9160635		
Variance	51.07490841	653.034062		
Observations	5	5		
Pooled Variance	352.0544852			
Hypothesized Mean Difference	0			
df	8			
t Stat	2.416655523			
P(T<=t) one-tail	0.021034521			
t Critical one-tail	1.859548038			
P(T<=t) two-tail	0.042069043		0.003367	TRUE
t Critical two-tail	2.306004135			

The post- hoc- corrected t-tests analysis reports as "true'' for liposome compared to LOV implies that there is 95% of chance of difference between LOV and liposome. The effect of TEER is significantly higher for liposome compared to LOV.

t-Test: Two-Sample Assuming Equal Variances	LOV vs micelles			
	Variable 1	*Variable 2*		
Mean	91.594118	69.572692		
Variance	51.07490841	498.3269211		
Observations	5	5		
Pooled Variance	274.7009147			
Hypothesized Mean Difference	0			
df	8			
t Stat	2.100803295			
P(T<=t) one-tail	0.034425718			
t Critical one-tail	1.859548038			
P(T<=t) two-tail	0.068851436		0.003367	TRUE
t Critical two-tail	2.306004135			

The post- hoc- corrected t-tests analysis reports as "true'' for micelles compared to LOV implies that there is 95% of chance of difference between LOV and micelles. The effect of TEER is significantly higher for micelles compared to LOV.

The post- hoc- corrected t-tests analysis reports as "true'' for LMH, liposome and micelles compared to free LOV implies that the effect of nanocarriers on the TEER is significantly higher compared to the free LOV.

APPENDIX E

Page 5-24; Figure 5-5 the extent of drug loading varies significantly with the increased drug quantity.

Anova: Single Factor					
SUMMARY					
Groups	*Count*	*Average*	*Variance*		
Liposome (PTX)	4	4.715	0.158567		
Micelles (PTX)	4	2.1975	0.018692		
Micelles (5-FU)	4	3.170326	0.009893		
ANOVA					
Source of Variation	SS	MS	F	P-value	F crit
Between Groups	12.894	6.44681	103.3412	0.000000619	4.256495
Within Groups	0.5615	0.062384			

There is significant difference ($p< 6.1 \times 10^{-7}$) of PTX loading in liposome and micelles.

t-Test: Two-Sample Assuming Equal Variances				
	Liposome PTX	*Micelles PTX*		
Mean	4.715	2.1975		
Variance	0.158566667	0.018691667		
Observations	4	4		
Pooled Variance	0.088629167			
Hypothesized Mean Difference	0			
df	6			
t Stat	11.9590352			
P(T<=t) one-tail	1.03567E-05			
t Critical one-tail	1.943180281			
P(T<=t) two-tail	0.0000207134		0.00000690	TRUE
t Critical two-tail	2.446911851			

The post- hoc- corrected t-tests analysis reports as "true'' for liposome (PTX) compared to micelles (PTX) implies that there is 95% of chance of difference between PTX loading in liposome and micelles. The effect of PTX loading is significantly higher for liposome compared to micelles.

t-Test: Two-Sample Assuming Equal Variances				
	Liposome PTX	*Micelles 5-FU*		
Mean	4.715	3.17032565		
Variance	0.158566667	0.009892945		
Observations	4	4		
Pooled Variance	0.084229806			
Hypothesized Mean Difference	0			
df	6			
t Stat	7.526950022			
P(T<=t) one-tail	0.000142448			
t Critical one-tail	1.943180281			
P(T<=t) two-tail	0.000284895		0.000006904	TRUE
t Critical two-tail	2.446911851			

The post- hoc- corrected t-tests analysis reports as "true'' for liposome (PTX) compared to micelles (5-FU) implies that there is 95% of chance of difference between PTX and 5-FU loading in liposome and micelles. The effect of PTX loading is significantly higher for liposome compared to 5-FU in micelles.

t-Test: Two-Sample Assuming Equal Variances				
	Micelles PTX	*Micelles 5FU*		
Mean	2.1975	3.17032565		
Variance	0.018691667	0.009892945		
Observations	4	4		
Pooled Variance	0.014292306			
Hypothesized Mean Difference	0			
df	6			
t Stat	-11.50797359			
P(T<=t) one-tail	1.29342E-05			
t Critical one-tail	1.943180281			
P(T<=t) two-tail	0.00002587		0.0000069	TRUE
t Critical two-tail	2.446911851			

The post- hoc- corrected t-tests analysis reports as "true'' for PTX in micelles compared to 5-FU in micelles implies that there is 95% of chance of difference between PTX and 5-FU loading in micelles. The effect of PTX loading is significantly higher compared to 5-FU in micelles.

The post- hoc-corrected t-tests analysis reports as "true'' for liposome (PTX), micelles (PTX) and micelles (5-FU) implies that the extent of drug loading varies significantly with the increased drug quantity.

APPENDIX F

Figure 5-10 Statistical difference between **the releases of PTX from TPGS micelles at 37°C and 42°C**

Anova: Single Factor						
SUMMARY						
Groups	*Count*	*Sum*	*Average*	*Variance*		
0	2	0	0	0		
1	2	88.08306	44.04153	688.3148		
2	2	107.2571	53.62854	527.6909		
4	2	112.9557	56.47783	379.9706		
6	2	126.546	63.27301	214.7744		
8	2	130.7154	65.3577	280.2625		
24	2	136.8322	68.41609	222.1143		
48	2	156.086	78.043	117.7535		
ANOVA						
Source of Variation	*SS*	*df*	*MS*	*F*	*P-value*	*F crit*
Between Groups	8042.740464	7	1148.963	3.781223	0.040905	3.500464
Within Groups	2430.881034	8	303.8601			
Total	10473.6215	15				

From the Single Factor ANOVA data analysis it is found that a statistically significant ($P < 0.04$) differences between the extent of drug release at elevated temperature 42 ° C and 37° C.

APPENDIX G

Page 5-32; Figure 5-13 a statistically significant difference between **the releases of PTX from liposome at 37°C and 42°C**

Anova: Single Factor

SUMMARY

Groups	*Count*	*Sum*	*Average*	*Variance*
1	2	79.67053	39.83527	226.2756
2	2	107.1021	53.55107	72.66127
4	2	126.1454	63.07271	154.8897
6	2	142.5123	71.25613	31.95777
8	2	144.2573	72.12865	33.53404
24	2	155.2937	77.64683	33.18599
48	2	176.2625	88.13126	2.559476

ANOVA

Source of Variation	*SS*	*df*	*MS*	*F*	*P-value*	*F crit*
Between Groups	3073.785076	6	512.2975	6.460667	0.013457	3.865969
Within Groups	555.0638108	7	79.29483			
Total	3628.848887	13				

From the Single Factor ANOVA data analysis it is found that a statistically significant ($p <$ 0.0134) differences between the extent of drug release at elevated temperature 42 ° C and 37° C.

APPENDIX H

Page 5-33; Figure 5-15 a statistical significant difference between **the releases of PTX from hybrid at 37°C and 42°C**

Anova: Single Factor

SUMMARY

Groups	*Count*	*Sum*	*Average*	*Variance*
0	2	0	0	0
1	2	14.82	7.41	15.7922
2	2	29.08	14.54	56.8178
4	2	43.51	21.755	87.78125
6	2	60.56	30.28	76.1378
8	2	76.9	38.45	55.3352
24	2	105.63	52.815	103.2485
48	2	117	58.5	144.5

ANOVA

Source of Variation	*SS*	*df*	*MS*	*F*	*P-value*	*F crit*
Between Groups	6177.094075	7	882.442	13.0826	0.000828	3.500464
Within Groups	539.6127	8	67.45159			
Total	6716.706775	15				

From the Single Factor ANOVA data analysis it is found that a statistically significant ($p < 8.2 \times 10^{-4}$) differences between the extent of drug release at elevated temperature 42 ° C and 37° C.

APPENDIX I

Page 5-37, Figure 5-17: The % release of A) PTX from liposome bilayer of PTX-5-FU-LMH for 24 hours (inset graph) and 192 hours,

Anova: Single Factor						
SUMMARY						
Groups	*Count*	*Sum*	*Average*	*Variance*		
Row 1	2	16.56847	8.284235	21.28383		
Row 2	2	22.12241	11.061205	43.87587		
Row 3	2	26.58905	13.294525	53.51934		
Row 4	2	30.30584	15.15292	69.45796		
Row 5	2	35.64718	17.82359	75.68437		
Row 6	2	47.27512	23.63756	28.19119		
Row 7	2	47.78851	23.894255	26.55521		
Row 8	2	60.31139	30.155695	20.35979		
Row 9	2	69.08449	34.542245	22.64046		
Row 10	2	71.33282	35.66641	20.35118		
Row 11	2	83.46189	41.730945	18.15652		
Row 12	2	90.10159	45.050795	14.00014		
Row 13	2	102.5776	51.28879	131.4771		
Row 14	2	125.3456	62.67282	680.7703		
ANOVA						
Source of Variation	*SS*	*df*	*MS*	*F*	*P-value*	*F crit*
Between Groups	6982.123602	13	537.0864309	6.131507	0.00091	2.507263
Within Groups	1226.323242	14	87.5945173			
Total	8208.446844	27				

A statistically significant ($p < 9.1 \times 10^{-4}$) differences between the extent of drug release at elevated temperature 42 ° C and 37° C.

Page 5-37, Figure 5-17B) 5-FU from PTX-5-FU-LMH micelles for 24 hours (inset graph) and 192 hours at 37°C and 42°C

Anova: Single Factor

SUMMARY

Groups	*Count*	*Sum*	*Average*	*Variance*
0	2	64.43103	32.21552	148.3043
1	2	166.81969	83.40985	2.680979
2	2	172.16029	86.08015	4.118479
4	2	168.57559	84.2878	10.58704
8	2	167.7087	83.85435	7.814449
24	2	161.33535	80.66768	10.91935
36	2	169.9297	84.96485	5.838355
48	2	155.84992	77.92496	26.89187
72	2	154.95861	77.47931	11.34656
96	2	155.61486	77.80743	3.734754
120	2	158.68182	79.34091	32.81667
144	2	155.71909	77.85955	39.79167
168	2	156.2828	78.1414	50.88125
192	2	153.09436	76.54718	0.608062

ANOVA

Source of Variation	*SS*	*df*	*MS*	*F*	*P-value*	*F crit*
Between Groups	4630.315884	13	356.1781	13.99388	0.00000787	2.507263
Within Groups	356.3338145	14	25.45242			
Total	4986.649699	27				

A statistically significant ($p < 7.8 \times 10^{-6}$) differences between the extent of drug release at elevated temperature 42° C and 37° C.

Page 5-38, Figure 5-18: The release of 5-FU from micelles for 24 hours (inset graph) and 120 hours at 37°C and 42°C in release media (PBS + PEG-400 0.5% with pH 7.4). Each data represents the (mean ± SD, n = 3).

Anova: Single Factor

SUMMARY

Groups	*Count*	*Sum*	*Average*	*Variance*
0	2	78.05918	39.02959	6.459065
1	2	179.15504	89.57752	0.226101
2	2	180.84959	90.4248	0.318665
4	2	175.71344	87.85672	0.00392
8	2	178.02287	89.01144	4.788306
24	2	169.31327	84.65664	29.71935
36	2	164.43536	82.21768	22.42357
48	2	168.62076	84.31038	10.66065
72	2	170.42507	85.21254	19.04377
96	2	169.77533	84.88767	34.36843
120	2	200.046	100.023	0

ANOVA

Source of Variation	*SS*	*df*	*MS*	*F*	*P-value*	*F crit*
Between Groups	4786.436696	10	478.6437	41.12964	0.0000002904	2.853625
Within Groups	128.011828	11	11.63744			
Total	4914.448524	21				

A statistically significant ($p < 2.9 \times 10^{-6}$) differences between the extent of drug release at elevated temperature 42 ° C and 37° C.

APPENDIX J

Page 5-39; Figure 5-19 statistically significant for comparisons of diffusion coefficients.

Anova: Single Factor						
SUMMARY						
Groups	*Count*	*Sum*	*Average*	*Variance*		
Micelles	3	7.02	2.34	0.0025		
Liposome	3	4.47	1.49	0.0004		
LMH (PTX in micelles' core)	3	1.797	0.599	4E-06		
LMH (PTX in bilayer)	3	0.312	0.104	0.000016		
ANOVA						
Source of Variation	*SS*	*df*	*MS*	*F*	*P-value*	*F crit*
Between Groups	8.785	3	2.9282948	4011.362671	4.792E-13	4.066180551
Within Groups	0.006	8	0.00073			
Total	8.791	11				

A statistically significant ($p < 0.05$) differences of diffusion coefficient between the micelles, liposome and LMH (micelles core and bilayer).

Anova: Single Factor						
SUMMARY						
Groups	*Count*	*Sum*	*Average*	*Variance*		
LMH (PTX in bilayer) 37° C	3	1.797	0.599	4E-06		
LMH (PTX in bilayer) 42° C	3	3.42	1.14	0.0009		
ANOVA						
Source of Variation	*SS*	*df*	*MS*	*F*	*P-value*	*F crit*
Between Groups	0.439022	1	0.439022	971.2865	6.32E-06	7.708647
Within Groups	0.001808	4	0.000452			
Total	0.44083	5				

A statistically significant ($p < 0.05$) differences of diffusion coefficient between the PTX release kinetics from LMH (bilayer) at different temperatures 42°C and 37°C.

Anova: Single Factor						
SUMMARY						
	Count	*Sum*	*Average*	*Variance*		
LMH (PTX in micelles' core) 37°	3	1.797	0.599	4E-06		
LMH (PTX in micelles' core) 42 °C	3	3.42	1.14	0.0009		
ANOVA						
Source of Variation	*SS*	*df*	*MS*	*F*	*P-value*	*F crit*
Between Groups	0.43902	1	0.4390215	971.2865	6.32E-06	7.708647
Within Groups	0.00181	4	0.000452			
Total	0.44083	5				

A statistically significant ($p < 0.05$) differences of diffusion coefficient between the PTX release kinetics from LMH (micelles core) at different temperatures 42°C and 37°C.

t-Test: Two-Sample Assuming Equal Variances				
	Micelles	*H-bilayer*		
Mean	0.541	0.1275		
Variance	0.050562	5E-07		
Observations	2	2		
Pooled Variance	0.02528125			
Hypothesized Mean Difference	0			
df	2			
t Stat	2.600616072			
P(T<=t) one-tail	0.060746949			
t Critical one-tail	2.91998558			
P(T<=t) two-tail	0.121493898		0.058051	TRUE
t Critical two-tail	4.30265273			

The post- hoc- corrected t-tests analysis reports as "true'' for micelles compared to H-bilayer implies that there is 95% of chance of difference between micelles and H-bilayer. The release kinetics of PTX is significantly higher for micelles compared to H-bilayer.

t-Test: Two-Sample Assuming Equal Variances				
	Micelles	*H-core*		
Mean	0.541	3.595		
Variance	0.050562	6.44405		
Observations	2	2		
Pooled Variance	3.247306			
Hypothesized Mean Difference	0			
df	2			
t Stat	-1.694756956			
P(T<=t) one-tail	0.116102906			
t Critical one-tail	2.91998558			
P(T<=t) two-tail	0.232205811		0.058051	TRUE
t Critical two-tail	4.30265273			

The post- hoc- corrected t-tests analysis reports as "true'' for micelles compared to H-core implies that there is 95% of chance of difference between micelles and H- core. The release kinetics of PTX is significantly higher for micelles compared to H- core.

t-Test: Two-Sample Assuming Equal Variances				
	Micelles	*Liposome*		
Mean	0.541	3.595		
Variance	0.050562	6.44405		
Observations	2	2		
Pooled Variance	3.247306			
Hypothesized Mean Difference	0			
df	2			
t Stat	-1.69475696			
P(T<=t) one-tail	0.116102906			
t Critical one-tail	2.91998558			
P(T<=t) two-tail	0.232205811		0.058051	TRUE
t Critical two-tail	4.30265273			

The post- hoc- corrected t-tests analysis reports as "true'' for micelles compared to liposome implies that there is 95% of chance of difference between micelles and liposome. The release kinetics of PTX is significantly higher for micelles compared to liposome.

The post- hoc- corrected t-tests analysis reports as "true'' for micelles compared to liposome, H-core and H-bilayer implies that there is 95% of chance of difference between micelles, liposome, H-core and H-bilayer. The release kinetics of PTX is significantly higher for micelles compared to liposomes and LMH (H-core and H-bilayer).

APPENDIX K

Page 5-41; Figure 5-21 the post hoc test to determine the difference (differences)

Anova: Single Factor

SUMMARY

Groups	*Count*	*Sum*	*Average*	*Variance*
Micelles	9	404.75	44.97222222	436.9703167
Liposome	9	391.18	43.46444444	36.42248889
Hybrid	9	239.306667	26.58962963	341.6083318

ANOVA

Source of Variation	*SS*	*df*	*MS*	*F*	*P-value*	*F crit*
Between Groups	1874.857	2	937.4287189	3.450653046	0.048174	3.402826
Within Groups	6520.009	24	271.6670458			
Total	8394.867	26				

A statistically significant ($p < 0.048$) differences of diffusion coefficient between the nanocarriers.

t-Test: Two-Sample Assuming Equal Variance (Micelles Vs Liposome)

	54.98666667	*42.42666667*
Mean	43.72041667	43.59416667
Variance	483.2767569	41.45261508
Observations	8	8
Pooled Variance	262.364686	
Hypothesized Mean	0	
df	14	
t Stat	0.015588657	
P(T<=t) one-tail	0.493891266	
t Critical one-tail	1.761310136	
P(T<=t) two-tail	0.987782532	
t Critical two-tail	2.144786688	
	0.329260844	
	FALSE	

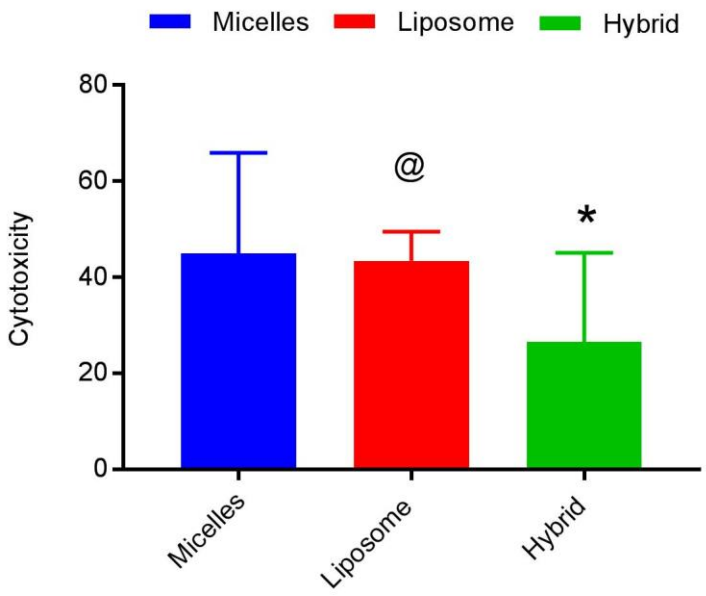
The post- hoc- corrected t-tests analysis reports as false for micelles vs liposome implies that there is no significant difference between micelles and liposome.

t-Test: Two-Sample Assuming Equal Variances		(Micelles VS Hybrid)		
	54.98666667	*52.92666667*		
Mean	43.72041667	23.2975		
Variance	483.2767569	278.9317421		
Observations	8	8		
Pooled Variance	381.1042495			
Hypothesized Mean Difference	0			
df	14			
t Stat	2.092309203			
P(T<=t) one-tail	0.027555661			
t Critical one-tail	1.761310136			
P(T<=t) two-tail	0.055111323			0.329261
t Critical two-tail	2.144786688			
				TRUE

The post- hoc- corrected t-tests analysis reports as "true'' for micelles vs hybrid implies that there is 95% of chance of difference between micelles and hybrid. The cytotoxicity of micelles is significantly lower for hybrid compared to micelles

t-Test: Two-Sample Assuming Equal Variances		(Liposome vs hybrid)		
	42.42666667	*52.92666667*		
Mean	43.59416667	23.2975		
Variance	41.45261508	278.9317421		
Observations	8	8		
Pooled Variance	160.1921786			
Hypothesized Mean Difference	0			
df	14			
t Stat	3.207259212			
P(T<=t) one-tail	0.003164256			0.329261
t Critical one-tail	1.761310136			
P(T<=t) two-tail	0.006328511			TRUE
t Critical two-tail	2.144786688			

The post- hoc- corrected t-tests analysis reports as "true'' for liposome vs hybrid implies that there is 95% of chance of difference between liposome and hybrid. The cytotoxicity of liposome is significantly lower compared to hybrid.



The post- hoc- corrected t-tests analysis reports as false for micelles vs liposome and "true'' for liposome vs hybrid implies that there is 95% of chance of difference between LMH and liposome. The cytotoxicity of micelles is significantly difference from liposome; however, it is significantly lower for hybrid compared to micelles.

APPENDIX L

Page 5-45; Figure 5-24 the post hoc test to determine the difference (differences)

Anova: Single Factor — Within a 2 hours period

SUMMARY

Groups	*Count*	*Sum*	*Average*	*Variance*
LMH	4	0.82073	0.2051825	1.04E-06
Liposome	4	0.73477	0.1836925	4.46E-05
Micelles	4	0.64613	0.1615325	9.19E-06

ANOVA

Source of Variation	*SS*	*df*	*MS*	*F*	*P-value*	*F crit*
Between Groups	0.003810944	2	0.001905472	104.1708	0.0000005983	4.256495
Within Groups	0.000164626	9	1.82918E-05			
Total	0.00397557	11				

A statistically significant difference ($P < 5.98 \times 10^{-7}$) between the nanocarriers.

t-Test: Two-Sample Assuming Equal Variance	(PTX vs LMH)				
	0.0751	*0.20536*			
Mean	0.075933333	0.205123333			
Variance	0.000124103	1.54123E-06			
Observations	3	3			
Pooled Variance	6.28223E-05				
Hypothesized Mean	0				
df	4				
t Stat	-19.96262595				
P(T<=t) one-tail	1.85789E-05				
t Critical one-tail	2.131846786				
P(T<=t) two-tail	3.71578E-05		9.28945E-06		TRUE
t Critical two-tail	2.776445105				

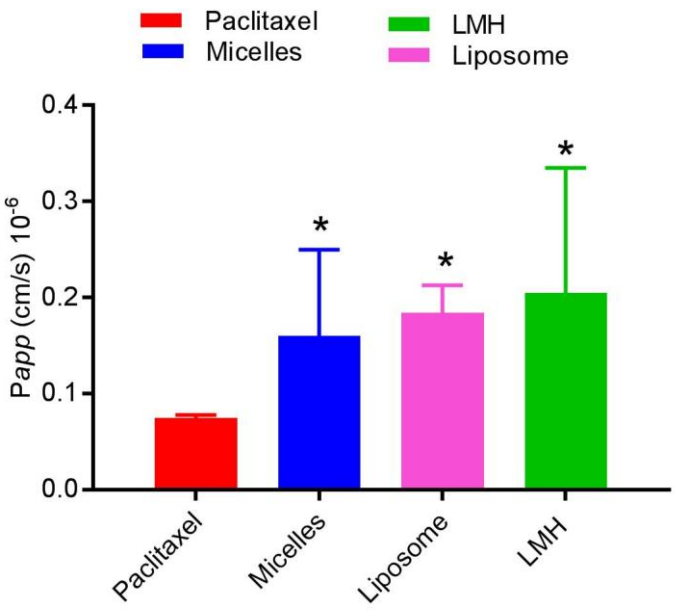
The post- hoc- corrected t-tests analysis reports as "true'' for LMH compared to free PTX implies that there is 95% of chance of difference between LMH and PTX. The permeability of PTX is significantly lower for LMH compared to free PTX.

t-Test: Two-Sample Assuming Equal Variances	(PTX vs Liposome)				
	0.0751	*0.19254*			
Mean	0.075933333	0.180743333			
Variance	0.000124103	1.47772E-05			
Observations	3	3			
Pooled Variance	6.94403E-05				
Hypothesized Mean	0				
df	4				
t Stat	-15.40432272				
P(T<=t) one-tail	5.1814E-05				
t Critical one-tail	2.131846786				
P(T<=t) two-tail	0.000103628			0.0000092894	TRUE
t Critical two-tail	2.776445105				

The post- hoc- corrected t-tests analysis reports as "true'' for liposome compared to free PTX implies that there is 95% of chance of difference between liposome and PTX. The permeability of PTX is significantly lower for liposome compared to free PTX.

t-Test: Two-Sample Assuming Equal Variances		(PTX vs Micelles)			
	0.0751	*0.16352*			
Mean	0.075933333	0.16087			
Variance	0.000124103	1.11547E-05			
Observations	3	3			
Pooled Variance	6.7629E-05				
Hypothesized Mean Difference	0				
df	4				
t Stat	-12.64952758				
P(T<=t) one-tail	0.000112446				
t Critical one-tail	2.131846786				
P(T<=t) two-tail	0.000224891		0.0000092894		TRUE
t Critical two-tail	2.776445105				

The post- hoc- corrected t-tests analysis reports as "true'' for micelles compared to free PTX implies that there is 95% of chance of difference between micelles and PTX. The permeability of PTX is significantly lower for micelles compared to free PTX.



The post- hoc- corrected t-tests analysis reports as "true'' for micelles, liposome and LMH compared to free PTX implies that there is 95% of chance of difference between LMH and liposome. The permeability of PTX is significantly higher for micelles, liposomes and LMH compared to free PTX.

APPENDIX M

Page 5-46, Figure 5-25 Percent permeability of LY (100 µM) from A→B; added to the apical chamber of CCM treated with 100 µM PTX and 100 µM PTX incorporated into each nanocarrier; micelles, liposomes, and LMH; were incubated for 1-hour with 100 µM LY. After 1-hour samples were collected from the basal chamber. Here the control was only the cells. LY was measured by fluorescence intensity at excitation and emission wavelengths of 485 and 520 nm, respectively. Results are means ± SD (n = 4).

Anova: Single Factor

SUMMARY

Groups	*Count*	*Sum*	*Average*	*Variance*
Control (cell only)	3	0.045	0.015	0.000004
Paclitaxel	3	2.37	0.79	0.0004
Micelles	3	0.87	0.29	1E-04
Liposome	3	0.904	0.301333333	5.3333E-06
LMH	3	1.29	0.43	0.0676

ANOVA

Source of Variation	*SS*	*df*	*MS*	*F*	*P-value*	*F crit*
Between Groups	0.951084267	5	0.190216853	12.5676732	0.000767	3.481659
Within Groups	0.136218667	9	0.015135407			
Total	1.087302933	14				

From the Single Factor ANOVA data analysis it is found that a statistically significant ($p < 7.6 \times 10^{-4}$) differences within control, PTX and nanocarriers permeability.

t-Test: Two-Sample Assuming Equal Variances

	Variable 1	*Variable 2*		
Mean	0.79	0.29		
Variance	0.0004	1E-04		
Observations	3	3		
Pooled Variance	0.00025			
Hypothesized Mean Difference	0			
df	4			
t Stat	38.72983346			
P(T<=t) one-tail	1.32743E-06			
t Critical one-tail	2.131846786			
P(T<=t) two-tail	0.00000265		0.0000008850	TRUE
t Critical two-tail	2.776445105			

t-Test: Two-Sample Assuming Equal Variances					
	Variable 1	*Variable 2*			
Mean	0.79	0.301333333			
Variance	0.0004	5.33333E-06			
Observations	3	3			
Pooled Variance	0.000202667				
Hypothesized Mean Difference	0				
df	4				
t Stat	42.04043323				
P(T<=t) one-tail	9.56789E-07				
t Critical one-tail	2.131846786				
P(T<=t) two-tail	0.0000019136				
t Critical two-tail	2.776445105			0.0000008850	TRUE

t-Test: Two-Sample Assuming Equal Variances				
	Variable 1	*Variable 2*		
Mean	0.79	0.43		
Variance	0.0004	0.0676		
Observations	3	3		
Pooled Variance	0.034			
Hypothesized Mean Difference	0			
df	4			
t Stat	2.391160191			
P(T<=t) one-tail	0.037536559			
t Critical one-tail	2.131846786			
P(T<=t) two-tail	0.075073118		8.85E-07	TRUE
t Critical two-tail	2.776445105			

The post- hoc- corrected t-tests analysis reports as "true'' for micelles, liposome and LMH compared to free PTX implies that there is 95% of chance of difference between LMH and liposome. The LY permeability of PTX is significantly lower for micelles, liposomes and LMH compared to free PTX.

APPENDIX N

Page 5-48, Figure 5-26: PTX transported across Caco-2 monolayers after 24 hours of incubation in the A→B direction at 37°C in the presence of micelles, liposome, and LMH containing 100 µM of PTX and PTX 100 µM, expressed as a percentage of the initial concentration of 100 µM PTX, added to the apical compartment, as a function of time, mean ± SD (n=4).

Anova: Two-Factor Without Replication						
SUMMARY	*Count*	*Sum*	*Average*	*Variance*		
1	4	0.1848	0.0462	0		
2	4	113.778585	28.4446463	33.45242519		
4	4	136.2071475	34.0517869	26.24620062		
8	4	216.97267	54.2431675	33.60911304		
12	4	253.7947425	63.4486856	39.18271951		
24	4	350.2226125	87.5556531	66.29011971		
Paclitaxel	6	228.625515	38.1042525	778.7970628		
LMH	6	284.081525	47.3469208	945.9978868		
Liposome	6	266.5350075	44.4225013	939.1805805		
Micelles	6	291.91851	48.653085	1096.456132		
ANOVA						
Source of Variation	*SS*	*df*	*MS*	*F*	*P-value*	*F crit*
Rows	18602.99	5	3720.59767	280.20775	2.95E-14	2.901295
Columns	397.1718	3	132.390593	9.970674998	0.000729	3.287382
Error	199.17	15	13.277997			
Total	19199.33	23				

From the Single Factor ANOVA data analysis it is found that a statistically significant ($p < 7.3 \times 10^{-4}$) differences between PTX and nano-carriers.

t-Test: Two-Sample Assuming Equal Variances				
	PTX	*LMH*		
Mean	38.1042525	47.34692083		
Variance	778.7970628	945.9978868		
Observations	6	6		
Pooled Variance	862.3974748			
Hypothesized Mean Difference	0			
df	10			
t Stat	-0.545135241			
P(T<=t) one-tail	0.298803955			
t Critical one-tail	1.812461123			
P(T<=t) two-tail	0.597607911		0.149402	TRUE
t Critical two-tail	2.228138852			

t-Test: Two-Sample Assuming Equal Variances				
	PTX	*Liposome*		
Mean	38.1042525	47.34692083		
Variance	778.7970628	945.9978868		
Observations	6	6		
Pooled Variance	862.3974748			
Hypothesized Mean Difference	0			
df	10			
t Stat	-0.545135241			
P(T<=t) one-tail	0.298803955			
t Critical one-tail	1.812461123			
P(T<=t) two-tail	0.597607911		0.149402	TRUE
t Critical two-tail	2.228138852			

t-Test: Two-Sample Assuming Equal Variances				
	PTX	*Micelles*		
Mean	38.1042525	48.653085		
Variance	778.797063	1096.4561		
Observations	6	6		
Pooled Variance	937.626597			
Hypothesized Mean Difference	0			
df	10			
t Stat	-0.5966918			
P(T<=t) one-tail	0.28198841			
t Critical one-tail	1.81246112			
P(T<=t) two-tail	0.56397682		0.149402	TRUE
t Critical two-tail	2.22813885			

The post- doc- corrected t-tests analysis reports as ‘‘true’’ for micelles, liposome and LMH compared to free PTX implies that there is 95% of chance of difference between LMH and liposome. The transport of free PTX was significantly lower compared to PTX-nanocarriers.